UAB
Universitat Autònoma de Barcelona

Synthetic (Bio)Receptors for Electrochemical Biosensing: Development of Molecularly Imprinted Polymers and Aptamers for ACLF-associated Small-Molecule Biomarkers

Jose Alfonso Marrugo Ramírez

ADVERTIMENT. L'accés als continguts d'aquesta tesi queda condicionat a l'acceptació de les condicions d'ús establertes per la següent llicència Creative Commons: https://creativecommons.org/licenses/?lang=ca

ADVERTENCIA. El acceso a los contenidos de esta tesis queda condicionado a la aceptación de las condiciones de uso establecidas por la siguiente licencia Creative Commons: https://creativecommons.org/licenses/?lang=es

WARNING. The access to the contents of this doctoral thesis it is limited to the acceptance of the use conditions set by the following Creative Commons license: https://creativecommons.org/licenses/?lang=en

UAB
Universitat Autònoma de Barcelona

Synthetic (Bio)Receptors for Electrochemical Biosensing: Development of Molecularly Imprinted Polymers and Aptamers for ACLF-associated Small-Molecule Biomarkers

Jose Alfonso Marrugo Ramírez

Ph.D. Thesis

Ph.D. in Biotechnology

Directors:

Prof. Arben Merkoçi Hyka

Dr. Andrew Piper

Dr. Giulio Rosati

Catalan Institute of Nanoscience and Nanotechnology

Department of Chemical, Biological and Environmental Engineering

2024

The present thesis, entitled "Synthetic (Bio)Receptors for Electrochemical Biosensing: Development of Molecularly Imprinted Polymers and Aptamers for ACLF-associated Small-Molecule Biomarkers", is presented by Jose Alfonso Marrugo Ramírez to obtain the degree of doctor by the Universitat Autònoma de Barcelona. This work was performed at the Nanobioelectronics and Biosensors Group at the Institut Català de Nanociencia i Nanotecnología (ICN2), under the supervision of Prof. Dr. Arben Merkoçi (ICREA Professor and Group Leader), Dr. Andrew Piper, and Dr. Giulio Rosati.

The author:

_____

Jose Alfonso Marrugo Ramírez
(Ph.D. candidate)

The supervisors:

_____	_____	_____
Prof. Arben Merkoçi Hyka	Dr. Andrew Piper	Dr. Giulio Rosati
(Supervisor and Co-Director)	(Co-Director)	(Co-Director)

The present thesis was performed also under the doctoral program studies "Doctorat en Biotecnologia" at the Faculty of Chemical Engineering, Universitat Autònoma de Barcelona, under the tutorship of Professor Arben Merkoçi Hyka.

The tutor

_____

Prof. Arben Merkoçi

Bellaterra, September 2024

Acknowledgments for the financial and logistic support:

















"The important thing is to never stop questioning (or learning)."

—Albert Einstein

"Science means constantly walking a tightrope between blind faith and curiosity; between bias and openness; between experience and epiphany; between ambition and passion; and between arrogance and conviction – in short, between an old today and a new tomorrow."

—Henrich Rohrer

ACKNOWLEDGMENTS

I would like to begin by thanking Arben Merkoçi for welcoming me to his research group and giving me the opportunity to become part of his team. I would also like to thank you for all the opportunities you gave me and for all they entailed.

I want to thank my thesis co-supervisors, Andrew and Giulio, for guiding and supervising me during my good and bad experiences. I greatly appreciate all your advice, our conversations, and training sessions (Wushu). They made me realize how strong I can be and how much I still need to learn not to continue thinking so innocently about academia and science. Andrew, I would like to thank you too and tell you that I appreciate it as you can't imagine all the help and support you have given me during this time, without need and with such a short time of having known each other. Thank you for your unlimited patience with my "last questions" and for always having the best attitude to have fruitful discussions, both super scientific and highly banal.

Lourdes. Gracias a ti tuve una increíble experiencia en el IBEC y eres una de las razones por las que terminé en el ICN2. Gracias por ser mi "mamá" de la ciencia. Por haberme impulsado siempre a ser mejor y a no dejarme noquear por lo que me tira el doctorado. Eres una de las primeras personas que comenzó a ayudarme a moldear y desarrollar mi forma extraña de pensar. Estaré agradecido contigo de por vida.

Anna!! Me has salvado la vida como unas 30 veces, mínimo. Honestamente, solo puedo decir que no existiría NB&B sin Anna Puig. Para mí siempre fuiste nuestro faro. Entre Dani y tu son los que más daban alegría al grupo. Gracias a ambos las tantas conversaciones y consejos durante estos años.

I want to give special thanks to Cecilia. I admire your passion, humility, positive attitude, patience, and desire to teach. You are a role model for many of us, and it has been a great honor to share some fantastic scientific discussions with you.

Ruslán y Marianna, el dúo dinámico. Gracias por las experiencias vividas. Por las fiestas, las conversaciones profundas, las barbacoas, los bailes de salsa y bachata, y, sobre todo, por la manera de bromear y tratar de mantener el ambiente siempre a flote. I also had the opportunity to meet Qiuyue, Lei, and Liming. I enjoyed our conversations, Lei's meals and resilience, the chillness of Qiuyue and her happiness, and how Liming accomplished whatever she set out to do. I miss the great and quirky scientific discussions we used to have with the amazing Sinan.

From that first period, I also have very fond memories of Vern, Matheus, Mayla, Chiara, Anna G, Eleonora, Ane, and Andrea "El Presidente". Also, David Panáček (Dr. Šulin) for his amazing attitude and contagious positivity. I was pleased to have coincided with you, my friend. Martina e Angela, le ragazze del fuoco! Grazie per le feste super divertenti e per avermi insegnato che le 7 del mattino sono solo un numero!

Leylosh (kara küçük xrxspu), thank you so much for the amazing times doing MIPs and for the amazing conversations and food! Massimo and Greg. Thanks for the amazing experiences and great conversations. Las fiesticas en Urbalucho nunca se olvidarán! #4LifeBro

I would like to express my gratitude to the Leicester Biotechnology Group, particularly Prof. Sergey Piletsky, Alvaro, and Chris. Thank you for teaching me so much about (nano)MIPs and for your patience in addressing the long list of questions that I had. I will always appreciate it. Nestor and Marco, thank you for making my stay in Leicester so much more enjoyable. I hope we can meet again soon!

Al final de mi doctorado tuve el honor de encontrarme con Danilito. En tan poco tiempo pudimos construir una amistad increíble y muy bonita basada siempre en el respeto mutuo. Eres a quien más le he

aprendido cosas del doctorado. ¡Tienes un futuro brillante! Espero vernos en Colombia o en cualquier parte del mundo. Andy. Tu también en poco tiempo te volviste un amigo muy cercano. Gracias por las conversaciones tan fructíferas y la actitud siempre tan positiva.

Enrico, Su, Jessica y Sabas. Ustedes tienen guardado uno de los capítulos más importantes de mi vida. Mi vida en Barcelona y durante el doctorado hubiese sido demasiado diferente si no hubiésemos coincidido. El pisito del Raval y La Terraza Gracias por todo el apoyo y el cariño. Espero volvernos a ver pronto.

Celia Maria, Nerea Maria y Laura Maria. Tantas cosas que podría decir que me quedaría más larga esta parte que la tesis misma. Nerea y Laura, ustedes eran las más jóvenes del grupo, pero de las personas a las que más les aprendí. Su perseverancia, pasión, resiliencia, inteligencia emocional, profesionalismo, humildad, y, sobre todo, su forma de ser y ganas de ayudar a los demás, son de las mejores cosas con las que me pude encontrar en estos años. Celia Celia Celia. Creo que ni siquiera sé cómo ni por donde comenzar a darte las gracias. Te has convertido en una de las personas que más me conoce y que más ha marcado mi vida. Sin ti y sin tu apoyo emocional no hubiera sido capaz de hacer este último sprint. El SELEX PANDA TEAM y "la centralita" a punta de redbulls siempre serán parte de mí.

Casi que desde el inicio de mi doctorado tuve la gran fortuna y el honor de poder compartir "oficina" con Gabo y Enriquito. Pienso que no alcanzan las palabras para describir la manera como me han marcado la vida. Digo "oficina" por decirlo, pero para mí era otro hogar. Gracias, por tanto. Por la hermandad que pudimos crear, por la confianza depositada, por los miles de conversaciones, chistes, consejos, salidas, viajes… Espero de verdad que en algún momento volvamos a coincidir en una misma "oficina". #4LifeBro

Finalmente, quiero mostrar mi eterna gratitud a mi familia. Mis padres, mi hermana y mis abuelos. A pesar de no haber estado tan presente para ustedes en estos últimos años, ustedes estuvieron conmigo en cada paso que di y en cada decisión que tomé. Gracias por el apoyo incondicional. Por siempre creer en mí, incluso en mis momentos más difíciles. Por impulsarme siempre hacia adelante y por enseñarme que, incluso con adversidades y dificultades, siempre se puede buscar la mejor forma de salir adelante. Ustedes son unos de los grandes motores de mi vida, y este logro no es solo mío. Es de ustedes también.

Finalmente, quiero darle infinitas gracias a Ivana. Solo puedo decir que me cambiaste la vida. Gracias por ser mi norte. Mi brújula. Mis pies en la tierra (o al menos uno). Gracias por apoyarme, ayudarme y aguantarme incondicionalmente durante este periodo. No sé qué hubiera sido de mi sin ti. Eres mi motor más grande y mi modelo a seguir.

PREFACE

The state-of-the-art studies led to a book chapter publication:

1) Marrugo-Ramírez, J., Karadurmus, L., Aroca, M. A., Nguyen, E. P., De Carvalho Castro E Silva, C., Rosati, G., Osma, J. F., Ozkan, S. A., & Merkoçi, A. (2022). Nanomaterials-Based Wearable Biosensors for Healthcare. In CRC Press eBooks (pp. 345–379). https://doi.org/10.1201/9781003189435-19

As a result of the experimental work performed, several articles have been either published or, as of thesis submission date, under review in high-impact scientific journals:

1) Marrugo-Ramírez, J.; Rosati, G.; Piper, A.; Zaleski, C.; Garcia-Cruz, A.; Junot, C.; Simon, S; Trebicka, J.; Piletsky, S.A.; Merkoçi, A. Electroactive NanoMIPs for Early Detection of Acute-on-Chronic Liver Failure (ACLF)-Associated Small-Molecule Biomarkers. *Advanced Functional Materials*, 2024, 252, 116142.

Additionally, the collaborations performed during the PhD resulted in the participation in several review publications not part of the thesis:

2) Echeverri, D.; Calucho, E.; Marrugo-Ramírez, J.; Álvarez-Diduk, R.; Orozco, J.; Merkoçi, A. Capacitive immunosensing at gold nanoparticle-decorated reduced graphene electrodes fabricated by one-step laser nanostructuration. *Biosensors & Bioelectronics*, 2024, 252, 116142.
3) Castelli, F. A., Rosati, G., Moguet, C., Fuentes, C., Marrugo-Ramírez, J., Lefebvre, T., Volland, H., Merkoçi, A., Simon, S., Fenaille, F., & Junot, C. (2021). Metabolomics for personalized medicine: the input of analytical chemistry from biomarker discovery to point-of-care tests. Analytical and Bioanalytical Chemistry/Analytical & Bioanalytical Chemistry, 414(2), 759–789. https://doi.org/10.1007/s00216-021-03586-z

THESIS OVERVIEW

The thesis endeavors to contribute to innovative biosensing systems by employing aptamers and molecularly imprinted polymers (MIPs) for the precise and sensitive detection of small molecules. These synthetic (bio)receptors aim to address significant challenges in biorecognition and sensor performance, particularly for small-molecule biomarkers in point-of-care applications. The primary focus will be on the synthesis, characterization, and electrochemical detection methods of MIPs and MIP nanoparticles (nanoMIPs), alongside the utilization of *in vitro* isolation of aptamers through Systematic Evolution of Ligands by EXponential enrichment (SELEX). Advanced techniques such as magnetic bead-based partitioning and next-generation sequencing (NGS) will be incorporated in the aptamer selection .

Chapter 1 provides an extensive overview of the challenges associated with traditional antibody-based methods for detecting small molecules, particularly within Acute-on-Chronic Liver Failure (ACLF). It emphasizes the difficulties posed by the size, lack of immunogenicity, and structural similarity of small molecules to endogenous compounds, which complicates their detection using antibodies. The chapter introduces aptamers and MIPs as promising alternatives, highlighting their advantages, such as specificity, high affinity, ease of synthesis, and stability. It discusses the SELEX technique for aptamer selection and the potential of MIPs for small molecule recognition. Additionally, it underscores the importance of integrating advanced biorecognition elements into biosensing platforms for enhanced diagnostic, prognostic, and disease monitoring applications in ACLF, setting the stage for the following experimental chapters.

Chapter 2 outlines the objectives of the thesis.

Chapter 3 explores MIPs as synthetic recognition elements. MIPs are created by polymerizing functional monomers in the presence of a template molecule, which is later removed to leave a cavity that matches the target molecule in shape and chemical functionality. The chapter highlights MIPs' robustness, reusability, and the ability to tailor their selectivity and affinity through careful design and synthesis. Applications of MIPs in biosensing for small molecule detection are discussed, demonstrating their potential in clinical diagnostics, environmental monitoring, and food safety.

Chapter 4 focuses on advanced SELEX methodologies for aptamer selection, specifically magnetic bead-based SELEX (MB-SELEX) and Joint One-Pot SELEX (jOP-SELEX) for single- and multi-target aptamer isolation, respectively. These methods use magnetic beads to partition aptamers based on their binding to target molecules, enhancing the selection process's efficiency and specificity. The chapter describes using NGS and custom MATLAB analysis to identify and track aptamer sequences across SELEX rounds, facilitating early detection of promising candidates. The potential application of this bioinformatic workflow in other SELEX processes is discussed, and its utility in sequence tracking and aptamer selection is validated.

Chapter 6 contains a summary highlighting each chapter's conclusions, milestones, and future perspectives.

List of Abbreviations

AcB: Acetate Buffer
ACN: Acetonitrile
ACLF: Acute-on-Chronic Liver Failure
AFM: Atomic Force Microscopy
AHT: 6-Amino-1-hexanethiol
aPCR: Asymmetric PCR
Apt:Tg: Aptamer:Target
ASSURED: Affordable, Sensitive, Specific, User-friendly, Robust and rapid, Equipment-free, Deliverable to those who need them
bp: base pair
BSA: Bovine serum albumin
CA: Chronoamperometry
CV: Cyclic Voltammetry
DMSO: Dimethyl sulfoxide
dsDNA: double-stranded DNA
EDC: N-Ethyl-N'-(3-dimethylaminopropyl)carbodiimide
ELISA: Enzyme-Linked ImmunoSorbent Assay
e-MIPs: Electropolymerized MIPs
e-nanoMIPs: Electroactive nanoMIPs
EP: Electropolymerization
EtOH: Ethanol
FcMMA: Ferrocenylmethyl methacrylate
GB: Glass beads
HRP: Horseradish peroxidase
IUPAC: International Union of Pure and Applied Chemistry
jOP-SELEX: Joint OP-SELEX
KA: Kynurenic Acid
mABs: Monoclonal antibodies
MB: Magnetic beads
M:T: Monomer:Template ratio
MES: 2-(N-morpholino)ethanesulfonic acid
MIPs: Molecularly Imprinted Polymers
MRI: Magnetic Resonance Imaging
NANA: N-acetylneuraminic acid
nanoMIPs: MIPs nanoparticles
NGAL: Neutrophil Gelatinase-Associated Lipocalin
NGS: Next-Generation Sequencing
NHS: N-hydroxysuccinimide
nt: Nucleotides
NTC: Non-Template Control
oPD: ortho-phenylenediamine
OP-SELEX: One-Pot SELEX
pAbs: Polyclonal antibodies
PAGE. PolyAcrylamide Gel Electrophoresis
PBS: Phosphate Buffered Saline
PBST: Phosphate Buffer Saline with Tween
PCR: Polymerase Chain Reaction
PEG400: Polyethylene Glycol 400
Phe: Phenylalanine
POC: Point-of-Care
POCT: Point-of-Care testing
PoPD: poly(ortho-phenylenediamine)
QA: Quinolinic Acid
R: round
SELEX: Systematic Evolution of Ligands by EXponential enrichment
SEM: Scanning Electron Microscopy
sGBs: Silanized GBs
SMs: Small molecules
ssDNA: Single-stranded DNA
TBAB: Tetrabutylammonium Bromide
TMB: 3,3',5,5'-tetramethylbenzidine
λ: lambda exonuclease

Table of Contents

CHAPTER 1 General Introduction
1.1. Acute-on-Chronic Liver Failure (ACLF) Diagnosis ... 3
1.2. From Sensing to Biosensing ... 5
1.3. Bioreceptors in Biosensing Technology ... 6
1.3.1. Traditional Bioreceptors ... 7
1.3.1.1. Antibodies ... 7
1.3.1.2. Enzymes ... 8
1.3.2. Synthetic Receptors ... 10
1.3.2.1. Molecularly Imprinted Polymers ... 10
1.3.2.2. Aptamers ... 14
1.3.3. The Role of Noncovalent Interactions ... 16
1.4. Integration of Transducers with MIPs and Aptamers ... 17
1.4.1. Optical ... 17
1.4.2. Electrochemical ... 19
1.4.3. Other transduction principles ... 21
1.5. Applications and Limitations of MIPs- and Aptamer-based (Bio)sensors ... 21
1.5.1. Existing Diagnostic Methods for ACLF ... 24
1.6. Future Perspectives in Biosensing ... 25
1.7. References ... 29
CHAPTER 2 Thesis Objectives ... 43
CHAPTER 3 Molecularly Imprinted Polymers: An Alternative Biomimetic Approach for Small-Molecule Detection ... 45
3.1. INTRODUCTION ... 47
3.1.1. The Ubiquitous Role of Noncovalent Interactions ... 47
3.1.2. Molecular Imprinting as A Biomimicking Strategy ... 47
3.1.2.1. The Role of Functional and Structural Elements ... 49
3.1.2.2. Enhancing Functionality through Combinatorial Chemistry ... 50
3.1.2.3. Solvent Management ... 52
3.1.3. Approaches for Molecular Imprinting ... 52
3.1.3.1. Electropolymerization for Small Molecule Imprinting ... 53
3.1.3.2. Polymeric nanoparticles' synthesis ... 55
3.1.3.3. Cooperative binding ... 57
3.1.3.4. Solid-Phase Polymerization ... 59
3.1.4. Applications and Limitations ... 62
3.1.5. Proposed Approach ... 66

3.2. CHAPTER OBJECTIVES 67
3.3. MATERIALS AND METHODS 68
3.3.1. Materials 68
3.3.2. Methods 69
3.3.2.1. e-MIPs 69
3.3.2.1.1. Characterization of the precomplex 69
3.3.2.1.2. Electropolymerization 69
3.3.2.1.3. Template Removal 69
3.3.2.2. nanoMIPs 70
3.3.2.2.1. Silanization of glass beads 70
3.3.2.2.2. Dansyl Chloride Test 70
3.3.2.2.3. NanoMIPs fabrication 70
3.3.2.2.4. Photopolymerization procedure 71
3.3.2.2.5. DLS and Solvent Evaporation 72
3.3.2.2.6. nanoMIPs Immobilization on Gold Electrodes 72
3.3.2.2.7. Electrochemical measurements 73
3.4. RESULTS AND DISCUSSION 74
3.4.1. e-MIPs for Kynurenic Acid determination 74
3.4.1.1. Spectrophotometric analysis of binding interactions 74
3.4.1.2. e-MIPs Performance 77
3.4.1.2.1. Electropolymerization 77
3.4.1.2.2. Template Removal 78
3.4.2. nanoMIPs 79
3.4.2.1. Fabrication 80
3.4.2.2. Characterization and Verification 80
3.4.2.2.1. Dansyl Chloride Test 80
3.4.2.2.2. Dynamic Light Scattering 81
3.4.2.2.3. Competitive bead-ELISA 81
3.4.2.2.4. Solvent evaporation Method 83
3.4.2.3. Electrochemical Approach 83
3.4.2.3.1. Optimization 86
3.4.2.3.2. Temporal and Cyclic Stability 88
3.4.2.3.3. Performance 89
3.5. CONCLUSIONS AND FUTURE PERSPECTIVES 93
3.6. REFERENCES 95

CHAPTER 4 Simultaneous *In Vitro* Isolation of Multiple Target-Specific Aptamers Towards Small-Molecule Biomarkers 103
4.1. INTRODUCTION 107
4.1.1. Aptamers as Biorecognition Elements 107
4.1.1.1. Thermodynamics of Aptamer-Target Interaction 108
4.1.2. Systematic Evolution of Ligands by Exponential enrichment 109
4.1.2.1. Oligonucleotide Library 112
4.1.2.2. Library Conditioning 113
4.1.2.3. Partitioning Strategy 114
4.1.2.4. Selection Conditions 114
4.1.2.5. Next-Generation Sequencing Analysis 115
4.1.2.6. Binding Assays 115
4.1.3. SELEX Approaches 117
4.1.3.1. Applications and Limitations for Small Molecules 119
4.1.4. Joint One-Pot SELEX: three-target simultaneous aptamer selection 121
4.2. CHAPTER OBJECTIVES 123
4.3. MATERIALS & METHODS 124
4.3.1. Materials 124
4.3.2. SsDNA library and primers 124
4.3.3. Target-conjugated magnetic beads 125
4.3.4. Verification of target conjugation 125
4.3.5. SELEX conditions 126
4.3.6. PCR amplification 128
4.3.7. Regeneration of ssDNA 128
4.3.7.1. Asymmetric PCR 128
4.3.7.2. Lambda Exonuclease Digestion 129
4.3.8. Spin column ssDNA purification 129
4.3.9. ssDNA & dsDNA quantification measurements 129
4.3.10. Agarose gel electrophoresis 130
4.3.11. Next-Generation Sequencing – Bioinformatic Analysis 130
4.4. RESULTS & DISCUSSION 132
4.4.1. Design and rationale behind the SELEX strategies 132
4.4.1.1. Magnetic bead target-conjugation and verification 133
4.4.2. SELEX progress 135
4.4.2.1. Enrichment monitoring during the SELEX process 142
4.4.2.2. NGS Bioinformatic Analysis 144

4.5. CONCLUSIONS.....148
4.6. REFERENCES.....150
CHAPTER 5 General Conclusions and Future Perspectives.....155

CHAPTER 1:

GENERAL INTRODUCTION

Identifying Acute-on-Chronic Liver Failure (ACLF)-associated small-molecule biomarkers presents notable challenges due to their size, lack of immunogenicity, and complexity when using traditional bioreceptors, such as antibodies, enzymes, and nucleic acids. Synthetic (bio)receptors, including aptamers and molecularly imprinted polymers (MIPs), exhibit promising potential in addressing these challenges. Their antibody-like specificity and affinity offer valuable alternatives for the detection of small-molecule targets, offering the potential to significantly impact clinical decisions and therapeutic strategies. Ultimately, these advancements could contribute to effectively managing this complex condition and improving patient outcomes.

This chapter provides an in-depth exploration of the fundamental elements of MIPs and aptamer technology, emphasizing their benefits in comparison to traditional bioreceptors. These advantages include synthetic production, ease of labeling, and stability. Additionally, the chapter discusses the thermodynamics of MIPs- and aptamer-target interactions and the SELEX method, which is utilized to isolate high-affinity aptamers. Furthermore, the chapter explores the synthesis, factors influencing selectivity and affinity, and potential biosensing applications of aptamers and MIPs, setting the stage for subsequent chapters that will detail their practical applications and technological advancements in the context of ACLF and other related conditions.

1.1. Acute-on-Chronic Liver Failure (ACLF) Diagnosis

Any chronic liver injury, such as alcohol overuse, chronic hepatitis C, metabolic-associated steatotic liver disease (MASLD), and cholestatic and genetic disease, can lead over time to liver cirrhosis. As shown in Figure 1.1, while compensated cirrhosis is rather silent and may impact outcome as a comorbidity, complications of liver cirrhosis may lead to the so-called decompensation stage. Decompensated cirrhosis is mainly defined by ascites, but precipitants such as bacterial infections, alcohol-related hepatitis, and gastrointestinal bleeding can lead to organ failures, not only of the diseased liver but also of extrahepatic organs. [1–3] This syndrome is called Acute-on-Chronic Liver Failure (ACLF), which has a high risk of short-term mortality and multiple organ failure. The main driver of ACLF is systemic inflammation and dysregulation of immune cell function, where the main pathways identified associated with inflammation seem to be via the kynurenic acid (KA), which seems to be closely linked to metabolic dysfunction and even predicts short-term outcomes. [4–6]

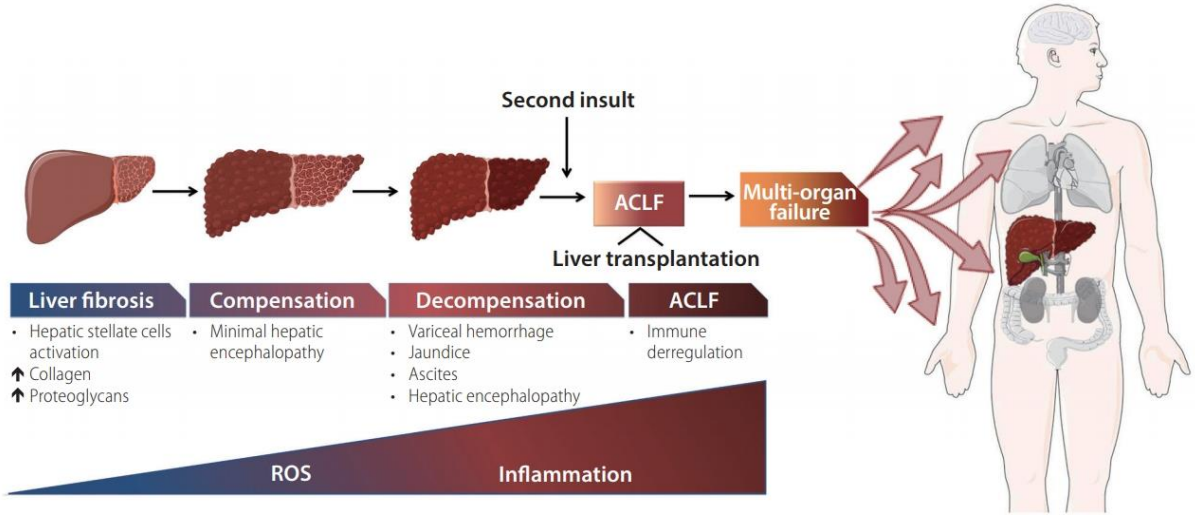
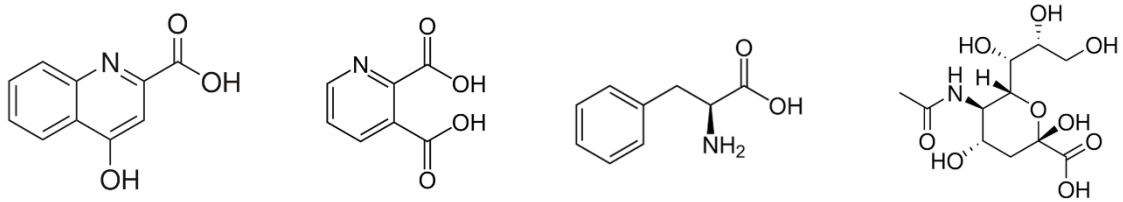


Figure 1.1*. Schematic representation of the evolution of the disease progression in ACLF. Retrieved from* [7]

The global significance and existing understanding of cirrhosis and ACLF underscore the importance of identifying biomarkers and their underlying mechanisms.[8] This would be achieved by exploring the human microbiome, which is the central objective of MICROB-PREDICT (https://microb-predict.eu/). Additionally, the project aims to develop Point-of-care (POC) nanobiosensors and propose treatment approaches that target the microbiome, as well as other strategies outlined within the project.

It is essential to prioritize the design of different biosensors for detecting a range of preliminary biomarkers associated with ACLF.[9] Following comprehensive omics analyses including proteomics, genomics, metabolomics, and bacteriomics, metabolomics emerged as particularly significant for the diagnosis, prognosis, and monitoring of the disease. Specifically, Neutrophil Gelatinase-Associated Lipocalin (NGAL), phenylalanine (Phe), quinolinic acid (QA), N-acetylneuraminic acid (NANA), and KA were identified as key biomarkers. [10] Interest in the last four biomarkers (Scheme 1.1) has grown

significantly in the detection of cirrhosis, although it is worth noting that most of the commercially available ELISA kits rely on the use of conjugated targets rather than free in solution.



Kynurenic Acid 187.17 g/mol | **Quinolinic Acid** 167.12 g/mol | **Phenylalanine** 165.19 g/mol | **N-acetylneuraminic acid** 309.27 g/mol

Scheme 1.1. Four ACLF-associated small-molecule biomarkers with their respective molecular weights.

KA and QA are byproducts of the kynurenine pathway. KA exhibits neuroprotective properties, acting as an antagonist at excitatory receptors such as NMDA and AMPA, while QA acts as an agonist at NMDA receptors, leading to excitotoxicity.[11–14] Elevated levels of both metabolites could potentially be associated with increased neuroinflammation and oxidative stress. The imbalance between neuroprotective KA and neurotoxic QA may lead to the development of hepatic encephalopathy and other mental disorders in ACLF patients. [13,15–18] Phe is an essential amino acid involved in protein synthesis and as the precursor in the biosynthesis of various neurotransmitters. When the hepatic metabolism is disrupted, Phe levels can become elevated, leading to hyperphenylalaninemia. Additionally, NANA, also known as Neu5Ac, is one of the most common types of sialic acid, which plays a crucial role in cell signaling and immunological response. Elevated NANA levels in ACLF have been linked to inflammation and liver damage, indicating potential alterations in sialylation and increased immunological activity.[16,19–21]

Therefore, monitoring the levels of these small-molecule biomarkers could offer insights into the extent of liver damage and ACLF stage, significantly aiding in early diagnosis and prognosis, severity assessment, and the guidance of targeted treatment strategies.[8,10] Nevertheless, (bio)sensing small molecules is a complex task that poses various challenges related to analytical performance, selectivity towards structurally similar or co-occurring molecules, stability in complex media, and consistency in batch-to-batch (bio)receptor synthesis. Traditional biorecognition elements, such as antibodies, enzymes, and nucleic acids, encounter difficulties in effectively detecting small molecules due to several reasons, including but not limited to (i) potential lack of epitopes or functional groups for strong binding; (ii) non-immunogenic or toxic nature, relying on carrier proteins, a.k.a. haptens, to activate the animal model's immune system and trigger antibody generation. Moreover, antibodies synthesized using a hapten may exhibit lower binding performance compared to the unconjugated target, compromising desired applications and potentially leading to false-positive or false-negative results. Additionally, enzymes and antibodies can be further influenced by their surrounding environment. To overcome these obstacles, novel molecular tools have been studied.[22–26]

1.2. From Sensing to Biosensing

Before discussing humanity's advancement in the constant pursuit of selectivity in detection and quantification methods, it is important to emphasize the progression from sensing to biosensing technologies. Early humans relied on chemical processes and visual observations to detect poisons and predict weather patterns. These "simple" sensing methods laid the historical foundations for the concepts of sensing and biosensing, as observed in Figure 1.2.

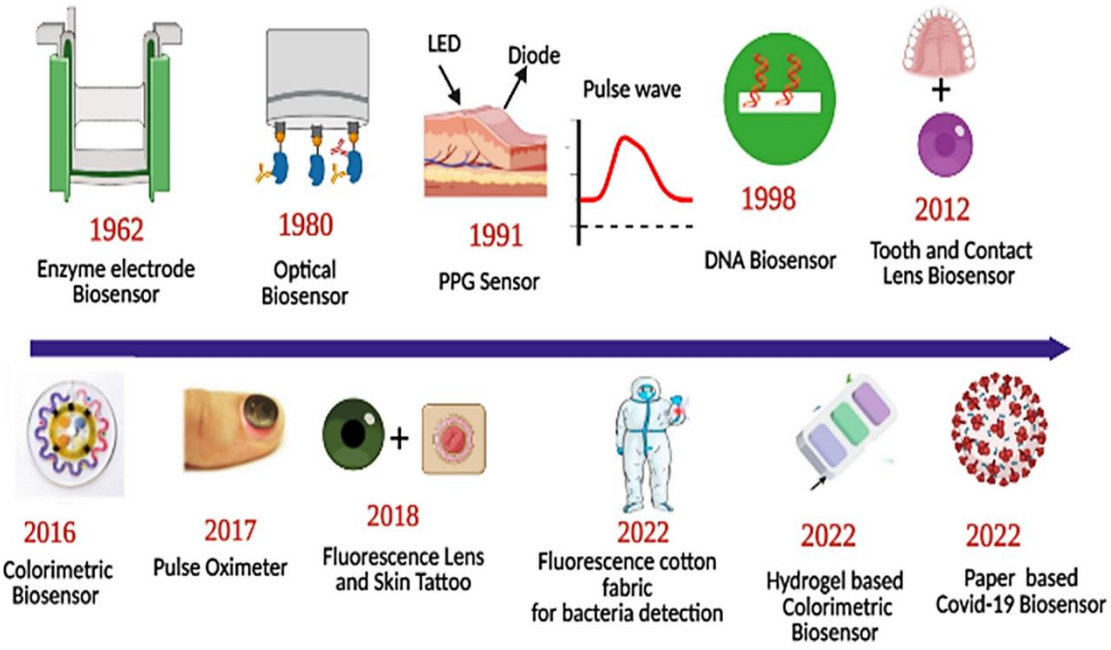


Figure 1.2. *Historical timeline of the discovery of various sensors and their development with respect to materials (green), sensor technologies (blue). Retrieved from* [27]

A significant advancement occurred with Galileo's invention of the Galilean thermometer in the 16th century, introducing the concept of quantifiable measurements. Later, in the early 20th century, more sophisticated equipment was developed by Prof. Arnold Orville Beckman, including but not limited to the spectrophotometer and pH meter, enabling more precise chemical analyses. Furthermore, the discovery of glucose oxidase (GOx) in 1928 was a significant milestone in biosensing.[28] Nevertheless, Clark and Lyons's groundbreaking work in 1962 truly marked the transition from traditional sensing to biosensing, as it attempted to incorporate or mimic binding mechanisms found in nature.[29] Their development of the first glucose biosensor, which combined an enzymatic activity with electrical transduction systems, provided high specificity and sensitivity, paving the way for developing a plethora of (bio)sensors.

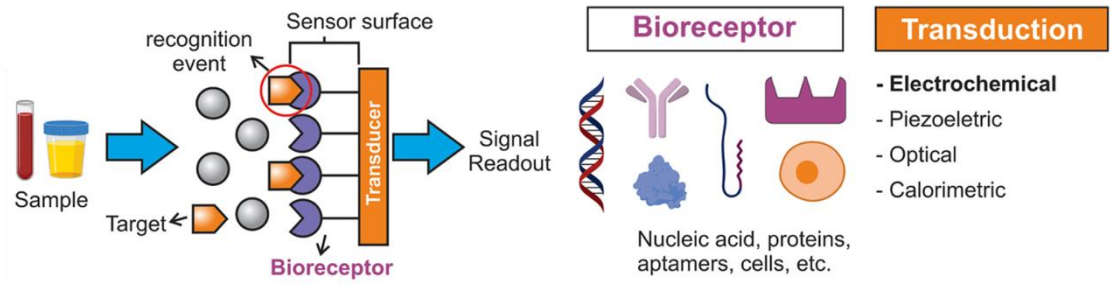


Figure 1.3. *Schematic representation of biosensing principle, showing the typical components of a biosensor. Retrieved from* [30]

IUPAC defines biosensors as devices that use specific biochemical reactions facilitated by biologically derived receptors (enzymes, antibodies, tissues, organelles, or whole cells) to detect compounds using transduction strategies, including electrochemical, thermal, optical, and mass-based (Figure 1.3). Conversely, chemical sensors convert chemical information into a quantifiable signal from single- to multi-target analysis. Both sensors have two primary components connected in series: a receptor and a transducer. In chemical sensors, the receptor is of chemical (molecular) nature; while in biosensors, the receptor is biological or biologically derived. [31,32]

The ASSURED criteria (Affordability, Sensitivity, Specificity, User friendliness, Rapid and robust, Equipment-free, Deliverable to end-users) were established by the World Health Organization (WHO) in 2003 to provide guidance for treatment and clinical management decisions. These criteria are widely acknowledged as the gold standard for ideal point-of-care testing (POCT) and can be effectively utilized by healthcare providers at all levels, particularly in the developing world.[33] Land et al. (2019) have introduced two new criteria, R (real-time connectivity) and E (ease of specimen collection and environmental friendliness), to supplement the original ASSURED criteria. This has resulted in the creation of a new acronym, REASSURED. [34]

1.3. Bioreceptors in Biosensing Technology

The effectiveness of biosensing technologies mainly relies on (bio)receptors specifically detecting analytes either qualitatively or quantitatively. These (bio)receptors —namely antibodies, enzymes, nucleic acids (NA), peptides, cells, or synthetic receptors like molecularly imprinted polymers (MIPs) and other supramolecular systems (Figure 1.4)— selectively bind to target molecules through various noncovalent interactions such as electrostatic forces, hydrogen bonding, and van der Waals interactions, among others.[26,35–37]

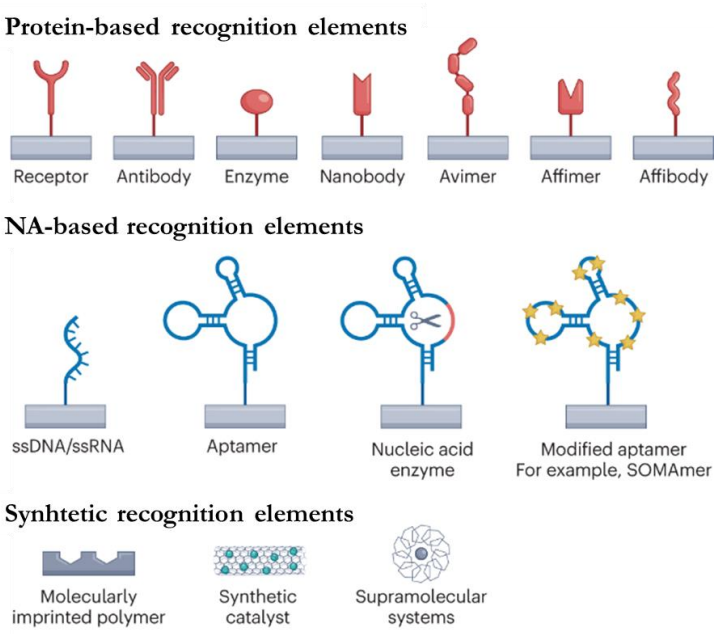


Figure 1.4. *Schematic representation of available recognition elements, including both traditional and synthetic receptors. Retrieved from* [35]

1.3.1. Traditional Bioreceptors

1.3.1.1. Antibodies

Antibodies (Ab), such as immunoglobulin G (IgG), are Y-shaped glycoproteins comprised of two disulfide-bonded heavy chains and two light chains. They contain a variable region, Fab, for antigen (Ag) binding and a constant region, Fc, as observed in Figure 1.5. The chemical nature of the Fab region enables the specific identification of a diverse range of antigens due to its molecular diversity. [37,38]

Antibody production involves the immunization of laboratory animal models, such as goats, rabbits, or mice, with antigens of interest in order to stimulate B cells and antibody generation. Polyclonal antibodies (pAbs), a combination of antibodies recognizing several antigen epitopes, are obtained from the anti-serum of an inoculated animal within weeks. Unlike pAbs, monoclonal antibodies (mAbs) are produced using the hybridoma technique, which involves fusing the inoculated animal's spleen cells with myeloma cells and cloning these hybrid cells capable of continuously producing a specific type of antibodies. Although they have high specificity and sensitivity, their fabrication process can take up to several weeks or months. Furthermore, recombinant antibodies are a more modern approach to antibody development. The genetic sequences of antibodies' heavy and light chains can be extracted from B cells or plasma cells of immunized animals and then replicated in a laboratory setting to yield recombinant antibodies, which are essentially monoclonal.[23,39] Distinct from those generated with hybridomas, antibodies produced using recombinant vectors involve introducing such vectors into host cells, such as E. coli. This recombinant methodology

minimizes batch-to-batch variability by mitigating genetic drift, which may otherwise induce disparities in monoclonal antibodies. [23,39–42]

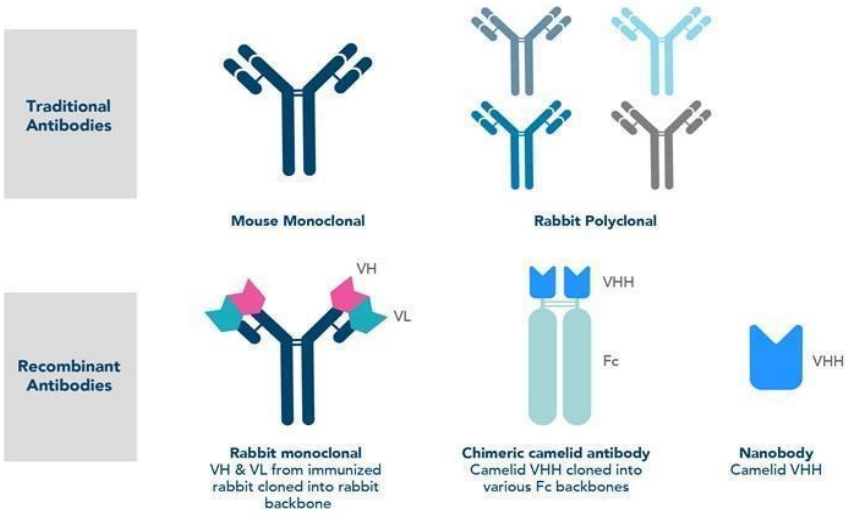


***Figure 1.5**. Schematic representation of the general structure of traditional and recombinant antibodies.*

Over the past two decades, there has been a noticeable shift towards using recombinant antibody libraries over animal-derived hybridomas for commercial antibody production. This shift is driven by the potential benefits of in vitro libraries, such as (i) improved product consistency, (ii) flexibility in modifying binding kinetics through stringent selection conditions, (iii) expanded targeting capabilities across a broader range of compounds, and (iv) reduced reliance on animals. Due to their exceptional performance, antibodies are considered the "gold standard" bioreceptor in biosensing applications, particularly in immunoassays such as Enzyme-Linked ImmunoSorbent Assays (ELISAs),[43,44] and Lateral Flow Assays (LFA).[45–47] Immobilizing antibodies on sensor surfaces further facilitates capturing the analyte from complex samples, and a resulting measurable signal could be obtained when coupled with several transduction mechanisms.[41,48,49]

1.3.1.2. Enzymes

Enzymes (E) are comprised of amino acid chains folded into complex three-dimensional structures forming active sites where substrates (S) selectively bind and are rapidly catalyzed into products (P). Two predominant models, the "lock-and-key" and the "induced fit" models, are potential explanations for enzyme-substrate specificity. Emil Fischer initially proposed the "lock-and-key" model in 1894, emphasizing the specific nature of enzymes and their geometric complementarity to the substrate. [50,51] However, the stabilization of enzymes' transition states is not considered by this theory. On the other hand, the "induced fit" model, introduced by Daniel Koshland in 1958, posits that the enzyme's active site undergoes continuous adjustments until the substrate is fully bound. At this point, the final shape and charge are determined. [52,53]

These bioreceptors play a crucial role in various natural processes, although it is important to note that the repeatability and performance of biosensors can be compromised if the enzymes used are unstable or strongly sensitive to environmental factors. Nevertheless, immobilizing enzymes — via physical adsorption, covalent binding, or entrapment in polymeric matrices — onto sensor surfaces stabilizes enzymatic activity and builds the foundation of enzymatic biosensors. [54,55] The most widely used enzymatic biosensor is the glucometer. There have been many generations of glucose sensors, but most use enzymes as bioreceptors. One example of how glucose sensors work is depicted in Figure 1.6, where immobilized GOx catalyzes the oxidation of β-D-glucose, producing gluconolactone and hydrogen peroxide, which can be monitored electrochemically.[54,56] The effectiveness of this approach has paved the way for the development of various types of enzymatic platforms for a variety of analytes.

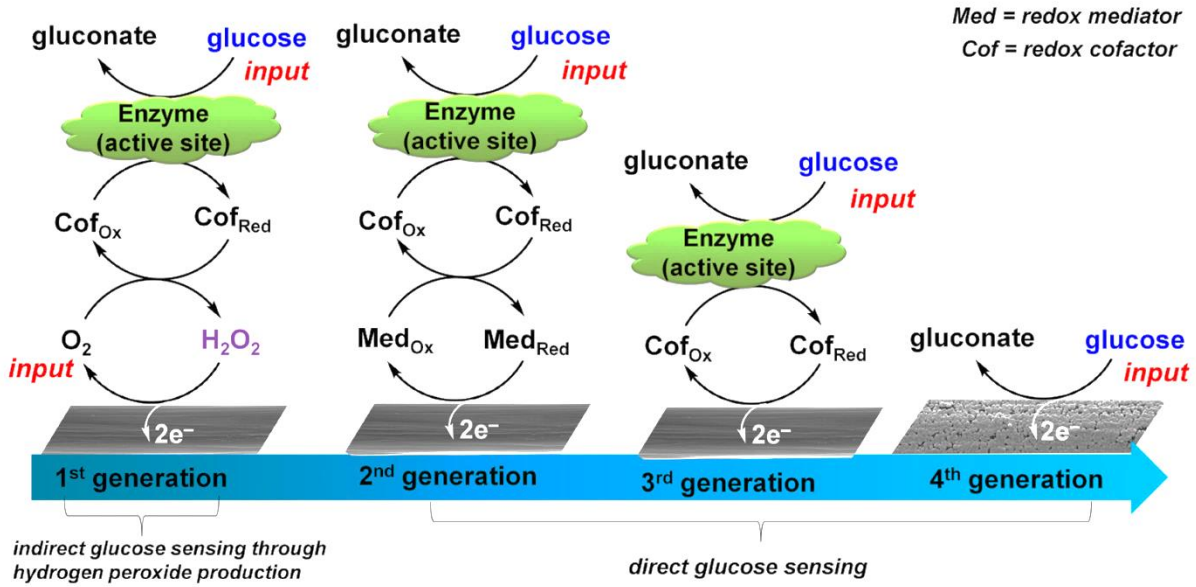


***Figure 1.6**. Evolution of enzymatic biosensing from indirect to direct substrate detection. Retrieved from* [57]

1.3.1.3. Nucleic acid sensors

DNA-based biosensors, also known as genosensors or DNA sensors, allow the examination of genomic or genetic information in various samples, including patient samples or sequences for pathogen invasion. The capability of DNA sensors to provide sequence-specific information is fundamental across various fields, especially in the scrutiny of food, environmental, and clinical samples, as evidenced during the COVID-19 pandemic (Figure 1.7).[58,59].

The fundamental principle of DNA sensor detection is the specific hybridization property between NA strands, which is widely utilized in diagnostic laboratories primarily due to its simplicity and is often preferred over the direct sequencing method. [58,60] The sensitivity of the measurement depends on factors such as the efficiency of sequence hybridization, the level of background signal, and the methods employed

for sequence amplification, such as polymerase chain reaction (PCR). Various factors can influence biosensing specificity, such as reaction temperature, ionic strength, the presence of nanomaterials, and specific components in a PCR mixture.

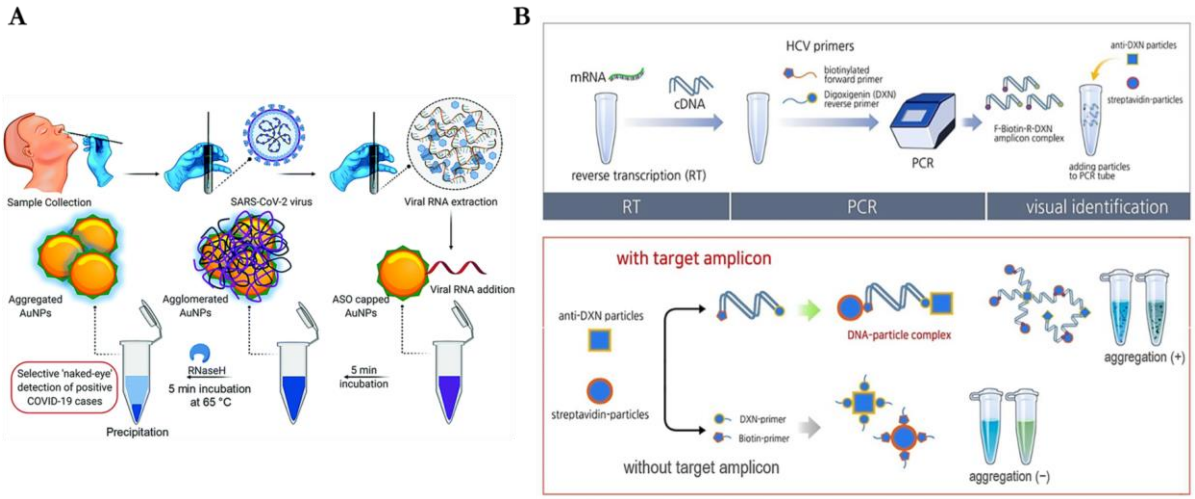


Figure 1.7. *Examples of nanoparticle-based NA optical biosensors for (A) SARS-CoV-2 viral RNA detection. Retrieved from* [59]*; (B) Hepatitis C viral RNA detection. Retrieved from* [58]

1.3.2. Synthetic Receptors

1.3.2.1. Molecularly Imprinted Polymers

Molecular imprinting of small-molecule targets, proposed by Polyakov in 1930, represents a remarkable achievement in molecular recognition as they are inspired by the binding mechanisms present in biological systems, such as E-S and Ab-Ag interaction. [22,61–63] MIPs can be classified into 2 approaches: (i) covalent approach, proposed by Wulff and colleagues in 1977;[64] and (ii) noncovalent approach, proposed by the Mosbach group in 1991[65–67] (which is the approach selected in this thesis). As depicted in Figure 1.8, these polymers are supramolecular systems whose functional monomers and crosslinkers interact with target molecules through multiple noncovalent interactions. During their synthesis, the target molecule serves as a template, guiding the polymerization of the monomers and cross-linkers. Upon completion of the polymerization, the template is removed, leaving cavities that closely mimic the target's physicochemical properties, such as size, shape, and functional group orientation/distribution.[68–70]

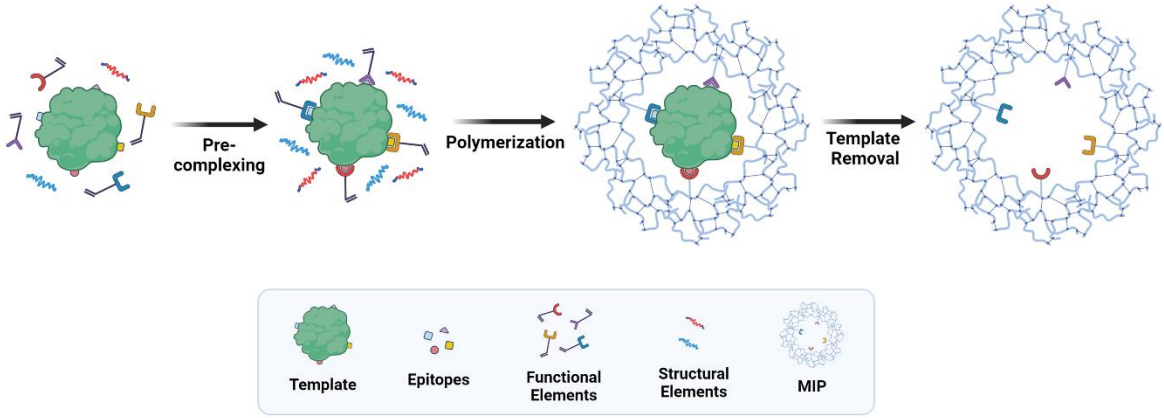


***Figure 1.8**. Schematic representation of MIPs fabrication, from pre-complex formation to target elution and subsequent cavity generation. Image generated using Biorender*

The tailored noncovalent interactions within MIPs' cavities play a pivotal role in their target affinity, ensuring that the binding sites within the polymer matrix exhibit exceptional selectivity for the target molecule, even in the presence of complex sample matrices or co-occurring molecules.

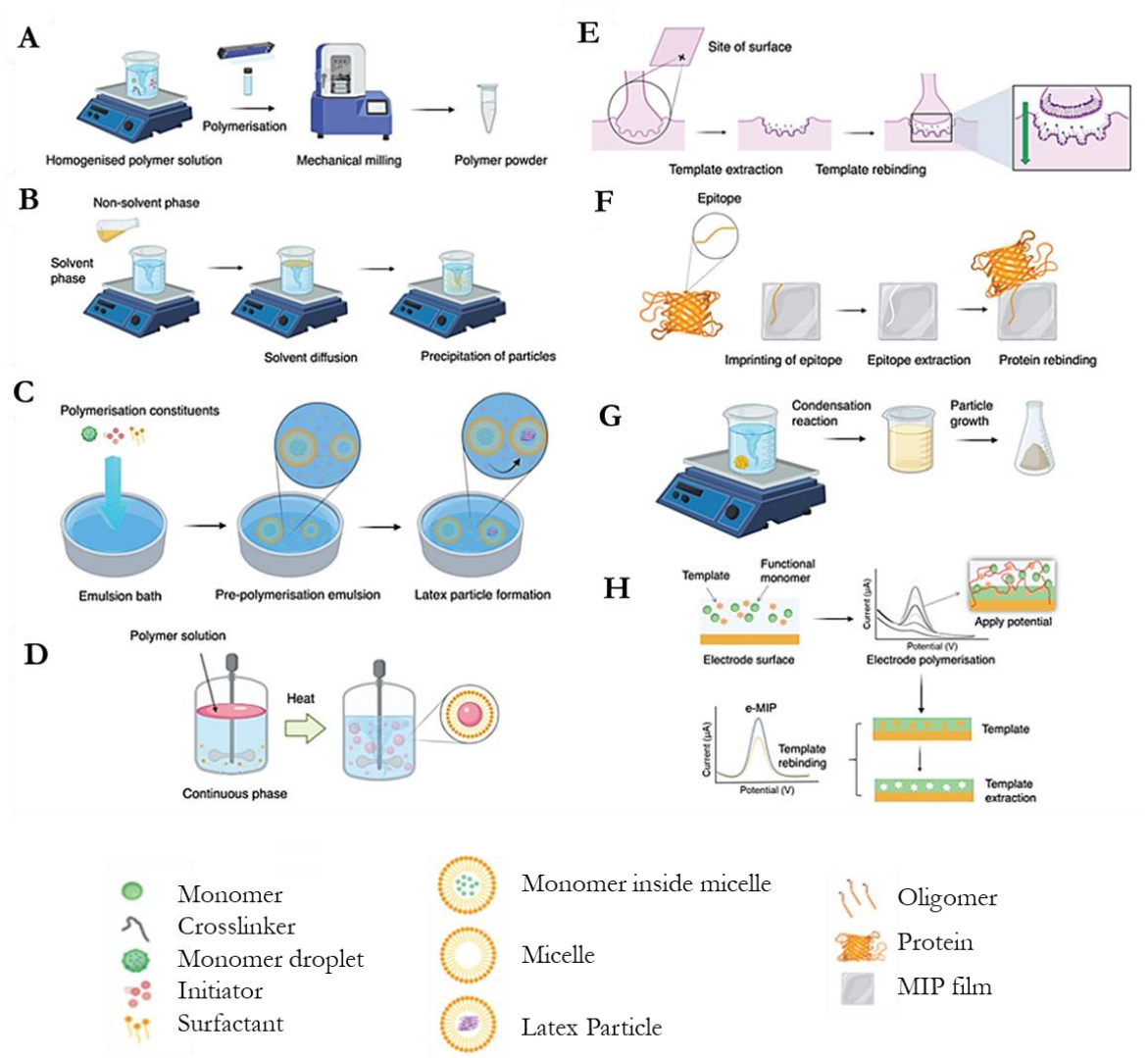


Figure 1.9. *Schematic representation of a range of different polymerisation techniques including: (a) bulk, (b) precipitation, (c) emulsion, (d) suspension, (e) surface, (f) epitope, (g) sol–gel, (h) electropolymerisation, and (i) legend for each technique. Retrieved from* [71]

Several fabrication methods for obtaining MIPs are shown in Figure 1.9, including but not limited to: sol-gel processes, emulsion, and precipitation polymerization.[71] These have all been shown to generate uniform particle sizes and decent target accessibility. As always, these methods have advantages and disadvantages (as seen in Table 1.1), and some challenges that need to be addressed when developing MIPs are (i) high binding site heterogeneity due to the highly "polyclonal" nature; (ii) an abundance of non-templated polymer, i.e. polymer lacking specific binding sites; (iii) the presence of residual template in the MIP; and (iv) the non-standard or labor-intensive procedures necessary for their production.[25,72–75]

Table 1.1. *Advantages and disadvantages of different nanoMIPs fabrication techniques. Adapted from* [75]

	Procedure	Advantages	Drawbacks
Bulk	• Use of organic solvents to obtain a • Block is then grounded and sieved	• Simple method	• Wide particle size distribution • Heterogeneity of active sites
Precipitation	• Polymer chains grow in a solution • Precipitation due to size-related insolubility	• Easy and fast with high yields • Low quantity of reagents required	• Low concentration of monomers may impair recognition events
Emulsion	• Use surfactants and high-shear homogenization • Emulsification of the water and organic phase	• Possible to obtain very small NPs (50 nm)	• Surfactants may disrupt the imprinting process • Difficulty to remove surfactants
Core-shell emulsion	• MIP layer deposition onto preformed nanoparticles • Core could be metals, silica, or polymers	• Suitable for large-scale production • High yields	• Surfactants and the aqueous phase may decrease the imprinting effect
Core-shell grafting	• Chemical linkage of MIP to modified nanoparticles with surface double bonds • Use of iniferter	• Excellent control over shell thickness • Sequential shell polymerization	• The shell may be too thin for bulky templates or too thick for small target diffusion.
Living radical	• Controlled growth of polymer chains • Use of nitroxide species, metal-containing, or dithiocarbonyl initiators	• Excellent control over particle size and PD • Useful for thermolabile templates	• Low yield • Catalyst removal needed • Not suitable for photolabile templates
Solid-phase	• Template immobilization onto solid support • High affinity nanoMIPs are collected by a temperature-based elution	• High affinity and selectivity (nano- or picomolar) • High purity with low template contamination • Fully automatable process.	• The template must have functional groups for immobilization. • Typically, one binding site per particle (low binding capacity)

In an attempt to circumvent these limitations, solid-phase polymerization (SPP) was proposed by Canfarotta & Piletsky in 2016, where the target is immobilized onto a solid substrate, and polymerization occurs around the target.[24,76] This allows for the tuning of the target density and availability on the solid surface, leading to high-affinity nanoMIPs with single- or multiple binding sites (Figure 1.10). Nevertheless, small molecules or targets with limited binding interaction sites remain a challenge, other types of noncovalent interactions and conjugation approaches may be more suitable in these cases. Among the different (nano)MIPs fabrication approaches (Figures 1.9 and 1.10), SPP stands out regarding enhanced "monoclonal" orientation and distribution of binding sites in the polymeric matrix. nanoMIPs via SPP exhibit lower binding capacity but faster binding kinetics, as the cavities would be only at the surface of the polymeric matrix. [76–78]

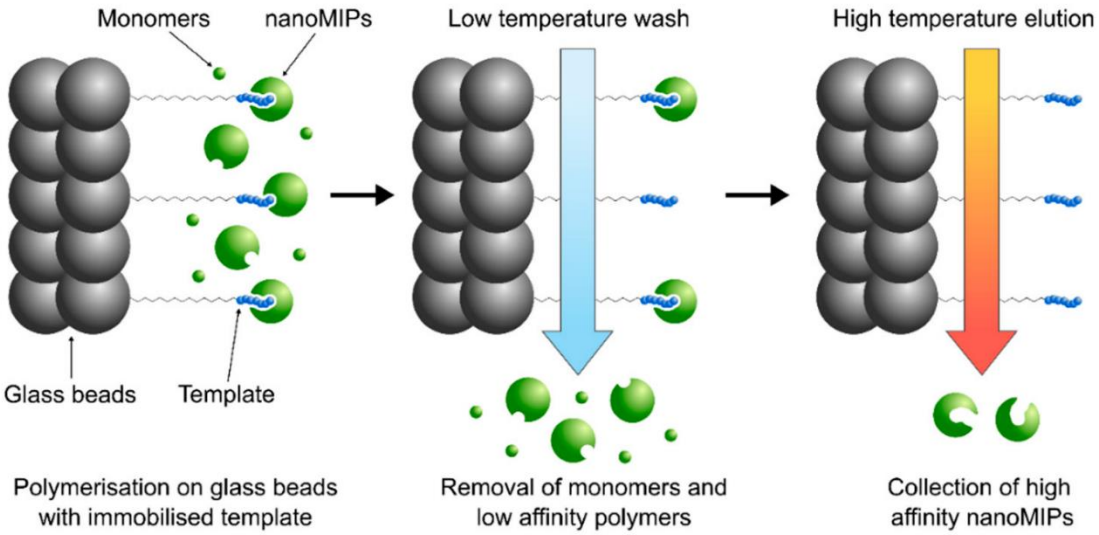


***Figure 1.10**. Schematic representation of nanoMIPs synthesis via SPP. Retrieved from* [79]

1.3.2.2. Aptamers

The development of NA binding in test tubes to interact with a wide range of analytes, beyond just DNA or RNA, has become possible through in vitro selection or systematic evolution of ligands by exponential enrichment (SELEX). This has resulted in creating high-affinity and highly specific binding NAs known as aptamers. The term aptamer is derived from the Latin word "aptus," meaning "to fit," symbolizing the specific and robust aptamer:target interactions, often related to the enzymatic models aforementioned. In recent decades, using aptamers as novel recognition elements in biosensors, known as aptasensors, garnered significant attention among researchers. [80–82]

Aptamers have demonstrated exceptional specificity and sensitivity for binding to various targets, including cells, proteins, whole viruses, tissues, and small molecules. These (bio)receptors fold into unique three-dimensional shapes to form highly robust antibody-like interactions with their target molecules, rendering them a viable alternative to traditional bioreceptors. [83,84]

The SELEX approach, which involves an iterative process of oligonucleotide selection, amplification and purification, is an effective combinatorial strategy for identifying and isolating aptamers with high affinity towards a desired molecule.[85,86] As observed in Figure 1.11, traditional SELEX starts with exposing a vast library pool of randomly generated oligonucleotide sequences to the desired target molecule. The subsequent steps include isolating the target-binding sequences and using the polymerase chain reaction (PCR) to amplify them. These target-binding aptamers are enriched with each selection round, aided by introducing negative and counter-selection steps for discarding sequences interacting with the sample matrix and structurally similar molecules, respectively. These selection steps require adjusting stringency conditions such as the buffer of choice, partition strategy, incubation times, and temperature. [85,87–89]

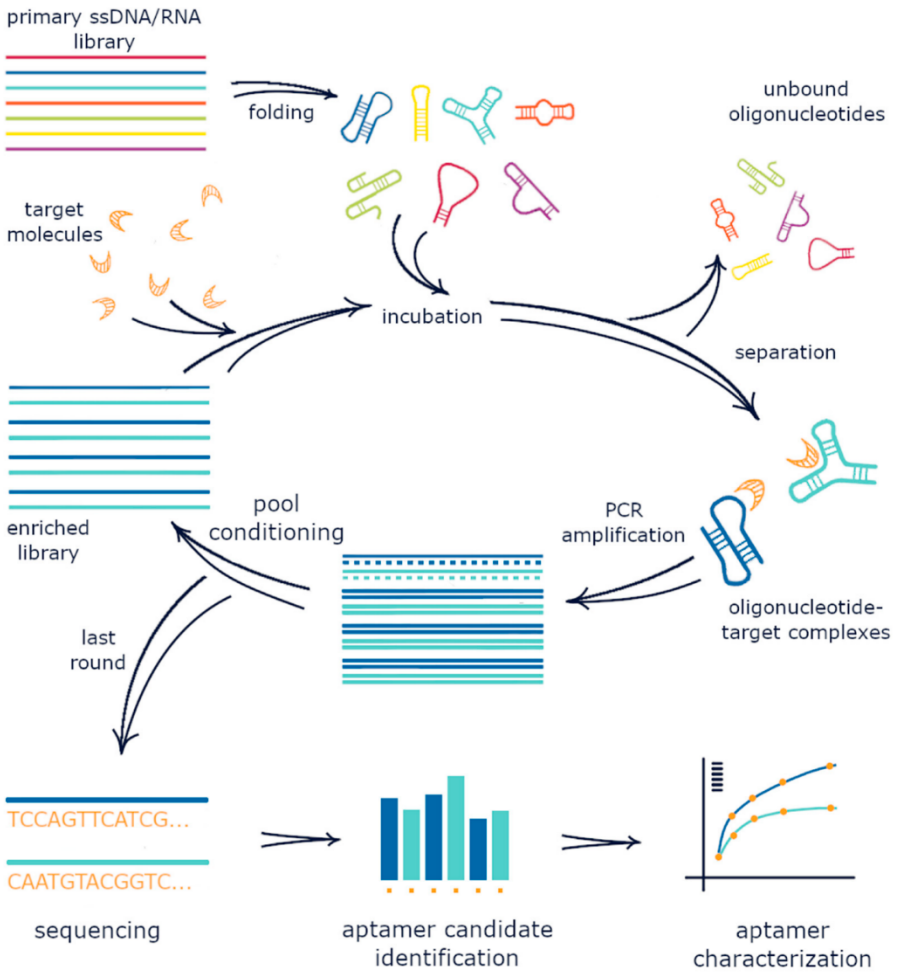


Figure 1.11. *Schematic representation of SELEX workflow for target-conjugated beads or target free in solution. Retrieved from* [85]

Furthermore, Next-Generation Sequencing (NGS) is crucial for identifying and analyzing the aptamer candidates enriched through the SELEX process, as it provides a complete assessment of all potential aptamer candidates. Furthermore, bioinformatics tools are used to analyze the sequencing data in order to predict secondary structures, identify common patterns (or motifs), and cluster the sequences into distinct families. This comprehensive approach is valuable for refining the pool of potential aptamers for further validation in binding assays, where their affinity and specificity are studied. [85,90–92] For instance, Surface Plasmon Resonance (SPR) is employed to assess kinetic parameters and dissociation constants (KD) by monitoring the real-time aptamer:target interactions. Alternatively, colorimetric, chemiluminescence, or fluorescence techniques have been used to investigate aptamer binding performance. [93–95]

There are several SELEX variations that rely on different partition strategies to separate target-bound and unbound sequences. Examples of partitioning approaches include nitrocellulose filters, agarose beads, magnetic beads (used in this thesis), graphene oxide, and electrophoretic mobility, among others.[96–100] Optimal tailoring of the noncovalent interactions during the SELEX process, such as library and primer designs, and modulation of stringency conditions, among others, ensures that the identified aptamers possess suitable binding properties for their intended applications.[85,88,101,102]

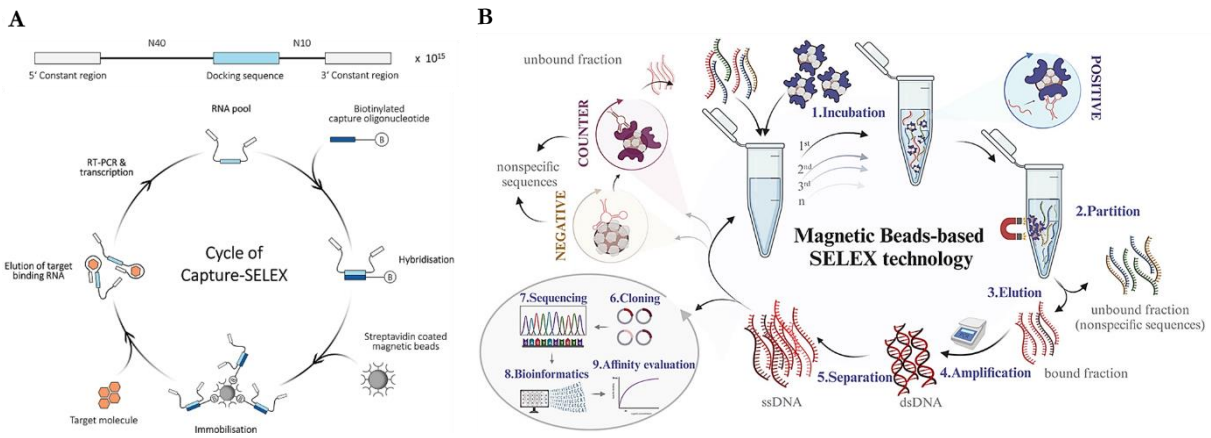


Figure 1.12. *Examples of different types of SELEX. (A) Capture-SELEX. Retrieved from* [103]*; (B) MB-SELEX. Retrieved from* [9589]*.*

1.3.3. The Role of Noncovalent Interactions

As stated before, molecular recognition processes typically rely on noncovalent interactions, which are crucial in biosensing systems. These interactions encompass various forces, such as van der Waals forces, electrostatic interactions, π-π stacking, and hydrogen bonding. The size and diversity of the target analytes can pose significant hurdles when detecting small molecules, as these often have limited binding areas, unlike macromolecules like proteins and NAs. It may be advantageous to optimize the fabrication conditions of MIPs and aptamers in such a way that they promote interactions complementary to the properties of the target analyte. This approach could potentially lead to the development of highly robust binding complexes, addressing some of the challenges highlighted in earlier sections.[104,105]

The extent to which a (bio)receptor binds to its target is influenced by these interactions' nature, strength, quantity, and physicochemical conditions. This is encompassed in the Gibbs free energy (ΔG), where lower dissociation constant (KD) values typically suggest more specific and robust binding. This highlights the necessity to harness these interactions in biosensing technologies. [106]

Regarding MIPs, the initial and most crucial step is selecting the appropriate functional monomers and cross-linkers to form the polymer matrix around the target molecule. For effective imprinting, the monomers must establish stable interactions with the target.[107] Computational modeling and molecular dynamics simulations can be employed to predict the optimal monomer combinations and 3-D spatial arrangements to enhance binding affinities. Furthermore, refining the polymerization parameters, including the ratio of polymerizing components, solvent selection, and temperature, can lead to high-affinity binding sites.[108–110] Post-synthesis procedures, including washing and conditioning methods, are vital for removing weakly attached template molecules and/or unreacted monomers and oligomers, resulting in enhancements in imprinting fidelity.

Similarly, tailoring the SELEX conditions could optimize aptamer:target interactions in aptamer selection. During selection rounds, carefully controlling parameters, such as ionic strength, pH, target concentrations, buffer's chemical nature, temperature, and even the presence of structurally similar or co-occurring molecules, promotes and potentially refines aptamer:target interactions. [88,98] Additional features can be introduced via post-SELEX modifications of the aptamer, such as truncation or incorporation of modified nucleotides, further improving binding strength and specificity. [111]

The strength and nature of these interactions determine the binding affinity and selectivity of molecular recognition elements, both natural and synthetic. Ultimately, biosensing technologies rely on their ability to selectively detect the target molecule among numerous other compounds in buffer conditions, initially, and subsequent adaptations for more complex biological or environmental matrices. [25,40,69]

1.4. Integration of Transducers with MIPs and Aptamers

The synergistic integration of bioreceptors with transducers is crucial in developing effective biosensing devices. Transducers convert biorecognition events into quantifiable signals, including but not limited to electrochemical, optical, thermal, or piezoelectric outputs. Considering several parameters is necessary to achieve optimal performance in integrating bioreceptors with transducers. For instance, if the immobilization approach is employed, bioreceptors tethered onto the transducer surface should maintain their biological activity and orientation to ensure efficient target binding. Furthermore, the selection of transducer technology should align with the bioreceptor's characteristics and intended use. For example, optical transducers are often used in immunosensors and genosensors.[112,113] Similarly, electrochemical transducers are commonly used with enzymes for their capacity to generate measurable signals via catalytic processes. [114–118]

1.4.1. Optical

The use of optical transducers is of great relevance in biosensing. These methods have proven to be invaluable in the field of colorimetric LFA, as can be observed in Figure 1.13.

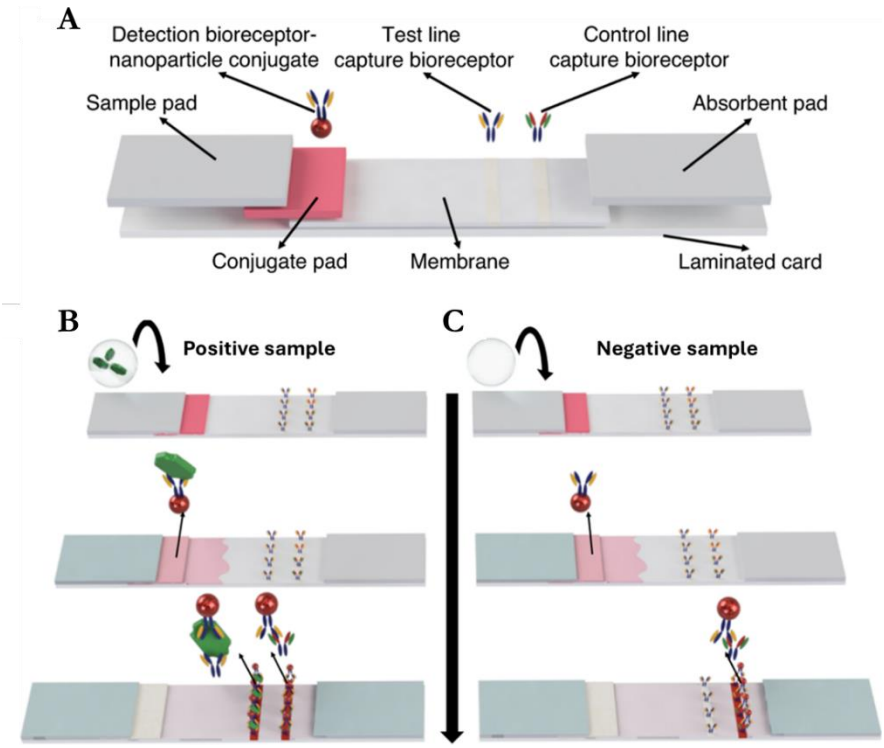


Figure 1.13. *Schematic representation of (A) a LFA; (B) Immunosandwich recognition in (B) presence and (C) absence of the target molecule. Retrieved from* [45]

SPR biosensors are widely favored due to their ability to perform the label-free detection of binding events, as they measure changes in the refractive index near the surface as target molecules bind to bioreceptors on a metal surface (typically gold). [119–121] Additionally, fluorescence-based sensors enable the quantitative measurement of binding events via fluorescence intensity or wavelength shifts. Another method, Fluorescence Resonance Energy Transfer (FRET), can sensitively detect molecular interactions through energy transfer between fluorophores. Furthermore, optical waveguide biosensors offer a reliable platform for detecting small molecules by assessing changes in light propagation via a waveguide upon target attachment. Examples of some aptamer-based sensing technologies are shown in Figure 1.14. [122]

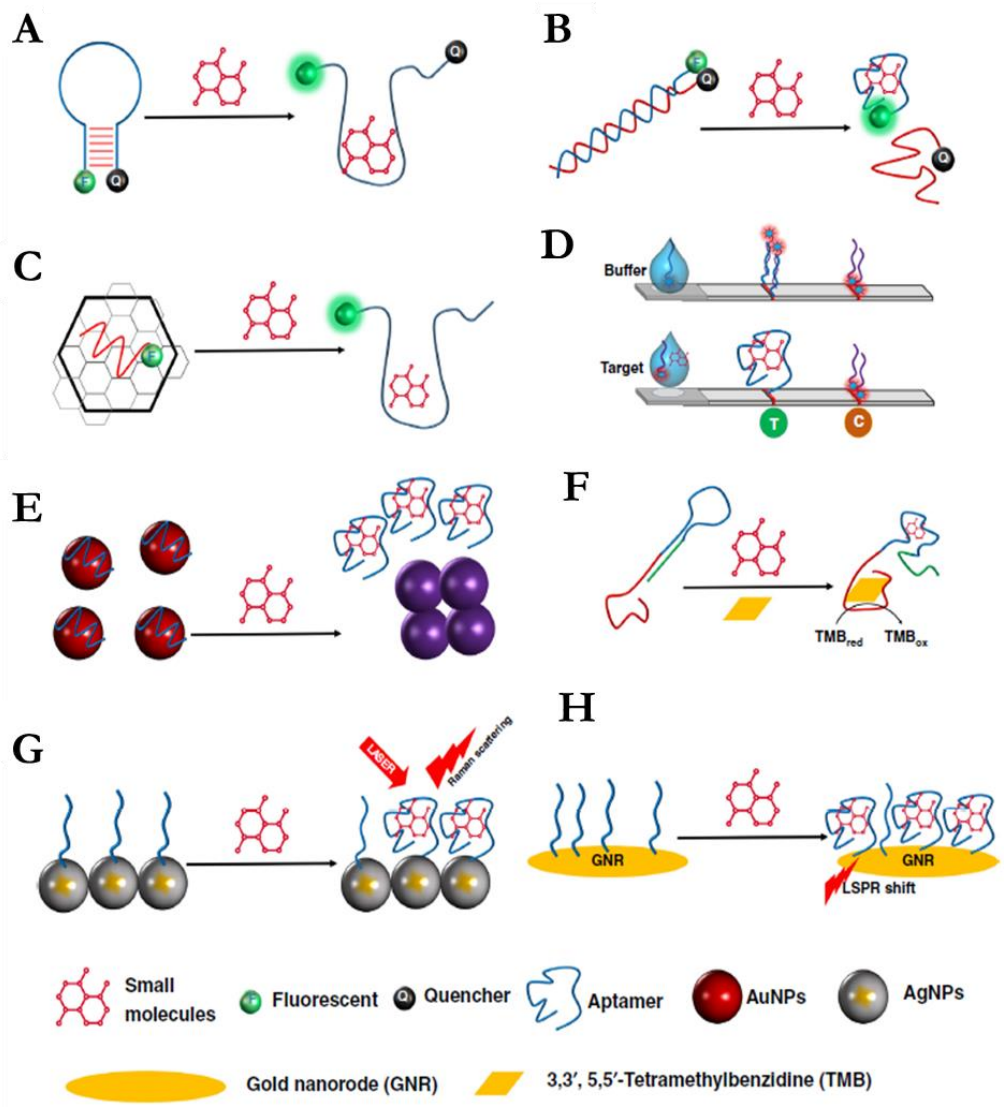


Figure 1.14. *Illustration of detection strategies of optical aptamer-based sensors: (a) Molecular Beacon, (b) complementary sequence, (c) graphene/CNT, (d) LFA, (e) gold-nanoparticle (AuNP) aggregation, (f) DNAzyme, (g) surface-enhanced Raman scattering (SERS), and (h) localized surface plasmon resonance (LSPR) shift. Retrieved from* [122]

1.4.2. Electrochemical

Similarly to their optical counterparts, electrochemical transducers are also compatible with downsizing and on-site analysis. These transducers transform biochemical recognition events into electrical signals, altering an electrochemical cell's impedance, voltage, or current. Electrochemical biosensors offer cost-efficiency and ease of use while providing sensitive quantitative analysis, rendering them highly valuable in various fields such as healthcare, environmental monitoring, and food safety.[122–125]

As depicted in Figure 1.15, electrochemical biosensing relies on essential methods such as electrochemical impedance spectroscopy (EIS), voltammetry, amperometry, and electrochemiluminescence. Voltammetry assesses the current response to a changing applied voltage over

time. Cyclic voltammetry (CV), for instance, is widely employed in electrochemical biosensors for characterization purposes in electrode surfaces and redox-active (bio)receptors or analytes. Furthermore, techniques such as differential pulse voltammetry (DPV) and square wave voltammetry (SWV) have demonstrated success in detecting small molecules, such as dopamine and pesticides, by combining the low KDs of (bio)receptors with the high sensitivity and resolution of these voltammetric methods. These techniques are designed to minimize or eliminate the contribution of capacitive currents' contribution to signal changes and focus solely on faradaic currents, making them more sensitive than voltammetric techniques. [126]

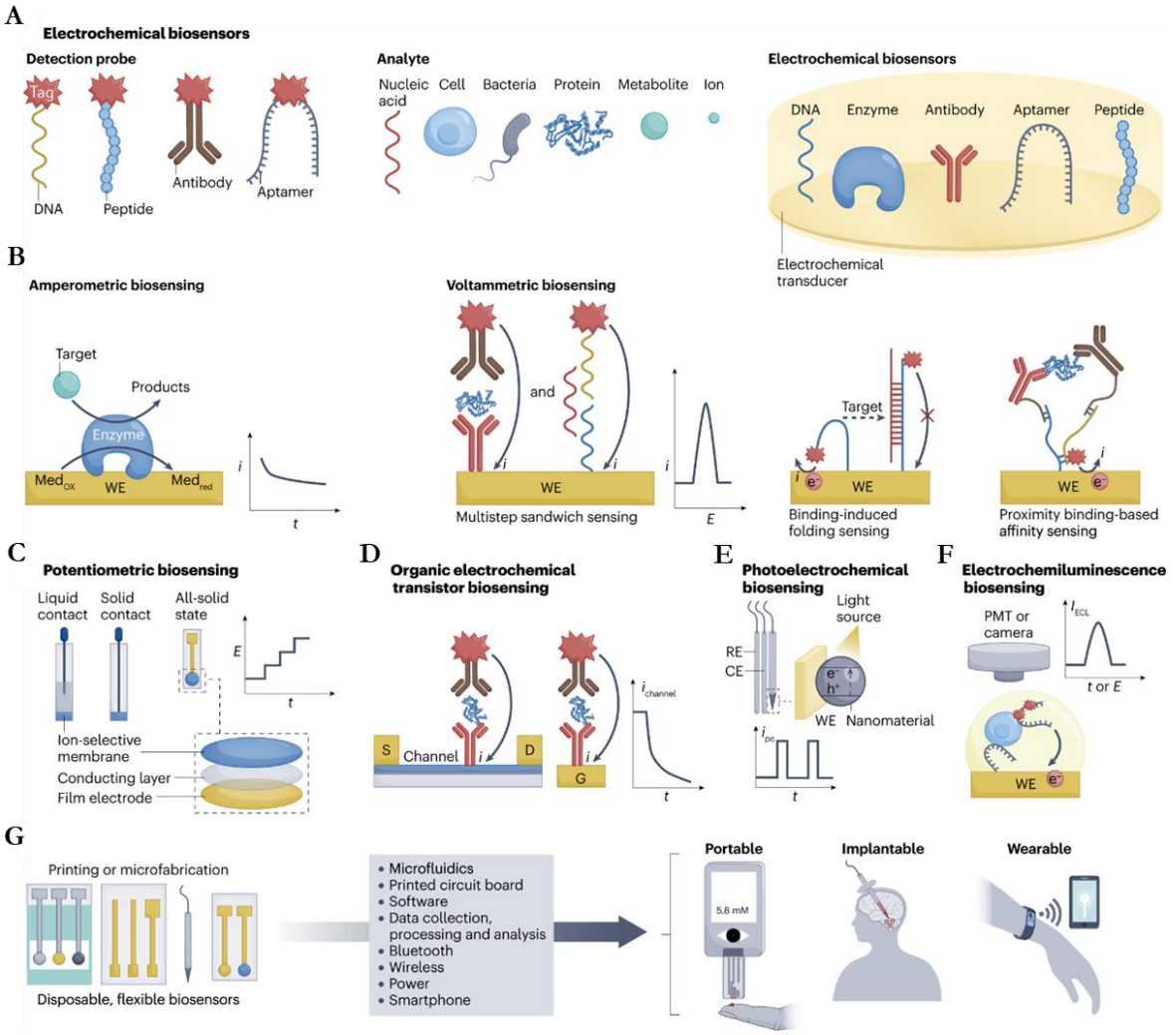


Figure 1.15. *(A) Schematic representation of electrochemical biosensors based on different (bio)receptors and detection probes; (B) Amperometric and voltammetric biosensing; (C) Ion-selective electrodes; (D) Organic electrochemical transistor sensors; (E) Photoelectrochemistry biosensing; (F) Aptamer-based electrochemiluminescence biosensing of cells. (G) Integration of electrochemical biosensors in portable/wearable devices. Retrieved from* [127].

Amperometry, on the other hand, measures the current flow due to a target-induced redox reaction at a constant voltage. The most widely recognized example is glucose biosensors using GOx, which is commonly used for continuous monitoring (Figure 1.6). Aptamer-based amperometric biosensors can

detect proteins, small molecules, and whole pathogens. For instance, aptamer-based thrombin aptamers have demonstrated high specificity and low detection limits, essential for many clinical applications. [121,128]

Another technique to study binding events and interfacial characteristics is EIS, which examines the impedance across various frequencies in the electrochemical cell. This method is particularly suitable for MIPs- and aptamer-based (bio)sensors due to its sensitivity to changes at the electrode surface, either by target-induced conformational change, positioning redox markers closer or further to the electrode surface, or even ionic alterations in the electrode vicinity. EIS has been used to detect analytes such as glucose, cholesterol, and heavy metals, among other small molecules.[125,129,130] Integrating these electrochemical methods with the high affinity and resilience of synthetic receptors can result in robust biosensing systems capable of detecting various small molecule targets in several samples.

1.4.3. Other transduction principles

Besides electrochemical and optical transducers, acoustic transducers, such as quartz crystal microbalance (QCM) and surface acoustic wave (SAW) devices, utilize sound waves to detect biomolecular interactions. QCM sensors measure changes in the resonant frequency of a quartz crystal due to mass variations, while SAW sensors detect alterations in surface acoustic waves caused by analyte binding. These transducers offer high sensitivity and the ability to monitor real-time interactions. [131,132] Based on the piezoelectric effect, piezoelectric transducers detect binding-induced mechanical changes in functionalized surfaces. Microcantilever-based biosensors, for instance, measure deflection or resonance frequency changes in small cantilevers upon target binding, providing label-free detection and real-time monitoring capabilities. [133–135] Thermal transducers detect changes in temperature resulting from biochemical interactions. Components like thermistors and thermocouples are commonly used in thermal transducers, providing precise temperature measurements. Calorimetric sensors measure the heat produced or absorbed, offering insights into the thermodynamics of binding events. [75,136]

When choosing a transduction mechanism, factors including the analyte's nature, desired sensitivity, biosensing response time, and the particular conditions of the type of sample to be used should be carefully evaluated. By harnessing the variety of approaches and considering their advantages and disadvantages, biosensors could be tailored to address the needs of diverse fields, such as medical diagnostics and environmental monitoring.

1.5. Applications and Limitations of MIPs- and Aptamer-based (Bio)sensors

MIPs and aptamers present various advantages over traditional bioreceptors, particularly in detecting small molecules. MIPs have demonstrated remarkable stability in harsh environmental conditions, and their

reversible binding process. However, certain limitations should be considered as challenges may arise in imprinting very small or highly hydrophilic molecules. Aptamers, for instance, also provide consistency in production and batch uniformity due to their chemical nature, eliminating variability in biological manufacturing processes. Nevertheless, the need for stability modification should be addressed, as their high specificity may render them susceptible to degradation by nucleases in biological materials.

As aforementioned, sensitivity is a critical factor in biosensing, particularly when detecting ultra-low concentrations of a small-molecule target within complex biological matrices. Despite the higher stability and antibody-like affinity of these alternative receptors, achieving the required sensitivity can be challenging mainly due to nonspecific binding, depicted in Figure 1.16.

Nonspecific binding has posed challenges in biosensing for several decades, especially in clinical scenarios involving complex biological matrices like blood, urine, or feces. This may lead to (i) false-positive results, (ii) reduced specificity, (iii) increased background noise, and (iv) reduced accuracy, making it difficult to accurately distinguish between true and false signals. This is due to their biological nature, as they typically contain various proteins, salts, and metabolites that can interact nonspecifically with the sensor surface. These interactions can interfere with or compete against target binding, impacting the sensitivity and detection limits of the biosensor, along with hindering reliable and consistent measurements. [137,138] Nonetheless, certain bodily fluids such as urine, sweat, and tears offer the benefit of being externally sampled in a non-invasive manner. In comparison to serum or plasma, their protein content may present a less intricate approach while still providing clinically relevant information, which can be correlated with other bodily fluids.

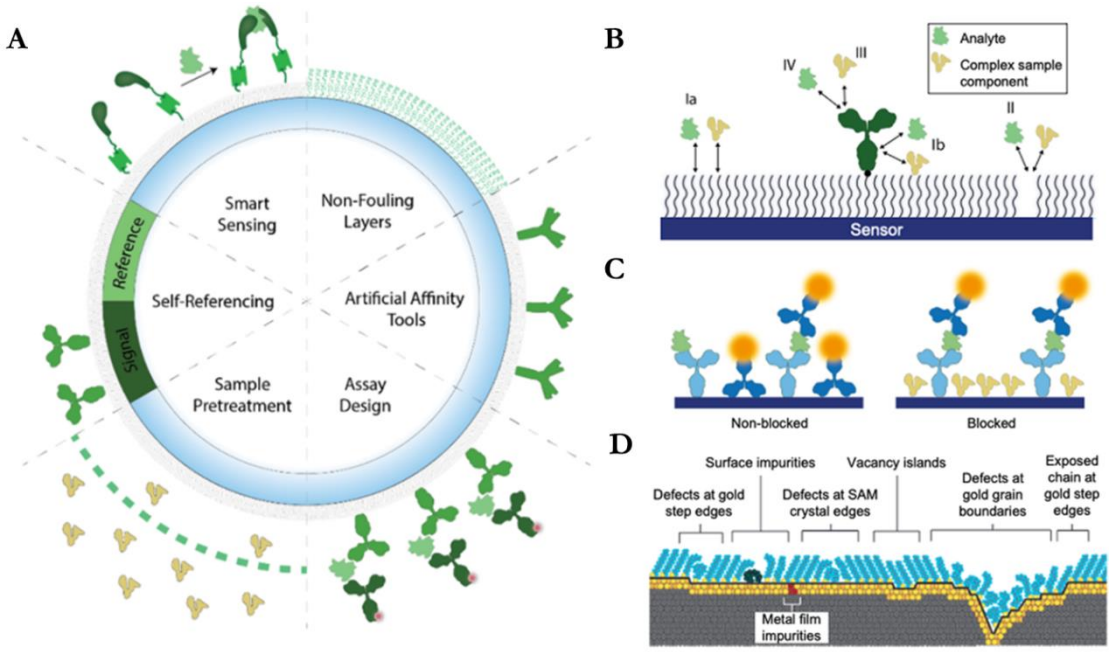


Figure 1.16. *(A) Approaches to minimize nonspecific binding. (B) Different possibilities on a sensor surface: direct binding (I) to the surface (Ia) or to the bioreceptor (Ib), binding to surface defects (II), binding to the bioreceptor's paratope (III), specific binding (IV). (C) Surface blocking to avoid I and II interactions. (D) Different types of surface defects (II) that may induce nonspecific binding. Retrieved from* [138]

Several strategies can be employed to mitigate nonspecific binding. Surface modifications with anti-fouling materials such as polyethylene glycol (PEG) or BSA can create a hydrophilic layer that resists protein adsorption. Using blocking agents like casein or synthetic peptides can occupy nonspecific binding sites, while proper sample preparation techniques such as centrifugation, filtration, and pH adjustment can remove interfering substances.[138–140] Advanced detection techniques, including differential measurements and multi-step washing procedures, can further reduce nonspecific contributions. These approaches are essential to improve biosensing platforms' sensitivity and reliability in clinical diagnostics, particularly for detecting small molecules.

Stability is also a key concern, requiring a deep understanding of supramolecular interactions in polymer synthesis, aptamer selection methods, and the development of practical test formats. MIPs demonstrate exceptional stability and endurance, making them suitable for various scenarios as their specificity can be precisely tailored for specific target molecules using several imprinting procedures.[141] On the other hand, aptamers offer flexibility, simplicity of modification, and tuning control, making them an appealing alternative to traditional antibodies, enzymes, and NA.

Reproducibility is another critical consideration, particularly in the synthesis of MIPs. Consistently producing high-quality MIPs (or nanoMIPs) with homogenous binding sites necessitates careful management of the imprinting process to avoid batch-to-batch discrepancies that could compromise the biosensors' performance. [142,143] Furthermore, enhancing sensitivity by incorporating nanomaterials and signal amplification strategies (Figure 1.17) is crucial to developing more accurate detection platforms.

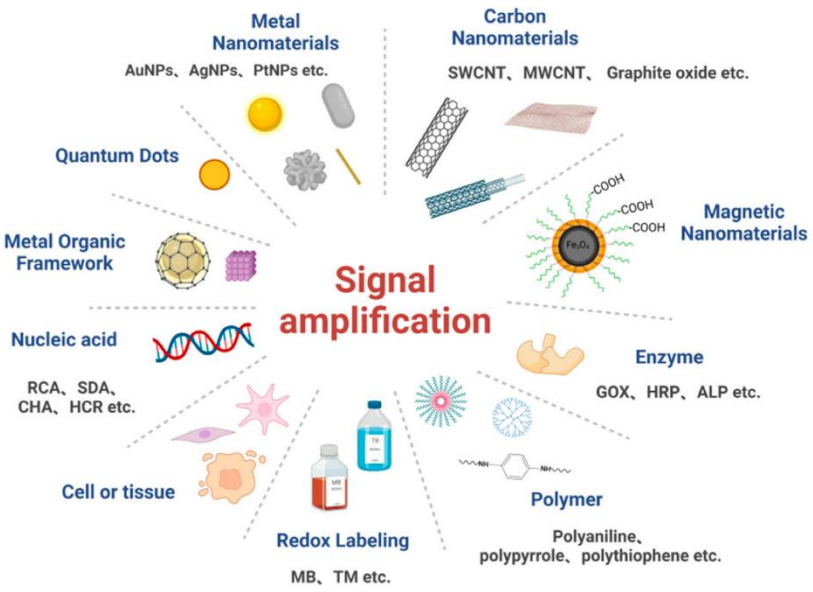


Figure 1.17. *Signal amplification strategies commonly used in biosensing technologies. Retrieved from* [144]

Furthermore, MIPs and aptamers are finding new avenues in biotechnological research, industrial process control, and security. Aptamer-based biosensors have proven particularly valuable in early disease detection and monitoring by identifying metabolites and small-molecule biomarkers, such as estradiol, progesterone, and testosterone, as they are involved in many physiological processes and are relevant biomarkers in cancer diagnostics. [145]

Notable advancements have been made in creating MIP-based sensors capable of identifying biomarkers in various biological fluids[146–149], and initial efforts have been made to commercialize MIP technology for public or private acquisition (MIP Discovery, UK) [150]. In summary, the use of MIPs and aptamers demonstrates great potential for the advancement of next-generation small-molecule biosensing. Their robustness and specificity provide a promising solution to the intricate aforementioned challenges, thereby laying the groundwork for reliable and efficient biosensors with broad relevance and accessibility.

1.5.1. Existing Diagnostic Methods for ACLF

Existing methods such as ELISAs, Mass spectrometry (MS), and High-Performance Liquid Chromatography (HPLC), have proven effective in identifying biomarkers. However, they come with certain drawbacks such as high costs, lengthy processing times, and the requirement for expensive equipment and highly skilled personnel to operate and interpret them. Aptamers and MIPs may present some advantages as diagnostic and prognostic tools for ACLF.[16,151] Additionally, modifications can be made to aptamers to enhance their stability and resistance to nucleases. Moreover, the synthetic nature of aptamer generation eliminates the uncertainties and ethical considerations associated with animal-derived antibodies.

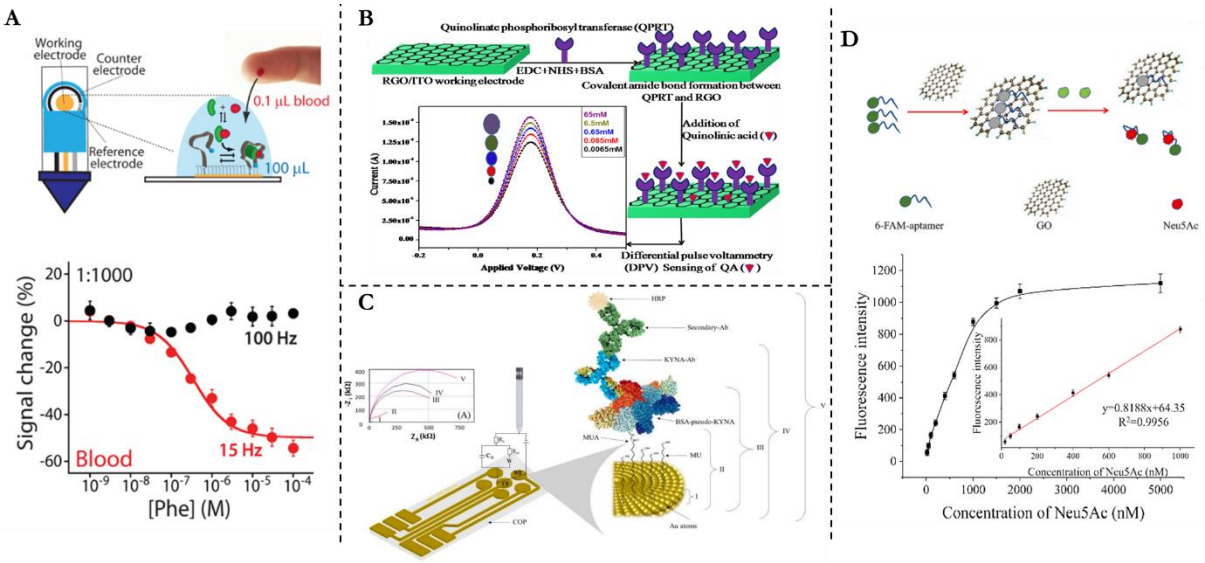


Figure 1.18. *(A) Aptamer-based electrochemical detection of Phenylalanine. Retrieved from [152]; (B) Enzymatic detection of quinolinic acid via RGO/ITO modified electrodes. Retrieved from [153]; (C) Electrochemical immunosensor for the detection of kynurenic acid. Retrieved from [154]; (D) GO-*

enabled detection of N-acetylneuraminic acid (Neu5Ac or NANA) after aptamer isolation via SELEX, along with its fluorescent detection. Retrieved from [100]

Some examples of biosensors for the previously mentioned ACLF-associated biomarkers are shown in Figure 1.18. [100,153,155] Additionally, nanoporous gold electrodes have been functionalized with Neutrophil Gelatinase Associated Lipocalin (NGAL)-specific aptamers for ACLF diagnosis. The electrochemical detection was performed via an affordable smartphone-based platform in both PBS and artificial urine. This method concurrently ensured continuous monitoring of AKI at a POC setting. [156]

Additionally, in a study comparing target- or library-immobilized MB-SELEX against NANA, sequences with high affinity are more effectively enriched employing the latter. [100] Aptamer candidates against NANA were obtained, exhibiting an almost a two-fold enhancement in binding affinities after post-SELEX optimization using rational design and molecular docking simulations for truncation purposes. Consequently, this study suggests that library-immobilized approaches may represent the optimal choice for screening aptamers targeting the small-molecule targets to be investigated in this work (Figure 1.18D).

1.6. Future Perspectives in Biosensing

As aforementioned, the ability to create supramolecular systems exhibiting strong binding affinities has opened the door to biosensors with outstanding performances for detecting ultra-low concentrations of several types of targets, highlighting their contributions to the detection of small molecules. [105,157,158]

The ongoing advancements in the field are expected to enhance the adaptability of aptamer- and MIPs-based (bio)sensing of small molecules in the foreseeable future. Researchers have recently focused on integrating nanomaterials with these synthetic receptors to improve their performance. For instance, a (poly) o-phenylenediamine (o-PD) MIP-based sensors enhanced with gold nanoparticles was developed for glucose detection, reaching nanomolar KDs. [159,160] Similarly, incorporating graphene and carbon nanotubes into these supramolecular systems has resulted in enhanced electronic characteristics, leading to lower LODs and improved signal transduction.

Techniques such as microfluidic-enabled MIP synthesis (either membrane or particle) and high-throughput SELEX (HT-SELEX) enable the rapid development of highly specific receptors. [102,161,162] Furthermore, advancements in MIP manufacturing, including surface imprinting and SPP, result in nanoMIPs with more homogeneously distributed and easily accessible binding sites, thus enhancing their effectiveness in biosensing applications.

Regarding aptamer isolation, HT-SELEX coupled with NGS bioinformatic analysis has significantly contributed to the aptamer screening process by enabling the simultaneous examination of vast nucleic acid libraries. This has accelerated the discovery of high-affinity aptamers for small molecules. For instance, HT-SELEX was employed to produce aptamers against 3 out of 5 small-molecule targets, namely KA, 3-

hydroxykynurenine (3-HK), and xanthurenic acid (XA), with dissociation constants ranging from high nanomolar to low micromolar, as observed in Figure 1.19. [163]

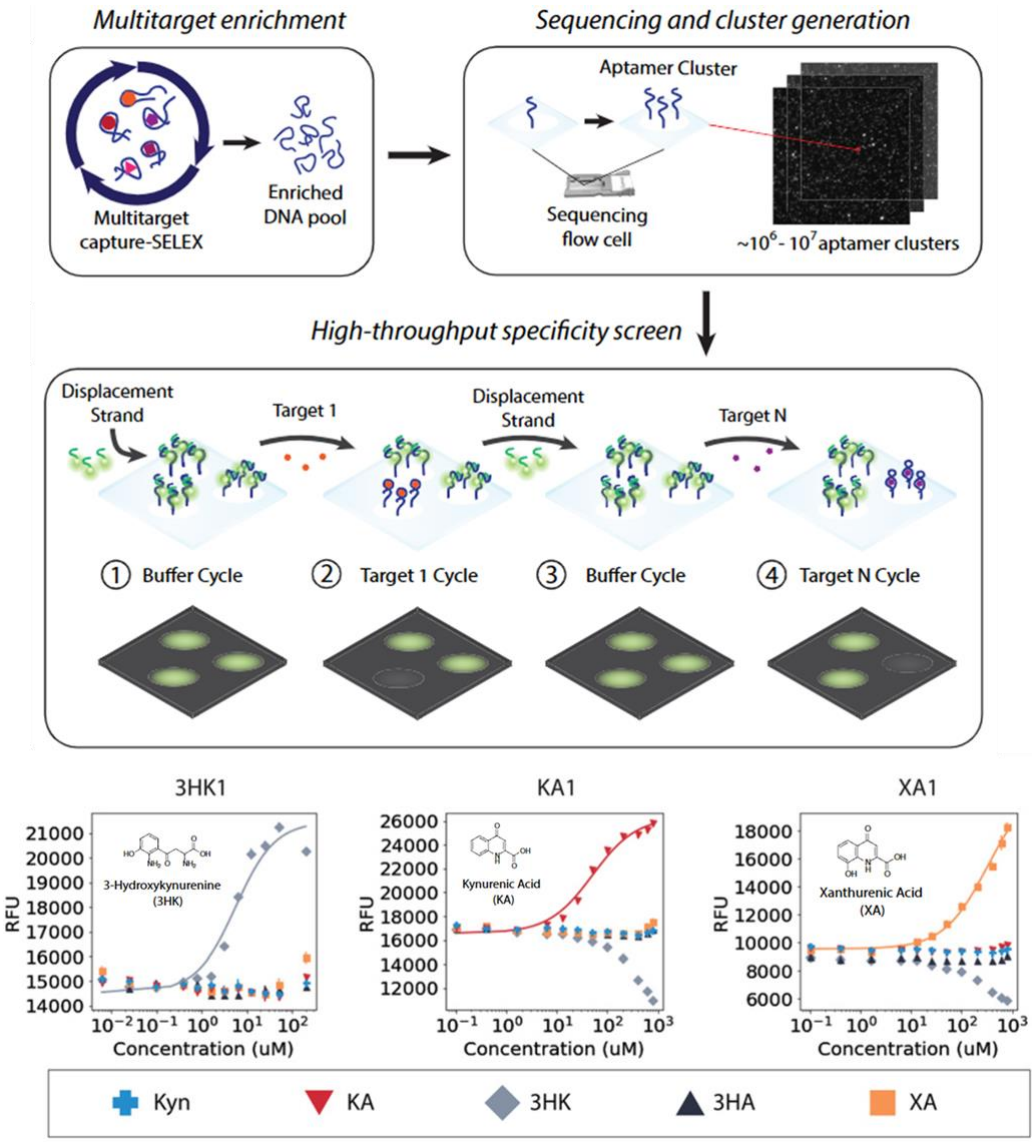


Figure 1.19. *Multi-target Capture-SELEX for isolation of target-specific aptamers for 3HK1, KA and XA. Retrieved from* [163]

These advancements facilitate the integration of biosensing assays into compact, more portable devices, streamlining (i) sample preparation, (ii) biorecognition reaction, and (iii) detection on a single chip. This would improve detection speed and efficiency while minimizing sample volume and reagent use. Such integration holds considerable promise for the advancement of POCT in diagnostics and environmental monitoring technologies that demand on-site analysis. [164–166]

The current landscape shows that while many integrated biosensor devices offer high portability, their sensitivity is often limited as they typically rely on traditional bioreceptor, such as enzymes or antibodies. Conversely, fluorescence-based systems demonstrate excellent sensitivity, albeit impractical for on-site diagnostics due to the need for additional equipment.[167] Meanwhile, electrochemical biosensors have shown

significant sensitivity improvements through advancements in nanomaterials and nanotechnologies. Researchers continue to strive for enhanced capabilities across various platforms. For instance, integrating flexible materials and electrodes into battery-free wireless devices represents a promising development, as depicted in Figure 1.20. When paired with conventional smartphones, these devices have the potential to provide reliable data in real-time, thus paving the way for potential commercialization. [168]

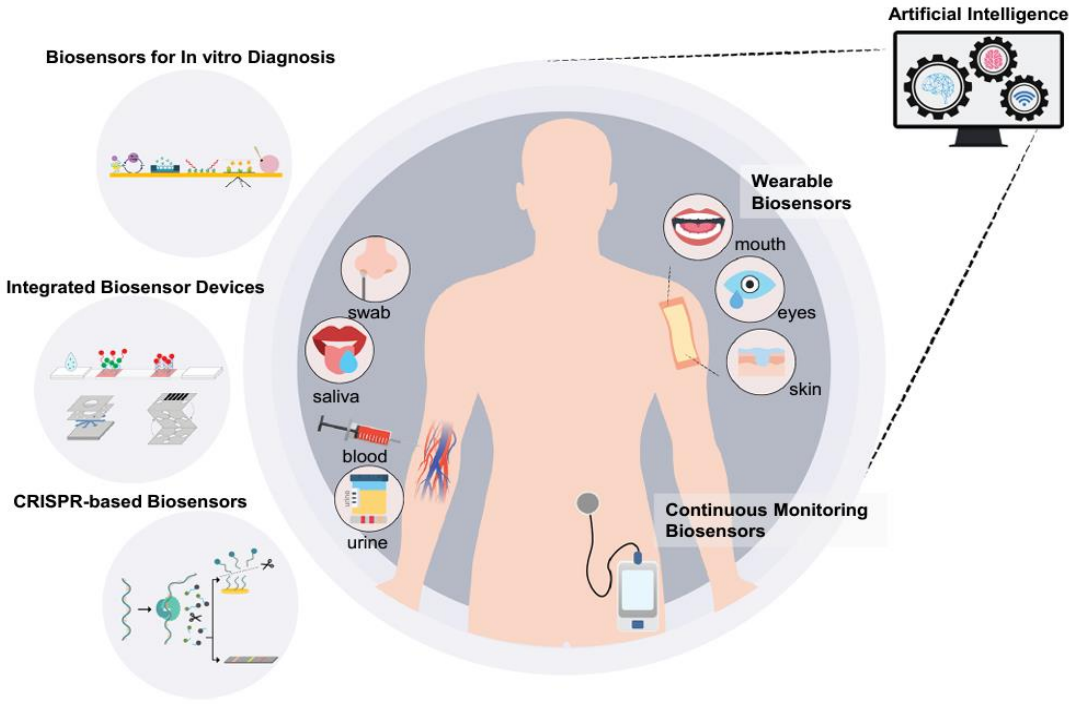


Figure 1.20. *Several types of biosensor for health applications based on their use in in vitro sampling (blood, saliva, urine, etc.), for continuous monitoring, and adaptation to wearable sensing. Retrieved from* [168]

A recent development has arisen, bringing the potential of utilizing artificial intelligence (AI) as a tool for several applications including interpreting the signals generated by biosensors, and aiding in the in-silico design and selection of constituents for highly specific supramolecular structures. [24,105,169] The current state of biosensors and the trend of continuous monitoring indicate that AI-supported biosensors will undoubtedly have a crucial role in the biosensing field, assisting with diverse tasks ranging from initial data analysis utilizing machine learning to the unveiling of new biomarkers.

Nevertheless, several considerations must be considered to enable biosensors to fulfill their potential as sensitive and reliable tools, and subsequently successful transition from the laboratory to clinical settings. Firstly, scalable and standardized manufacturing processes are essential to ensure the batch-to-batch repeatability of these synthetic receptors. Secondly, preserving their stability and performance under diverse physiological conditions is vital to their application in clinical settings. Lastly, maximizing the integration of these (bio)receptors into transducer technologies, coupled with battery-free readout devices with wireless communication protocols, such as Near-Field Communication (NFC), is necessary for real-time on-site detection and monitoring of small-molecule biomarkers. [170,171]

In resource-limited settings, the need for portable and cost-effective biosensing platforms is paramount; thus, these platforms should comply with the REASSURED criteria. [34] Additionally, consideration should be given to long-term storage and stability. One application of electrochemical biosensors is disposable test strips that can be read using a portable reader. For instance, blood glucose test strips often have a long shelf life when stored in dry conditions at room temperature, eliminating the need for a cold chain during shipping or storage.[146,172,173] Owing to integrating electrochemical biosensors in wearable platforms, individuals can now conveniently monitor their health and diagnose illnesses by measuring biomarkers in their homes.

In summary, biosensors not only enable point-of-care testing, leading to improved patient outcomes and expedited decision-making, but they have also revolutionized several fields, such as environmental monitoring, food safety, and security. Their invaluable contributions to science and technology are undeniable, and their ongoing progress promises to further enhance their capacity to tackle diverse analytical problems.

1.7. References

1. Medina Avalos E, Higuera de la Tijera M, Pérez Hernández J, Carmona Castillo M, Teutli Carrión S, Dorantes Nava C, et al. Characteristics of patients with acute over chronic liver failure (ACLF) and risk of mortality due to amount of alcohol, MELD and MELD NA. Ann Hepatol. 2022 Dec 1;27:100817.

2. Chicas López R, Mejía Loza S, García Rodas O, Pinto García L, Sánchez Salinas F, Jaen Villanueva C, et al. Acute-on-chronic liver failure or Alcoholic Hepatitis? In patients with chronic alcoholic liver disease. Ann Hepatol. 2022 Dec;27:100816.

3. Moreau R, Jalan R, Gines P, Pavesi M, Angeli P, Cordoba J, et al. Acute-on-chronic liver failure is a distinct syndrome that develops in patients with acute decompensation of cirrhosis. Gastroenterology. 2013;144(7):1426-37.e9.

4. Asrani SK, Devarbhavi H, Eaton J, Kamath PS. Burden of liver diseases in the world. J Hepatol. 2019 Jan 1;70(1):151–71.

5. Ginés P, Quintero E, Arroyo V, Terés J, Bruguera M, Rimola A, et al. Compensated cirrhosis: natural history and prognostic factors. Hepatology. 1987;7(1):122–8.

6. Hernaez R, Solà E, Moreau R, Ginès P. Acute-on-chronic liver failure: an update. Gut. 2017 Mar 1;66(3):541–53.

7. López-Sánchez GN, Dóminguez-Pérez M, Uribe M, Nuño-Lámbarri N. The fibrogenic process and the unleashing of acute-on-chronic liver failure. Clin Mol Hepatol. 2019 Jan 1;26(1):7–15.

8. Fuentes-Chust C, Parolo C, Rosati G, Rivas L, Perez-Toralla K, Simon S, et al. The Microbiome Meets Nanotechnology: Opportunities and Challenges in Developing New Diagnostic Devices. Adv Mater. 2021 May 1;33(18):2006104.

9. Luo J, Li J, Li P, Liang X, Hassan HM, Moreau R, et al. Acute-on-chronic liver failure: far to go—a review. Crit Care 2023 271. 2023 Jul 1;27(1):1–13.

10. Castelli FA, Rosati G, Moguet C, Fuentes C, Marrugo-Ramírez J, Lefebvre T, et al. Metabolomics for personalized medicine: the input of analytical chemistry from biomarker discovery to point-of-care tests. Vol. 414, Analytical and Bioanalytical Chemistry. Analytical and Bioanalytical Chemistry; 2022. 759–789 p.

11. Clària J, Moreau R, Fenaille F, Amorós A, Junot C, Gronbaek H, et al. Orchestration of Tryptophan-Kynurenine Pathway, Acute Decompensation, and Acute-on-Chronic Liver Failure in Cirrhosis. Hepatology. 2019 Apr 1;69(4):1686–701.

12. Wirthgen E, Hoeflich A, Rebl A, Günther J. Kynurenic Acid: The Janus-faced role of an immunomodulatory tryptophan metabolite and its link to pathological conditions. Front Immunol. 2018 Jan 10;8(JAN):312707.

13. Vondroušová J, Mikoška M, Syslová K, Böhmová A, Tejkalová H, Vacek L, et al. Monitoring of kynurenine pathway metabolites, neurotransmitters and their metabolites in blood plasma and brain tissue of individuals with latent toxoplasmosis. J Pharm Biomed Anal. 2019;170:139–52.

14. Basile AS, Saito K, Al-Mardini H, Record CO, Hughes RD, Harrison P, et al. The relationship between plasma and brain quinolinic acid levels and the severity of hepatic encephalopathy. Gastroenterology. 1995;108(3):818–23.

15. Flieger J, Święch-Zubilewicz A, Śniegocki T, Dolar-Szczasny J, Pizoń M. Determination of tryptophan and its major metabolites in fluid from the anterior chamber of the eye in diabetic patients with cataract by liquid chromotography mass spectrometry (LC-MS/MS). Molecules. 2018;23(11).

16. Liu G, Wang X, Fan X, Luo X. Metabolomics profiles in acute-on-chronic liver failure: Unveiling pathogenesis and predicting progression. Front Pharmacol. 2022 Aug 19;13.

17. Clària J, Arroyo V, Moreau R. Roles of systemic inflammatory and metabolic responses in the pathophysiology of acute-on-chronic liver failure. JHEP Reports. 2023 Sep 1;5(9):100807.

18. Jalan R, D'Amico G, Trebicka J, Moreau R, Angeli P, Arroyo V. New clinical and pathophysiological perspectives defining the trajectory of cirrhosis. J Hepatol. 2021 Jul 1;75:S14–26.

19. Zaccherini G, Aguilar F, Caraceni P, Clària J, Lozano JJ, Fenaille F, et al. Assessing the role of amino acids in systemic inflammation and organ failure in patients with ACLF. J Hepatol. 2021;74:1117–31.

20. Coenraad MJ, Artru F. Amino acids in acute-on-chronic liver failure: Another piece of the puzzle? J Hepatol. 2021 May 1;74(5):1015–7.

21. Moreau R, Clària J, Aguilar F, Fenaille F, Lozano JJ, Junot C, et al. Blood metabolomics uncovers inflammation-associated mitochondrial dysfunction as a potential mechanism underlying ACLF. J Hepatol. 2020 Apr 1;72(4):688–701.

22. Parisi OI, Francomano F, Dattilo M, Patitucci F, Prete S, Amone F, et al. The Evolution of Molecular Recognition: From Antibodies to Molecularly Imprinted Polymers (MIPs) as Artificial Counterpart. J Funct Biomater. 2022;13(1).

23. Gray AC, Sidhu SS, Chandrasekera PC, Hendriksen CFM, Borrebaeck CAK. Animal-Friendly Affinity Reagents: Replacing the Needless in the Haystack. Trends Biotechnol. 2016 Dec 1;34(12):960–9.

24. Cowen T, Stefanucci E, Piletska E, Marrazza G, Canfarotta F, Piletsky SA. Synthetic Mechanism of Molecular Imprinting at the Solid Phase. Macromolecules. 2020;53(4):1435–42.

25. Canfarotta F, Cecchini A, Piletsky S. Nano-sized Molecularly Imprinted Polymers as Artificial Antibodies. In: Kutner W, Sharma PS, editors. Molecularly Imprinted Polymers for Analytical Chemistry Applications. The Royal Society of Chemistry; 2018. p. 0.

26. Tabushi I. Artificial allosteric systems. Pure Appl Chem. 1988;60(4):581–6.

27. Kaur B, Kumar S, Kaushik BK. Novel Wearable Optical Sensors for Vital Health Monitoring Systems—A Review. Biosensors. 2023 Feb 1;13(2).

28. Heller A, Ulstrup J. Detlev Müller's Discovery of Glucose Oxidase in 1925. Anal Chem. 2021 May 11;93(18):7148–9.

29. Clark LC, Lyons C. ELECTRODE SYSTEMS FOR CONTINUOUS MONITORING IN CARDIOVASCULAR SURGERY. Ann N Y Acad Sci. 1962 Oct 1;102(1):29–45.

30. Lopes LC, Santos A, Bueno PR. An outlook on electrochemical approaches for molecular diagnostics assays and discussions on the limitations of miniaturized technologies for point-of-care devices. Sensors and Actuators Reports. 2022 Nov 1;4:100087.

31. Turner APF, Wilson GS. Biosensors : Fundamentals and Applications. Oxford Univ Press. 1987;(January):786.

32. The IUPAC Compendium of Chemical Terminology. IUPAC Compend Chem Terminol. 2019;

33. Point-of-care tests for sexually transmitted infections: target product profiles [Internet]. [cited 2024 Jul 2]. Available from: https://www.who.int/publications/i/item/9789240077102

34. Land KJ, Boeras DI, Chen XS, Ramsay AR, Peeling RW. REASSURED diagnostics to inform disease control strategies, strengthen health systems and improve patient outcomes. Nat Microbiol 2018 41. 2018 Dec 13;4(1):46–54.

35. Flynn CD, Chang D, Mahmud A, Yousefi H, Das J, Riordan KT, et al. Biomolecular sensors for advanced physiological monitoring. Nat Rev Bioeng 2023 18. 2023 May 11;1(8):560–75.

36. Hussain M, Wackerlig J, Lieberzeit PA. Biomimetic strategies for sensing biological species. Biosensors. 2013;3(1):89–107.

37. Sela-Culang I, Kunik V, Ofran Y. The structural basis of antibody-antigen recognition. Front Immunol. 2013 Oct 8;4(OCT):64858.

38. Tsumoto K, Caaveiro JM. Antigen–Antibody Binding. Encycl Life Sci. 2016 Dec 14;1–8.

39. Conroy PJ, Hearty S, Leonard P, O'Kennedy RJ. Antibody production, design and use for biosensor-based applications. 2009 Feb 1;20(1):10–26.

40. Tiller T. Synthetic Antibodies Methods and Protocols. Vol. 1575, Methods in Molecular Biology. 2017.

41. Sharma S, Byrne H, O'Kennedy RJ. Antibodies and antibody-derived analytical biosensors. Essays Biochem. 2016 Jun 6;60(1):9.

42. de Freitas JVB, Reis AVF, Silva ADO, de Sousa ACC, Martins JRP, Nogueira KAB, et al. Monoclonal Antibodies in Nanosystems as a Strategy for Cancer Treatment. Cancer Nanotechnol. 2022 Jan 1;115–76.

43. Lequin RM. Enzyme immunoassay (EIA)/enzyme-linked immunosorbent assay (ELISA). Clin Chem. 2005 Dec;51(12):2415–8.

44. Cáceres C, Canfarotta F, Chianella I, Pereira E, Moczko E, Esen C, et al. Does size matter? Study of performance of pseudo-ELISAs based on molecularly imprinted polymer nanoparticles prepared for analytes of different sizes. Analyst. 2016 Feb 21;141(4):1405–12.

45. Parolo C, Sena-Torralba A, Bergua JF, Calucho E, Fuentes-Chust C, Hu L, et al. Tutorial: design and fabrication of nanoparticle-based lateral-flow immunoassays. Nat Protoc 2020 1512. 2020 Oct 23;15(12):3788–816.

46. Rubio-Monterde A, Quesada-González D, Merkoçi A. Toward Integrated Molecular Lateral Flow Diagnostic Tests Using Advanced Micro- and Nanotechnology. Anal Chem. 2023;95(1):468–89.

47. Sena-Torralba A, Álvarez-Diduk R, Parolo C, Piper A, Merkoçi A. Toward Next Generation Lateral Flow Assays: Integration of Nanomaterials. Chem Rev. 2022;122(18):14881–910.

48. Mollarasouli F, Kurbanoglu S, Ozkan SA. The Role of Electrochemical Immunosensors in Clinical Analysis. Biosensors. 2019 Sep 1;9(3).

49. Kausaite-Minkstimiene A, Ramanaviciene A, Kirlyte J, Ramanavicius A. Comparative study of random and oriented antibody immobilization techniques on the binding capacity of immunosensor. Anal Chem. 2010;82(15):6401–8.

50. Lemieux RU, Spohr U. How Emil Fischer was Led to the Lock and Key Concept for Enzyme Specificity. Adv Carbohydr Chem Biochem. 1994 Jan 1;50(C):1–20.

51. Wiley-VCH - The Lock-and-Key Principle [Internet]. [cited 2024 Jul 2]. Available from: https://www.wiley-vch.de/de/fachgebiete/naturwissenschaften/chemie-11ch/organische-chemie-11ch8/supramolekulare-chemie-11ch85/the-lock-and-key-principle-978-0-471-93902-3

52. Koshland DE. The Key–Lock Theory and the Induced Fit Theory. Angew Chemie Int Ed English. 1995 Jan 3;33(23–24):2375–8.

53. Holyoak T. Molecular Recognition: Lock-and-Key, Induced Fit, and Conformational Selection. Encycl Biophys. 2013;1584–8.

54. Raba J, Mottola HA. Glucose Oxidase as an Analytical Reagent. Crit Rev Anal Chem. 1995;25(1):1–42.

55. Engelmann C, Ekambaram N, Johannsen J, Fellechner O, Waluga T, Fieg G, et al. Enzyme Immobilization on Synthesized Nanoporous Silica Particles and their Application in a Bi-enzymatic Reaction. ChemCatChem. 2020;12(8):2245–52.

56. Wong CM, Wong KH, Chen XD. Glucose oxidase: Natural occurrence, function, properties and industrial applications. Appl Microbiol Biotechnol. 2008 Apr 1;78(6):927–38.

57. Holade Y, Tingry S, Servat K, Napporn TW, Cornu D, Kokoh KB. Nanostructured Inorganic Materials at Work in Electrochemical Sensing and Biofuel Cells. Catal 2017, Vol 7, Page 31. 2017 Jan 18;7(1):31.

58. Kim SK, Oh YH, Ko DH, Sung H, Oh HB, Hwang SH. Nanoparticle-Based Visual Detection of Amplified DNA for Diagnosis of Hepatitis C Virus. Biosensors. 2022 Sep 1;12(9):744.

59. Moitra P, Alafeef M, Alafeef M, Alafeef M, Dighe K, Frieman MB, et al. Selective Naked-Eye Detection of SARS-CoV-2 Mediated by N Gene Targeted Antisense Oligonucleotide Capped Plasmonic Nanoparticles. ACS Nano. 2020 Jun 23;14(6):7617–27.

60. Lalli MA, Langmade SJ, Chen X, Fronick CC, Sawyer CS, Burcea LC, et al. Rapid and extraction-free detection of SARS-CoV-2 from saliva with colorimetric LAMP. Clin Chem. 2020;

61. Alexander C, Andersson HS, Andersson LI, Ansell RJ, Kirsch N, Nicholls IA, et al. Molecular imprinting science and technology: A survey of the literature for the years up to and including 2003. J Mol Recognit. 2006 Mar;19(2):106–80.

62. Lei Y. Synthetic Strategies in Molecular Imprinting. Adv Biochem Eng Biotechnol. 2015;123(July 2015):127–41.

63. Meier F, Mizaikoff B. Molecularly Imprinted Polymers as Artificial Receptors. Artif Recept Chem Sensors. 2010 Dec 1;391–437.

64. Wulff G, Sarhan A. Über die Anwendung von enzymanalog gebauten Polymeren zur Racemattrennung. Angew Chemie. 1972 Apr 1;84(8):364–364.

65. Vlatakis G, Andersson LI, Müller R, Mosbach K. Drug assay using antibody mimics made by molecular imprinting. Nat 1993 3616413. 1993;361(6413):645–7.

66. Ramström O, Ye L, Mosbach K. Artificial antibodies to corticosteroids prepared by molecular imprinting. Chem Biol. 1996;3(6):471–7.

67. Mosbach K, Ramström O. The emerging technique of molecular imprinting and its future impact on biotechnology. Bio/Technology. 1996;14(2):163–70.

68. Karlsson BCG, O'Mahony J, Karlsson JG, Bengtsson H, Eriksson LA, Nicholls IA. Structure and dynamics of monomer-template complexation: An explanation for molecularly imprinted polymer recognition site heterogeneity. J Am Chem Soc. 2009 Sep 23;131(37):13297–304.

69. Liu Y, Wang L, Li H, Zhao L, Ma Y, Zhang Y, et al. Rigorous recognition mode analysis of molecularly imprinted polymers—Rational design, challenges, and opportunities. Prog Polym Sci. 2024 Mar 1;150:101790.

70. Mujahid A, Afzal A, Dickert FL. Transitioning from Supramolecular Chemistry to Molecularly Imprinted Polymers in Chemical Sensing. Sensors (Basel). 2023 Sep 1;23(17).

71. Mustafa YL, Keirouz A, Leese HS. Molecularly imprinted polymers in diagnostics: accessing analytes in biofluids. J Mater Chem B. 2022 Sep 28;10(37):7418–49.

72. Lorenzo RA, Carro AM, Alvarez-Lorenzo C, Concheiro A. To remove or not to remove? The challenge of extracting the template to make the cavities available in molecularly imprinted polymers (MIPs). Int J Mol Sci. 2011 Jul;12(7):4327–47.

73. Sullivan M V., Dennison SR, Archontis G, Reddy SM, Hayes JM. Toward Rational Design of Selective Molecularly Imprinted Polymers (MIPs) for Proteins: Computational and Experimental Studies of Acrylamide Based Polymers for Myoglobin. J Phys Chem B. 2019 Jul 5;123(26):5432–43.

74. Garg M, Pamme N. Strategies to remove templates from molecularly imprinted polymer (MIP) for biosensors. TrAC Trends Anal Chem. 2024 Jan 1;170:117437.

75. Canfarotta F, Czulak J, Betlem K, Sachdeva A, Eersels K, Van Grinsven B, et al. A novel thermal detection method based on molecularly imprinted nanoparticles as recognition elements. Nanoscale. 2018 Jan 25;10(4):2081–9.

76. Canfarotta F, Poma A, Guerreiro A, Piletsky S. Solid-phase synthesis of molecularly imprinted nanoparticles. Nat Protoc. 2016;11(3):443–55.

77. Shevchenko KG, Garkushina IS, Canfarotta F, Piletsky SA, Barlev NA. Nano-molecularly imprinted polymers (nanoMIPs) as a novel approach to targeted drug delivery in nanomedicine. RSC Adv. 2022 Jan 28;12(7):3957–68.

78. Testa V, Anfossi L, Cavalera S, Di Nardo F, Serra T, Baggiani C. The Amount of Cross-Linker Influences Affinity and Selectivity of NanoMIPs Prepared by Solid-Phase Polymerization Synthesis. Polymers (Basel). 2024;16(4).

79. Kassem S, Piletsky SS, Yesilkaya H, Gazioglu O, Habtom M, Canfarotta F, et al. Assessing the In Vivo Biocompatibility of Molecularly Imprinted Polymer Nanoparticles. Polymers (Basel). 2022 Nov 1;14(21):4582.

80. Nimjee SM, Rusconi CP, Sullenger BA. Aptamers: An emerging class of therapeutics. Annu Rev Med. 2005;56:555–83.

81. Weigand JE, Suess B. Aptamers and riboswitches: Perspectives in biotechnology. Appl Microbiol Biotechnol. 2009 Nov;85(2):229–36.

82. Daniels J, Wadekar S, DeCubellis K, Jackson GW, Chiu AS, Pagneux Q, et al. A mask-based diagnostic platform for point-of-care screening of Covid-19. Biosens Bioelectron. 2021 Nov 15;192:113486.

83. Mok W, Li Y. Recent progress in nucleic acid aptamer-based biosensors and bioassays. Sensors. 2008 Nov;8(11):7050–84.

84. Sequeira-Antunes B, Ferreira HA. Nucleic Acid Aptamer-Based Biosensors: A Review. Biomedicines. 2023 Dec 1;11(12).

85. Komarova N, Kuznetsov A. Inside the Black Box: What Makes SELEX Better? Mol 2019, Vol 24, Page 3598. 2019 Oct 7;24(19):3598.

86. Gold L, Ellington A. Introduction to SELEX. :2–47.

87. Ruscito A, McConnell EM, Koudrina A, Velu R, Mattice C, Hunt V, et al. In Vitro Selection and Characterization of DNA Aptamers to a Small Molecule Target. Curr Protoc Chem Biol. 2017;9(4):233–68.

88. Kohlberger M, Gadermaier G. SELEX: Critical factors and optimization strategies for successful aptamer selection. Biotechnol Appl Biochem. 2022 Oct 1;69(5):1771–92.

89. Manea I, Casian M, Hosu-Stancioiu O, de-los-Santos-Álvarez N, Lobo-Castañón MJ, Cristea C. A review on magnetic beads-based SELEX technologies: Applications from small to large target molecules. Anal Chim Acta. 2024 Apr 8;1297:342325.

90. Ruiz-Ciancio D, Veeramani S, Embree E, Ortman C, Thiel KW, Thiel WH. AptamerRunner: An accessible aptamer structure prediction and clustering algorithm for visualization of selected aptamers. bioRxiv Prepr Serv Biol. 2023 Nov 15;

91. Hoinka J, Backofen R, Przytycka TM. AptaSUITE: A Full-Featured Bioinformatics Framework for the Comprehensive Analysis of Aptamers from HT-SELEX Experiments. Mol Ther - Nucleic Acids. 2018 Jun 1;11:515–7.

92. Tolle F, Mayer G. Preparation of SELEX samples for next-generation sequencing. Methods Mol Biol. 2016;1380:77–84.

93. Thevendran R, Citartan M. Assays to Estimate the Binding Affinity of Aptamers. Talanta. 2022 Feb 1;238:122971.

94. Amano R, Takada K, Tanaka Y, Nakamura Y, Kawai G, Kozu T, et al. Kinetic and Thermodynamic Analyses of Interaction between a High-Affinity RNA Aptamer and Its Target Protein. Biochemistry. 2016 Nov 15;55(45):6221–9.

95. Wochner A, Menger M, Orgel D, Cech B, Rimmele M, Erdmann VA, et al. A DNA aptamer with high affinity and specificity for therapeutic anthracyclines. Anal Biochem. 2008;373(1):34–42.

96. Spiga FM, Maietta P, Guiducci C. More DNA-aptamers for small drugs: A capture-SELEX coupled with surface plasmon resonance and high-throughput sequencing. ACS Comb Sci. 2015;17(5):326–33.

97. Stoltenburg R, Reinemann C, Strehlitz B. SELEX-A (r)evolutionary method to generate high-affinity nucleic acid ligands. Biomol Eng. 2007 Oct;24(4):381–403.

98. Yu H, Alkhamis O, Canoura J, Liu Y, Xiao Y. Advances and Challenges in Small-Molecule DNA Aptamer Isolation, Characterization, and Sensor Development. Angew Chemie - Int Ed. 2021;60(31):16800–23.

99. Ruscito A, DeRosa MC. Small-molecule binding aptamers: Selection strategies, characterization, and applications. Front Chem. 2016 May 10;4(MAY):188509.

100. Yue H, Chen J, Chen X, Wang X, Zhang Y, Zhou N. Systematic screening and optimization of single-stranded DNA aptamer specific for N-acetylneuraminic acid: A comparative study. Sensors Actuators B Chem. 2021 Oct 1;344:130270.

101. Tolle F, Wilke J, Wengel J, Mayer G. By-Product Formation in Repetitive PCR Amplification of DNA Libraries during SELEX. PLoS One. 2014 Dec 9;9(12):e114693.

102. Ouellet E, Foley JH, Conway EM, Haynes C. Hi-Fi SELEX: A high-fidelity digital-PCR based therapeutic aptamer discovery platform. Biotechnol Bioeng. 2015 Aug 1;112(8):1506–22.

103. Kramat J, Suess B. Efficient Method to Identify Synthetic Riboswitches Using RNA-Based Capture-SELEX Combined with In Vivo Screening. Methods Mol Biol. 2022;2518:157–77.

104. Haupt K. Noncovalent Molecular Imprinting of a Synthetic Polymer with the Herbicide 2,4-Dichlorophenoxyacetic Acid in the Presence of Polar Protic Solvents. ACS Symp Ser. 1998;703:135–42.

105. Furlan De Oliveira R, Montes-García V, Ciesielski A, Samorì P. Harnessing selectivity in chemical sensing via supramolecular interactions: From functionalization of nanomaterials to device applications. Mater Horizons. 2021 Oct 1;8(10):2685–708.

106. Huynh TP, Chandra BKC, Sosnowska M, Sobczak JW, Nesterov VN, D'Souza F, et al. Nicotine molecularly imprinted polymer: Synergy of coordination and hydrogen bonding. Biosens Bioelectron. 2015;64:657–63.

107. Suryana S, Mutakin, Rosandi Y, Hasanah AN. An update on molecularly imprinted polymer design through a computational approach to produce molecular recognition material with enhanced analytical performance. Molecules. 2021;26(7).

108. Dong W, Yan M, Liu Z, Wu G, Li Y. Effects of solvents on the adsorption selectivity of molecularly imprinted polymers: Molecular simulation and experimental validation. Sep Purif Technol. 2007 Feb 25;53(2):183–8.

109. Holland N, Frisby J, Owens E, Hughes H, Duggan P, McLoughlin P. The influence of polymer morphology on the performance of molecularly imprinted polymers. Polymer (Guildf). 2010;51(7):1578–84.

110. Whitcombe MJ, Rodriguez ME, Villar P, Vulfson EN. A New Method for the Introduction of Recognition Site Functionality into Polymers Prepared by Molecular Imprinting: Synthesis and Characterization of Polymeric Receptors for Cholesterol. J Am Chem Soc. 1995;117(27):7105–11.

111. Fan Y, Li J, Amin K, Yu H, Yang H, Guo Z, et al. Advances in aptamers, and application of mycotoxins detection: A review. Food Res Int. 2023;170.

112. Moitra P, Alafeef M, Alafeef M, Alafeef M, Dighe K, Frieman MB, et al. Selective Naked-Eye Detection of SARS-CoV-2 Mediated by N Gene Targeted Antisense Oligonucleotide Capped Plasmonic Nanoparticles. ACS Nano. 2020 Jun 23;14(6):7617–27.

113. Mirón-Mérida VA, González-Espinosa Y, Collado-González M, Gong YY, Guo Y, Goycoolea FM. Aptamer–Target–Gold Nanoparticle Conjugates for the Quantification of Fumonisin B1. Biosensors. 2021;11(1):1–18.

114. Jarczewska M, Ziółkowski R, Górski Ł, Malinowska E. Application of RNA Aptamers as Recognition Layers for the Electrochemical Analysis of C-Reactive Protein. Electroanalysis. 2018;30(4):658–64.

115. Rosati G, Ravarotto M, Scaramuzza M, De Toni A, Paccagnella A. Silver nanoparticles inkjet-printed flexible biosensor for rapid label-free antibiotic detection in milk. Sensors Actuators, B Chem. 2019;280:280–9.

116. Arroyo-Currás N, Scida K, Ploense KL, Kippin TE, Plaxco KW. High Surface Area Electrodes Generated via Electrochemical Roughening Improve the Signaling of Electrochemical Aptamer-Based Biosensors. Anal Chem. 2017;89(22):12185–91.

117. Dauphin-Ducharme P, Plaxco KW. Maximizing the signal gain of electrochemical-DNA sensors. Anal Chem. 2016;88(23):11654–62.

118. Maroli G, Abarintos V, Piper A, Merkoçi A. The Cleanroom-Free, Cheap, and Rapid Fabrication of Nanoelectrodes with Low zM Limits of Detection. Small. 2023 Dec 1;19(51):2302136.

119. Puiu M, Bala C. Plasmonic Biosensors for Medical Applications. Vols. 1–4, Encyclopedia of Sensors and Biosensors: Volume 1-4, First Edition. 2022. 402–420 p.

120. Garcia Cruz A, Haq I, Cowen T, Di Masi S, Trivedi S, Alanazi K, et al. Design and fabrication of a smart sensor using in silico epitope mapping and electro-responsive imprinted polymer nanoparticles for determination of insulin levels in human plasma. Biosens Bioelectron. 2020;169(August):112536.

121. Balamurugan S, Obubuafo A, Soper SA, McCarley RL, Spivak DA. Designing highly specific biosensing surfaces using aptamer monolayers on gold. Langmuir. 2006;22(14):6446–53.

122. Nguyen VT, Kwon YS, Gu MB. Aptamer-based environmental biosensors for small molecule contaminants. Curr Opin Biotechnol. 2017 Jun 1;45:15–23.

123. Hwang HS, Jeong JW, Kim YA, Chang M. Carbon nanomaterials as versatile platforms for biosensing applications. Micromachines. 2020;11(9):1–27.

124. Gao W, Nyein HYY, Shahpar Z, Fahad HM, Chen K, Emaminejad S, et al. Wearable Microsensor Array for Multiplexed Heavy Metal Monitoring of Body Fluids. ACS Sensors. 2016;1(7):866–74.

125. Ramanathan S, Gopinath SCB, Ismail ZH, Md Arshad MK, Poopalan P. Aptasensing nucleocapsid protein on nanodiamond assembled gold interdigitated electrodes for impedimetric SARS-CoV-2 infectious disease assessment. Biosens Bioelectron. 2022;197.

126. Bard AJ, Faulkner LR. Polarography and Pulse Voltammetry. Electrochem Methods Fundam Appl. 2001 Dec;261–304.

127. Bocu R. Extended Review Concerning the Integration of Electrochemical Biosensors into Modern IoT and Wearable Devices. Biosens 2024, Vol 14, Page 214. 2024 Apr 25;14(5):214.

128. Baldrich E, Restrepo A, O'Sullivan CK. Aptasensor development: Elucidation of critical parameters for optimal aptamer performance. Anal Chem. 2005;76(23):7053–63.

129. Moulton SE, Barisci JN, Bath A, Stella R, Wallace GG. Studies of double layer capacitance and electron transfer at a gold electrode exposed to protein solutions. Electrochim Acta. 2004;49(24):4223–30.

130. Singla P, Kaur S, Jamieson O, Dann A, Garg S, Mahon C, et al. Electrochemical and thermal detection of allergenic substance lysozyme with molecularly imprinted nanoparticles. Anal Bioanal Chem. 2023;415(18):4467–78.

131. Zhang J, Wu Q, Zhang X, Wan H, Wang P. Acoustic Transducer and Its Applications in Biosensors. Handb Cell Biosens. 2021;1–19.

132. Ji J, Pang Y, Li D, Huang Z, Zhang Z, Xue N, et al. An aptamer-based shear horizontal surface acoustic wave biosensor with a CVD-grown single-layered graphene film for high-sensitivity detection of a label-free endotoxin. Microsystems Nanoeng 2020 61. 2020 Feb 10;6(1):1–11.

133. Tian Y, Zhu P, Chen Y, Bai X, Du L, Chen W, et al. Piezoelectric aptasensor with gold nanoparticle amplification for the label-free detection of okadaic acid. Sensors Actuators, B Chem. 2021 Nov 1;346.

134. Uludağ Y, Piletsky SA, Turner APF, Cooper MA. Piezoelectric sensors based on molecular imprinted polymers for detection of low molecular mass analytes. FEBS J. 2007 Nov 1;274(21):5471–80.

135. Chieng A, Wan Z, Wang S. Recent Advances in Real-Time Label-Free Detection of Small Molecules. Biosensors. 2024;14(2).

136. McClements J, Bar L, Singla P, Canfarotta F, Thomson A, Czulak J, et al. Molecularly Imprinted Polymer Nanoparticles Enable Rapid, Reliable, and Robust Point-of-Care Thermal Detection of SARS-CoV-2. ACS Sensors. 2022;7(4):1122–31.

137. Taufik S, Barfidokht A, Alam MT, Jiang C, Parker SG, Gooding JJ. An antifouling electrode based on electrode–organic layer–nanoparticle constructs: Electrodeposited organic layers versus self-assembled monolayers. J Electroanal Chem. 2016;779:229–35.

138. Frutiger A, Tanno A, Hwu S, Tiefenauer RF, Vörös J, Nakatsuka N. Nonspecific Binding - Fundamental Concepts and Consequences for Biosensing Applications. Chem Rev. 2021 Jul 14;121(13):8095–160.

139. Yarman A, Scheller FW. How reliable is the electrochemical readout of MIP sensors? Sensors (Switzerland). 2020 May 1;20(9).

140. Shiddiky MJA, Vaidyanathan R, Rauf S, Tay Z, Trau M. Molecular nanoshearing: An innovative approach to shear off molecules with AC-induced nanoscopic fluid flow. Sci Rep. 2014;4:1–7.

141. Arshady R, Mosbach K. Synthesis of substrate-selective polymers by host-guest polymerization. Die Makromol Chemie. 1981 Jan;182(2):687–92.

142. Prabowo BA, Cabral PD, Freitas P, Fernandes E. The challenges of developing biosensors for clinical assessment: A review. Chemosensors. 2021;9(11).

143. Yadav AK, Verma D, Dalal N, Kumar A, Solanki PR. Molecularly imprinted polymer-based nanodiagnostics for clinically pertinent bacteria and virus detection for future pandemics. Vol. 12, Biosensors and Bioelectronics: X. 2022.

144. Wang X, Lu D, Liu Y, Wang W, Ren R, Li M, et al. Electrochemical Signal Amplification Strategies and Their Use in Olfactory and Taste Evaluation. Biosens 2022, Vol 12, Page 566. 2022 Jul 26;12(8):566.

145. Jauset-Rubio M, Botero ML, Skouridou V, Aktas GB, Svobodova M, Bashammakh AS, et al. One-Pot SELEX: Identification of Specific Aptamers against Diverse Steroid Targets in One Selection. ACS Omega. 2019 Dec 3;4(23):20188–96.

146. Sequeira-Antunes B, Ferreira HA. Urinary Biomarkers and Point-of-Care Urinalysis Devices for Early Diagnosis and Management of Disease: A Review. Biomedicines. 2023 Apr 1;11(4).

147. Mairal Lerga T, Jauset-Rubio M, Skouridou V, Bashammakh AS, El-Shahawi MS, Alyoubi AO, et al. High Affinity Aptamer for the Detection of the Biogenic Amine Histamine. Anal Chem. 2019 Jun 4;91(11):7104–11.

148. Zou ZP, Yang Y, Wang J, Zhou Y, Ye BC. Coupling split-lux cassette with a toggle switch in bacteria for ultrasensitive blood markers detection in feces and urine. Biosens Bioelectron. 2022;214.

149. Hariri AA, Cartwright AP, Dory C, Gidi Y, Yee S, Fu K, et al. Continuous optical detection of small-molecule analytes in complex biomatrices. bioRxiv. 2023;2023.03.03.531030.

150. We design recognition. - MIP Discovery [Internet]. [cited 2024 Jul 2]. Available from: https://mipdiscovery.com/

151. Marginean CM, Pirscoveanu D, Popescu M, Vasile CM, Docea AO, Mitruţ R, et al. Challenges in Diagnosis and Therapeutic Approach of Acute on Chronic Liver Failure—A Review of Current Evidence. Biomed 2023, Vol 11, Page 1840. 2023 Jun 26;11(7):1840.

152. Idili A, Parolo C, Alvarez-Diduk R, Merkoçi A. Rapid and Efficient Detection of the SARS-CoV-2 Spike Protein Using an Electrochemical Aptamer-Based Sensor. ACS Sensors. 2021;6(8):3093–101.

153. Singh R, Kashyap S, Kumar S, Abraham S, Gupta TK, Kayastha AM, et al. Excellent storage stability and sensitive detection of neurotoxin quinolinic acid. Biosens Bioelectron. 2017 Apr 15;90:224–9.

154. Marrugo-Ramírez J, Rodríguez-Núñez M, Marco MP, Mir M, Samitier J. Kynurenic Acid Electrochemical Immunosensor: Blood-Based Diagnosis of Alzheimer's Disease. Biosens 2021, Vol 11, Page 20. 2021 Jan 12;11(1):20.

155. Idili A, Parolo C, Ortega G, Plaxco KW. Calibration-Free Measurement of Phenylalanine Levels in the Blood Using an Electrochemical Aptamer-Based Sensor Suitable for Point-of-Care Applications. ACS Sensors. 2019 Dec 27;4(12):3227–33.

156. Rosati G, Urban M, Zhao L, Yang Q, de Carvalho Castro e Silva C, Bonaldo S, et al. A plug, print & play inkjet printing and impedance-based biosensing technology operating through a smartphone for clinical diagnostics. Biosens Bioelectron. 2022;196:113737.

157. Schalley CA. Functional Supramolecular Architectures Dendrimer Chemistry Supramolecular Catalysis Calixarenes and Resorcinarenes Electrochemistry of Functional Supramolecular Systems Modern Supramolecular Chemistry Encyclopedia of Applied Spectroscopy. 2012. 814 p.

158. Omar J, Ponsford D, Dreiss CA, Lee TC, Loh XJ. Supramolecular Hydrogels: Design Strategies and Contemporary Biomedical Applications. Chem - An Asian J. 2022;17(9).

159. Shumyantseva V V., Bulko T V., Sigolaeva L V., Kuzikov A V., Archakov AI. Electrosynthesis and binding properties of molecularly imprinted poly-o-phenylenediamine for selective recognition and direct electrochemical detection of myoglobin. Biosens Bioelectron. 2016;86:330–6.

160. Yamaguchi I, Morisaka R. Synthesis and electrical properties of copolymers of o-phenylenediamine with aniline, 3,4-ethylenedioxythiophene and 2,3,5,6-tetrafluoroaniline. Polym Int. 2017;66(2):320–6.

161. Poma A, Guerreiro A, Caygill S, Moczko E, Piletsky S. Automatic reactor for solid-phase synthesis of molecularly imprinted polymeric nanoparticles (MIP NPs) in water. RSC Adv. 2014;4(8):4203–6.

162. Poma A, Guerreiro A, Whitcombe MJ, Piletska E V., Turner APF, Piletsky SA. Solid-Phase Synthesis of Molecularly Imprinted Polymer Nanoparticles with a Reusable Template-"Plastic Antibodies". Adv Funct Mater. 2013 Jun 13;23(22):2821–7.

163. Yoshikawa AM, Wan L, Zheng L, Eisenstein M, Soh HT. A system for multiplexed selection of aptamers with exquisite specificity without counterselection. Proc Natl Acad Sci U S A. 2022;119(12):1–18.

164. Ates HC, Brunauer A, von Stetten F, Urban GA, Güder F, Merkoçi A, et al. Integrated Devices for Non-Invasive Diagnostics. Adv Funct Mater. 2021;31(15).

165. Aubry G, Lee HJ, Lu H. Advances in Microfluidics: Technical Innovations and Applications in Diagnostics and Therapeutics. Anal Chem. 2023 Jan 10;95(1):444–67.

166. Bhardwaj T, Ramana LN, Sharma TK. Current Advancements and Future Road Map to Develop ASSURED Microfluidic Biosensors for Infectious and Non-Infectious Diseases. Biosensors. 2022 May 1;12(5).

167. Li J, Fang Y, Lin X, Hao Z, Yin Y, Zhao M, et al. Universal Nanoplatform for Ultrasensitive Ratiometric Fluorescence Detection and Highly Efficient Photothermal Inactivation of Pathogenic Bacteria. ACS Appl Bio Mater. 2021;4(8):6361–70.

168. Kim ER, Joe C, Mitchell RJ, Gu MB. Biosensors for healthcare: current and future perspectives. Trends Biotechnol. 2023 Mar 1;41(3):374–95.

169. Wang W, Liu L, Zhu J, Xing Y, Jiao S, Wu Z. AI-Enhanced Visual-Spectral Synergy for Fast and Ultrasensitive Biodetection of Breast Cancer-Related miRNAs. ACS Nano. 2024 Feb 27;18(8):6266–75.

170. Maroli G, Rosati G, Suárez-García S, Bedmar-Romero D, Kobrin R, González-Laredo Á, et al. Wearable, battery-free, wireless multiplexed printed sensors for heat stroke prevention with mussel-inspired bio-adhesive membranes. Biosens Bioelectron. 2024;260.

171. Olenik S, Lee HS, Güder F. The future of near-field communication-based wireless sensing. Nat Rev Mater. 2021;6(4):286–8.

172. Dincer C, Bruch R, Costa-Rama E, Fernández-Abedul MT, Merkoçi A, Manz A, et al. Disposable Sensors in Diagnostics, Food, and Environmental Monitoring. Adv Mater. 2019;31(30).

173. Wu J, Liu H, Chen W, Ma B, Ju H. Device integration of electrochemical biosensors. Nat Rev Bioeng. 2023;1(5):346–60.

THESIS OBJECTIVES

The main goal of this Ph.D. thesis is to develop and optimize advanced biosensing technologies for the early diagnosis, prognosis, and monitoring of Acute-on-Chronic Liver Failure (ACLF). This research aims to address critical clinical needs associated with ACLF, thereby contributing to improved patient outcomes through early intervention and tailored treatment strategies. The specific objectives of this Ph.D. thesis are shown below:

Synthesis and applications of electropolymerized MIPs and SPP-synthesized electroactive nanoMIPs

1. Development of e-MIPs for kynurenic acid (KA) sensing
    1.1. Investigation of binding interactions between o-phenylenediamine (o-PD) and KA via spectrophotometric analysis.
    1.2. Characterization of the electrode surface to comprehend its electrochemical properties and any surface modifications.
    1.3. Refinement the electropolymerization process and template removal to promote the creation of efficient binding sites.

2. Synthesis and Characterization of NanoMIPs via Solid-Phase Polymerization (SPP)
    2.1. Validation of target conjugation on silanized glass beads via Dansyl Chloride test.
    2.2. Study and selection of monomer composition in nanoMIPs' synthesis
    2.3. Determination of size distribution and stability of nanoMIPs through Direct Light Scattering (DLS) measurements.
    2.4. Evaluation of binding capacity and specificity using bead-ELISA.
    2.5. Assessment of yield through the solvent evaporation method.
    2.6. Optimization of DPV parameters to enhance sensitivity in electrochemical measurements.
    2.7. Analysis of temporal and cyclic stability of nanoMIPs.
    2.8. Determination of critical analytical parameters such as the limit of detection, dissociation constant, and limit of quantification.

Single- and Multi-target aptamer isolation via MB-SELEX and jOP-SELEX

1. Development of Conventional MB-SELEX for phenylalanine.

1.1. Use of maleimide magnetic beads conjugated to phenylalanine as the target molecule.
1.2. Selection of tryptophan as a counter-selection target to augment aptamer specificity.
1.3. Implementation of multiple rounds of SELEX to enrich aptamers specific to phenylalanine.
1.4. Utilize next-generation sequencing (NGS) analysis and custom-developed MATLAB code for comprehensive sequence comparison and identification of potential aptamer candidates.

2. Development of Joint One-Pot SELEX Process
   2.1. Conduct the positive incubation of three ACLF-related targets simultaneously during the initial SELEX rounds.
   2.2. Splitting of the process into three parallel SELEX streams. Each stream focuses on one target while using the remaining two targets as counter-selection targets.
   2.3. Utilize next-generation sequencing (NGS) analysis and custom-developed MATLAB code for comprehensive sequence comparison and identification of potential aptamer candidates.

3. Optimization and Validation of SELEX Processes
   3.1. Validate the efficacy of MATLAB code in identifying potential aptamer candidates at earlier rounds to accelerate the selection process.
   3.2. Enhance the specificity and reduce cross-reactivity of aptamers through rigorous selection and counter-selection strategies.

CHAPTER 3:

MOLECULARLY IMPRINTED POLYMERS: AN ALTERNATIVE BIOMIMETIC APPROACH FOR SMALL-MOLECULE DETECTION

This study investigates the use of molecularly imprinted polymers (MIPs), focusing on both electropolymerized MIPs (e-MIPs) and electroactive MIP nanoparticless (e-nanoMIPs), for the detection of ultra-low concentrations of Acute-on-Chronic Liver Failure (ACLF)-associated small molecule biomarkers, highlighting their potential clinical applications. MIPs, particularly nanoMIPs, offer numerous benefits, including high specificity, low production costs, and exceptional stability, making them viable alternatives to traditional antibodies and enzymes. This research focuses on synthesizing and characterizing e-MIPs for kynurenic acid detection and e-nanoMIPs for both kynurenic and N-acetylneuraminic acid detection. Both of these targets have been previously identified as biomarkers for ACLF, as mentioned in Chapter 1.

Key findings from this study demonstrate the superior performance of e-nanoMIPs in detecting small-molecule biomarkers at ultra-low concentrations, achieving low fM KDs in phosphate-buffered saline (PBS) and diluted synthetic urine. The synthesis and characterization processes, involving techniques such as solid-phase polymerization (SPP), dynamic light scattering (DLS), and electrochemical analysis, confirmed the e-nanoMIPs' high affinity and specificity towards their target molecules. The electroactive nature of these nanoMIPs provides enhanced sensitivity and stability, which is crucial for clinical applications. The potential applications of these e-nanoMIPs are vast, offering a promising avenue for developing reliable sensor devices for the prognosis and monitoring of biomarkers associated with various diseases. Future research should focus on optimizing large-scale production processes and further enhancing the stability and specificity of e-nanoMIPs in complex biological matrices to realize their full potential in biosensing and ensure a successful transition from laboratory settings to real-world applications.

3.1. INTRODUCTION

3.1.1. The Ubiquitous Role of Noncovalent Interactions

Living organisms rely on noncovalent interactions for communication between cells and within the body, e.g., antibody-antigen (Ab-Ag) binding, receptor-hormone interaction, or enzyme catalysis. Genetic information is contained in long strands of DNA, arranged as double helices held together by hydrogen bonds between complementary base pairs. In the same manner, the distinctive structure of a protein is maintained by a wide range of noncovalent interactions between its amino acids. For instance, the biotin-avidin pair is an excellent example of a strong connection where the dissociation constant is in the femtomolar range. Therefore, it highlights how combining various noncovalent weak forces can result in a remarkably strong binding.

Enzymes and antibodies have been extensively used for accurate diagnostic tools as they provide high reliability and exceptional sensitivity and specificity. Although antibodies are the "gold standard" for diagnostic purposes, they have certain limitations, such as a limited shelf life, high cost, and low stability under certain conditions. Additionally, developing antibodies for immunosuppressants and toxins can be challenging due to their impact on the immune response, rendering it difficult to detect small molecules, thus relying on haptens. Nevertheless, (bio)sensing small molecules is a complex task with challenges related to analytical performance, selectivity, stability in complex media, and consistency in receptor synthesis. Traditional biorecognition elements encounter difficulties in effectively detecting small molecules due to a potential lack of binding sites and a non-immunogenic (relying on haptens) or toxic nature, as aforementioned. [1,2] Therefore, novel molecular tools are being studied to overcome these obstacles. [3–7]

3.1.2. Molecular Imprinting as A Biomimicking Strategy

As mentioned in Chapter 1, scientists have been exploring Molecular Imprinting (MI) as an alternative to antibodies and enzymes, mimicking their ability to bind to biomarkers through noncovalent interactions while overcoming many limitations.[7,8] In the early 1970s, Wulff and Sahan introduced the concept of covalent molecular imprinting, which entails carrying out reversible covalent-based polymerization in the presence of a target or template (i.e., target analog).[9] Subsequently, almost twenty years later, Mosbach introduced the noncovalent approach, in which synthetic recognition sites complementary to specific molecules are formed within the polymeric matrix, as depicted in Figure 3.1. During the initial stage of molecularly imprinted polymers (MIPs), the template interacts with functional elements (FE), creating a 3-D prearrangement. These interactions are then locked in, with the aid of structural elements (SE), followed by template elution, forming a matrix containing recognition sites tailored for the template's physicochemical features. [10–12]

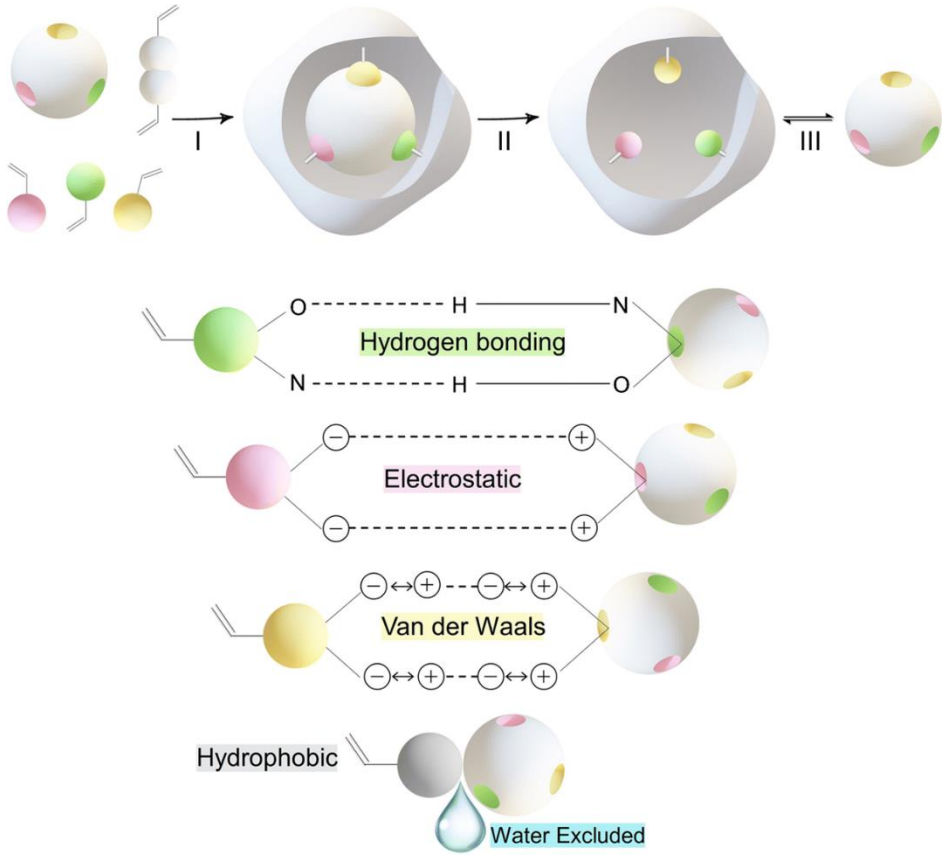


Figure 3.1. *Schematic representation of MIP synthesis indicating monomers (pink, green, and yellow), crosslinker (white), and a template. (top) I) Pre-complex formation and subsequent polymerization around the target. II) template elution and III) target re-binding. (bottom) Some examples of noncovalent interactions involved in MIP:target binding. Retrieved from* [13]

Traditional imprinting techniques require a template (i.e. target analog) to avoid contamination and achieve precise detection or separation at low levels. The selected sites should be carefully chosen based on their relevance to both the target and the template, indicating a strong similarity between them, i.e., the template must possess target-like chemical capabilities to interact with the functional monomer and be closely related to the target.[14,15]

As aforementioned, MIPs provide a promising alternative to antibodies in replicating natural binding sites, as can be seen in the evolution in Figure 3.2. [16,17] Their in vitro fabrication is more straightforward and cost-effective, and they also offer exceptional physicochemical stability while not requiring in vivo production (animal testing). With applications ranging from sensors to drug delivery, MIPs have been fabricated to recognize numerous targets, including small molecules, proteins, and whole cells. These features have made them suitable for various applications and scenarios, such as clinical use, environmental monitoring, food safety, etc.[11,18]

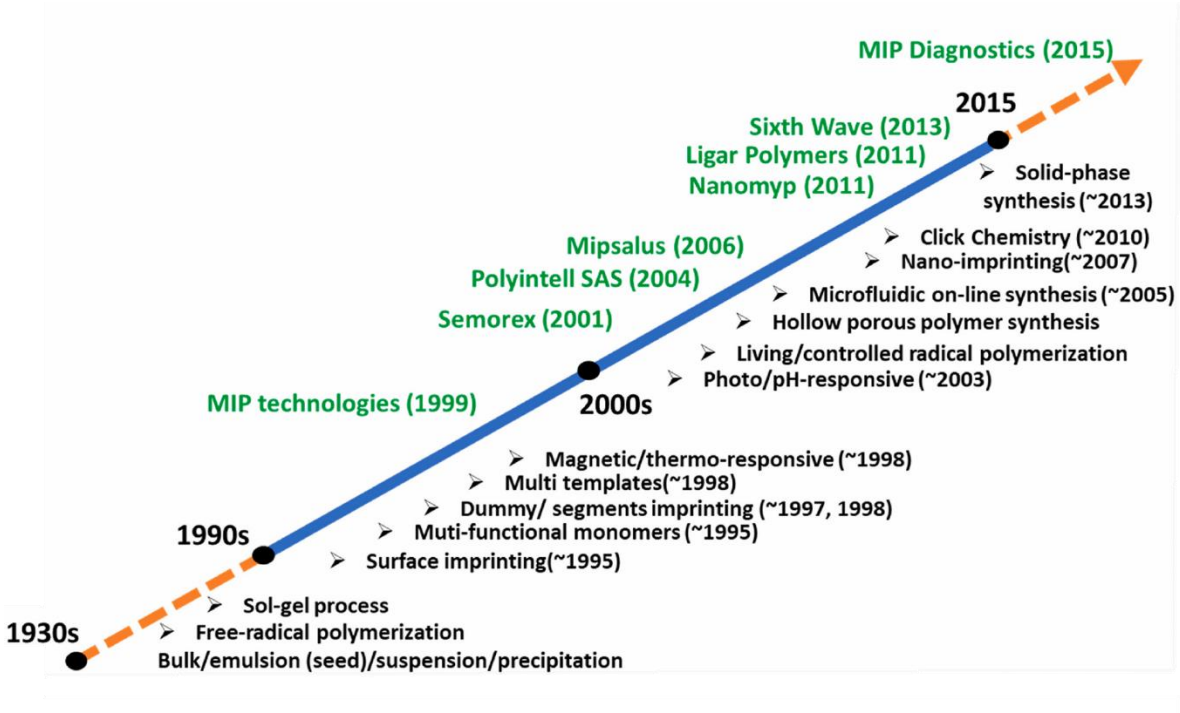


Figure 3.2. *The timeline presents an overview of several imprinting processes and strategies that have contributed to the evolution of MIPs. Additionally, it showcases the emergence of commercial platforms aimed at promoting the use of MIPs in numerous applications, encompassing diagnostics and environmental sectors. Retrieved from* [19]

Molecular recognition is the first step in developing MIPs, and, to maximize its efficiency, it is crucial to study the self-assembly of the template-FE complex due to the interactions between their moieties. Figure 3.1 illustrates the process of MIPs generation based on the template's physicochemical features, which have unique functionalities complementary to FEs. Each template has multiple types of noncovalent interactions, including crucial ones such as van der Waals forces, hydrogen bonding, ionic, and hydrophobic interactions. [20–23] These functionalities may be combined or used independently to form the polymeric matrix. There are a wide variety of monomers available from which MIPs can be fabricated, the choice of monomer can be used to target specific types of noncovalent interactions with the target. Given the wide choice of monomers available, MIPs have the potential to be developed for virtually most biomarkers. [16,22,24,25]

3.1.2.1. The Role of Functional and Structural Elements

As aforementioned, imprinting protocols use two types of construction elements: FEs and SEs. The FEs are monomers directly interacting with the template during polymerization and recognition. The SEs, on the other hand, are responsible for constructing and ensuring the proper recognition site's geometry, organizing the polymeric network, and locking the FEs in the correct 3-D structure. Although some FEs and SEs (if not all) can serve structural and functional purposes, distinguishing them may help identify possible MIP synthesis strategies.[10,26,27]

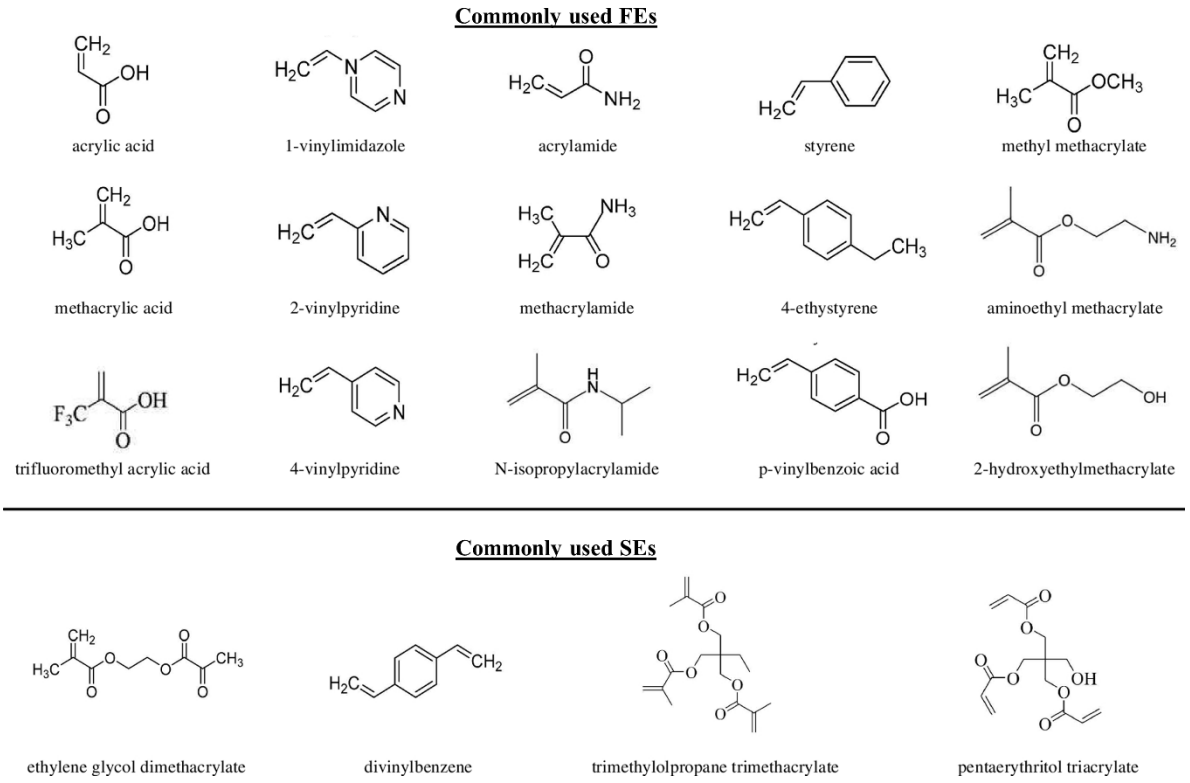


Figure 3.3. *Commonly used FEs and SEs in MIP's synthesis. Retrieved from* [28]

There has been a significant amount of research dedicated to the FEs. The monomers presented in Figure 3.3 have been categorized into two primary groups based on the nature of their chemical interactions with the target: (i) reversible covalent mechanisms[9], or (ii) noncovalent interactions[10,11]. The second group, which is the one selected to be used in this chapter, can be further subdivided based on their predominant interaction types, such as acidic, basic, hydrogen bonding, or π-π-stacking interactions.

Briefly, the noncovalent method, developed by Mosbach and his team, involves using pre-polymerized complexes between the monomer and the template through hydrogen bonding, electrostatic interactions, and hydrophobic interactions. An excess amount of monomer is typically used to stabilize the monomer:template (M:T) complex. This method is simpler and more adaptable than the reversible covalent approach, but the variability in the binding sites created can pose a challenge. [5,21]

3.1.2.2. Enhancing Functionality through Combinatorial Chemistry

The design of an ideal (bio)receptor with an enhanced strength of the receptor:target binding interactions may be achieved by delving into ligand-receptor and host-guest chemistry, as MIPs are considered supramolecular systems.[7,29,30] Therefore, using monomer combinations has frequently resulted

in improved affinity and selectivity, especially when FEs target distinct moieties on the template (Figure 3.4). Testing of M:T interactions under several solvents could serve as a preliminary screening method to identify potential monomers. Additionally, successful complexation through noncovalent interactions can be detected through NMR, UV-Vis, or fluorescence spectra changes. For example, as the monomer concentration increases or the solvent is changed, it can lead to variations in the characteristic spectroscopic signals of the template. These signals are commonly used to estimate the M:T association constants. [23,29,30]

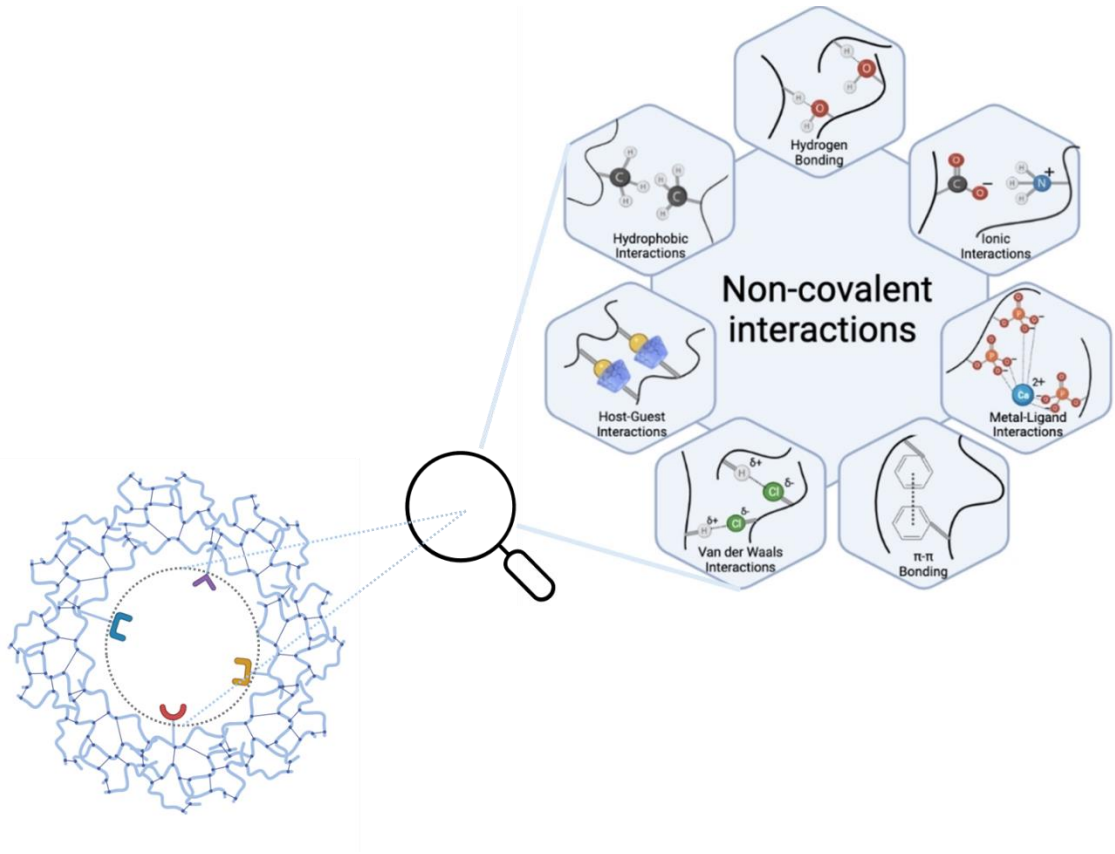


Figure 3.4. *Different noncovalent interactions taking place in MIP:target binding Modified with permission from* [31]

One of the most commonly used SEs over the years is ethylene glycol dimethacrylate (EDMA or EGDMA), which acts as a cross-linker in several procedures that involve acrylate or acrylamide functional monomers. However, there has been a growing trend of testing and demonstrating the superiority of trimethylolpropane trimethacrylate (TRIM) in many approaches. Both EGDMA and TRIM are insoluble in water; however, adding charged groups can improve their solubility, as long as these functional groups do not interfere with the recognition process. Therefore, other cross-linking monomers (SEs) are required for aqueous phase imprinting. [32,33]

3.1.2.3. Solvent Management

Managing solubility can often be challenging, particularly when working with small molecules. In MI, organic solvents like acetonitrile (ACN), chloroform, dichloromethane (DCM), tetrahydrofuran (THF), dimethylformamide (DMF), and toluene are commonly used due to their ability to induce porogenic effects while also effectively solubilizing a wide range of organic compounds. H-H interactions are essential in many functional M:T complexes, thus, solvents with strong H-H bonding properties can disrupt these complexes by competing with the monomers or targets involved. Therefore, selecting polar aprotic solvents is recommended in this situation. DCM, chloroform, and toluene are commonly used in these systems; however, alternatives such as ACN may be preferred due to health and environmental hazards. Conversely, it is important to note that polar solvents and higher temperatures tend to be more advantageous for M:T systems stabilized by apolar forces. [14,26,34–36]

Once the template has been removed, the polymeric matrix preserves recognition cavities that correspond to the target's size, shape, and functionality, i.e., the template's physicochemical features determine the arrangement of binding pockets within the polymer. However, removing the template is not always straightforward or successful, resulting in (i) target leaching from the polymer matrix, and (ii) incomplete target removal, producing inaccurate results in analytical applications. The size and accessibility of the imprinted sites are determined not only by the degree of cross-linking in the polymer network but also by the target removal procedure, which has a significant impact on the final structure and porosity of the final MIP, and consequently, its capacity to recognize the target. [6,16,33,37–41]

3.1.3. Approaches for Molecular Imprinting

Various techniques are used in MIPs fabrication, including but not limited to bulk, suspension, emulsion, miniemulsion, and precipitation polymerization. Each technique has its own advantages and disadvantages, such as the ability to control morphology, reproducibility, and, in some types, particle size. In addition, there are several other advanced methods employed, including sol-gel imprinting, bulk polymerization in porous templates, electropolymerization, surface imprinting, solid-phase imprinting (SPI), and post-polymerization modification. The method selection is typically based on the specific application and desired characteristics of the final MIP. A meticulous optimization process is necessary to achieve control over the imprinted sites and ensure reproducibility. [42–47] A breakdown of these techniques, along with their respective pros and cons, can be found in Table 3.1. Below are detailed the two main techniques used in this thesis: electropolymerization and SPI.

Table 3.1*. Pros and cons of different approaches for nanoMIPs synthesis. Adapted from* [40]

	Procedure	Advantages	Drawbacks
Bulk	• Use of organic solvents to obtain a • Block is then grounded and sieved	• Simple method	• Wide particle size distribution • Heterogeneity of active sites
Precipitation	• Polymer chains grow in a solution • Precipitation due to size-related insolubility	• Easy and fast with high yields • Low quantity of reagents required	• Low concentration of monomers may impair recognition events
Emulsion	• Use surfactants and high-shear homogenization • Emulsification of the water and organic phase	• Possible to obtain very small NPs (50 nm)	• Surfactants may disrupt the imprinting process • Difficulty to remove surfactants
Core-shell emulsion	• MIP layer deposition onto preformed nanoparticles • Core could be metals, silica, or polymers	• Suitable for large-scale production • High yields	• Surfactants and the aqueous phase may decrease the imprinting effect
Core-shell grafting	• Chemical linkage of MIP to modified nanoparticles with surface double bonds • Use of iniferter	• Excellent control over shell thickness • Sequential shell polymerization	• The shell may be too thin for bulky templates or too thick for small target diffusion.
Living radical	• Controlled growth of polymer chains • Use of nitroxide species, metal-containing, or dithiocarbonyl initiators	• Excellent control over particle size and PD • Useful for thermolabile templates	• Low yield • Catalyst removal needed • Not suitable for photolabile templates
Solid-phase	• Template immobilization onto solid support • High affinity nanoMIPs are collected by a temperature-based elution	• High affinity and selectivity (nano- or picomolar) • High purity with low template contamination • Fully automatable process.	• The template must have functional groups for immobilization. • Typically, one binding site per particle (low binding capacity)

3.1.3.1. Electropolymerization for Small Molecule Imprinting

Electropolymerization (EP) is another technique that can be used to create a polymer network containing template-specific imprinted sites. This is achieved by electrochemically oxidizing or reducing monomers in the presence of a target at the electrode surface. To perform this technique, an electrochemical cell comprising a working (WE), counter (CE), and reference (RE) electrode is required.[48] Successful molecular recognition relies on carefully selecting monomers capable of being electropolymerized (in this particular case) and interacting with the desired templates. The most common monomer is pyrrole, although o-aminophenol, o-phenylenediamine, dopamine, p-aminobenzoic acid, and aniline are also frequently employed for electropolymerized MIPs (e-MIPs). Some examples of less frequently used monomers include scopolein, 3-thiophene acetic acid, m-aminophenylboronic acid, gallic acid, p-aminothiophenol, and p-aminobenzene sulfonic acid. [44,49–51]

Even though using a combination of monomers may render optimization more difficult, the potential benefits of obtaining more precise e-MIP:analyte interactions may make the effort worthwhile.[30] Usually, conductive polymers like polypyrrole are used when doing voltammetric examination, whereas impedimetric analysis is typically based on the use of redox probes as required when using less conductive polymers like poly(o-phenylenediamine).[30]

Electrochemical characterization techniques, such as Cyclic Voltammetry (CV) or Electrochemical Impedance Spectroscopy (EIS), are commonly used to evaluate the properties of e-MIPs throughout their development. Furthermore, there are alternative methods, such as scanning electron microscopy (SEM), providing a perspective of the nanostructures produced and even enabling the measurement of certain characteristics; Fourier transform infrared (FTIR) and Raman spectroscopy, which offers valuable insights into the chemical interactions; and atomic force microscopy (AFM) which is useful for studying the physicochemical aspects of the cavities and gaining a better understanding of the MIPs morphology.[52,53] This is particularly useful when comparing MIPs to non-imprinted polymers (NIPs), the template-free controls used to guarantee a proper polymer formation.

The choice of electrolyte used for e-MIPs fabrication significantly impacts the M:T interactions, the solution's conductivity, and the monomers' redox behavior. By adjusting the applied voltage or current, it is possible to tune different features of the MIP film, such as the thickness, crosslinking degree, porosity, and electroactivity. e-MIPs are widely used as recognition elements in various applications, such as sensors, separation systems, and drug delivery. Additionally, EP is a more versatile multi-site approach allowing a finer tune of thickness and porosity, for instance, which will strongly influence adaptability, and specificity.[50,54–57]

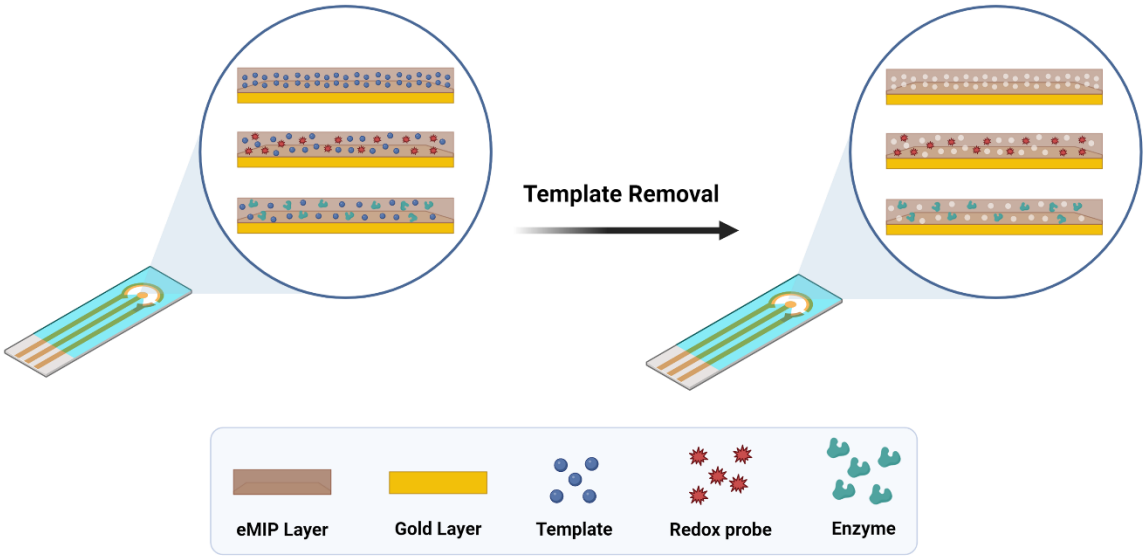


Figure 3.5. *Types of electropolymerized MIPs. (top) affinity chemosensor for electroactive target, (center) affinity chemosensor for non-electroactive target, aided by redox probes which enhances the signal obtained from target-induced conformational changes in polymeric matrix, (bottom) MIP-enabled enzymatic chemosensor. Adapted from* [40]

Once obtained, the final MIP can be used to detect a target with various electroanalytical techniques, including differential pulse voltammetry (DPV) and square-wave voltammetry (SWV), as these techniques could considerably diminish or even eliminate the contribution of capacitive currents and focus mainly on

faradaic ones. In cases where the analyte is not electroactive, a redox mediator, such as potassium ferricyanide, can be employed to make the detection quantifiable, as depicted in Figure 3.5.

Despite the seemingly straightforward nature of the e-MIP synthesis process, researchers have encountered numerous challenges. For example, (i) template removal, which can be done through electrochemical cleaning or solvent leaching, is a complex operation that may fail or damage the MIP, hence requiring extensive optimization, (ii) the cavities formed by the MIP may lack selectivity, meaning they may interact with interferents closely resembling the intended analyte, which is a common issue when testing complex samples, and (iii) scaling up from laboratory to commercial and clinical levels is a crucial challenge that requires further attention. Specifically, the focus should be on enhancing the robustness and antifouling properties of the final MIP-based sensor against expected interferents in real samples. This is necessary to ensure that the product can meet clinical and market standards. [24,33,36,38,47,58,59]

3.1.3.2. Polymeric nanoparticles' synthesis

NanoMIPs, also known as "plastic antibodies," are nanostructured (80-150 nm) polymer particles that can recognize a variety of targets with high specificity. They are a practical alternative to traditional antibodies and enzymes, gaining attention from researchers for their potential use in various diagnostic and therapeutic scenarios. Additionally, they can be used as drug delivery systems and sensing elements due to their unique properties. The colloidal stability of nanoMIPs is a fascinating characteristic that makes them ideal for in vitro research. Nevertheless, obtaining high-yield particle batches with a desired size range is essential for biomedical applications. Compared to natural ligands, nanoMIPs have two significant advantages: low production costs and ease of manufacture. [37,59,60]

The methods depicted in Figure 3.6 encompass a range of techniques for the preparation of nanoMIPs. While these approaches are applicable for both micro- and nanoMIPs, the resultant polymer particle size can vary based on the polymerization conditions. The target quantity utilized during nanoMIP synthesis may lead to the emergence of cooperativity effects, which could impact the final response of the nanoMIP. Furthermore, owing to the synthetic allosteric nature of MIPs, factors such as steric hindrance and cooperativity effects significantly influence the overall binding strength and the formation of single- to multiple binding sites. [16,59,61–63]

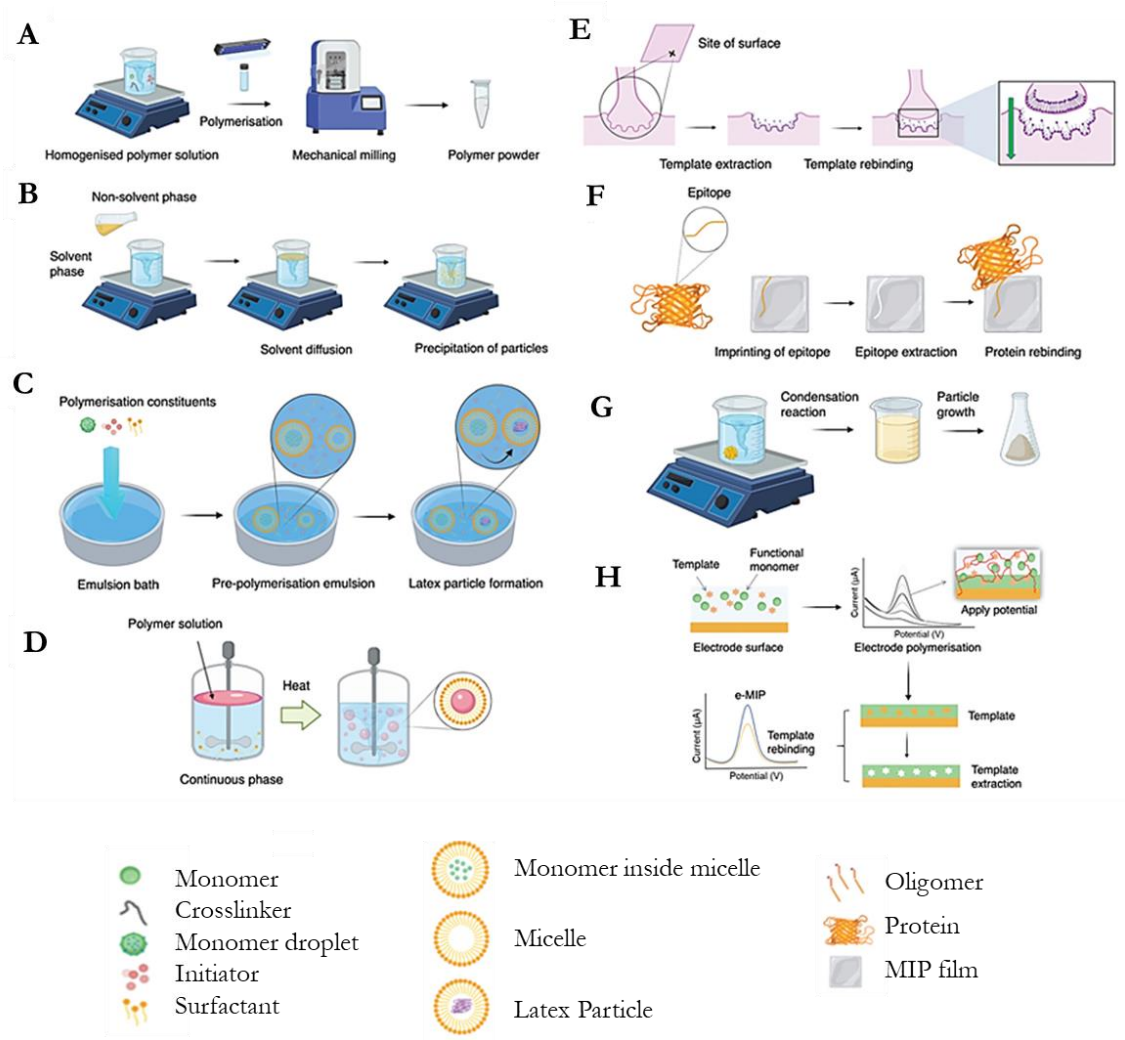


***Figure 3.6**. Schematic representation of several (nano)MIPs fabrication techniques, including but not limited to (a) bulk, (b) precipitation, (c) emulsion, (d) suspension, (e) surface, (f) epitope, (g) sol-gel, (h) electropolymerization. Adapted from* [64]

An alternative approach, so-called "semi-covalent imprinting", has been proposed by combining the noncovalent and covalent methods, as depicted in Figure 3.7. This involves using a template covalently attached to a solid support and designing the subsequent phase of analyte binding in a noncovalent manner. This approach reduces the issues of exhibiting multiple imprinted sites by immobilizing the template in a directional manner, which results in the creation of binding sites on the surface of the polymeric matrix. In contrast, when the template is available in solution, most imprinted sites are generated within the polymeric matrix, resulting in a lower accessibility for the target molecule. [59,65,66]

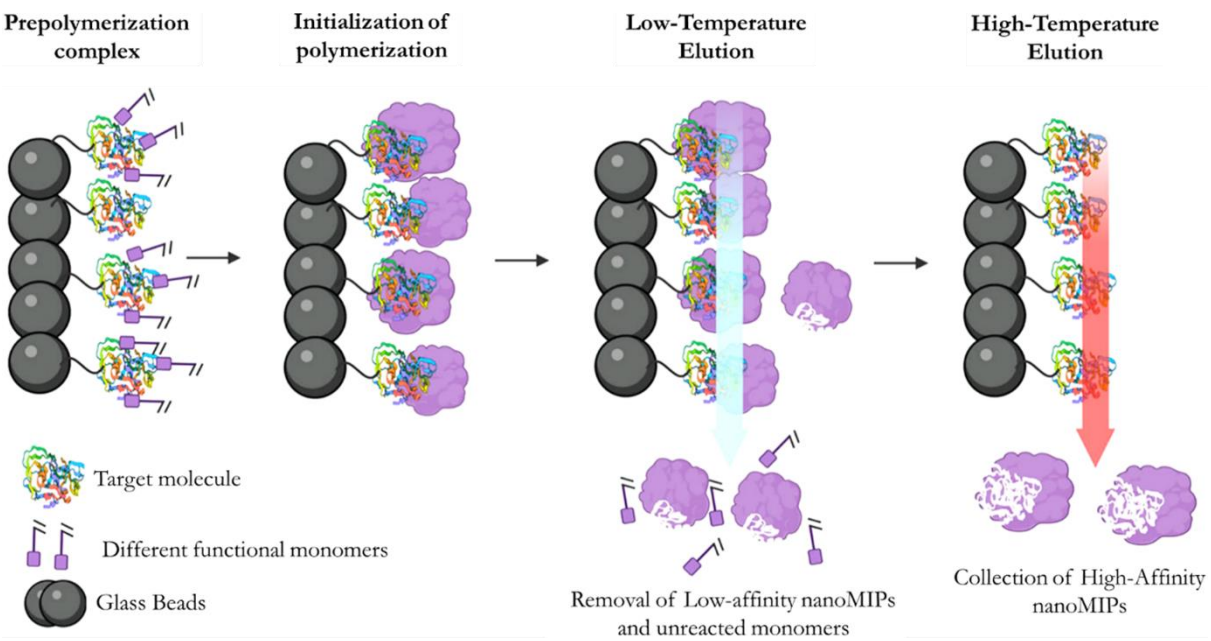


***Figure 3.7**. Semi-covalent approach for nanoMIPs synthesis, including a prepolymerization complex with its subsequent nanoMIP formation, followed by temperature-based elution steps for high-affinity nanoMIPs collection. Adapted from* [67]

3.1.3.3. Cooperative binding

Allosteric regulation is a phenomenon that occurs when the binding of one molecule affects the binding of other molecules in a positive or negative manner (Figure 3.8). These interactions only occur in receptor:ligand systems with three or more interacting parties, which may refer to the binding sites or the molecule that binds to them.[68] One well-known example of positive cooperativity and allosteric activation is the interaction between oxygen and the metalloprotein haemoglobin, which exhibits a positive cooperativity, i.e., the binding of oxygen triggers a conformational change in the shape of the remaining binding sites, making them more receptive to further binding. On the other hand, myoglobin exhibits negative cooperativity when binding to oxygen, as it only possesses one heme group. [61,69–71]

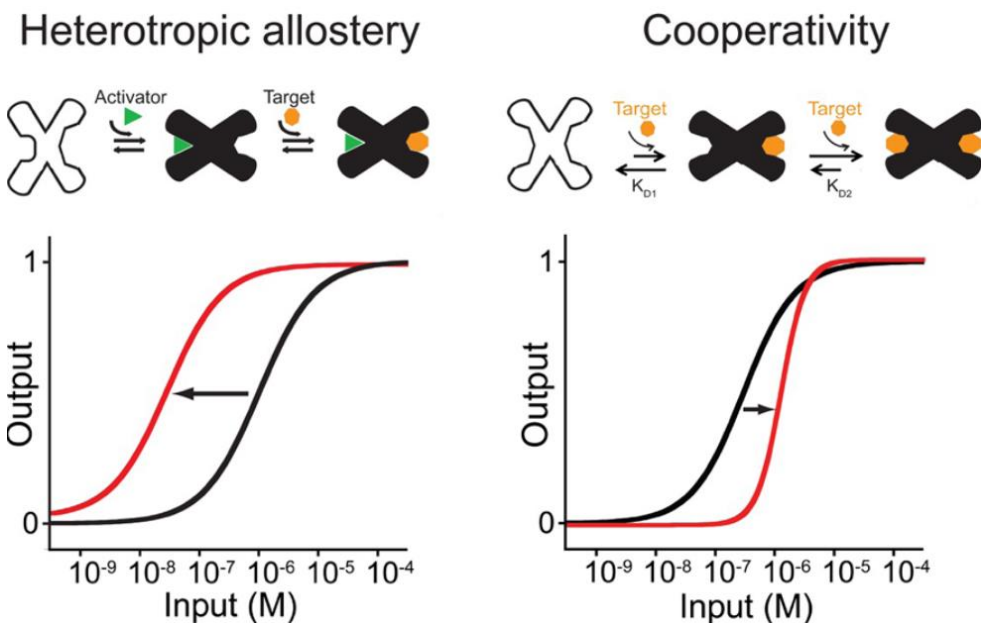


Figure 3.8*. Heterotropic allostery and cooperativity effects on binding events, and their consequence on the dynamic range and sensitivity of the receptor or sensor. Retrieved from* [72]

Remarkably, scarce documented instances offer proof of cooperative binding in (nano)MIPs.[61,69,71,73] In 1999, Andersson et al. conducted research using High-Performance Liquid Chromatography (HPLC) to investigate the retention of (-)nicotine. They discovered a significant increase in nicotine retention when a MIP with an affinity for (-)nicotine was used in the HPLC column. The resulting response indicated the presence of enhanced binding sites to templates in complex solutions. Cooperative binding behavior was evident as longer retention times were used. Subsequently, Svenson et al. conducted a 1H NMR to examine the interactions between template molecules (nicotine) in a MIP. This research demonstrated that the self-association of nicotine was intensified by the presence of the functional monomer counterpart, acetic acid. This study proved that template-template complexes are present in the polymerization mixture, resulting in the formation of selective binding sites for these complexes.[74,75]

According to [76] there are two molecular processes that may explain the cooperative binding behavior observed in receptor-ligand systems, which could potentially be applied to nanoMIP-template systems, assuming nanoMIPs contain multiple binding sites. This phenomenon was observed in (-)nicotine MIP cooperative binding experiments, which hindered the formation of the nanoMIP-template complex due to template-template complexes. The first mechanism involves a weak contact, such as a noncovalent interaction, between template T1 and template T2; while the second mechanism involves conformational changes in the nanoMIP structure when template T1 binds, which can affect its affinity towards T2. This can result in changes in the shape of the binding cavity, making it more, or less, accessible to template molecules. [76]

During nanoMIPs synthesis, the target density and spatial distribution are crucial for determining cooperativity effects. For a nanoMIP to exhibit cooperative binding, the binding sites would likely

"cooperate" to bind to multiple templates, i.e., the template molecules should be sufficiently close to each other so that the distance among them is smaller than the intended size of the nanoMIP (80-150 nm). By precisely tuning the template spacing, it is theoretically possible to pre-determine the average number of template-binding sites on the nanoMIP. Research into cooperative binding in nanoMIPs can be modeled using the surface plasmon resonance (SPR) binding assay. As aforementioned, the literature scarcely mentions cooperative binding in nanoMIPs; however, researchers have hypothesized that high-affinity nanoMIPs with one or two binding sites per particle could be synthesized using template-derivatized solid support.[59,77,78]

Figure 3.9 shows two strategies that can be employed for tuning the target density when utilizing solid supports: optimizing the linker's surface density and length. Figure 3.9 (left) depicts a correlation between the target proximity and the emergence of single- and multi-binding sites on the nanoMIPs surface. When utilizing aminated linkers (Figure 3.9, right), the length of the alkyl chain may contribute to improved stability and separation among linkers as electrostatic interaction becomes more prominent.

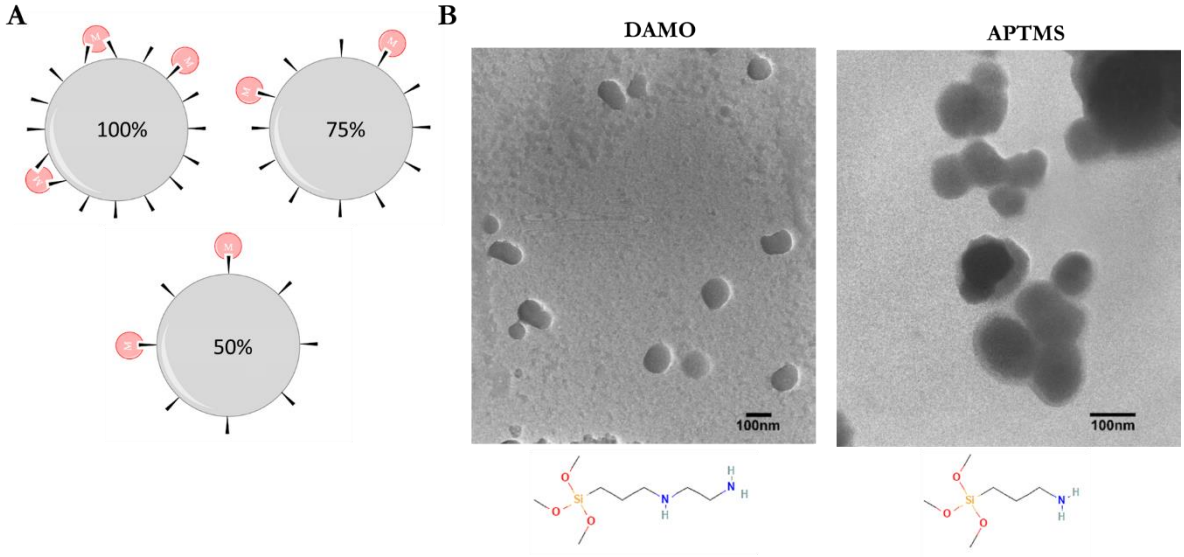


Figure 3.9. *Effect of (A) template density and (B) linker size on binding site generation. Retrieved from* [71]

3.1.3.4. Solid-Phase Polymerization

An advantage of solid-phase polymerization (SPP), also described here as the semi-covalent approach, is that it permits control over the orientation and placement of the template in relation to the monomers. This orientation depends on several factors, including the solid support's chemical functionality, size, the structural complexity, and solubility of the target. Furthermore, it allows the imprinting of insoluble templates by attaching them to a soluble carrier, which is required to detect small molecules in clinical and environmental settings. [4,53,59,65,79]

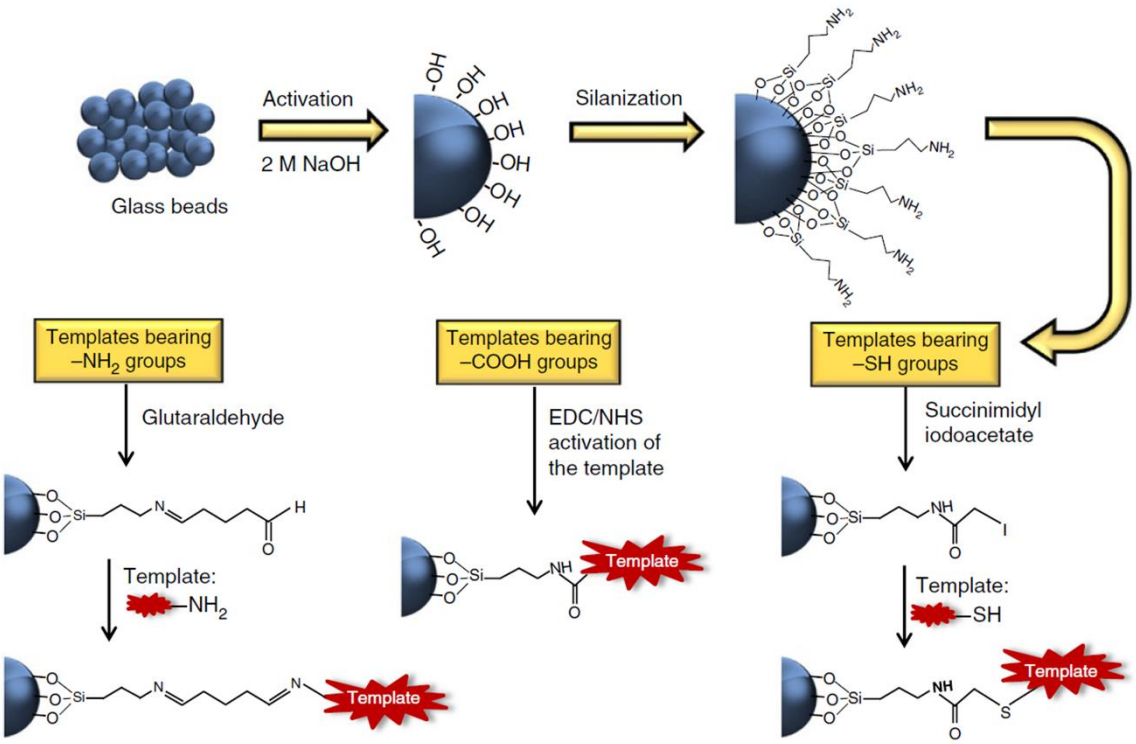


Figure 3.10. *Approaches for target conjugation based on target's bearing groups. Retrieved from* [80]

As shown in Figure 3.10, the target's functional groups dictate the immobilization approach to attach to the solid substrate. N-(3-dimethylaminopropyl)-N'-ethylcarbodiimide (EDC)/N-hydroxysuccinimide (NHS) coupling is a method for attaching -COOH groups to solid phase templates. However, glutaraldehyde (GA) may be used to generate a Schiff base, which can immobilize templates containing -NH2 groups. The reactivity of thiols with haloacetyl groups allows for the immobilization of templates with -SH groups, such as peptides with a cysteine residue for directed immobilization, via N-succinimidyl iodoacetate or bromoacetate.[80] [80–83]

Selecting functional monomers for nanoMIPs via SPP is analogous to the conventional methods of producing MIPs. Another option is to modify previously reported MIP compositions to obtain functional monomers that meet the requirements, i.e., adjust the cross-linker/monomer/initiator ratios while incorporating new monomers according to the desired noncovalent interactions with the template. Additionally, monomers with specific properties might be incorporated in order to generate multifunctional nanoMIPs with electroactive or optical features. Moreover, their surfaces could be further modified with stabilizing agents, such as PEG, to avoid agglomeration. [14,40,84–88]

The presence of a cross-linker in the polymerization mixture significantly impacts the nanoMIP's binding properties and morphological characteristics. In conventional MI techniques, the cross-linker is present in high concentrations, up to 90 mol%. However, in the SPS method, it is present in low concentrations, usually not exceeding 2 mol%, where the main contribution to molecular recognition

properties are given by the dominant functional monomers in the pre-polymerization mixtures.[4,5,14,63] The difference in cross-linking degrees of the polymer can also affect its stiffness and structural stability, where a low value may result in excessive chain flexibility, making it difficult for the polymer structure to rearrange itself in the binding sites around the ligand, reducing the nanoMIPs' binding affinity. [32,63,89,90]

However, as the degree of cross-linking rises, the binding sites become more structurally stable, and the polymer's three-dimensional structure becomes proportionately more rigid. When the polymer reaches a particular cross-linking degree, approximately 10 mol%, rearrangement of the binding sites around the ligands becomes challenging, resulting in a loss of binding affinity.

nanoMIPs produced via SPP may be synthesized in two ways: (i) an aqueous-based approach using persulfate-initiated polymerization, and (ii) an organic solvent-based approach employing a UV-initiated procedure. The target's molecular characteristics dictate the choice of technique; for instance, the aqueous-based approach involves imprinting peptides and proteins onto water-soluble monomers, where proteins may retain their native state and structural stability, facilitating their binding availability. The organic solvent-based approach, on the other hand, has demonstrated a greater efficacy in imprinting small molecules. This is due to water forming hydrogen bonds which disrupt the M:T interactions. Therefore, while larger proteins can be imprinted in aqueous media, the organic solvent approach is more suitable for imprinting water-insoluble molecules with limited chemical functionalities and, therefore, interaction sites with the monomer, as happens with many small molecules. [35,36,59,91–93]

Usually, monomers (such as methacrylic acid (MAA) or acrylamide) and cross-linkers (such as TRIM or EGDMA) are commonly used for UV-initiated processes, and their selection is depending on the template. TRIM is often used over EGDMA because of superior recognition capabilities, and, with the incorporation of an iniferter (initiator, transfer agent, and terminator in one molecule), such as benzyl diethyldithiocarbamate, particle size might be even more precisely tuned than with other radical polymerizations; i.e., as the growth rate of the polymer chains is more consistent, it allows the progressive grafting of numerous layers around the particle core. A small quantity of a chain transfer agent (such as alkyl thiols) may be added to further tune the polymerization process. [94–96]

Redox polymers and ferrocene derivatives have many desirable characteristics, including rapid electron transfer, and redox stability, making them perfect for use as mediators and reporters. In nanoMIPs, the reporting mechanism is closely linked to the template recognition at the binding sites since a conformational change of the polymer can affect the density of ferrocene moieties exposed on their surface, leading to a detectable electrochemical signal change that can be used to analyze the binding behavior (as illustrated in Figure 3.11). [50,53,97–100]

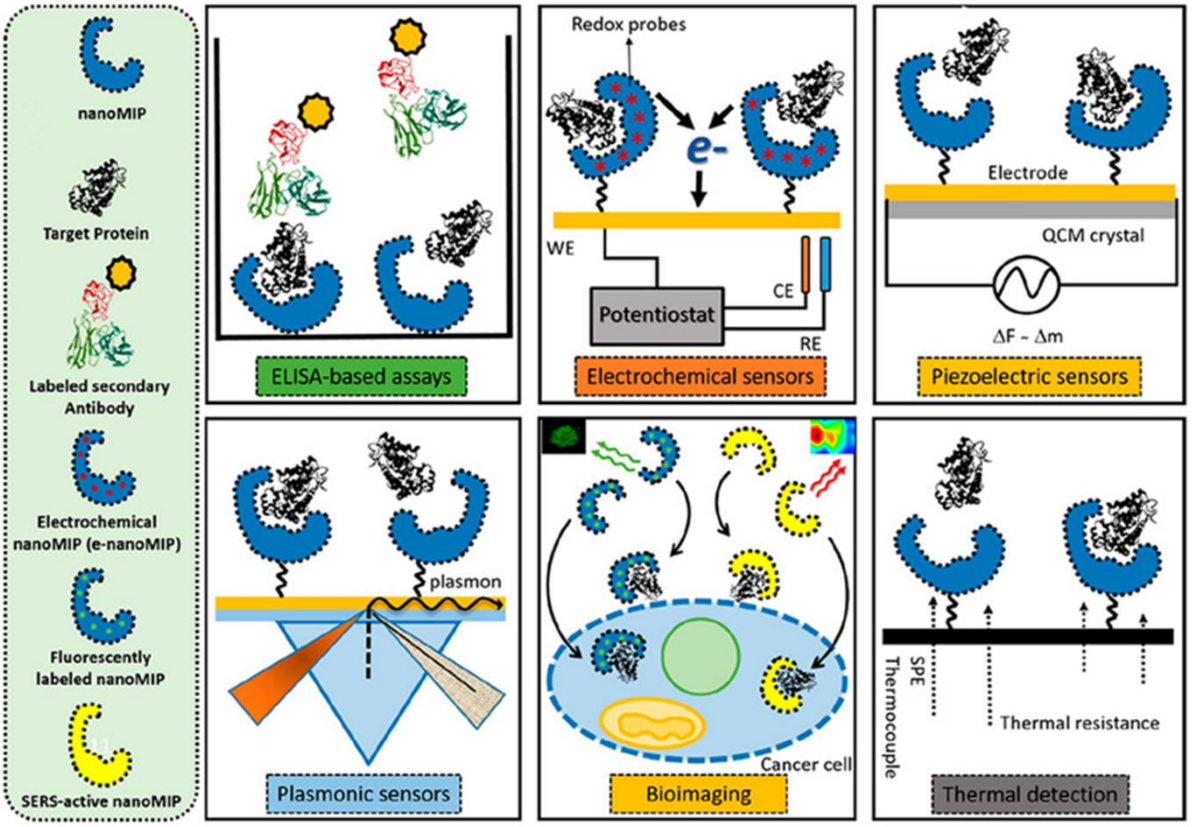


Figure 3.11. *Several applications of nanoMIPs-based sensors based on their transduction principle, including optical (ELISA, plasmonic, bioimaging) electrochemical, piezoelectric, and thermal. Adapted from* [100].

3.1.4. Applications and Limitations

The current use of enzymes and antibodies in diagnostics is widespread. Still, it is essential to consider their drawbacks, such as manufacturing periods, in vivo nature, high production costs, and limited stability, especially under extreme pH and temperature conditions. Additionally, these bioreceptors have a short shelf-life at ambient temperature. These limitations may be addressed by using (nano)MIPs, which offer advantages such as avoiding the need for animal involvement in synthesis and being a more cost-effective solution. Furthermore, the tailored design of (nano)MIPs makes them suitable for various targets, exhibiting exceptional stability and sensitivity. Given that (nano)MIPs do not require a cold chain, they can be utilized in chemosensors or assays deployed in remote areas where ambient temperature storage is the only viable option. [37,53,101,102] Some examples are shown in Figure 3.12

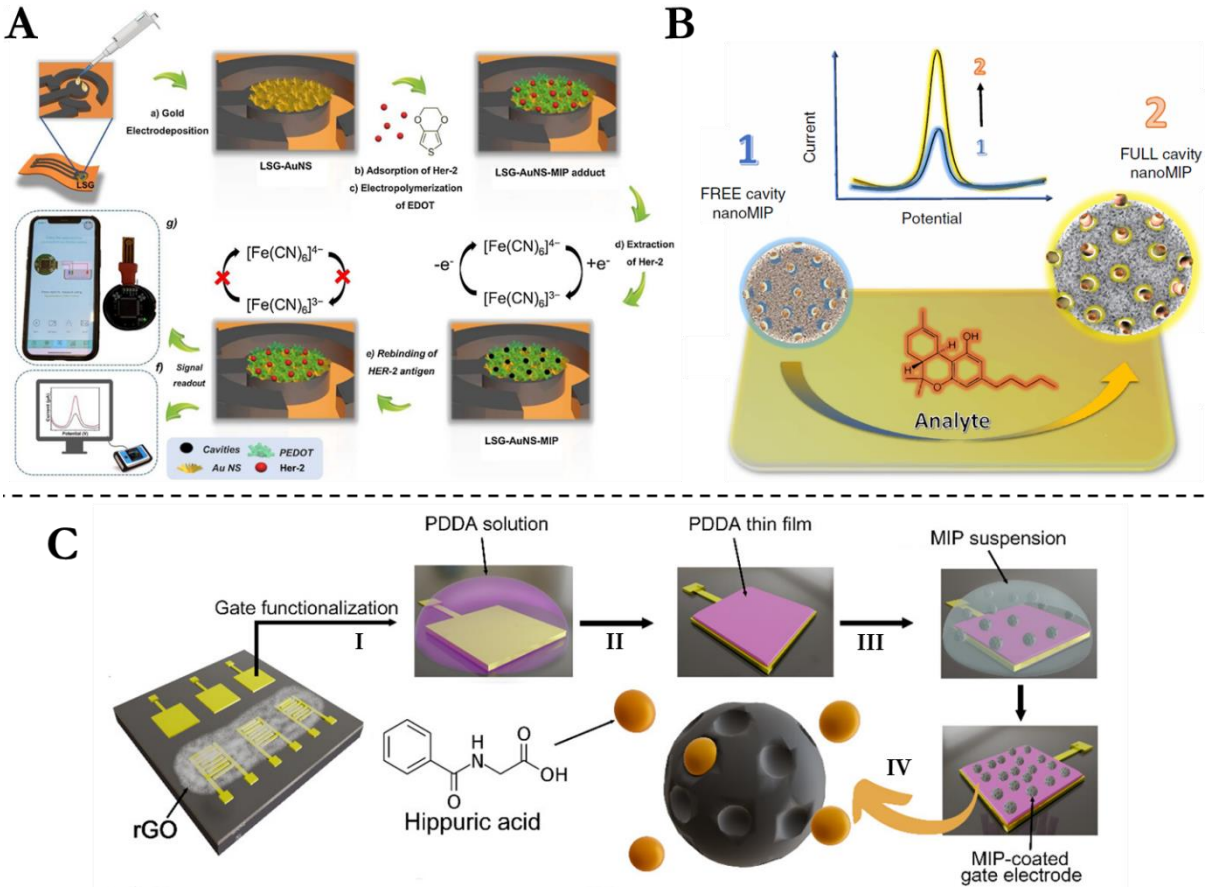


***Figure 3.12**. Several (nano)MIPs examples for electrochemical applications: (A) e-MIP for the detection of HER-2 antigen. Retrieved from* [103]*; (B) nanoMIP-based sensor for the detection of tetrahydrocannabinol (THC). Retrieved from* [78]*; (C) nanoMIP-based sensor for hippuric acid. Retrieved from* [104]*.*

As aforementioned, nanoMIPs are promising alternatives to antibodies, as evidenced by their current application in several diagnostic fields (Figure 3.13), with recent successful uses in cells and in vivo experiments, highlighting their diagnostic potential. Nevertheless, optimizations are needed in synthesizing nanoMIPs, specifically in achieving uniform particle sizes, homogeneous binding sites, and large-scale production. The SPP synthesis has proven to be the most widely applicable and cost-effective method for producing synthetic molecular receptors with antibody- and enzyme-like properties. Due to their unique ability to penetrate cell membranes, they are promising approaches to target intracellular proteins that have previously been challenging to access. [77,105,106]

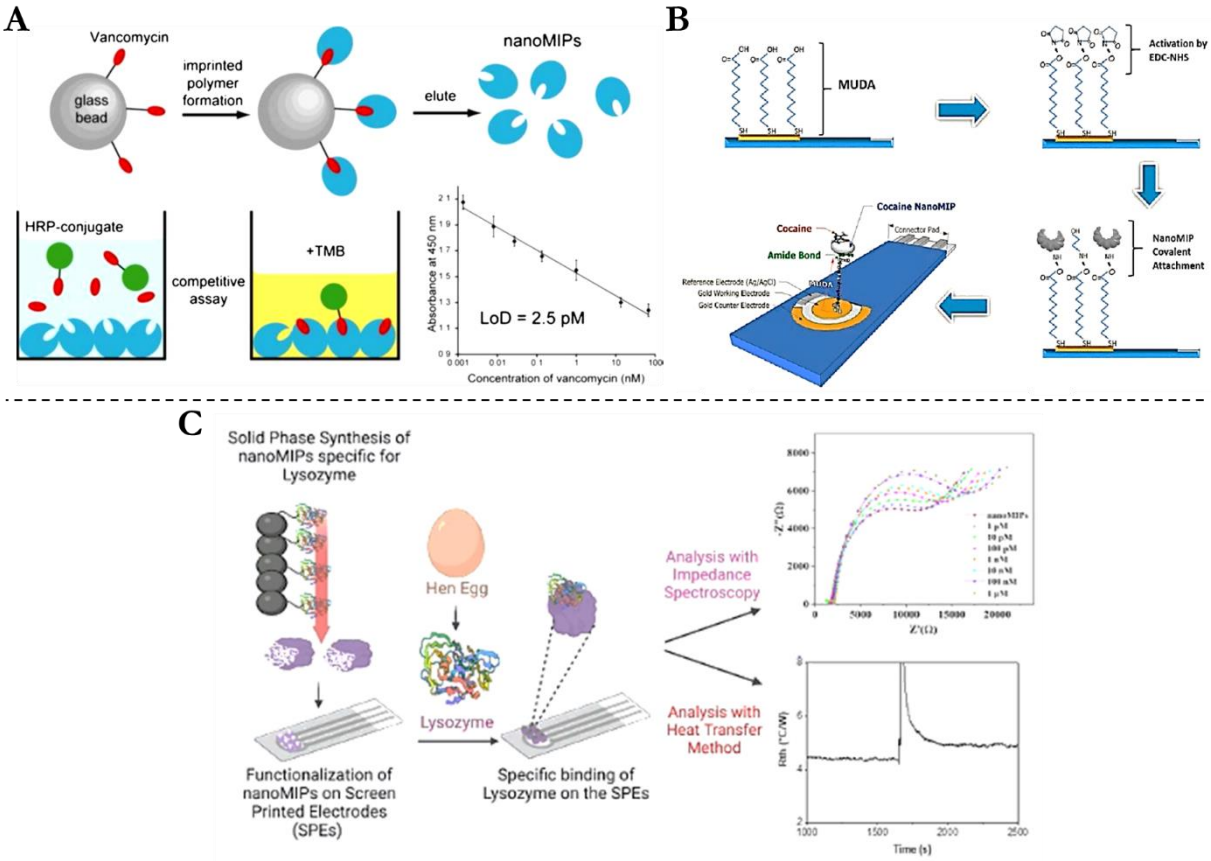


Figure 3.13. *Several examples of nanoMIPs (via SPP) in several applications: (A) vancomycin nanoMIPs for enzyme-linked molecularly imprinted nanoparticle assay. Retrieved from* [60] *. (B) electrochemical detection of cocaine. Retrieved from* [91]*; (C) impedimetric lysozyme detection. Retrieved from* [67].

The SPP technique could also be fully automatable, making it a potential choice for large-scale manufacturing of nanoMIPs-based chemosensors. Major corporations have shown a keen interest in nanoMIPs, such as MIP Discovery. As a result, it has become essential to develop operator-independent procedures for synthesizing nanoMIPs. There are difficulties in the large-scale synthesis of MIPs, much research has been devoted to addressing this.[62,107] One noteworthy example is the work of Piletsky et al., who have developed an automated SPP reactor to reproducibly fabricate nanoMIPs on an industrial scale (Figure 3.14), leading to improved batch-to-batch repeatability, enhanced reaction yield and, most importantly, the reduction of human error and increased throughput. With this automated reactor, it has become possible to create functionalized nanoMIPs, including those with fluorophores, electroactive groups, or PEG, as well as nanoMIPs with a uniform distribution of binding site affinities (typically one recognition cavity per nanoparticle). [5,77,108]

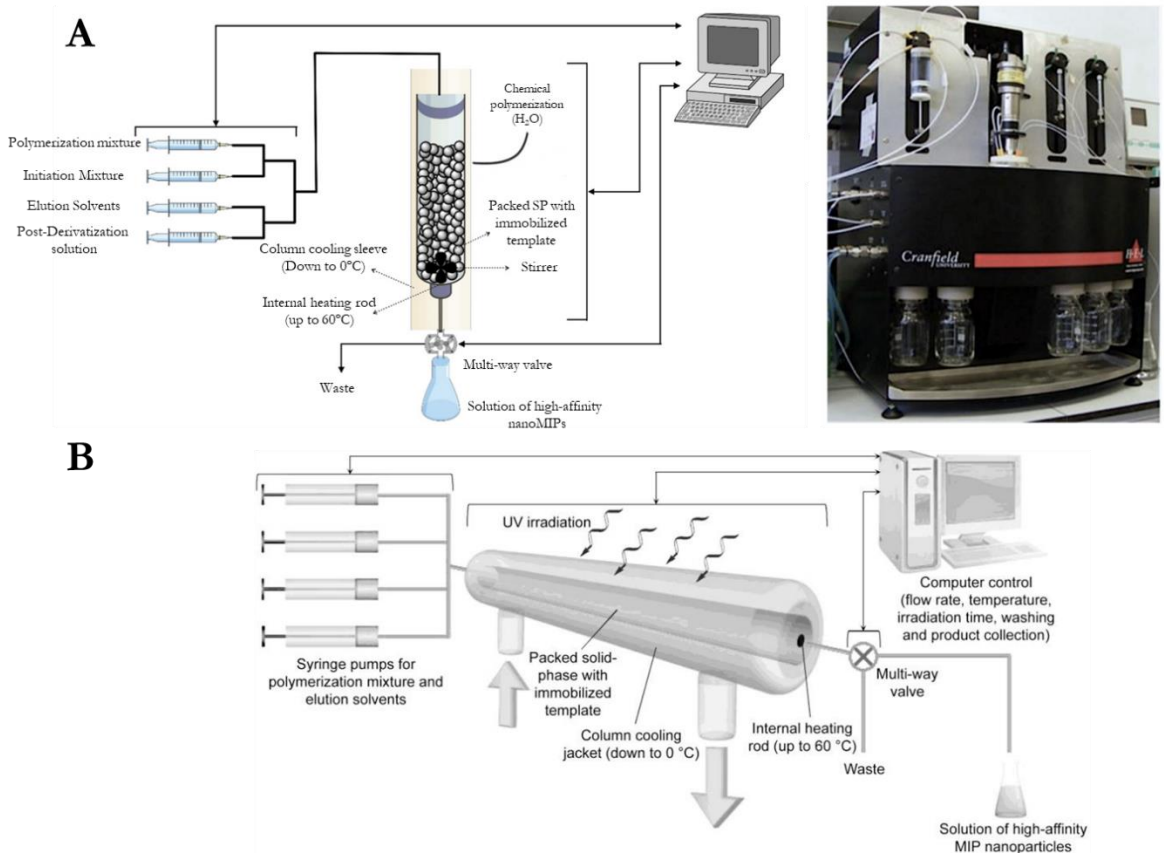


Figure 3.14. *Automated reactor for nanoMIPs fabrication via (A) chemical polymerization in H_2O. Retrieved from* [88]*; and (B) photopolymerization in Acetonitrile. Retrieved from* [109]

Unlike traditional bioreceptors, (nano)MIPs can be reused without losing their "memory effect" as long as the imprinted cavities remain stable. Moreover, as non-proteins, MIPs are not susceptible to degradation by bacteria or proteolysis. Furthermore, lateral flow tests and microfluidics using nanoMIPs are anticipated in the coming years, with the latter potentially enabling multiplexed analysis via fluorescent, colorimetric, or electrochemical readout within a single chip. [110,111]

In summary, MI shows promising potential despite facing several challenges. Although achieving optimal imprinting efficacy and selectivity, especially for complex molecular structures, remains a formidable obstacle, there has been significant progress in this field. Incorporating hierarchical structures, multisite imprints, and nanomaterials into MIPs has improved their functionality and adaptability, which has opened up a wide range of applications where customized synthetic receptors with specific recognition characteristics can be developed. The continuous expansion of MI applications and the refinement of imprinting processes have contributed to the growing influence of MIPs across diverse scientific and technological domains.

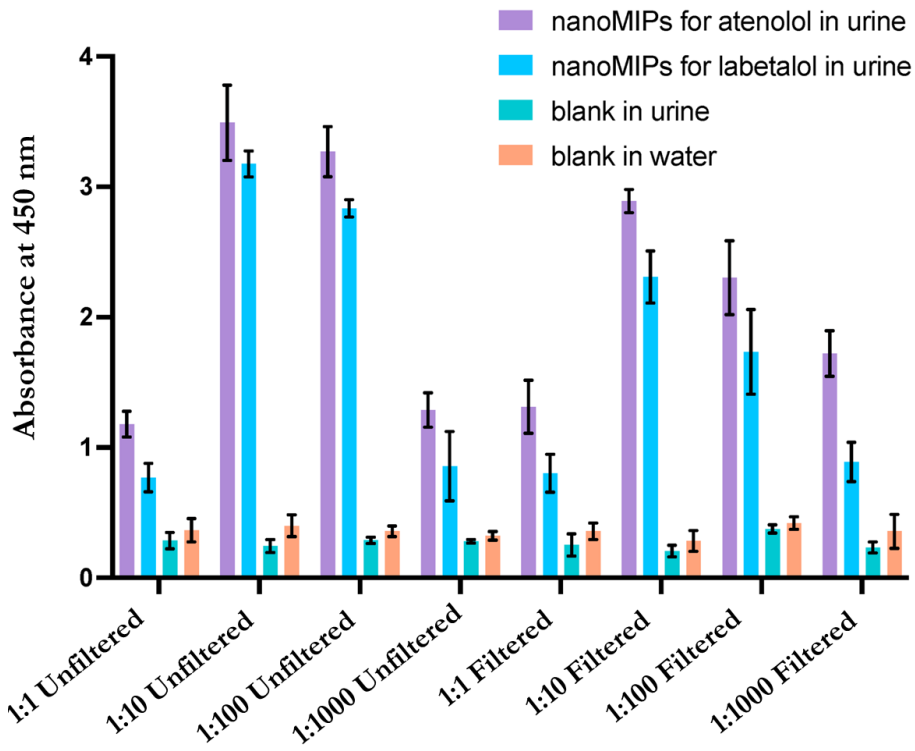


Figure 3.15. *Responses obtained in human filtered and unfiltered urine for different dilutions of the HRP-Atenolol and HRP-Labetalol conjugates and controls. Adapted from* [112]

3.1.5. Proposed Approach

This chapter seeks to offer an analysis of the experimental approaches utilized in the development of MIPs and nanoMIPs for the electrochemical detection of ACLF-associated small-molecule biomarkers, namely kynurenic acid (KA) and N-acetylneuraminic acid (NANA). Briefly, the focus will be on two projects: (i) feasibility study on e-MIPs for KA determination, which aims to refine the development of e-MIPs for KA detection through spectrophotometric analysis, electrode surface characterization, and optimization of electropolymerization and template removal; (ii) e-nanoMIPs for KA and NANA detection, which will focus on synthesizing and characterizing nanoMIPs, optimizing DPV parameters, and evaluating sensor stability and specificity. The primary objective is to further the practical application of MIPs and nanoMIPs in clinical diagnostics, thereby contributing to the development of reliable sensor devices for the prognosis and monitoring of ACLF-associated biomarkers.

3.2. OBJECTIVES

This chapter aims to provide a comprehensive overview of the experimental approaches employed in developing e-MIPs and e-nanoMIPs for electrochemical detection of ACLF-associated small-molecule biomarkers. This chapter is structured around two primary projects:

In Project 1, the main objective will be developing e-MIPs for KA sensing. The first part of the project involves conducting spectrophotometric analysis to explore the binding interactions between o-phenylenediamine (o-PD) and kynurenic acid (KA). Following this, the focus will be on characterizing the electrode surface to gain insights into its electrochemical properties and any surface modifications. Another significant aspect of this project is optimizing the electropolymerization process and template removal. Various approaches were explored for electropolymerizing o-PD in the presence of KA, as well as removing the template from the polymer matrix to create the necessary binding sites.

The second project involves the synthesis of nanoMIPs via SPP, which also incorporates electroactive monomers. The characterization of nanoMIPs includes (i) performing the Dansyl Chloride test to confirm target conjugation, (ii) utilizing DLS measurements to determine size distribution and stability, (iii) conducting bead-ELISA for a qualitative assessment of binding capacity and specificity, and (iv) employing the solvent evaporation method to evaluate the yield of the synthesized nanoMIPs. Furthermore, the project also study the optimization of DPV parameters to enhance the sensitivity and accuracy of electrochemical measurements. Additionally, the temporal and cyclic stability of the nanoMIPs will be studied to ensure reliable performance, and the targets will be quantified by determining key analytical parameters such as the limit of detection (LoD), dissociation constant (KD), and limit of quantification (LoQ).

3.3. MATERIALS AND METHODS

3.3.1. Materials

KA (C10H7NO3, MW = 189.17 g/mol), oPD dihydrochloride peroxidase substrate (C6H8N2·2HCl, MW = 181.06 g/mol), DMSO (C2H6OS, MW = 78.13 g/mol, 99.9 %), tetrabutylammonium bromide (TBAB, C16H36BrN, MW = 322.37 g/mol), Phosphate Buffered Saline tablets (PBS), potassium chloride (KCl, MW = 74.55 g/mol, d = 1.98 g/mL, 99.0-100.5 %), acetic acid (C2H4O2, MW = 60.05 g/mol, d = 1.049 g/mL, 99.8-100.5 %), and sodium acetate (C2H3NaO2, MW = 82.03 g/mol) were purchased from Sigma-Aldrich. Potassium Hexacyanoferrate (III) (Ferri, K3[Fe(CN)6], MW = 329.26 g/mol) and Potassium Hexacyanoferrate (II) 3-hydrate (Ferro, K4Fe(CN)6·3H2O, MW = 422.41 g/mol) were purchased from ITW Reagents (Spain) . Sodium hydroxide Standard Solution (NaOH, 0.1 M) was purchased from Fluka, ethanol (EtOH, C2H6O, MW = 46.07 g/mol, 96%) from Labbox.

Stock 10mM solutions of PBS in Milli-Q water, and TBAB in both EtOH and Milli-Q water, were prepared. Acetate Buffer (AcB) was prepared from acetic acid and sodium acetate, obtained from Sigma Aldrich, at a final concentration of 5 mM, pH 5.2. Finally, the ferro/ferricyanide redox solution contained 5 mM equimolar concentration of potassium ferro- and ferricyanide and 0.1 M KCl in Milli-Q water. Screen printed gold (SPGE, C220AT) and carbon electrodes (SPCE, C11L) were obtained in Metrohm DropSens, Spain.

N-acetylneuraminic acid (NANA), tryptophan (Trp), and quinolinic acid (QA), acrylamide (AAm) N-isopropylacrylamide (NIPAm) N,N-methylene-bis-acrylamide (BIS), ethylene glycol dimethacrylate (EGDMA), trimethylolpropane trimethacrylate (TRIM), itaconic acid (ITA), 2-hydroxyethyl methacrylate (HEMA), pentaerythritol tetrakis(3-mercaptopropionate) (PETMP), N,N-dimethylformamide (DMF), N,N-diethyldithiocarbamic acid benzyl ester (Iniferter), 1-ethyl3-(3-dimethylaminopropyl)-carbodiimide hydrochloride (EDC), N-hydroxysuccinimide (NHS), 2-(N-morpholino)ethanesulfonic acid (MES) and [3-(2-Aminoethylamino)propyl]trimethoxysilane (AEAPTMS, or DAMO) and 1,2-Bis(triethoxysilyl)ethane (BTSE) were purchased from Sigma-Aldrich, UK. Ferrocenylmethyl methacrylate (FcMMA) Acetonitrile (ACN), Dimethylformamide (DMF), Dansyl chloride (DNSCL) ethanolamine, tris(2-carboxyethyl)phosphine (TCEP). 6-mercaptohexanoic acid (MCH), and 11-mercaptoundecanoic acid (MUA) was obtained from Aldrich (Deisenhofen, Germany). Glass beads (Spheriglass 2429 CP005 53-106 μm diameter) were purchased from Blagden Chemicals, UK. In all experiments, milli Q water was used. All chemicals and solvents were of analytical or HPLC grade and used without further purification. Glass funnel filter with sintered glass (GFF-SG) from Sigma-Aldrich. Acetic anhydride (AAn) was provided by University of Leicester. Synthetic urine was prepared following a previously reported study.

3.3.2. Methods

3.3.2.1. e-MIPs

3.3.2.1.1. Characterization of the precomplex

Precomplex solutions were prepared using a 4:1 M:T ratio in three different solvents: PBS, TBAB in EtOH, and AcB. Stock solutions of 50 Mm KA and oPD were prepared in DMSO and then diluted to concentrations of 0.5 mM and 2 mM, respectively, in the solvent being studied (at a 1:4 ratio). The solutions were then further diluted in a 1:10 ratio (to avoid signal saturation due to high concentrations) and analyzed using UV-Vis spectroscopy on a SHIMADZU UV-1900 spectrophotometer. All measurements were taken using the same quartz cuvette, which was cleaned with acetone and ethanol between measurements.

3.3.2.1.2. Electropolymerization

The electropolymerization (EP) was carried out with Autolab potentiostat (PGSTAT302N) with a connector for commercial ceramic electrodes, which were SPCE. WE and CE are carbon and RE electrode is Ag/AgCl. The MIPs synthesis was performed based on previous studies, although some parameters were adapted. Initially, each electrode was subjected to an electrochemical cleaning procedure, which consisted of cleaning the electrode using 10 cycles of CV between -0.2 – 1.5 V at 100 mV/s in 0.5 M H_2SO_4. Afterwards, EP was carried out with either Cyclic voltammetry (CV) or Chronoamperometry (CA). For the CV, the parameters were potential range of 0.2-0.8 V, 10 cycles at 25 mV/s (step potential: 0.01 V); whereas for CA were 0.9 V was imposed for 10 min.

3.3.2.1.3. Template Removal

Once polymerized, the template removal process was attempted using several approaches: chemical, via incubations with several solvents (NaOH, DMSO, etc) with/out agitation; electrochemical using CV with a potential window of 0-1.3 V, 5 cycles at 25 mV/s (step potential: 0.01 V), or CA (1.2 V for 5 mins several times).

For surface characterization purposes, a CV was performed between each step using 5 mM Ferro/Ferricyanide (3 cycles), checking the respective redox peaks and the shape of the voltammogram. Afterwards, the electrodes were thoroughly cleaned with milli-Q water and gently dried with N2 after each step and measurement. In parallel, the respective NIP was also prepared as the negative control by following the same steps but without the target molecule in the solution.

3.3.2.2. nanoMIPs

3.3.2.2.1. Silanization of glass beads

A 4 M NaOH solution was prepared for 200 g of GBs by adding 64 g of NaOH to 400 mL of DI H2O (NaOH was added first, then DI H2O slowly while in stirring conditions). Before weighing the GBs, they were passed through a sieve tower using the top 125 μm sieve and weighed 200 g of GBs (65-125 μm size) on a dry recipient using a funnel. The GBs were mixed with 4 M NaOH in a round-bottom flask and incubated for 15 minutes at 100 ºC, using a heating jacket to maintain the heat. The filter was washed with GFF-SG and DI H2O under vacuum and a filtering flask was used to collect the waste.

To complete the process, the hot GBs solution was poured onto GFF-SG before adding an excess of DI H2O, 5 mM PBS, and then DI H2O again. The beads were dried under vacuum adding acetone and vacuuming until completely dry, obtaining a powder-like substance. Once dried, the GBs were placed on a metal tray in an oven at 120-150 ºC for 30-45 mins to ensure complete dryness.

A silane solution was prepared by mixing 12 mL DAMO (6% v/v), 6 mL BTSE (3% v/v), and 182 mL dry toluene. The solution was added to the dried GBs in a round bottom flask and swirled slightly, placed on a heater with open reflux and incubated for 6-8 h at 110 ºC, avoiding toluene evaporation. The silanized GBs (sGBs) solution was swirled in toluene, poured it into GFF-SG and added to hot dry toluene. Then, once at RT, dry acetone was added with vacuum waiting for 20-40 mins until it was completely dried. The sGBs looked like powder without any acetone smell. Finally, the sGBs were stored for further conjugations at 4 ºC, and covered with parafilm.

3.3.2.2.2. Dansyl Chloride Test

3 mL of DNSCL solution (10 mg/mL in DMF) was prepared and poured into 1g of GBs, sGBs or target-conjugated GBs. Both bead solutions were incubated in dark conditions for 1 hour. After the incubation period, a solid-phase extraction (SPE) cartridge was used to wash them both with excess DMF at RT and subsequently tested for fluorescence signal under a UV lamp. The aminated bead should appear fluorescent.

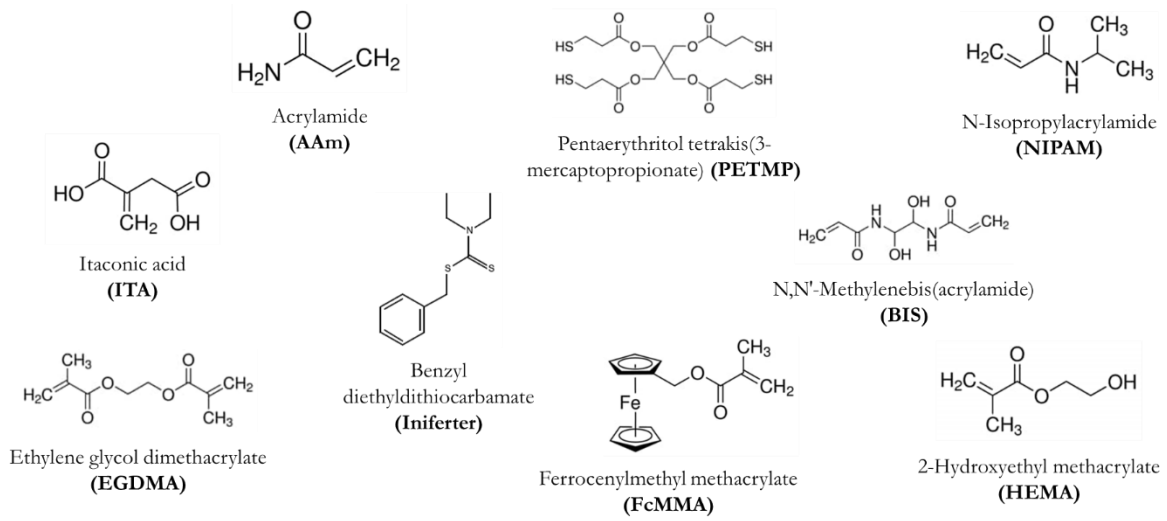
3.3.2.2.3. NanoMIPs fabrication

To immobilize the targets NANA or KA on GBs, 30 g sGBs and 60 mL of 10 mM PBS were used. Briefly, 24 mL of 10 mM PBS was added to the sGBs, swirled, and then 1.86 g EDC (161.7 mM), 1.68 g NHS (243.28 mM), and 300 mg NANA (16.16 mM) were added, and volume was made up to 30 mL with 10 mM PBS. The solutions were mixed, vortexed, and incubated for 45 mins. The target-conjugated GBs were poured into a SPE cartridge and 200 mL of 10 mM PBS and 200 mL of DI H2O were added for washing purposes. Vacuum was gently applied so the beads were left wet.

60 mL of 2.5% v/v Acetic Anhydride (AAn) was prepared by mixing 1.53 mL of AAn with 58.47 mL of Acetonitrile (ACN). This solution was mixed with the target-conjugated GBs and incubated for 30 minutes with gentle stirring to block any unreacted amine groups. Then, the solution containing the modified-GBs was poured into the SPE cartridge, 200 mL of ACN and 200 mL of DI H2O were added, and vacuum was applied until completely dry. The modified GBs were used directly for polymerization or stored at 4ºC. DNSCL test was performed to confirm the blocking of free amines with NANA and AAn.

3.3.2.2.4. Photopolymerization procedure

Each reagent (see Table 1) was dissolved separately in 1 mL of ACN and vortexed vigorously until complete dissolution. For BIS and ITA, 5 mL of ACN was used for their dissolution, and if necessary, sonication was used to help dissolve them. The solutions were mixed, the container was filled with ACN, purged with N2, sonicated, and then the dry beads were added. The solution was exposed to UV for 3 minutes, then a cold wash was performed using 200 mL of ACN, and 200 mL of cold DMF (previously cooled in the freezer 1h prior to the step) were placed in an SPE cartridge. Finally, a hot wash was carried out using 2x 50 mL of 65-70ºC EtOH, and the filtered solution was collected and concentrated using a rotary evaporator until 3-10 mL remained. The obtained cloudy solution was used for experiments or stored in a covered flask at room temperature.



Scheme 3.1*. Monomer composition for the synthesis of nanoMIPs*

Table 1. *Monomers and crosslinkers used for KA- and NANA-nanoMIPs*

Reagent	Amount	Concentration (mM)
Acrylamide **(AAm)**	60 mg	24.118
N,N'-Methylenebis(acrylamide) **(BIS)**	85 mg	15.753
2-Hydroxyethyl methacrylate **(HEMA)**	56.96 µL	12.504
Itaconic acid **(ITA)**	22.5 mg	4.941
Ferrocenylmethyl methacrylate **(FcMMA)**	14 mg	1.408
Ethylene glycol dimethacrylate **(EGDMA)**	153.55 µL	22.133
Trimethylolpropane trimethacrylate **(TRIM)**	152.83 µL	12.904
N-isopropylacrylamide **(NIPAM)**	14 mg	3.535
Benzyl diethyldithiocabamate **(Iniferter)**	33.48 µL	3.996
Pentaerythritol tetrakis(3-mercaptopropionate) **(PETMP)**	7.03 mg	0.411

3.3.2.2.5. DLS and Solvent Evaporation

The hydrodynamic size of nanoMIPs was determined using dynamic light scattering (DLS). Prior to the measurement, the nanoMIPs solution underwent ultrasonication for 3 minutes and was subsequently analyzed at 25°C using a Nano-S Zetasizer. Yields were also determined by evaporating 100 µL aliquots of both target-specific nanoMIPs, which were dissolved in EtOH solvent, on sterilized glass slides, and then weighting the resulting dry mass.

3.3.2.2.6. nanoMIPs Immobilization on Gold Electrodes

The process for covalently immobilizing the e-MIPs onto the gold surfaces of screen-printed electrodes has been previously described and adapted to the experimental requirements. Briefly, SPGEs were electrochemically cleaned using 75 CV cycles from 0-1.25 V (vs. Ag RE) in 0.5 M H2SO4 (scan rate: 100 mV/s). Meanwhile, MUA was incubated with TCEP for 1h under dark conditions in order to reduce the disulfide bonds between MUA molecules. Then, 15uL of 200 uM MUA was drop-cast on the WE and incubated overnight (under dark and humid conditions, 4ºC). Then, TCEP and 5 mM MCH were incubated

for 1h under dark conditions. Afterwards, 15 uL of 500 uM MCH was dropcast onto the modified WE for 2h under dark and humid conditions.

Once the electrode was rinsed thoroughly with milliQ H2O, a solution of 1:4 EDC/NHS in 100 mM MES buffer was employed in order to activate the carboxylic groups of the MUA. Then, a solution of 1:5 nanoMIPs:MES was dropcast onto the WE, in order for the free amines on the nanoMIPs to bind to the activated carboxylic surface. After rinsing with MES buffer, an excess of ethanolamine (EtAm) was used to block any remaining unreacted succinimide. Finally, the electrodes were rinsed once with MES and thrice with 5 mM PBS and left under a drop of PBS until measurements for signal and conformational stabilization could be performed.

3.3.2.2.7. Electrochemical measurements

All experiments were carried out using an Ivium Octostat instrument. DPV was recorded from −0.2 to 0.6 V, at a scan rate of 25mV/s, a step potential of 1mV and potential amplitude 100 mV, and a pulse time of 5 ms vs a Ag RE and gold CE.

3.4. RESULTS AND DISCUSSION

3.4.1. e-MIPs for Kynurenic Acid determination

3.4.1.1. Spectrophotometric analysis of binding interactions

This section of the project concerned a feasibility study based on developing e-MIPs for detecting KA. Therefore, it was deemed prudent to start by analyzing the o-PD:KA interactions, as KA can exist in various charge states, determining the chemical properties of the biomolecule (Figure 3.16A). By analyzing the behavior under different solvents using UV-Vis spectroscopy, it was possible to identify three or four distinct peaks from the different ionic species present, as shown in Figure 3.16B: (i) 320 nm, corresponding to an equilibrium between cationic and anionic species; (ii) 330 nm representing the mono-anionic specie; (iii) 340 nm corresponding to the neutral keto form of KA; and (iv) 355-360 nm representing the protonated anion. Although the wavelengths may shift depending on the solvent used, these distinct peaks permit a better understanding of the chemical properties of the biomolecule in solution and how it might behave in different solvents. [113,114]

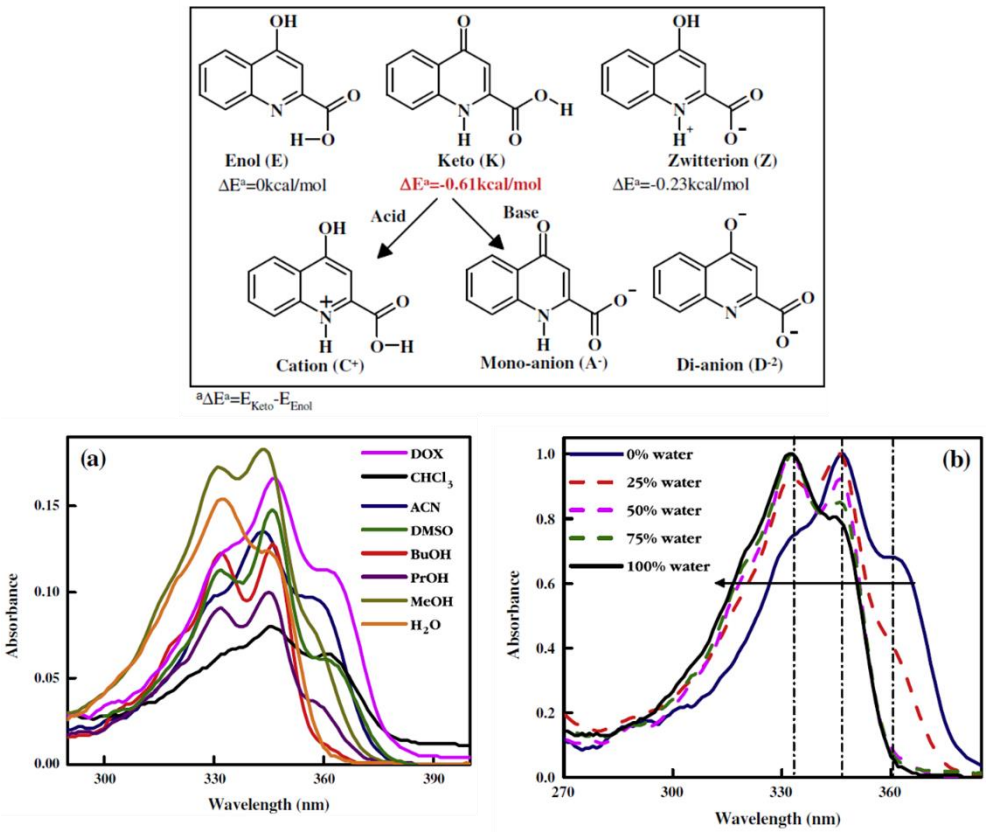


Figure 3.16. *Spectrophotometric analysis of KA under several solvents. A) Schematic representation of different KA species depending on pH and buffer nature; B) Absorption spectra of KA under different solvents at RT; C) effect of solvent mixture (organic (1,4-dioxane)+H_2O) on normalized KA absorption spectra. Retrieved from* [113]

This feasibility study investigated the impact of different solvents (PBS, AcB, and EtOH+TBAB) on the M:T interactions (oPD:KA) using spectrophotometric analysis. The results shown in Figure 3.17 and Figure 3.18 showed that the absorbance spectra of solutions that only contain oPD remained consistent across all the solvents tested, whereas the spectra of KA changed in each solvent. Even though there are relatively small absorbance differences between PBS and AcB, they exhibited similar overall spectra mostly due to the presence of mono-anionic species, which can be attributed to their aqueous nature and their similar dielectric constants (around 79). On the other hand, KA in TBAB in EtOH showed a distinct behavior, as EtOH is the most hydrophobic solvent of the three and has a dielectric constant of approximately 36, causing a shift in the KA species contribution ratio towards the keto form.

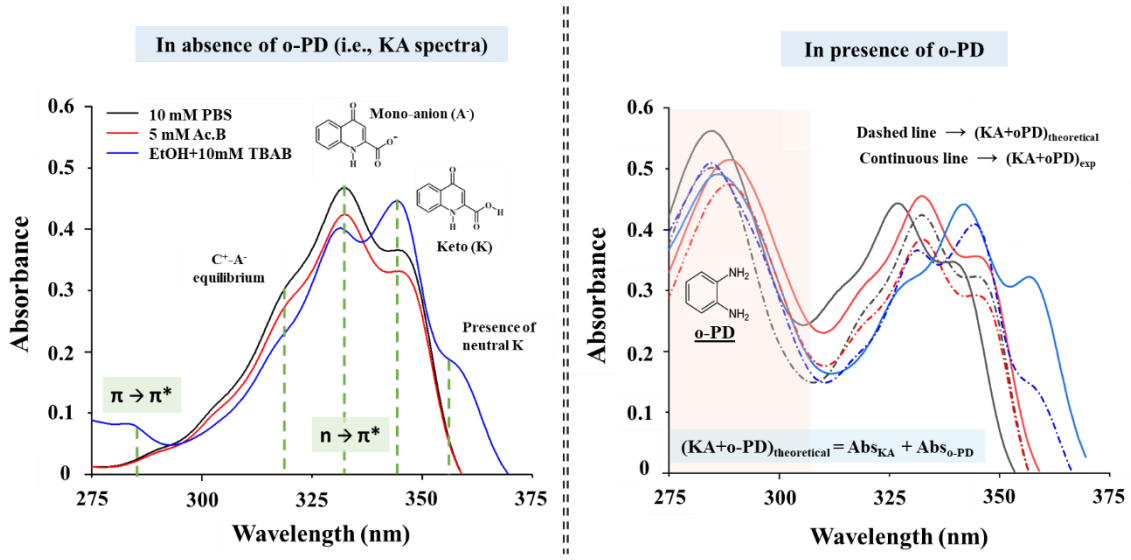


Figure 3.17. *Absorbance spectra of target:monomer interactions under several solvents. Dash and continuous lines indicate theoretical and experimental absorbances, respectively.*

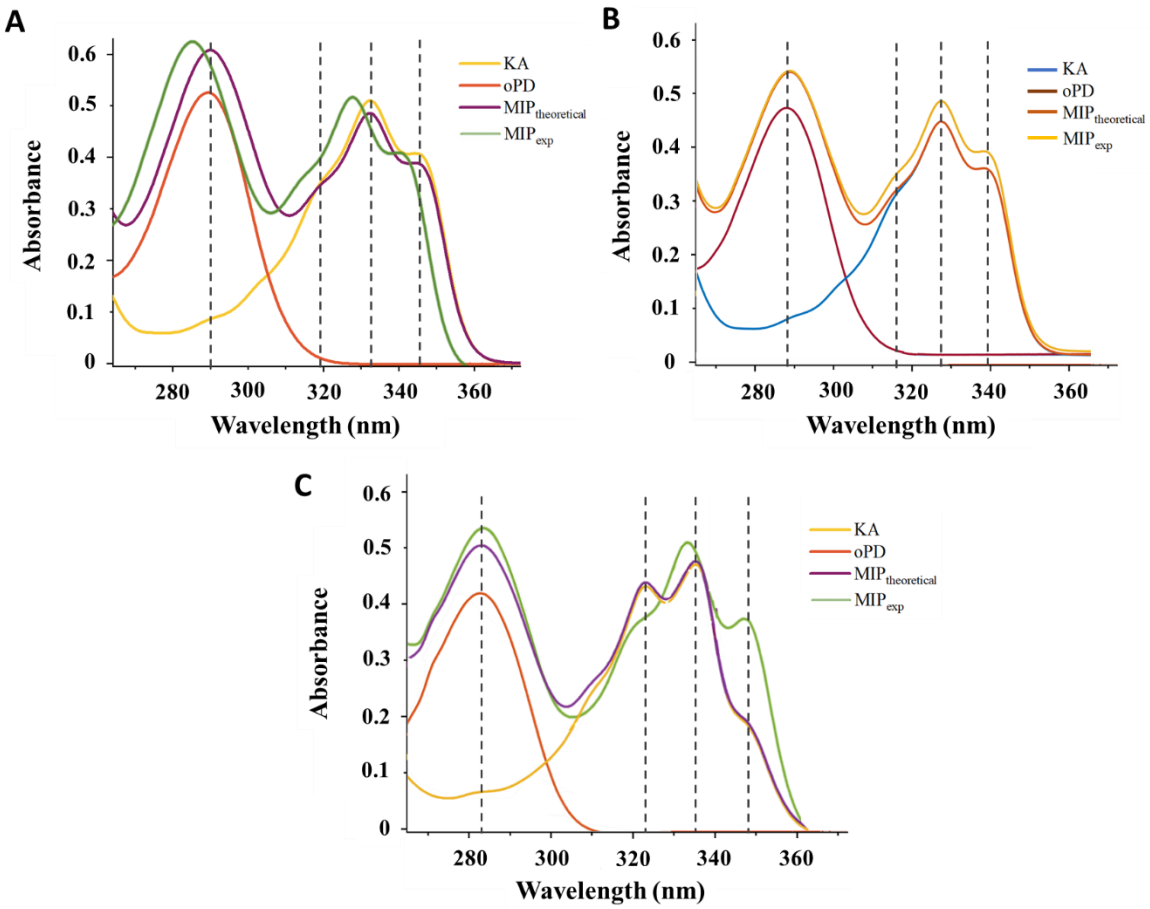


Figure 3.18. *Absorbance spectra of target:monomer interactions for (A) 10 mM PBS, (B) 5 mM Ac.B, and (C) EtOH + 10 mM TBAB*

When KA and oPD are combined (Figure 3.17 and Figure 3.18), the resulting spectra displayed differences between the calculated sum of template and monomer spectra (based on Beer's Law for multi-component systems[115–117]) and the experimental measurement. As shown in Figure 3.18A, in PBS, a blue shift in the wavelength and a slight increase in the absorbance is observed. Conversely, in AcB, no shift is detected, but the absorbance is also increased (Figure 3.18B). Furthermore, TBAB in EtOH elicits distinct changes in each KA peak, indicating a difference in the contribution of each ionic species (Figure 3.18). This suggests several noncovalent interactions between KA and oPD in EtOH, which might be stronger than in PBS and AcB. These results imply that KA and oPD exhibit different behaviors depending on the solvent used and that, in organic solvents, their interactions rely solely on M:T and do not compete with possible H-H bonds of the solvent.

It is noteworthy that the observed increase in the experimental spectrum, compared with the theoretical one, may result from a possible combination of π- π stacking between aromatic rings, H-H bonding, charge-dipole, and van der Wals forces between the desired molecules, hinting to a possible correlation to absorbance changes and wavelength shifts. Therefore, this feasibility study successfully demonstrated the impact of solvents on the M:T interactions.

3.4.1.2. e-MIPs Performance

3.4.1.2.1. Electropolymerization

To ensure accurate readings, it was important to perform an electrochemical activation procedure (in 0.5 M H2SO4) on the bare SPCE before using 5 mM Ferro/Ferricyanide solution as a redox label (Figure 3.19). This step established a reliable basis for subsequent measurements, as it helped to characterize the electrode surface. As expected, the current significantly decreased after electropolymerization due to the polymer partially preventing the diffusion of the electrolyte and redox probe to the electrode surface. After this, an increased shift at the peak currents could indicate the polymer porosity increasing.

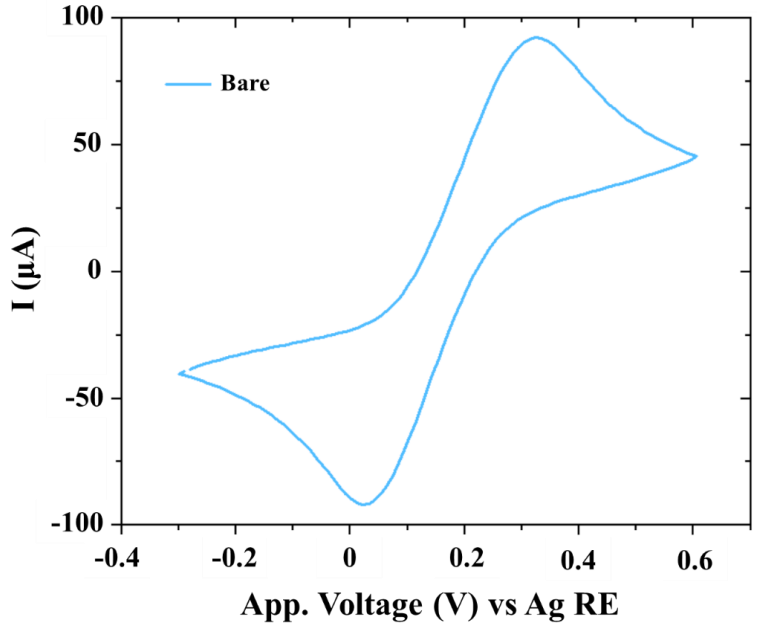


Figure 3.19. *Signal of the bare SPCE after 10 cycles of electrochemical activation in 0.5 M H_2SO4 activation using 5 mM ferro/ferricyanide*

Although EtOH+TBAB produced a more distinguishable response than other solvents in the spectrophotometric analysis (Figure 3.18C, green line), it was crucial to have a stable carbon surface before the polymer deposition. However, an organic solvent may destabilize and weaken the carbon surface, rendering it difficult to deposit the polymer. Additionally, the template and monomer are both organic molecules that may interact in solution, but they are likely too stable in the hydrophobic solvent to be deposited on the surface. This may result in polymerization occurring within the solvent as suspended polymer particles before being deposited. This precomplex solution may benefit other types of MIP polymerizations, such as photopolymerization, but could entail some drawbacks in electropolymerization scenarios. A more detailed analysis of the solvent's properties and M:T interactions could provide further insights into the polymerization process and the resulting characteristics of the final polymer.

Several electrochemical tests were conducted using CV and CA to investigate the effectiveness of TBAB as an organic salt for MIP synthesis in aqueous solutions. This was done after it was determined that ethanol (EtOH) was no longer a viable solvent option as the polymer matrix was unstable, which led to its

degradation. To carry out EP of NIP and MIP, three new solvents were used: 10 mM PBS, 10 mM TBAB in water, and 0.5 M Acetate Buffer (AcB).

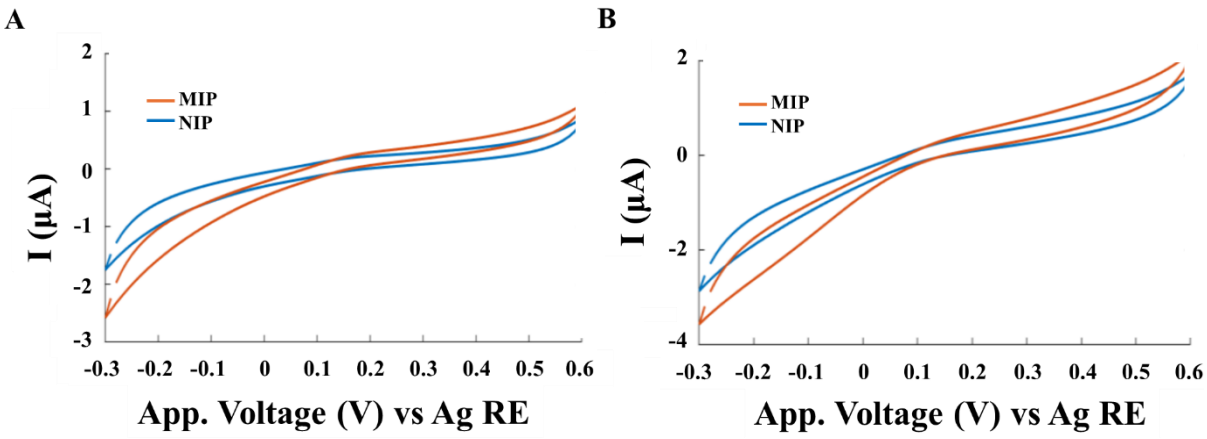


Figure 3.20. *Results obtained by EP in 5 mM PBS A) CA and B) CV.*

The results in Figure 3.20 and S1 exhibit that all EPs were successful (PBS shown in Figure 3.20). Similar signals were obtained for both NIP and MIP, except for the CV with TBAB in water. In this case, the resulting MIP showed a similar redox behavior as in the bare electrode, while the NIP signal did not exhibit the expected current decrease due to the presence of an insulating layer (polymer) on the electrode surface. Therefore, it was decided that all these electropolymerized electrodes should be taken forward to the removal step.

3.4.1.2.2. Template Removal

Upon removal of the template, the redox peaks are expected to increase. Nevertheless, even after the removal process, the peaks of the bare electrode are still expected to be higher than those of the polymer since the MIP remains on the electrode and offers a slight resistance to the current. The polymer also has the characteristic cavities for the template (KA), which influences the behavior of the voltammograms. Several removal procedures were tested, but many were unsuccessful. Those removal procedures that were found not to work included soaking the electrode in a solution of 0.1 M NaOH with/without stirring, drop-casting on the electrode, or soaking in a "removal solution" (0.1 M NaOH in EtOH:H2O 5:1) for 30 s to 10 mins min (See Figure S2). [33,38,41]

Several studies have shown that electrochemical removal, using either CV or CA, has yielded promising results. Figure 3.21 provides similar evidence for CA-based removal method, which involves 3 or 4 electric pulses at a voltage equal to the oxidative potential of KA. On the third pulse, it became apparent that there was a marked contrast between the NIP and MIP signals. While the NIP remained relatively constant, the MIP exhibited a significant surge in the Ferro/Ferricyanide redox peaks, proving that KA was released

from the polymeric matrix. Once the template is successfully re-bound, the peaks are expected to decrease considerably as the cavities get filled. The gradual decrease in peak height is indicative of the increasing concentration of the target bound to the MIP. Therefore, as the concentration of the target increases, the behavior of the voltammograms should tend towards but never exceed the voltammogram of the MIP prior to the removal process since there is a gradual increase in the surface concentration of the target.

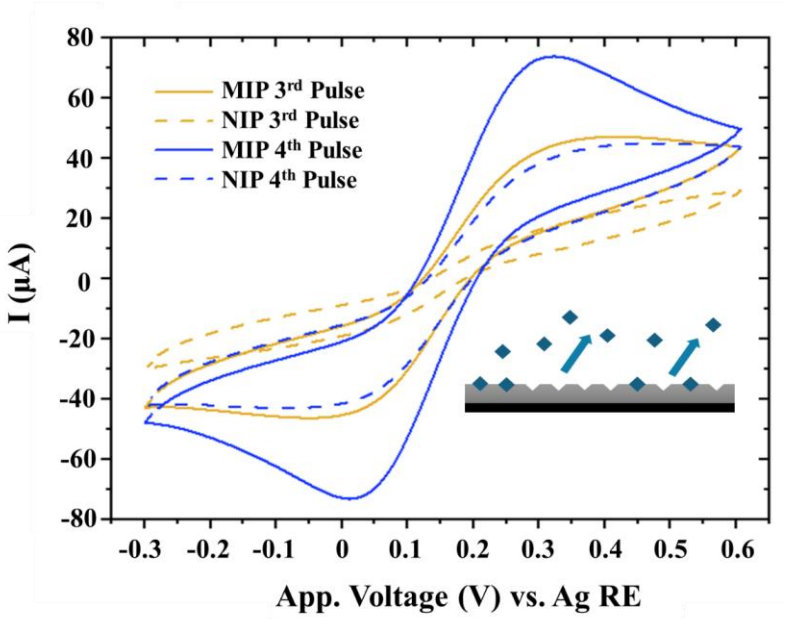


Figure 3.21. *Electrochemical template removal via sequential chronoamperometric measurements at 1.2 V for MIP and NIP.*

It is worth noting that both MIP and NIP showed an increase in the signal during the fourth pulse. Nevertheless, even with this increase, the MIP was still significantly different from the negative control, hinting at a higher KA release. It is also worth considering the potential damage to the polymer matrix or alterations in pore size as an opportunity for further exploration and optimization of the experiment. It's important to remember that this study is primarily focused on assessing the potential impact of the polymerization solvent on the sensitivity and electrochemical performance of the final platform, using o-PD and KA as a template monomer and target molecule.

3.4.2. nanoMIPs

Regarding the development of nanoMIPs, KA and NANA were utilized as target molecules for bead conjugation and subsequent electrochemical analysis. Based on and adapted from literature,[53,66,80,91] nanoMIPs were synthesized through solid-phase polymerization to achieve more uniformly distributed binding cavities on the surface of these supramolecular systems, leading to accelerated binding kinetics.

3.4.2.1. Fabrication

Briefly, there are three stages in the protocol for making nanoMIPs: (i) template immobilization, (ii) SPP, and (iii) nanoMIP purification and characterization.

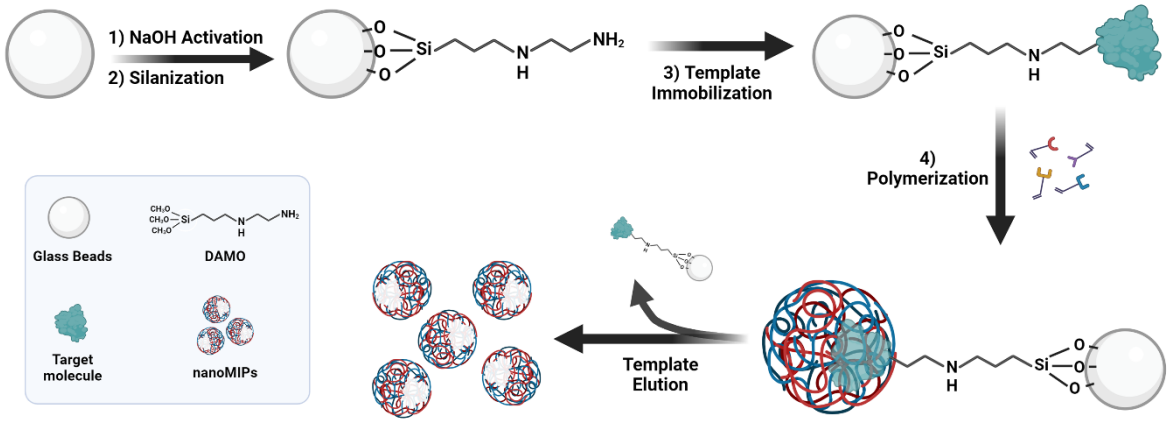


Figure 3.22. *Schematic representation of the procedure for nanoMIPs synthesis*

Well-established protocols were used to synthesize nanoMIPs with electroactive properties dictated by the FcMMA. Briefly, a mixture of monomers (see Figs. 3.8 and 3.1) undergoes a controlled polymerization in the presence of the template previously conjugated to glass beads, which are typically used as solid-phase support (see Figure 3.22).

3.4.2.2. Characterization and Verification

3.4.2.2.1. Dansyl Chloride Test

The DNSCL test is an important step in verifying that the targets (KA and NANA) were successfully conjugated onto the silanized GB (sGB). The test detects the presence of amines on the surface of the sGB by reacting DNSCL with primary and secondary amines to form a sulfonamide product with green or turquoise fluorescence, respectively. These results imply that the target's activated carboxylic groups were unable to bond to the DAMO's free amines; i.e., if there are primary amines in the beads' surfaces, the DNSCL test would give a green fluorescence, as shown in Figure 3.23B, because amine-terminated linkers were used. As the targets were immobilized via EDC/NHS, creating an amide bond on the GB, this would interfere with the DNSCL test, as fewer amines would be accessible (Figure 3.23C) and KA has no 1ry or 2ry amines in the pH and buffer used, only a pyridine ring. In the case of NANA conjugation, an interesting phenomenon was observed: the presence of secondary amines in the target interacted with the DNSCL resulting in a turquoise-like fluorescence (Figure 3.23D).[118,119] It is important to note that this observation does not affect the success of the conjugation process, as it only gave the fluorescence due to the presence of the target.

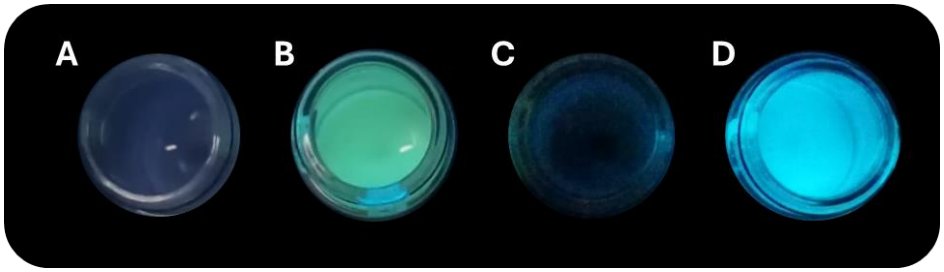


Figure 3.23. *DNSCL Test on GBs and modified GBs. (A) GBs, (B) sGBs, (C) KA-conjugated GBs, and (D) NANA-conjugated GBs.*

3.4.2.2.2. Dynamic Light Scattering

Target-specific nanoMIPs were further characterized by DLS, the results are represented in Figure 3.24. The obtained polydispersity index (PDI) for KA nanoMIPs was 0.036 with a hydrodynamic diameter (HD) of 135.8 ± 2.6 nm. Similarly, for NANA nanoMIPs, the PDI was 0.089 with a hydrodynamic diameter of 147.1 ± 0.7 nm. These results strongly correlate with those found in the literature with nanoMIPs for small molecules, such as histamine, glucose, cortisol, and testosterone. [53,120,121]

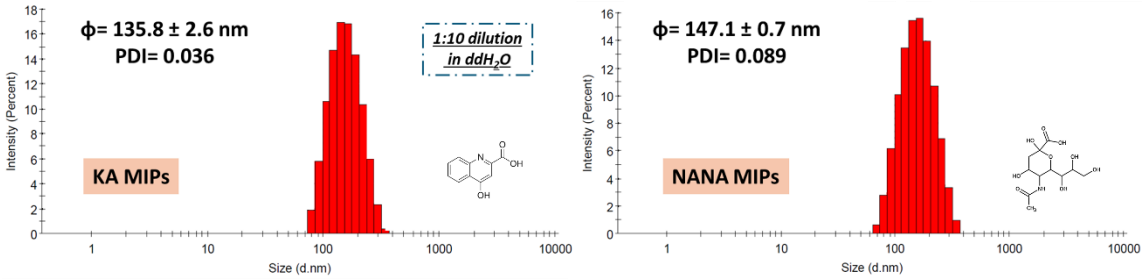


Figure 3.24. *DLS measurements on (left) KA- and (right) NANA MIPs using a 1:10 dilution in ddH_2O*

3.4.2.2.3. Competitive bead-ELISA

Prior to the electrochemical measurements, a bead-based ELISA was performed to qualitatively assess the performance of the e-nanoMIPs towards their respective targets. The test was carried out using target-conjugated magnetic beads (MB) that were synthesized as follows (Figure 3.25): (i) maleimide moiety of the MB interacted with thiol moieties in the linker (AHT) and backfiller (BT) via click chemistry; (ii) carboxylic groups of the template were activated using EDC/NHS, which were then bound to the amine moiety of AHT; and (iii) sulfo-NHS-acetate was used to block any unreacted primary amines.[82,83,122,123]

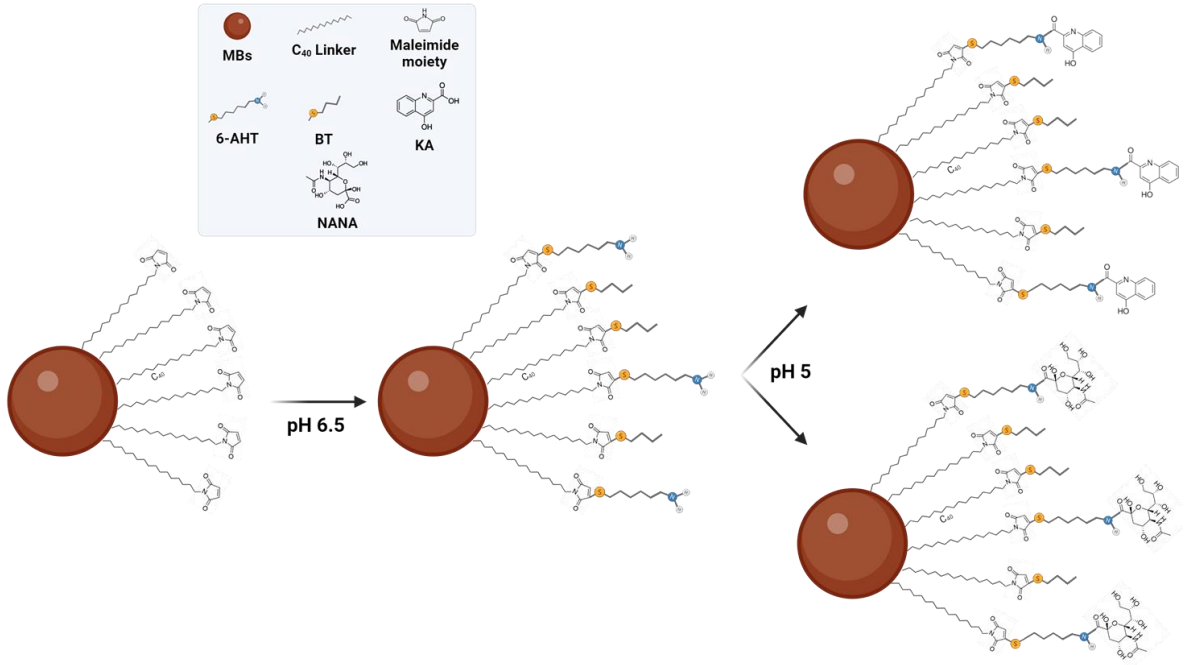


Figure 3.25. *Schematic representation of target conjugation via click chemistry (for linker and backfiller) and EDC/NHS (for targets immobilization).*

The competitive assay was conducted by incubating target-specific antibodies and nanoMIPs as depicted in Figure 3.26:

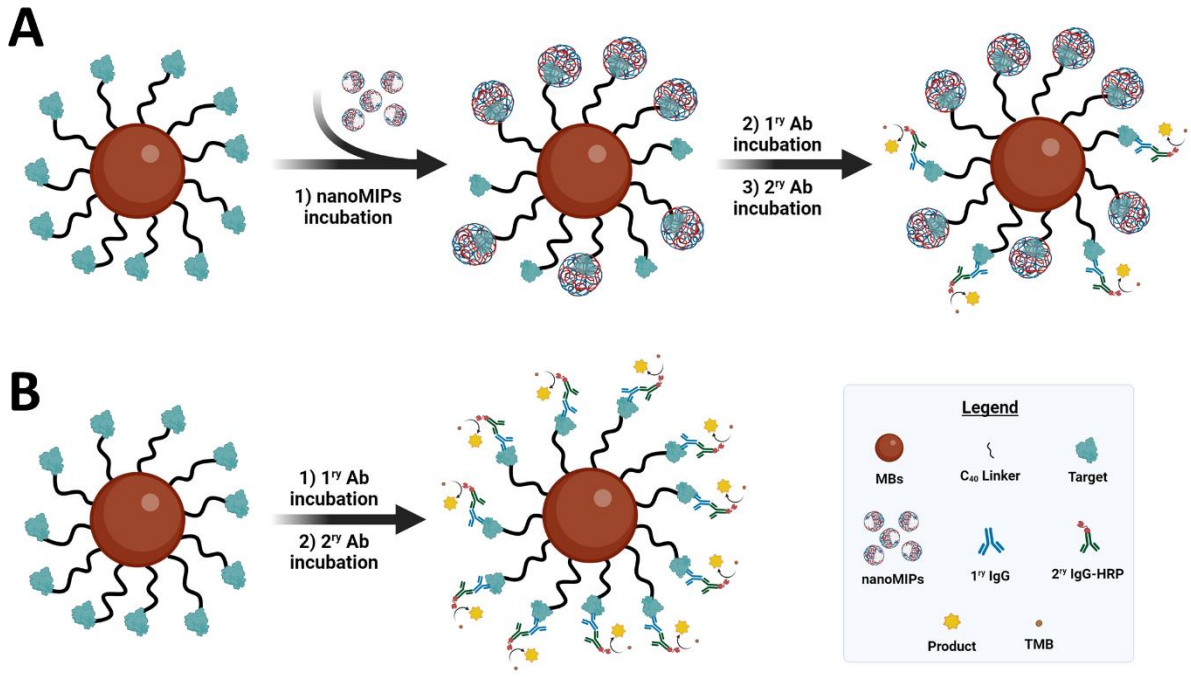


Figure 3.26. *Schematic representation of the competitive bead-ELISA procedure. (A) with an additional nanoMIP incubation step, and (B) without nanoMIPs incubation*

where "target-MB" is the target-conjugated MB, and "target-MB*" refers to the supernatant obtained from the previous incubation step using magnetic separation. The results are presented in Table 3.2, where

a clear decrease in the absorbance was observed for both targets when the nanoMIPs incubation step was introduced. As expected, in the presence of nanoMIPs as a competing factor, the absorbance was 0.1045 ± 0.0123 and 0.0891 ± 0.0211 for KA and NANA, respectively. Whereas in the absence of nanoMIPs, signals of 0.2491 ± 0.0586 and 0.3095 ± 0.021 were obtained for KA and NANA, respectively, which is in accordance with findings in other studies.

Table 3.2. *Absorbances of the competitive bead-ELISA at 450 nm with and without nanoMIPs incubation (N=3).*

	With nanoMIPs			Without nanoMIPs		
KA	0.119	0.096	0.1	0.321	0.219	0.22
NANA	0.115	0.079	0.078	0.331	0.289	0.31

3.4.2.2.4. Solvent evaporation Method

Different methods like dialysis, solvent evaporation, and lyophilization are commonly used to purify and determine the concentration of nanoMIPs in solution. For this experiment, a combination of the roto evaporator and the solvent evaporation technique. According to the results presented in Table 3.3, the concentration of KA and NANA e-nanoMIP synthesis was found to be 15.2 ± 2.21 mg/mL and 21.233 ± 2.702 mg/mL, respectively. These values fall within the expected range for nanoMIPs synthesis via SPP based on the available literature. [53,80]

Table 3.3. *KA- and NANA-nanoMIPs yield using the solvent evaporation method (N=3).*

	Before (g)	Variation (mg)	Amount (mg nanoMIPs/mL)
KA-1	5.230	1.77	17.70
KA-2	5.140	1.35	13.50
KA-3	5.387	1.44	14.40
NANA-1	5.218	2.02	20.20
NANA-2	5.148	2.43	24.30
NANA-3	5.403	1.92	19.20

3.4.2.3. Electrochemical Approach

While many studies use silanized surfaces to interact with the carboxylic moieties on the nanoMIPs surface, their monomeric composition also includes amine, hydroxyl, ferrocenyl, and other moieties prone to interact. To determine the best immobilization strategy for the electrochemical measurements, the nanoMIPs were added to an EDC/NHS solution (1:4). Consequently, as shown in Figure 3.27, both the

PDI and hydrodynamic diameter considerably increased (PDI=0.517 and HD=1384± 143.3 nm) due to the tendency of nanoMIPs to form amide bonds among them, leading to the formation of large clusters and subsequent agglomeration.

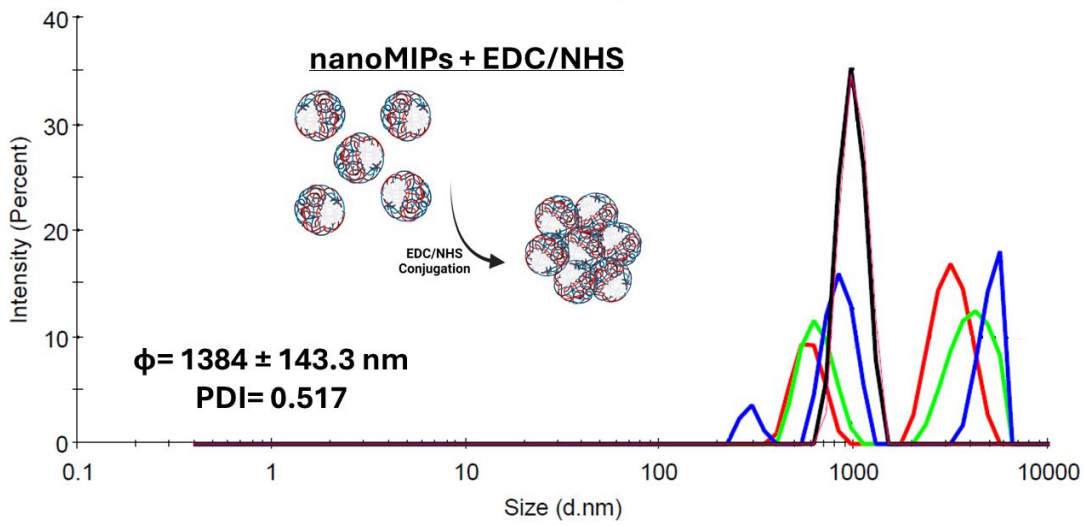


Figure 3.27. *Agglomeration of nanoMIPs via EDC/NHS. Different colors are repetitions (N=5)*

The "surface-silanized" approach provides an opportunity to develop complex systems containing multiple single-binding site receptors that are covalently joined together, as in IgM. This will significantly impact various parameters of the system's final response, such as electroactive properties, binding mechanism, LOD, dynamic range, and cooperativity, among others. To meet the requirements of the desired targets, several published procedures were adapted, as explained in the next sections.

The process of covalently immobilizing e-nanoMIPs onto screen-printed gold electrodes (Figure 3.28) consisted of several steps, as adapted from published studies: (i) immobilization of a mixed self-assembled monolayer (SAM) consisting of MUA (as a linker) and MCH (as a backfiller) via gold-thiol bonds; (ii) Activation of the carboxylic groups on the linker via EDC/NHS; (iii) conjugation to primary amines in acrylamide moieties on the nanoMIPs' surface; and (iv) Blocking of any unreacted carboxylic groups from the linker via EtAM to avoid nonspecific interactions.

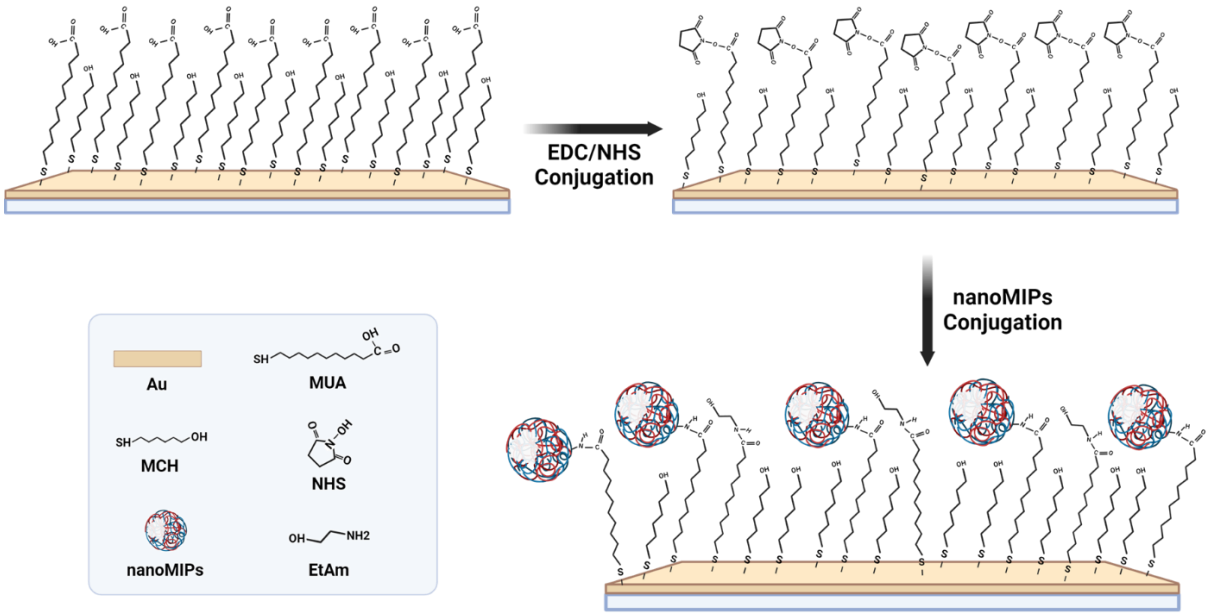


Figure 3.28. *Schematic representation of nanoMIPs immobilization on SPGE using EDC/NHS conjugation*

To achieve accurate readings, electrochemical activation was performed on the bare SPGE in 0.5 M H2SO4 until signal stabilization (see Figure 3.29), as it was essential to properly characterize the electrode surface prior to subsequent analysis.

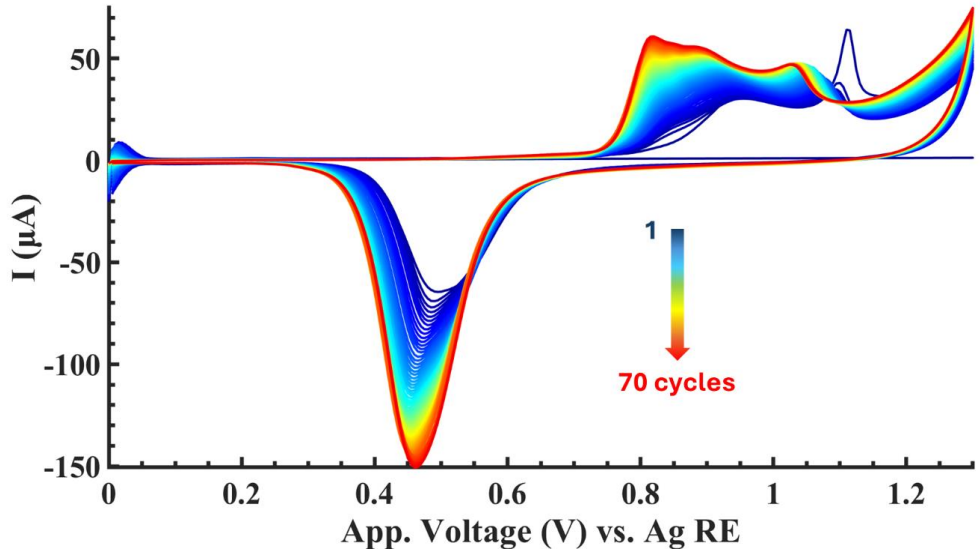


Figure 3.29. *Voltammogram of SPGE electrochemical cleaning using 70 cycles in 0.5 M H_2SO_4. Parameters are shown in "Methods" section*

The sensor response was measured using CV and DPV in order to study the redox behavior of the ferrocene moiety. The redox peaks can be seen after the addition of 5 mM PBS, located around E0= 5 mV. Therefore, several CV cycles were performed to characterize the system, and it was noted that the ferrocene peaks increased with subsequent scans until signal stabilization, as observed in Figure 3.30. Additionally, the sharpness of the peaks indicated that the electrochemical reaction is occurring at a fast rate in relation

to mass transport, suggesting that the system is likely surface-confined rather than diffusion-controlled. This is due to the redox reaction predominantly occurring at the electrode surface, where the reactants (redox species) are in close proximity to the electrode interface, allowing rapid electron transfer without significant mass transport limitations. This information can be valuable for understanding the binding mechanism and kinetics of the electrochemical process under investigation (Figure 3.30).

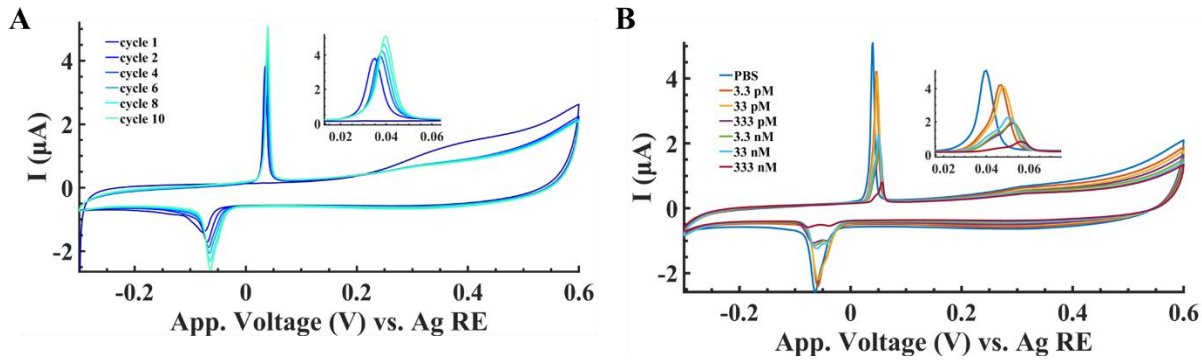


Figure 3.30. *A) Ferrocene peak evolution after several cycles first in 50 µL nanoMIPs in EtOH and then incorporation of 50 µL of 5 mM PBS ; (B) Cyclic stability of NANA-nanoMIPs in 5 mM PBS, B) Quantification of NANA at different concentrations from 3pM to 333 nM.*

3.4.2.3.1. Optimization

Prior to the quantification of the targets, several DPV parameters were optimized in order to enhance the final response of the surface-confined system: (i) Pulse amplitude, (ii) Pulse time, and (iii) Scan rate. Figure 3.31A exhibits the crucial role of the pulse amplitude in influencing the final electrochemical signal, where increasing it generally leads to an increase in the peak current; however, excessively high amplitudes (200 mV) may lead to (i) broader peaks, as mass transport limitations may start to become significant, and (ii) overpotential effects, which might shift the redox peak potential. Additionally, sharp and well-defined peaks are often observed in surface-confined systems. [48,124,125] Therefore, 100 mV was selected for the following experiments.

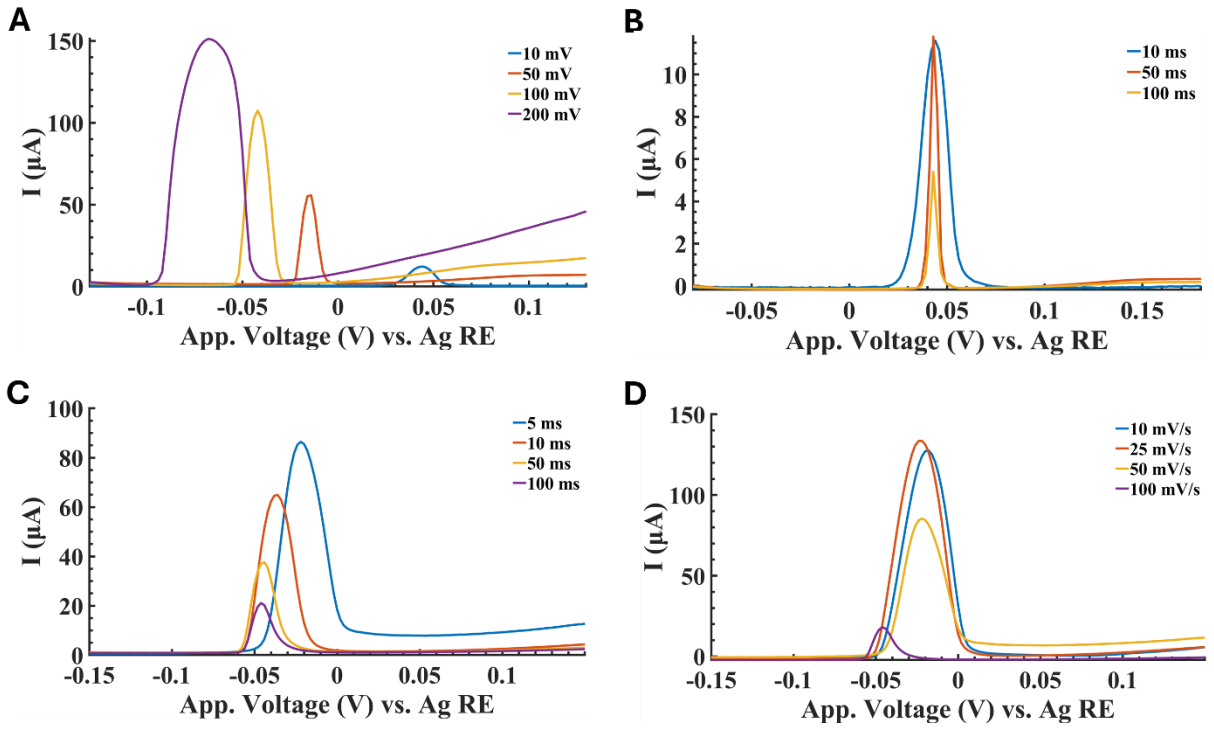


Figure 3.31. *Optimization of DPV parameters: (A) Pulse amplitude, (B) Pulse Time, (C) pulse time at 100 mV amplitude, and (D) Scan rates at 100 mV amplitude and 5 ms pulse time.*

Furthermore, analyzing the pulse time can also provide insight into the redox reactions of the system. As shown in Figure 3.31B, shorter pulse times allow for a finer temporal resolution, i.e., the potential pulse is applied for a shorter duration, providing a more precise snapshot of the electrochemical processes occurring at the electrode surface. [48,124,125] This can also lead to sharper and more well-defined peaks in the voltammogram, providing a clearer visualization of electron transfer events. Therefore, based on the data obtained (Figure 3.31C), 5 ms and 100 mV were selected as pulse time and amplitude for further experiments.

Once the pulse amplitude and time were optimized, a study of the effect of the scan rate was performed. In general, higher scan rates typically lead to an increase in peak current for a redox reaction, even in a surface-confined system. In other words, this behavior is due to the diffusion-limited current, as all the redox agents in the immediate vicinity of the electrode have reacted, thus relying on the flux of molecules to the electrode for reaction. As the scan rate increases, the flux of the redox agent also increases, leading to the expansion of the diffusion layer. Consequently, faster scan rates result in a larger flux and correspondingly larger peaks. [48,124,125] Interestingly, as shown in Fig 3.25D, the results obtained suggest an apparent increase in the peak intensity of the ferrocene moieties with lower scan rates. According to the literature, this might be because, as the redox reaction at the electrode surface is limited by kinetic factors rather than mass transport, lower scan rates may allow more time for the redox processes to occur, leading to the higher observed current responses. Therefore, 25 mV/s for further experiments was selected.

3.4.2.3.2. Temporal and Cyclic Stability

As aforementioned, e-nanoMIPs are made of polymeric materials that are susceptible to shrinking, swelling, and solvation effects. These effects play a crucial role in determining the redox states of the ferrocene moieties, which in turn affect the electrochemical properties of the e-nanoMIPs. Solvation is important not only for maintaining the structural stability and consistent electrochemical performance of the e-nanoMIPs, but also for their ion mobility, conductivity, particle hydrodynamic size, and cyclic stability. To better understand the behavior of e-nanoMIPs in PBS, DPV measurements were taken one, three (used for next sections), and five days after the sensor was fabricated, the MIPs were stored in PBS during these days. The electrodes' response to increasing target concentrations was difficult to observe after 1 day (Figure 3.32A), possibly due to the polymeric structure still undergoing structural stabilization, highlighting the strong contribution of solvation effects. Conversely, as shown in Figure 3.32B, it was possible to observe the expected decrease in peak intensity with increasing target concentrations ranging from 0.33 aM to 333 nM in 5 mM PBS after days 3 and 5.

Three days after fabrication were chosen for further experiments. To demonstrate the versatility of the proposed approach, electrochemical sensors were developed for the two targets: KA and NANA. In all experiments conducted, the current response of the respective e-nanoMIPs decreased proportionally to the concentration of the analyte, and control experiments (nanoMIPs-free) varied erratically (Figure 3.32C).

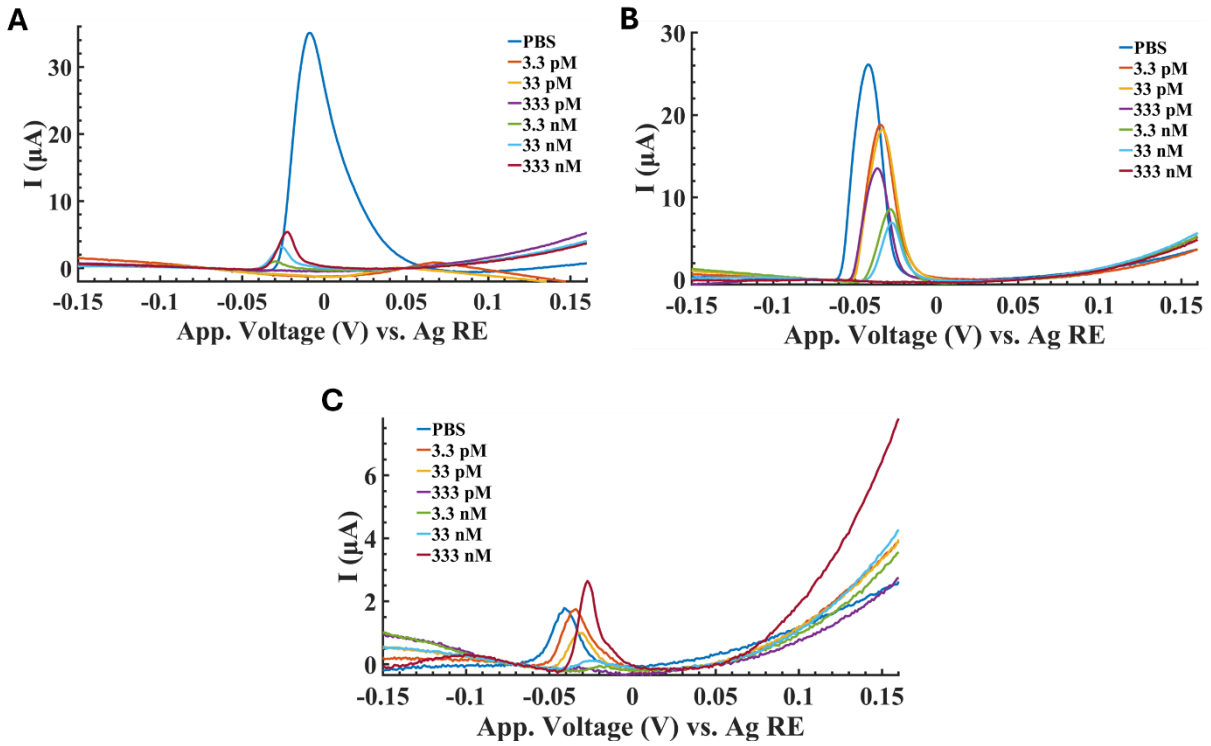


Figure 3.32. *Representatives of (A) 1-day and (B) 5-day incubation in 5 mM PBS, along with (C) control without nanoMIPs.*

It is important to highlight that the solvation process may take a few days. Interestingly, no significant difference is observed between days 3 and 5, indicating that a stable solvation degree is achieved after day 3. This suggests that while complete solvation may not be essential for functionality, it is optimal for reproducibility. Therefore, exploring solvation rates in other solutions, such as Milli-Q water, would be valuable to assess if acceleration is possible. This could be a focus for future research, potentially involving more frequent sampling at shorter time intervals.

3.4.2.3.3. Performance

Some studies based on electrochemical detection using nanoMIPs have demonstrated a binding mechanism where an increase in peak current is observed with greater target concentrations, which might be caused by the immobilization method where highly silanized electrodes are used, increasing the nanoMIPs surface density. Nevertheless, this might also entail multisite-induced cooperativity effects, along with steric hindrance, influencing factors such as dissociation constant (KD), dynamic range, and LOD.

In this work, a decrease in ferrocene peak current was observed and attributed to binding-induced conformational changes, leading to the closure of cavities and the blocking of e-nanoMIP ferrocenes. These conformational changes may also result in the movement of ferrocene moieties away from the electrode surface, thereby impeding electron transfer. The density of e-nanoMIPs on the surface is deliberately kept low to avoid the formation of linker multilayers [126,127] and to enable rapid target detection within 15 minutes using equation 1 in order to study relative responses based on target-free signals. Therefore, as the blank signal would be zero based on the RR equation (equation 1), an alternative LOD was estimated using $3.33 \cdot \frac{\sigma_{LC}}{m}$, where σ_{LC} represents the standard deviation (n=5) of the lowest concentration tested (since the PBS RR would be equal to zero), and m is the slope of the linear region of the calibration curves.

$$RR(\%) = \frac{I_{PBS} - I_{target}}{I_{PBS}} * 100 \quad (1)$$

In buffer conditions (5 mM PBS), as observed in Figure 3.33A, the KA sensor had a sensitivity of 14.10 %/nM (R2=0.89), while exhibiting a LOD and limit of quantification (LOQ, $10 \cdot \frac{\sigma_{LC}}{m}$) of 0.57 aM and 8.05 aM, respectively (n=5), in a linear working range from 3.33 aM to 33.33 pM. The NANA sensor was even more sensitive, with a sensitivity of 16.04 %/nM (R2=0.85), and a LOD and LOQ of 0.01 aM and 0.66 aM in a similar linear range as the KA sensor (Figure 3.33B, n=5). Due to its polymeric nature, nonspecific contributions due to the solvent were expected, as observed in the linear contributions of 5 mM PBS in both target-specific e-nanoMIPs.

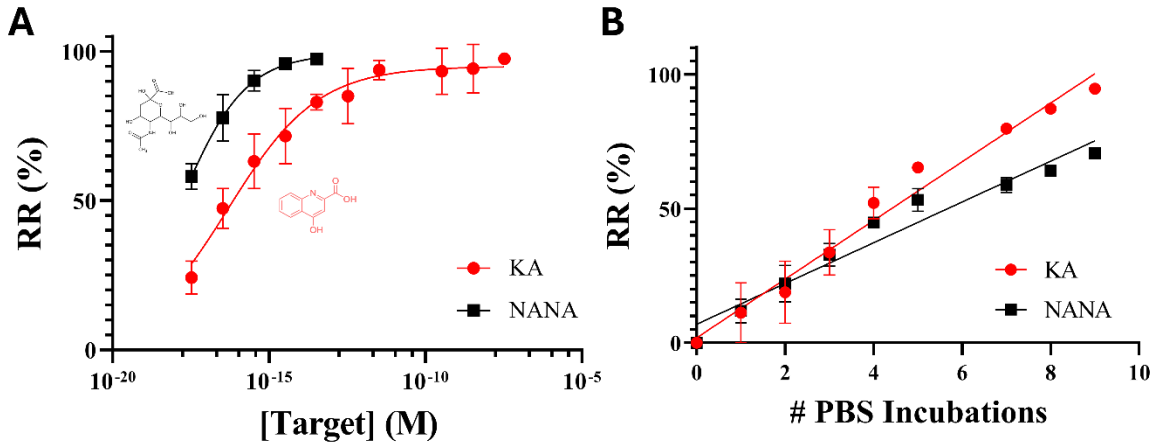


Figure 3.33. *(A) Calibration curves of nanoMIPs against their respective targets in 5 mM PBS (n=5), and (B) PBS contribution to the final signal (n=4).*

In order to study sensor performance in complex media, synthetic urine (SU) was prepared, as mentioned in the experimental section. Even after serial dilutions, SU still contains nM concentrations of components like urea, uric acid, and creatinine, which are structurally similar molecules leading to potential nonspecific binding interactions affecting sensor response. As observed in Figure 3.34A, the KA sensor demonstrated a sensitivity of 12.86 %/nM (R2=0.79) and a LOD of 1.62 aM in diluted SU (1:109). However, the NANA sensor encountered challenges in complex media (Figure 3.34B), which could potentially be attributed to heightened susceptibility to interferants. This susceptibility may be linked to the higher ratio between monomers/crosslinkers and the target in the NANA-e-nanoMIPs formulation, potentially leading to increased polymeric malleability and reduced ability to effectively "lock" the target in its respective cavity.

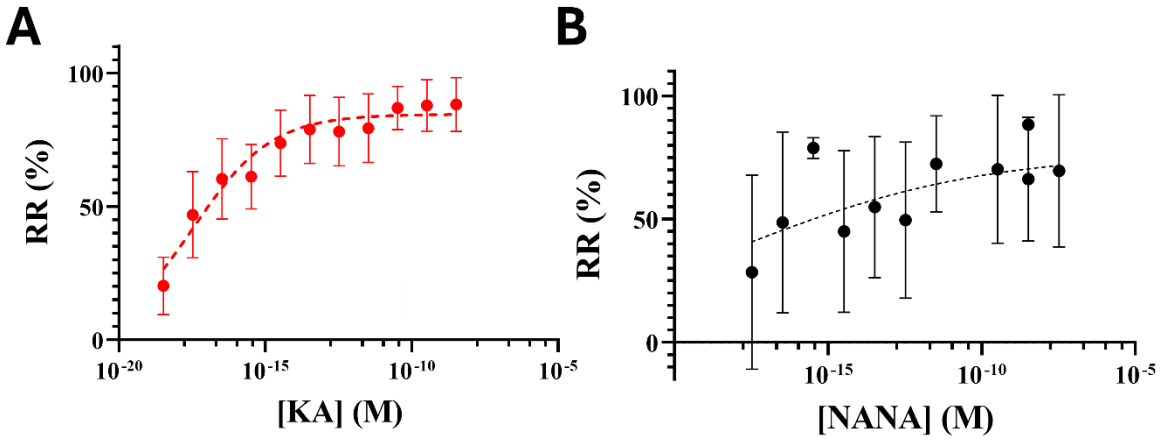


Figure 3.34. *Calibration curves in diluted SU (1:10⁹) of (A) KA-, and (B) NANA-nanoMIPs (n=8).*

e-nanoMIPs are proposed as an alternative to antibodies for synthetic recognition elements in biosensing applications. In the typical analysis of antibody binding, the Hill equation is employed to study the receptor-ligand binding process. Therefore, it was deemed prudent to fit the MIP calibration curves to

the same function. The Hill equation, shown below, is used to study the receptor:ligand binding, considering both cooperativity and sensitivity.

$$\theta = \frac{[L]^h}{K_D + [L]^h} \quad (2)$$

where L is the ligand being investigated (namely KA and NANA), KD represents the dissociation constant, and h is the Hill coefficient, which describes the cooperativity degree between the ligand and the receptor. Briefly, when h > 1, the receptor or ligand exhibits positive cooperativity, resulting in the presence of many binding sites facilitating binding events, displaying a sigmoidal shape in the calibration curve. When h = 1, the Hill equation simplifies to the Langmuir binding isotherm, where there are no interaction or cooperativity effects between the ligand and the receptor. If h < 1, on the other hand, the system demonstrates negatively cooperative binding, which implies that when a ligand binds to the receptor, its ability to bind to additional ligands diminishes. [101,128,129]

In PBS, the obtained KD for the KA sensor is 50.62 aM, with a hill coefficient (h) of 0.3. Similarly, the NANA sensor exhibited a more sensitive response with a KD of 1.47 aM (h=0.4). To the best of our knowledge and based on the literature, these values are among the lowest KDs obtained for e-nanoMIPs with electrochemical transduction in buffered conditions, especially for KA and NANA. Surprisingly, in diluted SU, the KA sensors exhibited an even lower KD of 3.6 aM (h=0.3). Our hypothesis is that it may be attributed to the elevated ionic strength of the solution resulting from the residual nanomolar levels of SU components, potentially leading to an augmentation in electron transfer, due to the change in the solvation of the e-nanoMIPs and ferrocene monomers.

In the assessment of the selectivity of synthetic receptors for kynurenic acid, it is advisable to consider quinolinic acid (QA), and tryptophan (Trp) as suitable target compounds for evaluation. QA, being structurally similar and metabolically related to KA, poses a significant challenge due to its high resemblance and co-occurrence in bodily fluids including urine. On the other hand, tryptophan, despite being less polar and a precursor for both KA and QA via the kynurenine pathway, offers valuable insights into the receptor's ability to differentiate between other aromatic and biologically relevant molecules. Therefore, including all three compounds ensures a comprehensive and thorough assessment of the receptor's selectivity. As shown in Figure 3.35, even though the KA sensor showed some cross-reactivity to 50 nM NANA (50%), QA (55%), and Trp (60%), it exhibited a 97% of RR towards 5 nM KA. The NANA sensor was tested against KA, QA, and Trp, which showed a similar behavior as in the KA sensor.

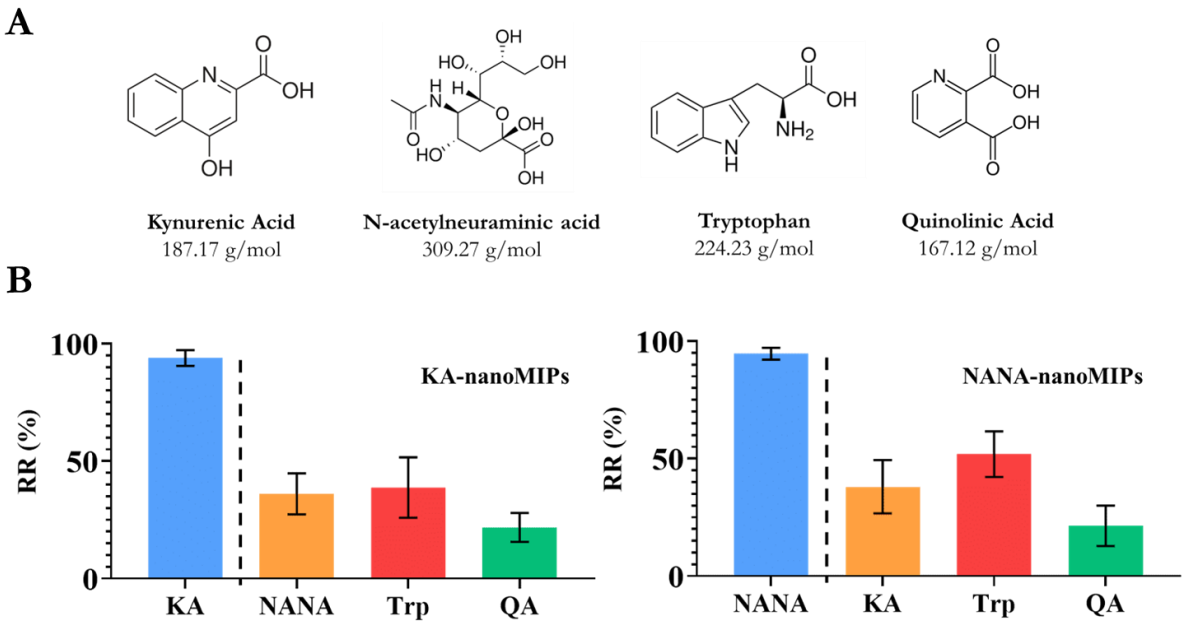


Figure 3.35. *Selectivity tests against 50 nM of interferents (n=3) and 5 nM of target (n=3).*

3.5. CONCLUSIONS AND FUTURE PERSPECTIVES

In conclusion, the spectrophotometric analysis of the M:T interactions in different solvents has provided valuable insights into the behavior of the biomolecule in solution. The distinct peaks identified from the different KA ionic species and the changes observed in the absorbance spectra of KA in different solvents indicate the significant impact of solvent selection on their interaction. The observed differences in the experimental spectra compared to the theoretical ones suggest the presence of several types of noncovalent interactions between KA and oPD, with potential correlations to absorbance changes and wavelength shifts.

Furthermore, the performance of e-MIPs, particularly in the context of electropolymerization, has been examined. The electrochemical activation procedure on the bare SPCE and the subsequent electropolymerization process provided a reliable basis for subsequent measurements. The impact of different solvents, such as EtOH+TBAB, on the response and stability of the carbon surface before polymer deposition has been highlighted. The potential challenges associated with organic solvents destabilizing the carbon surface and the stability of the template and monomer in hydrophobic solvents have been identified, providing essential considerations for the electropolymerization process.

Additionally, a multi-stage protocol has successfully achieved the fabrication, characterization, and verification of nanoMIPs against KA and NANA. The fabrication involved template immobilization, SPP, and purification, resulting in the synthesis of target-specific nanoMIPs with desirable electroactive properties given by the FcMMA. Several techniques were utilized for the characterization and verification steps, such as the DNSCL test, DLS, and Bead-ELISA, providing valuable insights into the binding and performance of the nanoMIPs. These results are consistent with existing literature and demonstrate the successful synthesis and characterization of nanoMIPs for KA and NANA. The electrochemical performance of the nanoMIPs as a synthetic receptor for KA and NANA was further investigated. The immobilization strategy for the electrochemical measurements was carefully considered, taking into account the composition of the nanoMIPs and their potential for surface interaction. The electrochemical approach revealed promising results, demonstrating KD's in the subfM level, and indicating their suitability for detecting and quantifying analytes for potential prognosis applications.

Even though these nanoMIPs have shown promise via manufacture, characterization, and application, several obstacles remain before they can be used in clinical settings. Improving the long-term durability and biocompatibility of nanoMIPs, developing more scalable and repeatable manufacturing procedures, and increasing selectivity and specificity in complex biological matrices are all critical topics that need to be addressed. There is a prevailing uncertainty regarding the ability of (nano)MIPs to establish a presence in the diagnostics industry, where antibodies and enzymes are currently the gold standard. The use of (nano)MIPs in diagnostics is expected to remain primarily within academic settings until reliable and robust (nano)MIPs-based sensors become readily accessible. This availability could potentially lead to MIPs serving

as direct antibody substitutes without requiring in vivo testing or significant infrastructure adjustments from device manufacturers.

Future research should optimize fabrication processes to guarantee a high yield and consistency in large-scale manufacturing. SPR and AFM are two examples of sophisticated characterization methods that may help improve nanoMIPs by providing more detailed information about binding interactions and surface characteristics. Furthermore, nanoMIPs, as well as MIPs in general, may be suited for in vitro, in vivo or ex vivo applications as the polymerization step is carried out in a solution closely resembling the final application sample, such as an aqueous buffer in this specific scenario. Alternatively, they can be functionalized with biocompatible materials to enhance stability and reduce cytotoxicity.

Finally, overcoming the shortcomings in scalability, specificity, stability, and integration is crucial to successfully use nanoMIPs for KA and NANA in clinical settings, even if their progress shows excellent promise. To improve medical diagnostics and patient care, it is necessary to conduct cutting-edge research and use strategic techniques to bring nanoMIPs from the lab into real-world applications.

3.6. REFERENCES

1. Kramer K, Hock B. Antibodies for Biosensors. 2004;3–22.
2. Marx V. Finding the right antibody for the job. Nat Methods. 2013 Aug;10(8):703–7.
3. Ayankojo AG, Reut J, Öpik A, Tretjakov A, Syritski V. Enhancing binding properties of imprinted polymers for the detection of small molecules. Proc Est Acad Sci. 2018;67(2):138–46.
4. Cowen T, Stefanucci E, Piletska E, Marrazza G, Canfarotta F, Piletsky SA. Synthetic Mechanism of Molecular Imprinting at the Solid Phase. Macromolecules. 2020;53(4):1435–42.
5. Cowen T, Karim K, Piletsky S. Computational approaches in the design of synthetic receptors – A review. Anal Chim Acta. 2016;936:62–74.
6. Spivak DA. Selectivity in molecularly imprinted matrices. Molecularly Imprinted Materials: Science and Technology. 2004. 395–417 p.
7. Mujahid A, Afzal A, Dickert FL. Transitioning from Supramolecular Chemistry to Molecularly Imprinted Polymers in Chemical Sensing. Sensors (Basel). 2023 Sep 1;23(17).
8. Hussain M, Wackerlig J, Lieberzeit PA. Biomimetic strategies for sensing biological species. Biosensors. 2013;3(1):89–107.
9. Wulff G, Sarhan A. Über die Anwendung von enzymanalog gebauten Polymeren zur Racemattrennung. Angew Chemie. 1972 Apr 1;84(8):364–364.
10. Arshady R, Mosbach K. Synthesis of substrate-selective polymers by host-guest polymerization. Die Makromol Chemie. 1981 Jan;182(2):687–92.
11. Mosbach K, Ramström O. The emerging technique of molecular imprinting and its future impact on biotechnology. Bio/Technology. 1996;14(2):163–70.
12. Vlatakis G, Andersson LI, Müller R, Mosbach K. Drug assay using antibody mimics made by molecular imprinting. 1993;361(6413):645–7.
13. Marfà J, Pupin RR, Sotomayor M, Pividori MI. Magnetic-molecularly imprinted polymers in electrochemical sensors and biosensors. Anal Bioanal Chem 2021 41324. 2021 Jun 23;413(24):6141–57.
14. Hasanah AN, Safitri N, Zulfa A, Neli N, Rahayu D. Factors affecting preparation of molecularly imprinted polymer and methods on finding template-monomer interaction as the key of selective properties of the materials. Molecules. 2021 Sep 2;26(18).
15. Chen L, Wang X, Lu W, Wu X, Li J. Molecular imprinting: Perspectives and applications. Chem Soc Rev. 2016 Apr 21;45(8):2137–211.
16. Tiller T. Synthetic Antibodies Methods and Protocols. Vol. 1575, Methods in Molecular Biology. 2017.
17. Ye L, Mosbach K. Molecular imprinting: Synthetic materials as substitutes for biological antibodies and receptors. Chem Mater. 2008 Feb 12;20(3):859–68.
18. Kang MS, Cho E, Choi HE, Amri C, Lee JH, Kim KS. Molecularly imprinted polymers (MIPs): emerging biomaterials for cancer theragnostic applications. Biomater Res. 2023;27(1):1–32.
19. Rajpal S, Mishra P. Next generation biosensors employing molecularly imprinted polymers as sensing elements for in vitro diagnostics. Biosens Bioelectron X. 2022 Sep 1;11:100201.
20. Moura SL, Fajardo LM, Cunha L dos A, Sotomayor MDPT, Machado FBC, Ferrão LFA, et al. Theoretical and experimental study for the biomimetic recognition of levothyroxine hormone on

magnetic molecularly imprinted polymer. Biosens Bioelectron. 2018;107(January):203–10.

21. Karlsson BCG, O'Mahony J, Karlsson JG, Bengtsson H, Eriksson LA, Nicholls IA. Structure and dynamics of monomer-template complexation: An explanation for molecularly imprinted polymer recognition site heterogeneity. J Am Chem Soc. 2009 Sep 23;131(37):13297–304.

22. Haupt K. Noncovalent Molecular Imprinting of a Synthetic Polymer with the Herbicide 2,4-Dichlorophenoxyacetic Acid in the Presence of Polar Protic Solvents. ACS Symp Ser. 1998;703:135–42.

23. Cram DJ. The Design of Molecular Hosts, Guests, and Their Complexes (Nobel Lecture). Angew Chemie Int Ed English. 1988;27(8):1009–20.

24. Karim K, Breton F, Rouillon R, Piletska E V., Guerreiro A, Chianella I, et al. How to find effective functional monomers for effective molecularly imprinted polymers? Adv Drug Deliv Rev. 2005;57(12):1795–808.

25. Poma A, Turner APF, Piletsky SA. Advances in the manufacture of MIP nanoparticles. Trends Biotechnol. 2010 Dec;28(12):629–37.

26. Ektirici S, Kurc O, Jalilzadeh M, Asır S, Türkmen D. Computational Investigation of the Monomer Ratio and Solvent Environment for the Complex Formed between Sulfamethoxazole and Functional Monomer Methacrylic Acid. ACS Omega. 2022 May 24;7(20):17175–84.

27. Borozniak R, Reut J, Tretjakov A, Lomaka A, Öpik A, Syritski V. A computational approach to study functional monomer-protein molecular interactions to optimize protein molecular imprinting. J Mol Recognit. 2017;30(10):1–9.

28. Kang MS, Cho E, Choi HE, Amri C, Lee JH, Kim KS. Molecularly imprinted polymers (MIPs): emerging biomaterials for cancer theragnostic applications. Vol. 27, Biomaterials Research. BioMed Central Ltd; 2023. p. 45.

29. Liu Y, Wang L, Li H, Zhao L, Ma Y, Zhang Y, et al. Rigorous recognition mode analysis of molecularly imprinted polymers—Rational design, challenges, and opportunities. Prog Polym Sci. 2024 Mar 1;150:101790.

30. Furlan De Oliveira R, Montes-García V, Ciesielski A, Samorì P. Harnessing selectivity in chemical sensing via supramolecular interactions: From functionalization of nanomaterials to device applications. Mater Horizons. 2021 Oct 1;8(10):2685–708.

31. Omar J, Ponsford D, Dreiss CA, Lee TC, Loh XJ. Supramolecular Hydrogels: Design Strategies and Contemporary Biomedical Applications. Chem - An Asian J. 2022;17(9).

32. Testa V, Anfossi L, Cavalera S, Di Nardo F, Serra T, Baggiani C. The Amount of Cross-Linker Influences Affinity and Selectivity of NanoMIPs Prepared by Solid-Phase Polymerization Synthesis. Polymers (Basel). 2024;16(4).

33. Yan M, Ramström O. Molecularly imprinted materials : science and technology. 2005;734.

34. Dong W, Yan M, Liu Z, Wu G, Li Y. Effects of solvents on the adsorption selectivity of molecularly imprinted polymers: Molecular simulation and experimental validation. Sep Purif Technol. 2007 Feb 25;53(2):183–8.

35. Piletsky SA, Piletska E V., Karim K, Freebairn KW, Legge CH, Turner APF. Polymer cookery: Influence of polymerization conditions on the performance of molecularly imprinted polymers. Macromolecules. 2002 Sep 10;35(19):7499–504.

36. Piletska E V., Guerreiro AR, Whitcombe MJ, Piletsky SA. Influence of the polymerization conditions on the performance of molecularly imprinted polymers. Macromolecules. 2009 Jul 28;42(14):4921–8.

37. Okutucu B. Biomedicine Application of Nano-Molecularly Imprinted Polymers (NanoMIPs).

Biomed Mater Devices. 2023;1(1):419–25.

38. Lorenzo RA, Carro AM, Alvarez-Lorenzo C, Concheiro A. To remove or not to remove? The challenge of extracting the template to make the cavities available in molecularly imprinted polymers (MIPs). Int J Mol Sci. 2011 Jul;12(7):4327–47.

39. Mahony JO, Nolan K, Smyth MR, Mizaikoff B. Molecularly imprinted polymers - potential and challenges in analytical chemistry. Anal Chim Acta. 2005 Apr 4;534(1):31–9.

40. Canfarotta F, Cecchini A, Piletsky S. CHAPTER 1: Nano-sized Molecularly Imprinted Polymers as Artificial Antibodies. RSC Polym Chem Ser. 2018;2018-Janua(28):1–27.

41. Garg M, Pamme N. Strategies to remove templates from molecularly imprinted polymer (MIP) for biosensors. TrAC Trends Anal Chem. 2024 Jan 1;170:117437.

42. Alexander C, Andersson HS, Andersson LI, Ansell RJ, Kirsch N, Nicholls IA, et al. Molecular imprinting science and technology: A survey of the literature for the years up to and including 2003. J Mol Recognit. 2006 Mar;19(2):106–80.

43. Cejner M, Dobrowolski R. Ion-imprinted polymers: synthesis, characterization and applications. Annales. 2015;LXX(2):67–85.

44. Liao C. Electrochemical polymerization. Chem Bull / Huaxue Tongbao. 2000;63(2):37–41.

45. Tse Sum Bui B, Mier A, Haupt K. Molecularly Imprinted Polymers as Synthetic Antibodies for Protein Recognition: The Next Generation. Small. 2023 Mar 29;19(13).

46. Haupt K, Medina Rangel PX, Bui BTS. Molecularly imprinted polymers: Antibody mimics for bioimaging and therapy. Chem Rev. 2020 Sep 9;120(17):9554–82.

47. Feroz M, Vadgama P. Molecular Imprinted Polymer Modified Electrochemical Sensors for Small Drug Analysis: Progress to Practical Application. Electroanalysis. 2020;32(11):2361–86.

48. Bard AJ, Faulkner LR. Polarography and Pulse Voltammetry. Electrochem Methods Fundam Appl. 2001 Dec;261–304.

49. Shumyantseva V V., Bulko T V., Sigolaeva L V., Kuzikov A V., Archakov AI. Electrosynthesis and binding properties of molecularly imprinted poly-o-phenylenediamine for selective recognition and direct electrochemical detection of myoglobin. Biosens Bioelectron. 2016;86:330–6.

50. Yarman A, Scheller FW. How reliable is the electrochemical readout of MIP sensors? Sensors (Switzerland). 2020 May 1;20(9).

51. Regasa MB, Refera Soreta T, Femi OE, Ramamurthy PC. Development of Molecularly Imprinted Conducting Polymer Composite Film-Based Electrochemical Sensor for Melamine Detection in Infant Formula. ACS Omega. 2020;5(8):4090–9.

52. Sehit E, Drzazgowska J, Buchenau D, Yesildag C, Lensen M, Altintas Z. Ultrasensitive nonenzymatic electrochemical glucose sensor based on gold nanoparticles and molecularly imprinted polymers. Biosens Bioelectron. 2020;165:112432.

53. Garcia-Cruz A, Ahmad OS, Alanazi K, Piletska E, Piletsky SA. Generic sensor platform based on electro-responsive molecularly imprinted polymer nanoparticles (e-NanoMIPs). Microsystems Nanoeng 2020 61. 2020 Oct 19;6(1):1–9.

54. Arrieta Almario AA, Tarazona Cáceres RL. Study of kinetic formation and the electrochemical behavior of polypyrrole films. J Chil Chem Soc. 2009;54(1):14–9.

55. Balčiūnas D, Plaušinaitis D. Study of Pyrrole Adsorption and Electropolymerization on Au Surface from PBS Solutions by using ESPR method. 2019;(May):6–7.

56. Vanossi D, Pigani L, Seeber R, Ferrarini P, Baraldi P, Fontanesi C. Electropolymerization of

ortho-phenylenediamine. Structural characterisation of the resulting polymer film and its interfacial capacitive behaviour. J Electroanal Chem. 2013;710:22–8.

57. Maouche N, Guergouri M, Gam-Derouich S, Jouini M, Nessark B, Chehimi MM. Molecularly imprinted polypyrrole films: Some key parameters for electrochemical picomolar detection of dopamine. J Electroanal Chem. 2012;685:21–7.

58. Luliński P, Maciejewska D, Bamburowicz-Klimkowska M, Szutowski M. Dopamine-imprinted polymers: Template-monomer interactions, analysis of template removal and application to solid phase extraction. Molecules. 2007 Nov;12(11):2434–49.

59. Canfarotta F, Cecchini A, Piletsky S. Nano-sized Molecularly Imprinted Polymers as Artificial Antibodies. In: Kutner W, Sharma PS, editors. Molecularly Imprinted Polymers for Analytical Chemistry Applications. The Royal Society of Chemistry; 2018. p. 0.

60. Chianella I, Guerreiro A, Moczko E, Caygill JS, Piletska E V., De Vargas Sansalvador IMP, et al. Direct replacement of antibodies with molecularly imprinted polymer nanoparticles in ELISA - Development of a novel assay for vancomycin. Anal Chem. 2013 Sep 3;85(17):8462–8.

61. Tabushi I. Artificial allosteric systems. Pure Appl Chem. 1988;60(4):581–6.

62. Mahony JO, Nolan K, Smyth MR, Mizaikoff B. Molecularly imprinted polymers - Potential and challenges in analytical chemistry. Anal Chim Acta. 2005;534(1):31–9.

63. Rampey AM, Umpleby RJ, Rushton GT, Iseman JC, Shah RN, Shimizu KD. Characterization of the Imprint Effect and the Influence of Imprinting Conditions on Affinity, Capacity, and Heterogeneity in Molecularly Imprinted Polymers Using the Freundlich Isotherm-Affinity Distribution Analysis. Anal Chem. 2004;76(4):1123–33.

64. Mustafa YL, Keirouz A, Leese HS. Molecularly imprinted polymers in diagnostics: accessing analytes in biofluids. J Mater Chem B. 2022 Sep 28;10(37):7418–49.

65. Shevchenko KG, Garkushina IS, Canfarotta F, Piletsky SA, Barlev NA. Nano-molecularly imprinted polymers (nanoMIPs) as a novel approach to targeted drug delivery in nanomedicine. RSC Adv. 2022 Jan 28;12(7):3957–68.

66. Poma A, Guerreiro A, Whitcombe MJ, Piletska E V., Turner APF, Piletsky SA. Solid-Phase Synthesis of Molecularly Imprinted Polymer Nanoparticles with a Reusable Template-"Plastic Antibodies". Adv Funct Mater. 2013 Jun 13;23(22):2821–7.

67. Singla P, Kaur S, Jamieson O, Dann A, Garg S, Mahon C, et al. Electrochemical and thermal detection of allergenic substance lysozyme with molecularly imprinted nanoparticles. Anal Bioanal Chem. 2023;415(18):4467–78.

68. Sela-Culang I, Kunik V, Ofran Y. The structural basis of antibody-antigen recognition. Front Immunol. 2013 Oct 8;4(OCT):64858.

69. Jie Z, Xiwen H. Study of the nature of recognition in molecularly imprinted polymer selective for 2-aminopyridine. Anal Chim Acta. 1999;381(1):85–91.

70. Ozer A, White BS, Lis JT, Shalloway D. Density-dependent cooperative non-specific binding in solid-phase SELEX affinity selection. Nucleic Acids Res. 2013 Aug 1;41(14):7167–75.

71. Mistry J, Guerreiro A, Moczko E, Piletska E, Karim K, Piletsky SA. Analysis of cooperative interactions in molecularly imprinted polymer nanoparticles. Mol Imprinting. 2016;3(1):55–64.

72. Ricci F, Vallée-Bélisle A, Simon AJ, Porchetta A, Plaxco KW. Using Nature's "tricks" to Rationally Tune the Binding Properties of Biomolecular Receptors. Acc Chem Res. 2016 Sep 20;49(9):1884–92.

73. Huynh TP, Chandra BKC, Sosnowska M, Sobczak JW, Nesterov VN, D'Souza F, et al. Nicotine molecularly imprinted polymer: Synergy of coordination and hydrogen bonding. Biosens

Bioelectron. 2015;64:657–63.

74. Andersson LI, Mosbach K. Enantiomeric resolution on molecularly imprinted polymers prepared with only non-covalent and non-ionic interactions. J Chromatogr A. 1990 Jan 1;516(2):313–22.

75. Andersson HS, Karlsson JG, Piletsky SA, Koch-Schmidt AC, Mosbach K, Nicholls IA. Study of the nature of recognition in molecularly imprinted polymers, II [1]: Influence of monomer-template ratio and sample load on retention and selectivity. J Chromatogr A. 1999;848(1–2):39–49.

76. Biologists E. Binding and Kinetics for Experimental Biologists. Computing. 2009;82(3):1–19.

77. Piletsky SS, Rabinowicz S, Yang Z, Zagar C, Piletska E V., Guerreiro A, et al. Development of molecularly imprinted polymers specific for blood antigens for application in antibody-free blood typing. Chem Commun. 2017;53(11):1793–6.

78. Garcia-Cruz A, Ahmad OS, Alanazi K, Piletska E, Piletsky SA. Generic sensor platform based on electro-responsive molecularly imprinted polymer nanoparticles (e-NanoMIPs). Microsystems Nanoeng. 2020 Oct 19;6(1):1–9.

79. Elfadil D, Lamaoui A, Pelle F Della, Amine A, Compagnone D. Molecularly imprinted polymers combined with electrochemical sensors for food contaminants analysis. Molecules. 2021;26(15):1–40.

80. Canfarotta F, Poma A, Guerreiro A, Piletsky S. Solid-phase synthesis of molecularly imprinted nanoparticles. Nat Protoc. 2016;11(3):443–55.

81. Moretta R, Terracciano M, Rea I, De Stefano L. Bioconjugation of Peptides to Hybrid Gold Nanoparticles. Methods Mol Biol. 2021;2355:105–15.

82. Hermanson GT. Bioconjugate Techniques: Third Edition. Bioconjugate Tech Third Ed. 2013;1–1146.

83. Sehgal D, Vijay IK. A Method for the High Efficiency of Water-Soluble Carbodiimide-Mediated Amidation. Anal Biochem. 1994 Apr 1;218(1):87–91.

84. Moczko E, Poma A, Guerreiro A, Perez De Vargas Sansalvador I, Caygill S, Canfarotta F, et al. Surface-modified multifunctional MIP nanoparticles. Nanoscale. 2013;5(9):3733–41.

85. Zhang H. Molecularly Imprinted Nanoparticles for Biomedical Applications. Adv Mater. 2020 Jan 1;32(3).

86. McClements J, Bar L, Singla P, Canfarotta F, Thomson A, Czulak J, et al. Molecularly Imprinted Polymer Nanoparticles Enable Rapid, Reliable, and Robust Point-of-Care Thermal Detection of SARS-CoV-2. ACS Sensors. 2022;7(4):1122–31.

87. Elbelazi A, Canfarotta F, Czulak J, Whitcombe MJ, Piletsky S, Piletska E. Development of a homogenous assay based on fluorescent imprinted nanoparticles for analysis of nitroaromatic compounds. Nano Res. 2019;12(12):3044–50.

88. Cáceres C, Moczko E, Basozabal I, Guerreiro A, Piletsky S. Molecularly Imprinted Nanoparticles (NanoMIPs) Selective for Proteins: Optimization of a Protocol for Solid-Phase Synthesis Using Automatic Chemical Reactor. Polymers (Basel). 2021 Jan 1;13(3):1–11.

89. Holland N, Frisby J, Owens E, Hughes H, Duggan P, McLoughlin P. The influence of polymer morphology on the performance of molecularly imprinted polymers. Polymer (Guildf). 2010;51(7):1578–84.

90. Sajini T, Mathew B. A brief overview of molecularly imprinted polymers: Highlighting computational design, nano and photo-responsive imprinting. Talanta Open. 2021 Dec 1;4.

91. D'Aurelio R, Chianella I, Goode JA, Tothill IE. Molecularly imprinted nanoparticles based sensor for cocaine detection. Biosensors. 2020;10(3):1–13.

92. Ashley J, Shukor Y, D'Aurelio R, Trinh L, Rodgers TL, Temblay J, et al. Synthesis of Molecularly Imprinted Polymer Nanoparticles for α-Casein Detection Using Surface Plasmon Resonance as a Milk Allergen Sensor. ACS Sensors. 2018;3(2):418–24.

93. Refaat D, Aggour MG, Farghali AA, Mahajan R, Wiklander JG, Nicholls IA, et al. Strategies for Molecular Imprinting and the Evolution of MIP Nanoparticles as Plastic Antibodies—Synthesis and Applications. Int J Mol Sci. 2019 Dec 2;20(24).

94. Lee S hui, Lin OH, Doong R an. Design of size-tunable molecularly imprinted polymer for selective adsorption of acetaminophen. Clean Technol Environ Policy. 2017;19(1):243–50.

95. Peeters M. Molecularly Imprinted Polymers (Mips) for Bioanalytical Sensors : Strategies for Incorporation of Mips into Sensing Platforms. Austin J Biosens Bioelectron. 2015;1(3):1–5.

96. Refaat D, Aggour MG, Farghali AA, Mahajan R, Wiklander JG, Nicholls IA, et al. Strategies for Molecular Imprinting and the Evolution of MIP Nanoparticles as Plastic Antibodies—Synthesis and Applications. Int J Mol Sci 2019, Vol 20, Page 6304. 2019 Dec 13;20(24):6304.

97. Glasscott MW, Vannoy KJ, Kazemi R, Verber MD, Dick JE. μ-MIP: Molecularly Imprinted Polymer-Modified Microelectrodes for the Ultrasensitive Quantification of GenX (HFPO-DA) in River Water. Environ Sci Technol Lett. 2020;7(7):489–95.

98. Haq I, Garcia Cruz A, Di Masi S, Cowen T, Allcock NS, Malitesta C, et al. Smart nano-actuators for electrochemical sensing of Metformin in human plasma. Sensors Actuators B Chem. 2023;376(PB):132928.

99. Zhang X, Caserta G, Yarman A, Supala E, Waffo AFT, Wollenberger U, et al. "Out of Pocket" Protein Binding—A Dilemma of Epitope Imprinted Polymers Revealed for Human Hemoglobin. Chemosensors. 2021;9(6).

100. Silva AT, Figueiredo R, Azenha M, Jorge PAS, Pereira CM, Ribeiro JA. Imprinted Hydrogel Nanoparticles for Protein Biosensing: A Review. ACS Sensors. 2023 Aug 25;8(8):2898–920.

101. Bossi AM, Marinangeli A, Quaranta A, Pancheri L, Maniglio D. Time-Resolved Fluorescence Spectroscopy of Molecularly Imprinted Nanoprobes as an Ultralow Detection Nanosensing Tool for Protein Contaminants. Biosensors. 2023;13(7).

102. Alanazi K, Garcia Cruz A, Di Masi S, Voorhaar A, Ahmad OS, Cowen T, et al. Disposable paracetamol sensor based on electroactive molecularly imprinted polymer nanoparticles for plasma monitoring. Sensors Actuators, B Chem. 2021 Feb 15;329(July 2020):129128.

103. Lahcen AA, Rauf S, Aljedaibi A, de Oliveira Filho JI, Beduk T, Mani V, et al. Laser-scribed graphene sensor based on gold nanostructures and molecularly imprinted polymers: Application for Her-2 cancer biomarker detection. Sensors Actuators B Chem. 2021 Nov 15;347:130556.

104. Lelis GC, Fonseca WT, de Lima AH, Okazaki AK, Figueiredo EC, Riul A, et al. Harnessing Small-Molecule Analyte Detection in Complex Media: Combining Molecularly Imprinted Polymers, Electrolytic Transistors, and Machine Learning. ACS Appl Mater Interfaces. 2023;

105. Smolinska-Kempisty K, Guerreiro A, Canfarotta F, Cáceres C, Whitcombe MJ, Piletsky S. A comparison of the performance of molecularly imprinted polymer nanoparticles for small molecule targets and antibodies in the ELISA format. Sci Rep. 2016;6(November):1–7.

106. El-Schich Z, Zhang Y, Feith M, Beyer S, Sternbæk L, Ohlsson L, et al. Molecularly imprinted polymers in biological applications. Biotechniques. 2020;69(6):407–20.

107. Wackerlig J, Schirhagl R. Applications of Molecularly Imprinted Polymer Nanoparticles and Their Advances toward Industrial Use: A Review. Anal Chem. 2016 Jan 5;88(1):250–61.

108. Poma A, Guerreiro A, Caygill S, Moczko E, Piletsky S. Automatic reactor for solid-phase synthesis of molecularly imprinted polymeric nanoparticles (MIP NPs) in water. RSC Adv.

2014;4(8):4203–6.

109. Muzyka K, Karim K, Guerreiro A, Poma A, Piletsky S. Optimisation of the synthesis of vancomycinselective molecularly imprinted polymer nanoparticles using automatic photoreactor. Nanoscale Res Lett. 2014 Mar 31;9(1):1–7.

110. Li S, Li J, Luo J, Xu Z, Ma X. A microfluidic chip containing a molecularly imprinted polymer and a DNA aptamer for voltammetric determination of carbofuran. Microchim Acta. 2018;185(6):1–8.

111. Raziq A, Kidakova A, Borozнjak R, Reut J, Öpik A, Syritski V. Development of a portable MIP-based electrochemical sensor for detection of SARS-CoV-2 antigen. Biosens Bioelectron. 2021;178.

112. Cáceres C, del Pilar Garcia Morgado M, Bozo FC, Piletsky S, Moczko E. Rapid Selective Detection and Quantification of β-Blockers Used in Doping Based on Molecularly Imprinted Nanoparticles (NanoMIPs). Polymers (Basel). 2022 Dec 1;14(24):5420.

113. Samanta A, Guchhait N, Bhattacharya SC. Photophysical aspects of biological photosensitizer Kynurenic acid from the perspective of experimental and quantum chemical study. Spectrochim Acta - Part A Mol Biomol Spectrosc. 2014;129:457–65.

114. Zelentsova EA, Sherin PS, Snytnikova OA, Kaptein R, Vauthey E, Tsentalovich YP. Photochemistry of aqueous solutions of kynurenic acid and kynurenine yellow. Photochem Photobiol Sci. 2013;12(3):546–58.

115. Brown CW, Obremske RJ. Multicomponent quantitative analysis. Appl Spectrosc Rev. 1984;20(3–4):373–418.

116. Wallace RM. Analysis of absorption spectra of multicomponent systems. J Phys Chem. 1960;64(7):899–901.

117. Gupta D, Bhardwaj S, Sethi S, Pramanik S, Kumar Das D, Kumar R, et al. Simultaneous spectrophotometric determination of drug components from their dosage formulations. Spectrochim Acta Part A Mol Biomol Spectrosc. 2022 Apr 5;270:120819.

118. Mantoanelli JOF, Gonçalves LM, Pereira EA. Dansyl Chloride as a Derivatizing Agent for the Analysis of Biogenic Amines by CZE-UV. Chromatographia. 2020 Jun 1;83(6):767–78.

119. Ayranci R, Vargün E, Ak M. Conjugated and Fluorescent Polymer Based on Dansyl-Substituted Carbazole: Investigation of Electrochromic and Ion Sensitivity Performance. ECS J Solid State Sci Technol. 2017 Mar 10;6(5):P211–6.

120. Feng X, Ashley J, Zhou T, Halder A, Sun Y. A facile molecularly imprinted polymer-based fluorometric assay for detection of histamine. RSC Adv. 2018 Jan 9;8(5):2365–72.

121. Diliën H, Peeters M, Royakkers J, Harings J, Cornelis P, Wagner P, et al. Label-Free Detection of Small Organic Molecules by Molecularly Imprinted Polymer Functionalized Thermocouples: Toward in Vivo Applications. ACS Sensors. 2017 Apr 28;2(4):583–9.

122. Devaraj NK, Finn MG. Introduction: Click Chemistry. Chem Rev. 2021 Jun 23;121(12):6697–8.

123. Northrop BH, Frayne SH, Choudhary U. Thiol–maleimide "click" chemistry: evaluating the influence of solvent, initiator, and thiol on the reaction mechanism, kinetics, and selectivity. Polym Chem. 2015 Apr 28;6(18):3415–30.

124. Mann MA, Bottomley LA. Cyclic Square Wave Voltammetry of Surface-Confined Quasireversible Electron Transfer Reactions. Langmuir. 2015;31(34):9511–20.

125. Brown AP, Anson FC. Cyclic and Differential Pulse Voltammetric Behavior of Reactants Confined to the Electrode Surface. Anal Chem. 1977;49(11):1589–95.

126. Piletsky SS, Cruz AG, Piletska E, Piletsky SA, Aboagye EO, Spivey AC. Iodo Silanes as Superior

Substrates for the Solid Phase Synthesis of Molecularly Imprinted Polymer Nanoparticles. Polymers (Basel). 2022 Apr 1;14(8):1595.

127. Zhu M, Lerum MZ, Chen W. How to prepare reproducible, homogeneous, and hydrolytically stable aminosilane-derived layers on silica. Langmuir. 2012 Jan 10;28(1):416–23.

128. Cattoni DI, Chara O, Kaufman SB, Flecha FLG. Cooperativity in Binding Processes: New Insights from Phenomenological Modeling. PLoS One. 2015 Dec 1;10(12):e0146043.

129. Goutelle S, Maurin M, Rougier F, Barbaut X, Bourguignon L, Ducher M, et al. The Hill equation: a review of its capabilities in pharmacological modelling. Fundam Clin Pharmacol. 2008 Dec 1;22(6):633–48.

CHAPTER 4:

SIMULTANEOUS *IN VITRO* ISOLATION OF MULTIPLE TARGET-SPECIFIC APTAMERS TOWARDS SMALL-MOLECULE BIOMARKERS

The use of aptamers, single-stranded DNA or RNA oligonucleotides, has garnered attention as a promising alternative to antibodies for the detection of small molecules (SM) due to their high specificity and affinity, as well as their ease of synthesis and better stability. This study emphasizes the development of aptamers targeting Acute-on-Chronic Liver Failure (ACLF)-associated small-molecule biomarkers using Magnetic Bead-based Systematic Evolution of Ligands by EXponential enrichment (MB-SELEX) and Joint One-Pot SELEX (jOP-SELEX) methodologies. The MB-SELEX method employed MBs conjugated to phenylalanine (Phe) to isolate single-target aptamers, with tryptophan (Trp) utilized as a counter-selection target. Additionally, the novel jOP-SELEX method sought to simultaneously select aptamers for multiple Acute-on-Chronic Liver Failure (ACLF)-associated targets, including kynurenic acid (KA), quinolinic acid (QA), and Phe, thereby enhancing specificity through a combination of negative and counter-selection steps.

Next-Generation Sequencing (NGS) and custom-developed MATLAB code were employed for sequence identification and tracking through the round to ensure the optimal performance of these SELEX methodologies. NGS facilitated a thorough analysis of the enriched libraries, allowing for the identification of sequence motifs and tracking of the enrichment process through the SELEX rounds. The bioinformatics workflow could validate the enrichment of potential aptamer candidates in the early SELEX rounds, showcasing the potential of this method to increase the speed of aptamer identification in other SELEX processes. The outcomes demonstrated the successful isolation and enrichment of aptamers specifically targeting ACLF biomarkers, highlighting the potential of advanced SELEX strategies and bioinformatics tools in creating highly targeted aptamers for clinical and diagnostic purposes.

4.1. INTRODUCTION

4.1.1. Aptamers as biorecognition elements

Synthesizing and characterizing new antibodies is a complex and time-consuming process that involves multiple steps, such as target preparation, animal immunization, antibody purification, and characterization.[1,2] Due to the in vivo nature of antibody production, controlling binding characteristics can be challenging. Immunosensors face several challenges when detecting small molecules (SM) due to their size, lack of immunogenicity, and available epitopes of the target molecules. Moreover, the resemblance of these molecules to endogenous compounds can activate host tolerance mechanisms, further complicating the detection process [3–5]

Aptamers, single-stranded DNA (ssDNA) or RNA oligonucleotides, offer an effective solution to this challenge as their specificity and high affinity towards the target could be tailored in a synthetic and more straightforward manner, as well as relying on various aspects such as shape complementarity, and noncovalent interactions such as hydrophobic, electrostatic interactions, π-π stacking, and hydrogen bonding, to bind to their target after folding into intricate three-dimensional conformations, as depicted in Figure 4.1. [6–8]

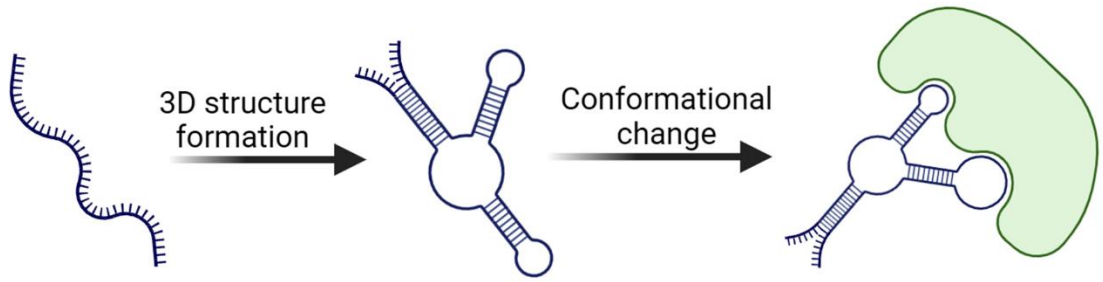


Figure 4.1. *Schematic representation of 3D structure and target-induced conformational changes of aptamers as bioreceptors. Figure from Biorender*

In the 1990s, several researchers successfully discovered the first small-molecule-binding aptamers by utilizing in vitro selection techniques to analyze the binding mechanisms of antibiotic ligands like chloramphenicol and aminoglycoside to nucleic acid motifs.[9–11] Since then, there have been numerous research studies on the isolation and further use of aptamers in several applications, such as (bio)sensors, drug delivery, and disease treatment. Nevertheless, while aptamers have been extensively studied for larger targets, such as proteins and cells, there is a relative scarcity of documented SM-binding aptamers, which can be mainly attributed to technical challenges associated with their selection and characterization, which will be discussed further in subsequent sections. [12–15]

Aptamers, besides offering ease of labeling, thermal stability, versatility, cost-effectiveness, and development time similar to polyclonal antibody production, have also been demonstrated to be highly stable. This is due to their resilient phosphodiester backbone, which sets them apart from protein-based bioreceptors (e.g., antibodies, peptides, or enzymes), as they could be reversibly denatured due to changes in pH, temperature, or ionic strength. Aptamers can also be restored to their original binding state after such changes, i.e., they can undergo several regeneration cycles; for instance, there are various published methods for reversing their conformation after target detection. [6,7,16,17] Ideally, a proper regeneration solution would have no impact on the aptamer's structure and would simply interfere with its interaction with the analyte. This advantage allows for the selection of aptamers based on their potential application.

The aptamer's conformational changes associated with target recognition play a crucial role in guaranteeing a proper binding affinity, i.e., the strength of the interaction between two or more molecules that bind reversibly.[18–20] Despite their potential usefulness, aptamers do have certain limitations: (i) their hydrophilicity and overall negative charge make them susceptible to rapid breakdown by nucleases; (ii) the range of secondary and tertiary structures they can adopt is limited, as they only contain four nucleic acids as building blocks. To address some of these issues, modifying the aptamer backbone or adding certain functional groups could improve their stability, albeit at a potentially higher financial cost. [21,22]

4.1.1.1. Thermodynamics of Aptamer-Target Interaction

Several techniques have been developed for isolating aptamer candidates from a diverse library based on their interactions with a specific target. These techniques utilize the dissociation constant (KD) or changes in Gibbs free energy (ΔG) to assess the binding affinity of the aptamer candidates to the target. ΔG, the driving force of the aptamer:target (Apt:Tg) complex, comprises both enthalpic (ΔH) and entropic (ΔS) components, collectively predicting the likelihood of a spontaneous and stable recognition occurring at constant pressure and temperature. [23–25]

$$\Delta G = \Delta H - T\Delta S \quad (1)$$

A more negative ΔG indicates a stronger affinity and a more stable Apt:Tg complex, leading to lower KD. Similarly, a negative ΔH suggests a higher frequency of Apt:Tg interactions, which enhances the stability of the complex. Nevertheless, enthalpy variations in the Apt:Tg binding process can be significantly influenced by the solvent of use as it could disrupt H-H bonds and van der Waals interactions in the Apt:Tg complex.[26]

The stability of Apt:Tg complex is also influenced by entropic changes. It has been observed that low-affinity aptamers exhibit nonspecific interactions with the solvent, leading to a significant entropic increase due to the increase in the randomness of the water molecules surrounding the aptamer during binding. Conversely, a negative ΔS arises from an entropic decrease caused by target-specific conformational

changes. These changes occur due to a loss of rotational and translational degrees of freedom of the aptamer in the Apt:Tg complex compared to free aptamers. [27,28] It is worth mentioning that aptamers' innate flexibility makes them highly susceptible to their environment, which can lead to conformational instability and reduced affinity and selectivity toward their desired target.

Enthalpy-driven recognition ligands may exhibit greater affinity and higher resistance to matrix interference in practical implementations compared to an entropy-driven ligand undergoing a comparable ΔG. This is mainly due to the increased bond frequency between the ligand and the target in the former case. Therefore, by optimizing these parameters, a more profound understanding of the thermodynamics governing the binding process can be attained. This, in turn, can provide valuable insights into the actual binding mechanism, facilitating a more accurate determination of experimental settings or adaptations to the aptamer structure or its isolation. [23,29]

4.1.2. Systematic Evolution of Ligands by Exponential enrichment

Identifying synthetic aptamers is a complex task that poses several challenges. Despite the implementation of computational methods and rational design approaches, the intricate nature of the Apt:Tg complex continues to be a formidable issue. [14] Therefore, the widely accepted approach for this purpose is based on Systematic Evolution of Ligands by EXponential enrichment (SELEX), a well-established in vitro selection technique. As aforementioned, the simultaneous introduction of SELEX in 1990 was done by Ellington and Szostak and Tuerk and Gold, which has been extensively used to identify aptamers. [9–11,30] Many protocols and reviews on the topic have been published, and researchers have documented numerous variants of the initial method to improve its efficacy. [31,32]

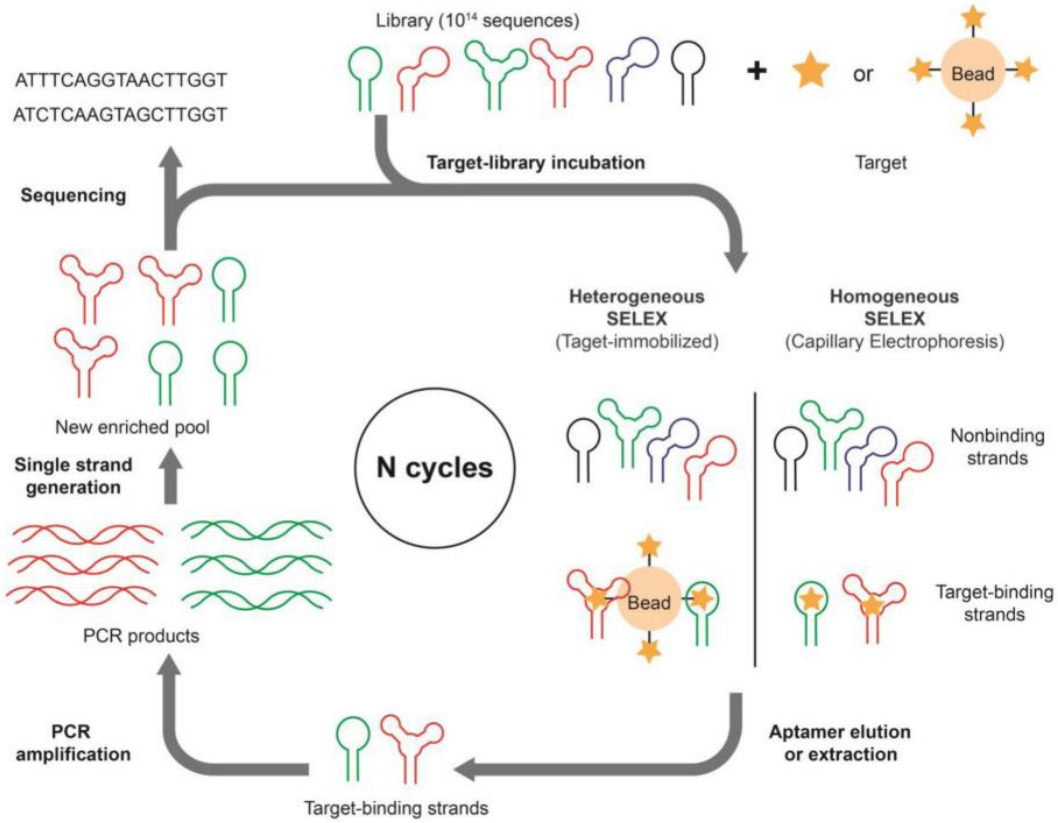


Figure 4.2. Schematic representation *of the SELEX technique. Retrieved with permission from* [15]

The SELEX method is a widely used combinatorial chemistry technique for identifying and isolating aptamers (target-specific sequences) from a pool of between 1015 and 1060 random ssDNA or RNA sequences [33–35] As suggested in Figure 4.2, the process is iterative and involves several steps, including exposing the random nucleic acid (NA) library to the target, isolating the target-bound aptamers, amplifying them via PCR, and then purifying them. This cycle is repeated, starting from the purified collection, until the enriched aptamers are isolated.

Typically, 6-25 selection rounds are required to observe the intended enrichment. However, some advanced protocols (e.g., atomic force microscopy SELEX, and microfluidic SELEX) can accomplish this in only three rounds.[36] The stringency requirements are progressively tightened throughout the SELEX course to ensure that the initial library accumulates sequences that exhibit strong affinity and specificity toward the target. [12]

SELEX, compared to antibody generation methodologies, offers distinct advantages. It allows for custom-made selection conditions that can be finely tuned throughout the process, enabling the selective enrichment of highly specific aptamers. Notably, small compounds, often non-immunogenic, may require the laborious process of conjugation to carrier proteins to induce a sufficient antibody response during immunization. In contrast, SELEX's in vitro approach enables the direct isolation of aptamers for virtually any SM, including toxic or non-immunogenic. This highlights the potential of SELEX as an alternative to antibody generation procedures, especially when considering the final application of the aptamers, where

several parameters, such as buffer ionic strength, pH, and matrix, should be considered for optimal performance. [13,37–39]

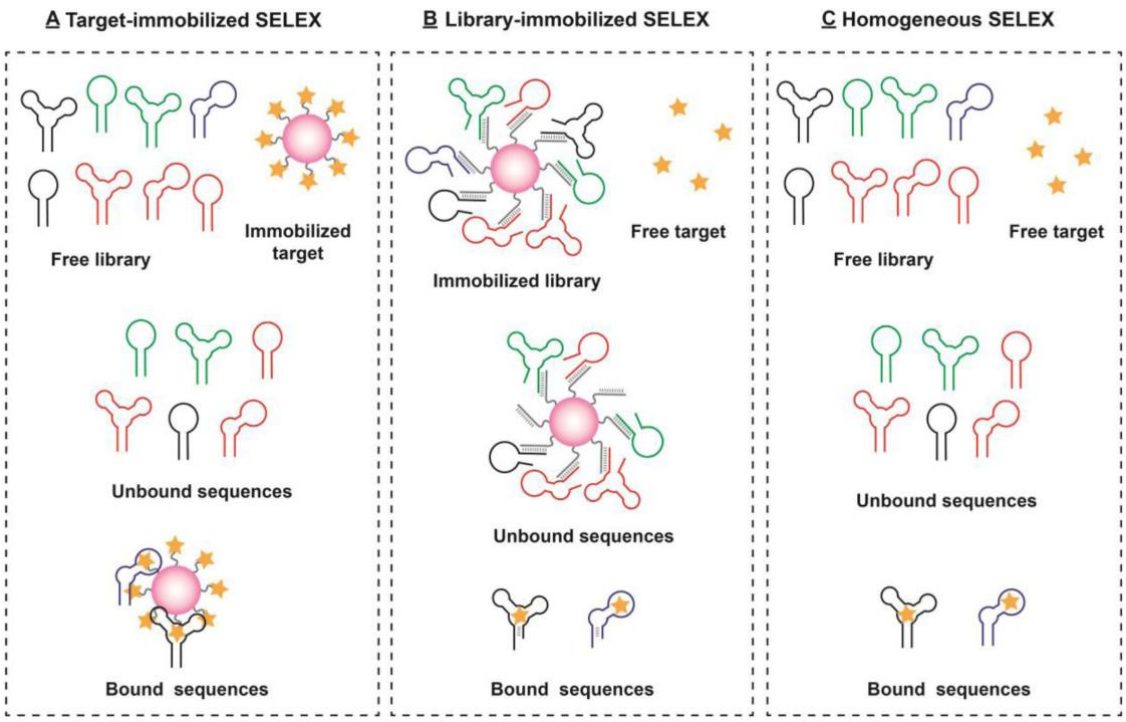


Figure 4.3. *SELEX approaches.* (A) Target-immobilized, (B) Library-immobilized SELEX, (C) Homogeneous SELEX. Retrieved from [15]

It is often observed that sequences exhibiting greater affinities tend to dominate the NA pool and are subsequently analyzed using Next-Generation Sequencing (NGS) techniques and bioinformatics to identify possible aptamer candidates. To validate them, further binding studies are carried out to determine their specificity and affinity towards their desired target. The success of aptamer selection largely depends on the SELEX strategy employed (depicted in Figure 4.3), including the NA library, partitioning strategies for isolating target-bound aptamers, PCR protocols, and regeneration and purification of RNA or ssDNA for further experimentation. [34,40,41]

As mentioned above, SELEX's ease of adaptability and duration is particularly beneficial when dealing with new and challenging targets, as developing monoclonal antibodies using traditional methods could take several months. Furthermore, aptamers tend to have significantly longer shelf lives than antibodies and enzymes due to their inherent ability to resist degradation and denaturation in extreme conditions. Additionally, oligonucleotide synthesis costs are comparatively lower, and their batch-to-batch heterogeneity is reduced as they can be chemically manufactured.

4.1.2.1. Oligonucleotide library

In the conventional sense, libraries encompass a large collection of diverse sequences consisting of two regions: a random central region (RCN), which varies from 10-80 nucleotides in length, and (ii) common flanking regions where primers may bind for amplification purposes. To ensure that aptamers effectively bind to their targets via the secondary or tertiary structures (mainly associated with nucleotides from their RCN), it is imperative to design primers that prevent dimerization and/or hairpins. As such, it is essential to guarantee a high level of heterogeneity in the starting library, typically including 1015-1030 unique sequences, leading to increases in the probability of having target-binding motifs in the initial pool. [34,35,42]

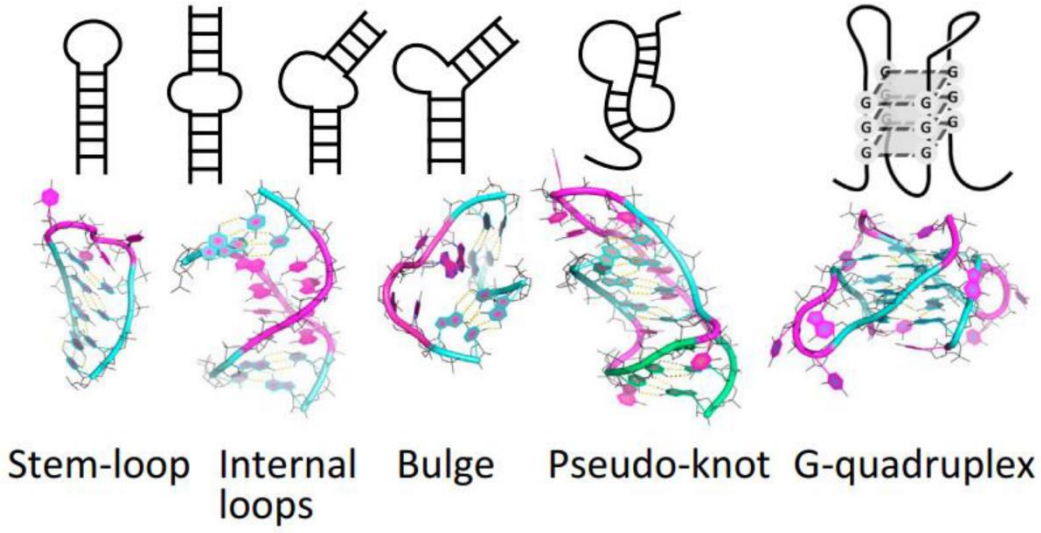


Figure 4.4. *Possible 2- and 3-D conformational structures that aptamers may adopt based on the nucleotide content and distribution. Retrieved with permission of* [43]

In the past, RNA libraries were commonly used as it was believed that only RNA could fold into functional patterns, although requiring an additional reverse transcription step. However, recent studies have shown that ssDNA has the same folding capability, as shown in Figure 4.4. While RNA aptamers tend to have more structural complexity, the practicality of ssDNA libraries has made them increasingly popular in recent years. Furthermore, ssDNA and RNA aptamers have comparable affinities for their targets, each providing a unique range of structural conformations. Nevertheless, ssDNA libraries are more straightforward to synthesize and offer enhanced chemical and biological stability. [42]

While more extensive libraries may have advantages, they can also pose potential challenges in PCR amplification and the generation of ssDNA or RNA. One crucial factor to consider is the RCN's length. A longer RCN can make the library less predictable, leading to undesired interactions; i.e., by increasing the RCN length, the library increases the chances of non-specific binding among unique strands. On the other hand, if the RCN is too short, it may lack target-specific motifs or the sequence would be unable to fold

into the necessary target-binding "pockets", thereby hindering its ability to interact specifically with the target[22,34,39]

Although the use of base-modified aptamers has been explored and extensively demonstrated in various research studies to enhance the binding affinities toward proteins, the efficacy of such aptamers in SM detection is still uncertain. Creating a library of short sequences for SMs could be a plausible alternative to overcome the size disparity between aptamers and SMs. However, this approach presents a dilemma as increasing the number of nucleotides also increases the potential conformations that sequences may assume, raising the possibility of successful aptamer isolation. Yet, the significant size disparity poses a challenge in the SELEX process, as nitrogenous bases can be similar in size to SMs. Therefore, multiple factors, such as the target's size, chemical functionality, and binding behavior, must be considered for a successful outcome. A thoughtfully designed library facilitates the integration of functionality and structural modifications during SELEX, which may reduce or eliminate the need for subsequent post-SELEX strategies. [35,44]

4.1.2.2. Library Conditioning

To achieve the desired enrichment in each SELEX cycle, it is essential to prioritize the yield and sequence quality of the initial step by conditioning the library, which plays a critical role in dictating the eventual outcome of the SELEX. For quite some time, generating ssDNA from the dsDNA template via PCR linearization has been the conventional approach within SELEX. However, there are four well-researched methods for ssDNA regeneration, namely: (i) streptavidin-biotin separation; (ii) denaturing polyacrylamide gel electrophoresis (PAGE) size separation; (iii) asymmetric polymerase chain reaction (aPCR) for ssDNA generation; and (iv) lambda (λ) exonuclease 5'→3' digestion in dsDNA. The literature suggests that the most favorable results, in terms of higher yields and quality, are achieved by combining aPCR and exonuclease digestion. [35,45,46]

PCR amplification is a crucial step in SELEX, as it ensures optimal enrichment of the pool, with every sequence ideally being amplified equally and effectively. However, PCR bias is a well-known issue that may occur due to certain sequences being favored over others, which could compromise the reliability of positive selection and SELEX per se. Various strategies could be implemented to mitigate this issue, such as reducing product (or amplicon) size, optimizing the PCR temperatures, increasing primer concentrations, etc. Additionally, using labeled primers and libraries could be an alternative option to quantify PCR bias. [47–49]

Optimizing the PCR process is essential for achieving accurate and efficient dsDNA synthesis. While increasing the number of PCR cycles can increase yields, it is essential to prevent overamplification and unwanted byproduct formation. The high heterogeneity of the PCR template, which is determined by the initial pool characteristics, can cause undesired interactions, such as product-primer (mispriming), product-

product, and primer-primer dimerization, thereby reducing SELEX efficiency. Therefore, balancing the number of amplification cycles, PCR conditions and selecting a bias-reduced DNA polymerase might ensure the desired quality of dsDNA synthesis.[47,50]

4.1.2.3. Partitioning strategy

Isolating target-bound aptamers from the rest of the pool is a crucial step in the selection process. A partitioning approach is commonly employed for this purpose; however, the level of effectiveness can vary and depends on the specific method used, as there is currently no universally accepted method for achieving this. More efficient elimination of non-binding aptamers can lead to a faster pool enrichment, ultimately resulting in fewer selection cycles needed for aptamer isolation. [12,35]

Various techniques, such as nitrocellulose filters, affinity-based columns, and magnetic beads (used in this chapter), are commonly used for partitioning purposes. [35] Over the years, numerous protocols have been published, including those that do not involve immobilization, such as Capillary electrophoresis SELEX and Sol-gel-based microfluidic SELEX. Additionally, there are protocols like Capture-SELEX, which require immobilization of the library while the target remains in solution, rendering it ideal for SMs or when the target has limited functionality and binding possibilities[51,52]

The conjugation of SMs can be challenging due to their reduced number of functional groups. Therefore, aptamers isolated from a conjugated SM have been demonstrated to exhibit less affinity for the free target. This finding implies that attaching linkers or moieties for conjugation could potentially modify the target's physiochemical properties. Various factors should be considered, including the target's size and complexity and the aptamer's intended use. However, practical considerations, such as the availability of laboratory equipment, financial resources, and research personnel, may also influence the selection process. [53,54]

Regarding SMs, bound and unbound sequences could be challenging to discern. This separation process can become further complicated due to the target's physicochemical properties, which may not result in a significant mass difference between the Apt:Tg complex and the unbound aptamer. As a result, it is often employed as common practice to immobilize one of the biomolecules.[55,56]

4.1.2.4. Selection conditions

As aforementioned, the selection conditions during SELEX significantly impact the Apt:Tg binding interactions. Selection buffers containing cations, such as Na+, Mg2+, and K+, shield the negatively charged DNA backbone, thereby preventing any non-specific electrostatic interactions and reducing the electrostatic repulsion between neighboring phosphates. [12,27,34]

It is often recommended to carefully consider the stringency settings throughout the process, as this can significantly influence the optimization of aptamer affinity. While implementing high-stringency conditions early on may seem like a viable strategy, it can also result in losing target-binding sequences that may have been present in low copy numbers during the initial rounds. Therefore, starting with less stringent conditions is generally advisable to ensure binding and gradually increase the stringency as the SELEX rounds progress. This can be achieved by adjusting various parameters, including but not limited to: (i) target or library concentration, as it can help displace weakly bound aptamers via competition, favoring sequences with stronger binding affinities; (ii) reducing incubation periods, as the isolation of picomolar KD aptamers might take several hours, while species with nano- or micromolar KD can be obtained in minutes; (iii) incubation temperatures; or (iv) buffer composition. However, it is recommended to include a washing step afterward to ensure the desired disassociation. [32,34,57,58]

Furthermore, considering the binding buffer's physicochemical properties is a sine qua non for ensuring aptamer isolation as it should closely resemble those of the actual sample matrix, guaranteeing a desired performance in real-world applications.

4.1.2.5. Next-Generation Sequencing Analysis

Compared to Sanger sequencing, which is the traditional method for aptamer identification (1 sequence per sample), high-throughput sequencing (HTS) offers the unique advantage, providing higher sequence coverage, enabling not only a comprehensive determination of each sequence in the pool and its enrichment compared to prior rounds but also aids the identification of motif-sharing sequences by further clustering and generating families based on similarities throughout the SELEX process. In other words, this feature allows (i) the discovery of enriched sequences from a large pool of millions of sequences, exhibiting unique binding qualities; (ii) isolating aptamers based on enrichment criteria, which can help overcome the influence of factors such as PCR bias on the read count. [34,40,59,60]

It is plausible to conduct an analysis of the Apt:Tg binding and pool enrichment round-wise by employing a combination of HTS and bioinformatics, even prior to the termination of SELEX. Based on the maximization of sequence enrichment, this approach allows for the study of binding and/or structural motifs at each round, which might prevent the need to test many potential aptamer candidates in binding assays for various parameters such as affinity, specificity, and cross-reactivity.

4.1.2.6. Binding Assays

After the SELEX process, numerous aptamers with similar binding affinities can be obtained. Subsequently, it is vital to evaluate the analytical performance of the selected candidates based on their binding affinities and specificity towards the target and structurally similar molecules.

One of the significant challenges in aptamer screening and characterization, particularly for small molecules, is the lack of universally accepted standard binding assays, rendering it challenging to determine which assay is reliable for affinity measurements. Moreover, highly sensitive assays are required to accurately study the Apt:SM interaction to ensure a high signal-to-noise ratio. Various assays have shown potential in measuring binding interactions based on two strategies: (i) heterogeneous approaches, such as Surface Plasmon Resonance (SPR), Quartz crystal microbalance (QCM), Enzyme-Linked Immunosorbent Assay , Enzyme-Linked Aptamer Assay (ELAA), bead-ELISA, and AptaPCR Affinity Assay (APAA); and (ii) homogeneous approaches, like Isothermal Titration Calorimetry (ITC), and Electrophoretic Mobility Shift Assay (EMSA). However, it is crucial to recognize that each assay has its own limitations, and their suitability may differ depending on the target's chemical functionality and downstream application.[8,22,37,43,61]

To obtain thermodynamic information about the Apt:Tg complex, several research studies have utilized ITC, which can provide outputs such as KD, ΔG, ΔH, ΔS, and the number of oligonucleotide binding sites for further studies. Additionally, when selecting the techniques, it is essential to consider the final use of the aptamer. For instance, heterogeneous approaches are recommended when the aptamers are attached to a substrate (either electrode or lateral flow assay), and homogeneous methods should be employed when the aptamer is used in a free environment. [24,29]

It has been observed that SELEX studies have primarily relied on a single method to determine the binding affinity of newly isolated aptamers. However, it is recommended that future studies employ the desired sample matrix in conjunction with at least two well-established techniques to determine binding affinities. This approach could offer valuable additional information and help circumvent the limitations of individual techniques. It has been documented that the same binding technique (for small molecule detection) can lead to significant variations in KD on different occasions. Therefore, using multiple techniques for validation purposes would be a prudent step toward obtaining more comprehensive and reliable results that could be used in real-world applications.[8,34,62]

Regarding aptamer immobilization techniques, it is pivotal to consider a variety of factors in order to make an informed decision. Specifically, aptamer type, buffer conditions, electrode material, analyte characteristics, and biosensor operating parameters can all play a role in determining the most appropriate immobilization method. This phase of the design process can significantly impact critical features such as binding affinity, stability, (bio)receptor accessibility, non-specific adsorption, and overall electrochemical performance, if electrochemical aptasensors are used.

Unfortunately, due to time limitations, it was not feasible to carry out binding assays in this work. However, it is hypothesized that the most suitable binding assays for small-molecule targets would include bead-adapted binding assays such as APAA, ELAA, and ABAA, as well as SPR and MST for targets or aptamers in solution. As previously mentioned, each of these methods offers valuable insights into sensitivity and specificity, facilitating the determination of KD values for further analysis. Therefore, it

would be advisable to consider using multiple assays to estimate binding efficiencies in both target-conjugated and target in solution scenarios.

4.1.3. SELEX Approaches

Since the first development of SELEX, more than 30 variants have been published, each distinguished primarily by the separation method between non-binding and target-bound sequences. These variants can be broadly classified into two categories: heterogeneous SELEX, where either the target or the library are immobilized onto solid supports, such as Classic-, FluMag-[63], Capture-[51,52], One Pot- (OP-)[64], and Toggle-SELEX; and homogeneous SELEX, where both components are in solution, including Capillary Electrophoresis (CE-)[50] and Cell-SELEX[65]. Some examples are shown in Figure 4.5.

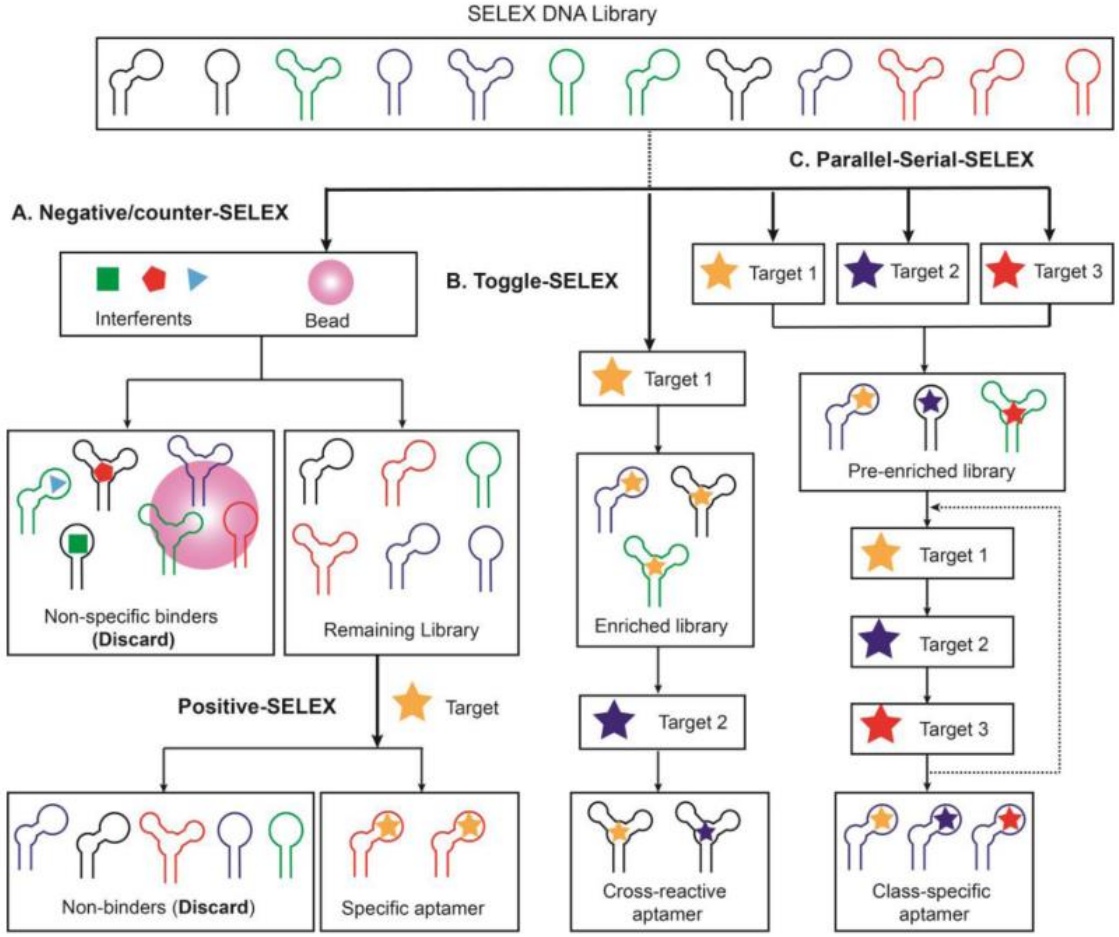


Figure 4.5. *Toggle SELEX design incorporating negative and counterselections, along with the parallel selection approach*. Retrieved from [53]

Despite its potential, target-immobilized SELEX faces some technical challenges that must be addressed. As aforementioned, conjugating small molecules to solid substrates can be complex, which may lead to aptamers with a lower binding affinity for the target free-in-solution. However, implementing negative and counter-selection strategies can help overcome this issue.[34,66]

For small molecules, Capture-SELEX, a.k.a. library-immobilized SELEX, is a promising approach (example in Figure 4.6A). In this method, docking sequences (DS) are immobilized onto beads, which then hybridize with the capture region on the ssDNA library. After target incubation, the target-binding sequences will undergo a conformational change that will release them from the beads, which will only retain non-binding sequences, allowing for a straightforward collection of the enriched pools. Compared to the target-immobilized methods, the background contribution is minimized as the targets are free in solution. However, the duration of the SELEX rounds may negatively impact the library-conjugated beads' efficiency due to spontaneous dissociation of the DS:library complex or weaker covalent bonds in DS-conjugated beads. Therefore, it is crucial to carefully consider the potential consequences of time effects on the final SELEX design.[51,67]

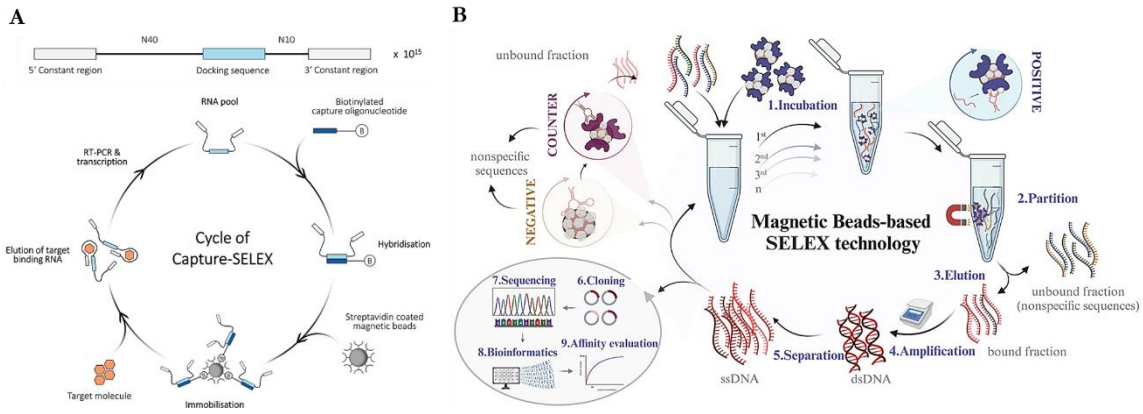


Figure 4.6. *Different types of SELEX approaches. (A) Capture-SELEX. Retrieved from [68]; and (B) MB-SELEX. Retrieved from [69].*

The Capture-SELEX method is a promising technique in the field, but it has some limitations. One of the potential challenges is the possibility of encountering sequences that interact irreversibly with the solid support or produce false-positive results due to weak interactions in the DS:library complex. Additionally, it may not always identify target-binding sequences if there are insufficient conformational changes during target incubation. Despite these potential limitations, the Capture-SELEX method remains an important tool for isolating aptamers towards SMs.[51,52]

An alternate strategy, known as OP-SELEX, was introduced by O'Sullivan et al. and is detailed in Figure 4.7C.[64] Aptamers were selected for three different steroids, estradiol, progesterone, and testosterone, with a preference for target estradiol. Due to the targets' co-occurrence and physicochemical similarities, testosterone and progesterone were utilized for counterselections. In the first rounds, the library was first exposed to target-free modified MBs and then estradiol-beads as positive selection. The incorporation of sequential incubations with the other targets was then introduced. This approach led to identifying and amplifying binding sequences enriched for estradiol while also selecting aptamers for the other steroids in the final rounds. By monitoring highly overrepresented sequences in only estradiol's sub-libraries, aptamer candidates with high affinities and nanomolar KD's were obtained for the three steroids. [64]

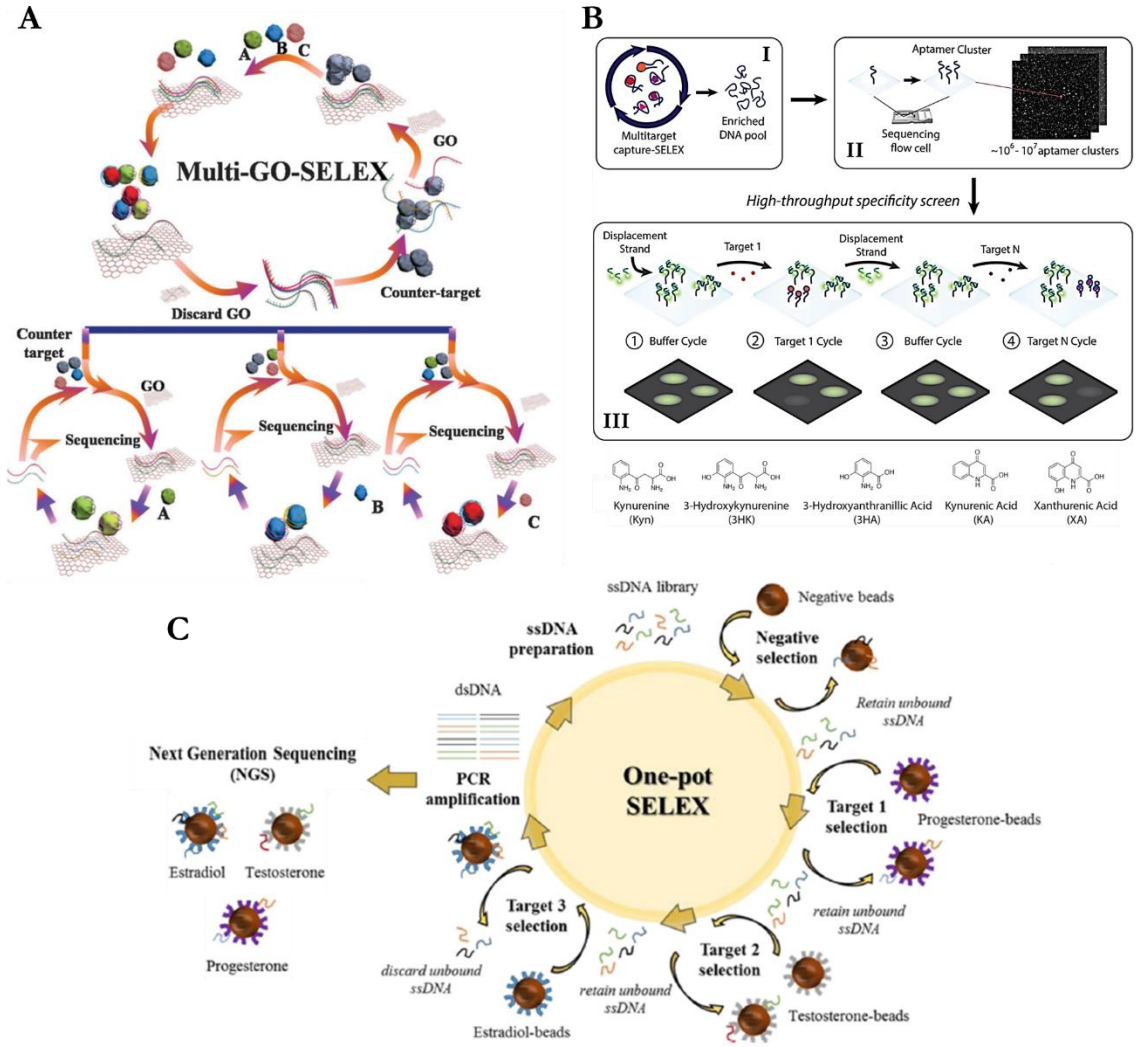


Figure 4.7. *Examples of multi-target SELEX approaches. (A) GO-SELEX. Retrieved from* [70]*; (B) Capture-SELEX. Retrieved from* [71]*; (C) OP-SELEX. Retrieved from* [64]

4.1.3.1. Applications and Limitations for Small Molecules

Aptamers' physicochemical properties, such as affinity, nuclease resistance, or chemical stability might be further enhanced through post-SELEX modifications, as depicted in Figure 4.8. Although optimizing the Apt:Tg complex can be challenging, truncation studies are often utilized to remove unnecessary nucleotide regions that do not contribute to any specific interaction, reducing fabrication costs. While smaller aptamers may offer some advantages, post-SELEX modifications could potentially disrupt any conformational change and stability of the aptamer. Therefore, to ensure the efficient aptamer design, determining the binding region/area and predicting the secondary/tertiary structures involved in target binding is crucial. [34,35,55,72,73]

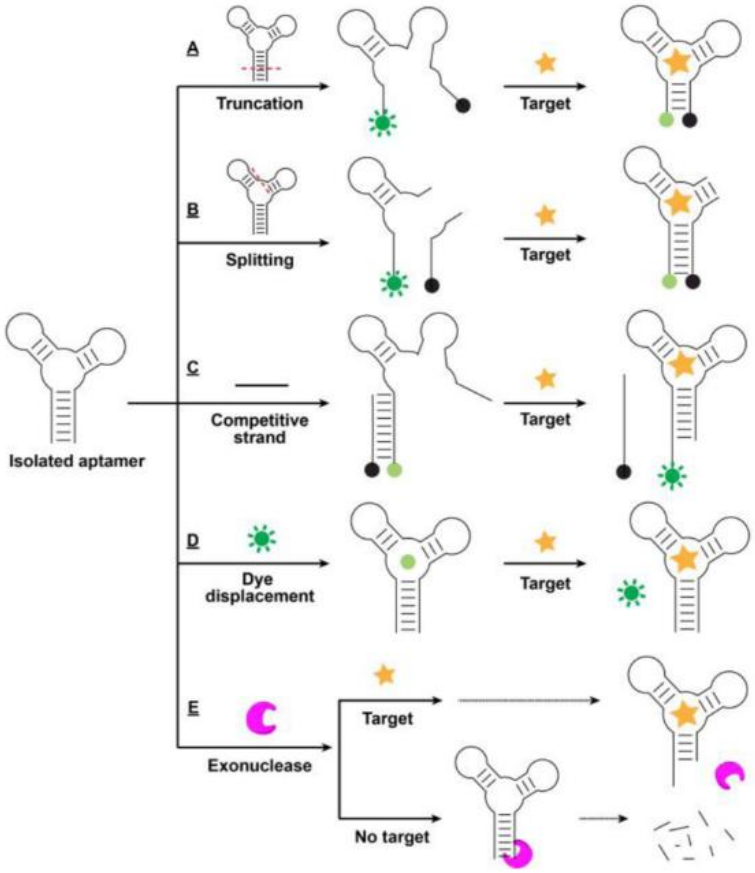


Figure 4.8. *Examples of post-SELEX modifications after aptamer isolation via NGS. Retrieved from* [53]

Although significant progress has been made in developing aptamer-based sensors for small molecule detection, it is important to consider that only a few of them have demonstrated the sensitivity and specificity required for real-world applications. There may be several factors contributing to this, including but not limited to (i) differences in the SELEX conditions and final application leading to a lack of affinity and specificity of aptamers for their targets; (ii) challenges in the characterization of Apt:Tg complex; (iii) the chosen strategy of aptamer conjugation onto solid substrates (nitrocellulose, beads, packed columns, etc) for sensing purposes may hinder possible conformational changes as the degrees of freedom are less than free in solution, as mentioned in previous sections; and (iv) scarcity of available epitopes or target functional groups for stabilizing the Apt:Tg complex.

It is crucial to carefully consider the optimal time to move from SELEX to HTS. Ending SELEX too soon could lead to a more heterogeneous library, possibly missing out on potential high-affinity aptamers. On the other hand, conducting too many rounds and implementing stringent conditions too early in the SELEX process may exclude promising target-binding sequences as well. [12,27,41,59,74]

Additionally, researchers have found that if a single aptamer cannot meet the requirements of a particular application, they have been able to adjust some sensor parameters, including limits of detection (LODs) and dynamic range, by combining two or more aptamers targeting different epitopes of the same target. Therefore, it may be necessary not to exclude what may at first appear to be less desirable aptamers.

To increase accuracy and reduce the possibility of errors during SELEX procedures, researchers have been exploring the implementation of robotic liquid-handling devices. While SELEX can be demanding and time-consuming, studies have demonstrated that adopting Automated-SELEX can facilitate the isolation of aptamers against multiple targets simultaneously, resulting in a significant reduction in the overall SELEX time, from several weeks or months to just a few days. The entire Automated-SELEX process, which includes strand separation and amplification, can now be performed on a single chip using microfluidic technologies. [75,76]

4.1.4. Joint One-Pot SELEX: three-target simultaneous aptamer selection

When isolating SM-binding aptamers, MB-SELEX and OP-SELEX are promising SELEX variants, with Capture-SELEX being another potential strategy. In the MB-SELEX method, target-conjugated magnetic beads isolate and capture target-binding sequences. Unbound sequences can be easily removed via magnetic separation and discarded after several washing steps. However, MBs exhibit significant nonspecific binding, therefore, incorporating a negative selection step is highly advantageous. It is possible to consider that OP-SELEX offers a potential multi-target strategy for aptamer isolation while taking into consideration time variables, physicochemical characteristics of the targets, and their co-occurrence.

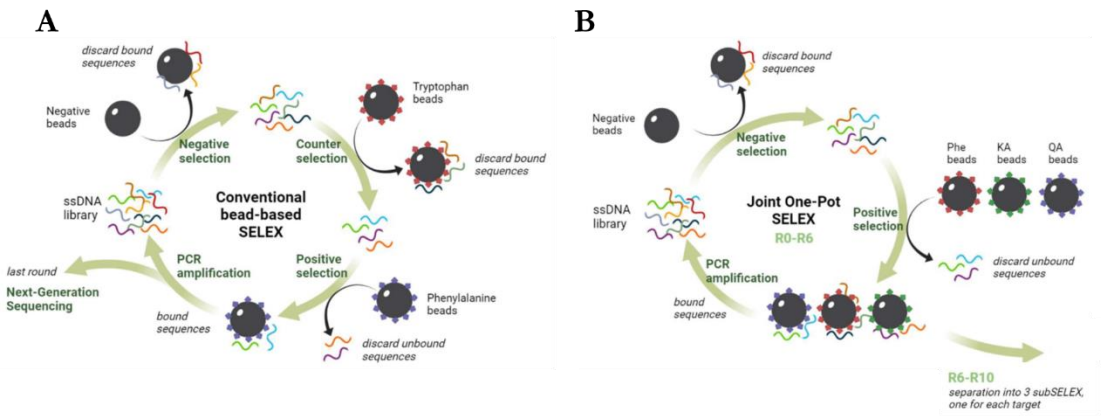
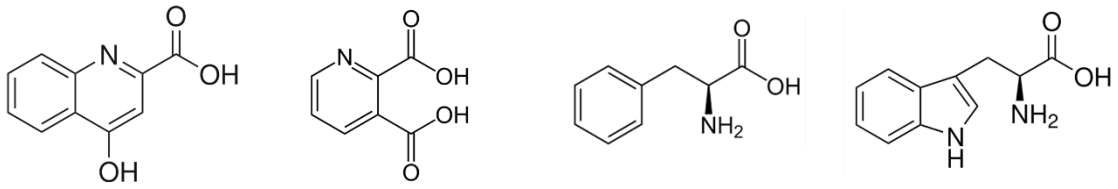


Figure 4.9. *Schematic of* conventional bead-based *SELEX and Joint One-Pot SELEX (initial stage)*

This chapter presents an innovative approach to aptamer selection called "Joint One-Pot SELEX" (jOP-SELEX) that involves the simultaneous selection of multiple targets associated to Acute-on-chronic Liver Failure (ACLF), shown in Scheme 4.1. Motivated by the OP-SELEX method, jOP-SELEX may provide a strategy to simultaneously enrich a pool of sequences for multiple structurally similar or co-occurring targets (Figure 4.9B), which could lead to the generation of several sequence families sharing motifs. It aims to achieve this objective within the same time frame as the MB-SELEX method using Phe as the target model

(Figure 4.9), which has been thoroughly studied in the literature. Furthermore, parallel SELEX processes (library separation) would be needed if target-specific aptamers are necessary.



Kynurenic Acid 187.17 g/mol | **Quinolinic Acid** 167.12 g/mol | **Phenylalanine** 165.19 g/mol | **Tryptophan** 224.23 g/mol

Scheme 4.1. *ACLF-associated small-molecule biomarkers employed for MB- and jOP-SELEX.*

4.2. OBJECTIVES

This chapter aims to develop and optimize SELEX processes for identifying aptamers targeting biomarkers associated with Acute-on-Chronic Liver Failure (ACLF). This will be achieved through the development of two distinct SELEX methodologies. Firstly, a conventional SELEX process will be developed, utilizing maleimide magnetic beads conjugated to phenylalanine as the target molecule. Tryptophan will be employed as a counter-selection target to enhance the specificity of the aptamers for phenylalanine. Multiple rounds of SELEX will be conducted to enrich the pool of aptamers specific to phenylalanine.

Simultaneously, a novel SELEX variation, termed Joint One-Pot SELEX, will be introduced and developed. This process involves the simultaneous incubation of three ACLF-related targets during the initial SELEX rounds. After several rounds, the process will be divided into three parallel SELEX streams, each focused on one of the three targets. In these parallel SELEX processes, the remaining two targets will serve as counter-selection targets to improve specificity and reduce cross-reactivity.

Next-generation sequencing (NGS) analysis will be employed to assess the SELEX process. Custom-developed MATLAB code will be used to facilitate an in-depth analysis of a more significant number of sequences, allowing for comprehensive sequence comparison both within rounds of the same SELEX process and between the parallel branches of the Joint One-Pot SELEX. This thesis chapter aims to contribute to aptamer development for ACLF biomarkers, where the insights and methodologies presented here could potentially be applied to other multiplexed SELEX processes.

4.3. MATERIALS & METHODS

4.3.1. Materials

The ssDNA library used in this work consists of 10^30 randomized 94 nt-long sequences purchased from Ella Biotech (Germany). All sequences are composed of the same structure, containing a random central region of 50 nucleotides flanked by fixed primer binding regions: 5'-AGCTCCAGAAGATAAATTACAGG-nt(50)-CAACTAGGATACTATGACCCC-3'. The library has a molecular weight of 29885 g/mol and was brought to a concentration of 100 μM. PCR was performed using library-specific primers, with a 23 nt-long forward primer (5'-AGCTCCAGAAGATAAATTACAGG-3') and a 21 nt-long 5'-phosphorilated reverse primer (5'-phosphate-GGGGTCATAGTATCCTAGTTG-3'). Both oligonucleotides were synthesized and purchased from LGC Biosearch Technologies (Denmark).

PureCube Maleimide Activated MagBeads (25 μm) were purchased from Cube Biotech (Germany). Quinolinic acid, kynurenic acid, phenylalanine and tryptophan molecules, HRP-conjugated goat anti-rabbit pAb, 6-Amino-1-hexanethiol hydrochloride, 1-butanethiol, PBS tablets, magnesium chloride, Tween-20, polyethylene glycol 400, 3,3',5,5'-tetramethylbenzidine(TMB), sulfuric acid, agarose, ethanol, N-hydroxysuccinimide (NHS), 2-Morpholinoethanesulfonic acid hydrate (MES), and dry skim milk were purchased from Merck (Germany). 1X PlatinumTM II Taq Hot Start Polymerase, 10X lambda exonuclease, 96-wells transparent microplates, GeneRuler Ultra Low Range DNA Ladder, SYBRTM Gold Nucleic Acid Gel Stain, TriTrack DNA Loading Dye, sulfo-NHS-acetate, and 1-ethyl-3-(3-dimethylaminopropyl) carbodiimide (EDC) were purchased from Thermo Fisher Scientific (US). GelGreen® Nucleic Acid Gel Stain was purchased from Biotium (US). Rabbit anti-quinolicic acid antibody and rabbit anti-kynurenic acid antibody were purchased from Abcam (Netherlands). Rabbit anti-phenylalanine antibody and rabbit anti-tryptophan acid antibody were purchased from Immusmol (France).

Mini 10 Horizontal Electrophoresis kit and accessories were purchased from VWR (US), SpectraMax iD3 from Molecular Devices (USA), Veriti™ 96-Well Fast Thermal Cycler from Thermo Fisher Scientific (USA), InGenius 3 Gel Doc System transilluminator from Syngene (UK), Oligo Clean & Concentrator kit was purchased from Zymo Research (US)

4.3.2. SsDNA library and primers

For this study, a ssDNA library of 1030 94-nt-long randomized sequences was employed, which were obtained from Ella Biotech (Germany). Each sequence consisted of fixed primer binding regions flanking a random central region of 50 nucleotides, namely, 5'-AGCTCCAGAAGATAAATTACAGG-nt(50)-CAACTAGGATACTATGACCCC-3'. The library's concentration, which has a molecular weight of 29885 g/mol, was increased to 100 μM, and PCR was conducted using specific primers designed for the library.

The forward primer, with a length of 23 nucleotides (5'-AGCTCCAGAAGATAAATTACAGG-3'), and the phosphorylated reverse primer, 5'-GGGGTCATAGTATCCTAGTTG-3', with a length of 21 nucleotides.

4.3.3. Target-conjugated magnetic beads

PureCube Maleimide Activated MagBeads (purchased from Cube Biotech, Germany) were used in the conjugation process with various target molecules. To ensure the validity of the results, seven independent conjugations were conducted, including kynurenic acid (KA), quinolinic acid (QA), tryptophan (Trp), two phenylalanine (Phe) conjugations, and two negative controls. All conjugation steps were carried out in a dark and temperature-controlled environment using a tube rotator. To eliminate any residual untethered target, the magnetic beads were washed thrice with the buffer of each coupling phase before and after incubation.

Briefly, 100 µL of MBs were put in a microcentrifuge tube, followed by three washes with 500 µL of 10 mM PBS (pH 6.5–7). Subsequently, 100 µL of 5.89 mM AHT in 10 mM PBS (pH 6.5–7) was added to the MBs, vortexed, and incubated for 2 h. The supernatant was removed via magnetic separation, and 100 µL of 100 mM BT in 10 mM PBS (pH 6.5–7) was added to AHT-modified beads and incubated for 2 h. After discarding the supernatant, modified MBs were then incubated for 2 hours in a solution containing 50 µL of 10 mM of the respective target, 50 µL of 644 mM EDC and 50 µL of 869 mM NHS in 0.1 M MES buffer at pH 5.0. Finally, the target-conjugated MBs were incubated for 1h with 100 µL of excess sulfo-NHS acetate in PBS (pH 7.5) to block remaining unreactive amine on the beads.

4.3.4. Verification of target conjugation

Target conjugation was validated via competitive bead-ELISA. QA and KA-conjugated beads were rinsed thrice with 200 µL of 10 mM PBS containing 0.1% Tween (PBST, pH 7.4). The beads were then treated for 30 mins with 200 µL of 2% dry skimmed milk (w/v) in PBST. Subsequently, each target-conjugated bead was incubated with 50 µL of a 1:10000 dilution of anti-target rabbit polyclonal antibody (pAb) - anti-QA and anti-KA, and anti-Phe and anti-Trp. The beads were then incubated for 1 h. Subsequently, each bead was incubated for 30 mins with 50 µL of HRP-conjugated goat anti-rabbit pAb at 1:20000 in 2% milk/PBST. For Phe- and Trp-MBs, the aforementioned procedure was replicated, with the exception of PEG400 being used for Phe and Trp instead of dry skim milk throughout.

The incubation was carried out in a controlled environment, in dark conditions, and at ambient temperature, on a tube rotator. After each incubation, the beads were thoroughly washed five times with 200 µL of PBST to ensure no residual substances were left behind. The negative beads, a target-free control, were synthesized similarly. To ensure accuracy, three replicates were performed. 50 µL of TMB was added

to each tube and incubated for 5-10 mins at ambient temperature (static, on the bench). The color development (blue) continued until the negative control beads showed a slightly discernible color. The enzymatic reaction was stopped by adding 50 µL of 1 M H2SO4. The absorbance was measured at 450 nm using a plate reader after transferring the supernatant of each tube to a 96-well microplate reader. The mean and standard deviation for each bead type were calculated using the three replicates.

4.3.5. SELEX conditions

During the initial phase of the process, 3 µL of the ssDNA library was diluted in 97 µL of SELEX binding buffer (BB), which consisted of 10 mM PBS and 1.5 mM MgCl2 (pH 6.4), resulting in a starting concentration of 3 µM. In subsequent rounds, the sub-libraries obtained at the end of each round were brought to 100 µL using BB. Prior to the selection process, the library was linearized at 95ºC for 5 minutes and then gradually cooled down to 25ºC, which facilitates conformational changes into their 3D structures. In the initial round (R0) of both SELEX procedures, only positive selection was achieved by incubating 100 µL of the library with 3 µL of Phe-MBs (for MB-SELEX) and with equal proportions of the three target-conjugated beads (1 µL each) for the jOP-SELEX .

Regarding MB-SELEX, after the incubation period, the supernatant was carefully discarded and the beads underwent three thorough washing steps with BB to ensure that only the target-bound sequences remained. To eliminate sequences that exhibited affinity towards the solid support, negative selection was incorporated in the subsequent round (R1) by incubating the library with negative beads (i.e., target-free MBs). The unbound sequences in the supernatant after incubation were then subjected to positive selection. As a counterselection step, an incubation with Trp-conjugated beads was introduced in R4, as can be seen in Table 4.1.

Table 4.1. *MB-SELEX conditions roundwise*

		R0	R1	R2	R3	R4	R5	R6	R7	R8-10
Volume of Library (µL)		100	100	100	100	100	100	100	100	100
Volume of beads (µL)	**(-)**		3	3	3	3	6	6	6	6
	c					3	3	3	3	3
	(+)	3	3	3	3	3	3	3	3	3
Incubation time (h)	**(-)**		2	2	2	2	2	2	2	2
	c					2	2	2	2	3
	(+)	2	2	2	2	2	2	2	2	1
Buffer		BB	BB	BB	BB	BB	BB	BB	BB	BB
Washing steps (repetitions with 100 µL)		3	3	2	2	2	3	5	3	3
Vortex time (s)		3	3	3x3	9	9	9	9	9	9

Regarding jOP-SELEX, negative selection was introduced in R1,while in R7, it was divided into three distinct MB-SELEX, one for each target. Following negative selection in R7, the resulting supernatant was split into three aliquots, each containing 33.33 µL, and brought to 100 µL for producing target-specific sublibraries. From R7 onwards, counterselection was employed by incubating each sub-library with equal amounts of their target-conjugated counterparts (1 µL each) in order to discard sequences that interact with structurally similar targets. The supernatant obtained after counter-selection was then subjected to positive selection by incubating it with the corresponding target-conjugated MBs. The incubations were carried out in microcentrifuge tubes, one for each SELEX procedure, using a tube rotator. Following each selection phase (negative, counter, and positive), the beads were resuspended in 20 µL of BB before amplification. The stringency binding conditions for both SELEX, which include the amount of beads, incubation times, buffer, number, and duration of washing, are shown in detail in Table 4.1 and 4.2.

***Table 4.2**. jOP SELEX conditions roundwise*

		R0	R1	R2	R3	R4	R5	R6	R7	R8-10
Volume of Library (µL)		100	100	100	100	100	100	100	100	100
Volume of beads (µL)	**(-)**		3	3	3	3	6	6	6	6
	c								1	3
	(+)	3	3	3	3	3	3	3	1	3
Incubation time (h)	**(-)**		2	2	2	2	2	2	2	2
	c								2	3
	(+)	2	2	2	2	2	2	2	2	1
Buffer		BB	BB	BB	BB	BB	BB	BB	BB	BB
Washing steps (repetitions with 100 µL)		3	3	2	2	2	3	5	3	3
Vortex time (s)		3	3	3x3	9	9	9	9	9	9

4.3.6. PCR amplification

Following the selection process, a Pilot PCR was employed to amplify the bound sequences of the positive, counter, and negative beads. To achieve this, a mixture of 10 µL of each bead suspension and 90 µL of PCR master mix (1X Master Mix, 0.4 µM forward primer, 0.4 µM reverse 5'-phosphorylated primer) was prepared. The final mixture was then divided into four 25-µL PCR tubes to perform amplification using several PCR cycles (5−25). A Veriti™ 96-Well Fast Thermal Cycler was employed in accordance with a predetermined protocol that included a 5-minute denaturation period at 95ºC, 5 to 25 repetitions at 95ºC, 55ºC, and 72ºC for 30 seconds each, and a final elongation step of 5 minutes at 72ºC. Gel electrophoresis was used to determine the quantity and quality of all bead suspensions, which was accomplished by loading 1µL of sample into 3% (w/v) non-denaturing agarose gels using 1µL TriTrack DNA Loading Dye.

4.3.7. Regeneration of ssDNA

4.3.7.1. Asymmetric PCR

The amplified products obtained from the Pilot PCR were utilized as a template for an asymmetric PCR (aPCR), with the number of PCR cycles selected based on signal enhancement. A 10 µL aliquot of the selected amplified product from the pilot PCR was added to 90 µL of aPCR master mix (1X Master Mix, 0.4 µM forward primer). The quantity of aPCR cycles was equivalent to the quantity of cycles used for the selected product in the Pilot PCR.

4.3.7.2. Lambda Exonuclease Digestion

After aPCR amplification, a final concentration of 1X of exonuclease (λ) reaction was added to each tube. Subsequently, all PCR tubes underwent thermal deactivation at 80ºC for 15 minutes after being incubated with 0.1U of λ at 37ºC for 5 minutes. The resultant product was analyzed via gel electrophoresis by loading 1 µL of sample onto 4% (w/v) non-denaturing agarose gels with 1 µL of TriTrack DNA Loading Dye tracking dye.

To perform the optimization, 10 µL 10X λ reaction buffer was added to 90 µL of ssDNA library after 10 PCR, together with 1 µL of a 1:10 diluted λ stock (0.1 U/µL). Then, 10 µL of the mixture was aliquoted into ten PCR tubes and incubated at 37 ºC. Following the various digestion periods, λ were deactivated by heating to 80 ºC for 15 minutes. Gel electrophoresis was used to validate the optimization outcomes; 2.5 µL of each timepoint was loaded with 1 µL of TriTrack DNA Loading Dye onto a 3% (w/v) non-denaturing agarose gel.

4.3.8. Spin column ssDNA purification

The ssDNA generated after λ digestion was purified and isolated using the Oligo Clean & Concentrator Kit via spin column purification. Following the protocol provided in the kit, 100 µL of the sample was mixed with 400 µL of ethanol (95-100%) and 200 µL of Oligo Binding Buffer. The flow-through was discarded after transferring the solution to a Zymo-Spin™ IC Column and centrifuging it in a collection tube. To purify the ssDNA, 750 µL of DNA Wash Buffer was added to the column, which was centrifuged twice to ensure complete buffer removal. The purified ssDNA was eluted by transferring the column into a sterile nuclease-free tube and adding 15 µL of nuclease-free water to the column before subjecting it to centrifugation. The eluted samples were collected and stored in PCR tubes at 4ºC. All centrifugation steps were performed using a Sigma 1-15 centrifuge at 14000 rpm (17530 G) for 30 seconds. The purified ssDNA was loaded onto 4% (w/v) non-denaturing agarose gels with 1 µL of TriTrack DNA Loading Dye for gel electrophoresis analysis.

4.3.9. ssDNA & dsDNA quantification measurements

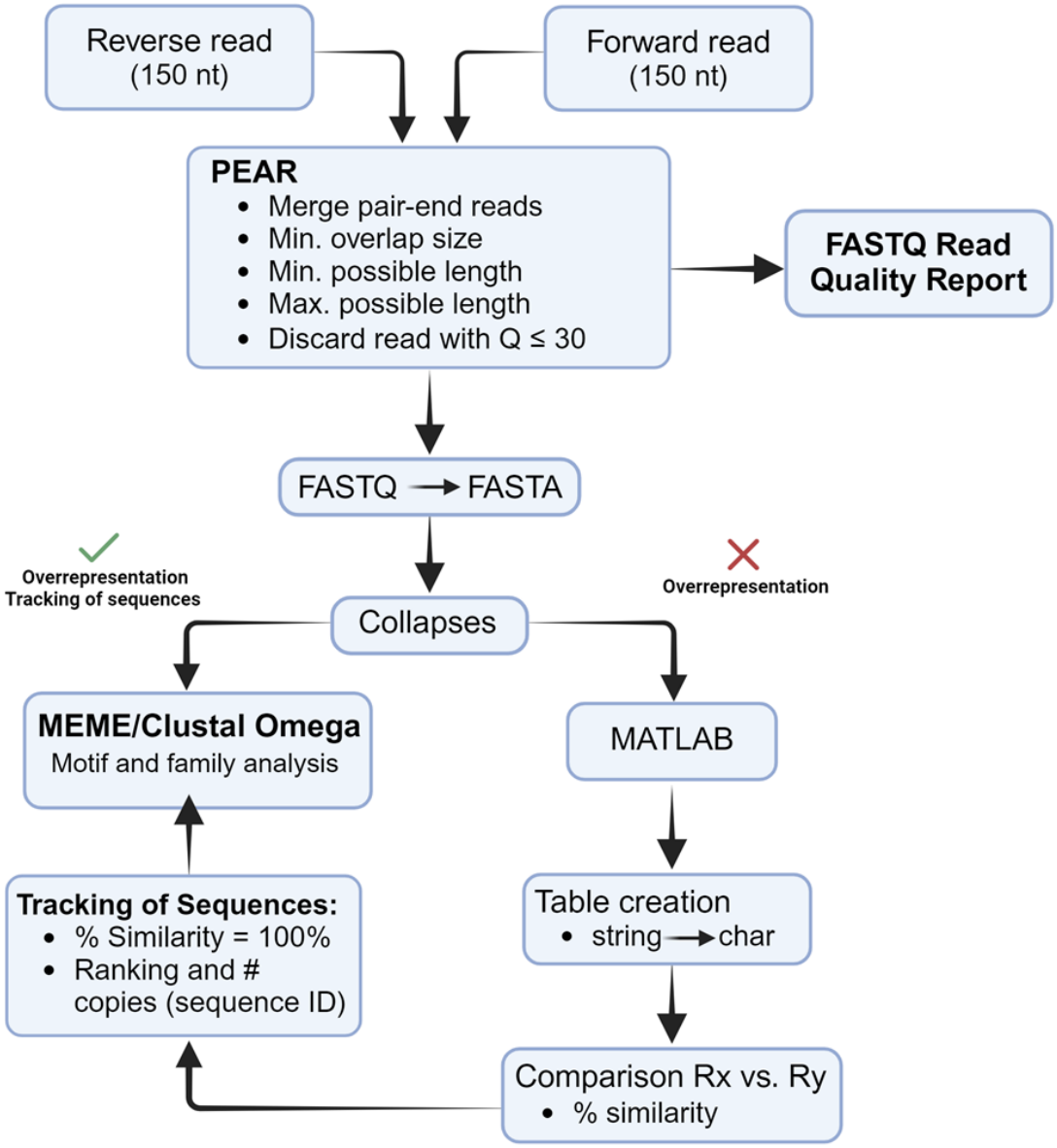
To quantify the ssDNA amount, a Nanodrop 2 000c UV-vis spectrophotometer was employed. The quantification was performed by measuring the absorbance at 260 nm using an extinction coefficient of 50 µg/mL for dsDNA and 33 µg/mL for ssDNA.

4.3.10. Agarose gel electrophoresis

A Mini 10 Horizontal Electrophoresis Kit was utilized to prepare agarose gels considering the size distribution of the ssDNA under investigation. Agarose gels containing 3-4% (w/v) were prepared for size determination and quantification, using GeneRuler Ultra Low Range DNA Ladder, which contains a 10-300 bp size marker. The application of 120 V for 40 or 50 minutes was carried out for the 3% and 4% gels, respectively. Two different staining procedures were used: (i) pre-cast in-gel staining method, employing 1X GelGreen, and (ii) post-electrophoresis staining technique, using 1X SYBR Gold in TBE buffer (1X), for 30 minutes. The staining process was conducted at RT, with gentle and consistent agitation. In both approaches, the gels were promptly observed using a UV-to-blue light converter screen affixed to an InGenius 3 Gel Doc System transilluminator operating under blue light excitation (≈450 nm).

4.3.11. Next-Generation Sequencing – Bioinformatic Analysis

Aliquots of R3, R6, R7, and R9 were processed and sequenced by Servei de Genòmica (Universitat Autònoma de Barcelona) using Illumina MiSeq (300 reads), generating around 230,000 reads. FASTQ files were obtained for pair-end reads of each sample. Bioinformatic analysis was performed using GALAXY (https://usegalaxy.org) and a custom-made MATLAB® code. The NGS data analysis workflow is shown in Scheme 4.2.



Scheme 4.2. *NGS data analysis workflow for both SELEX approaches*

4.4. RESULTS & DISCUSSION

4.4.1. Design and rationale behind the SELEX strategies

As discussed in the previous sections, OP-SELEX has the potential to overcome certain limitations associated with detecting small molecules. This technique effectively isolates aptamers against three structurally similar targets by incorporating negative and counterselections.

The MB-SELEX method, depicted in Figure 4.9, was employed for Phe aptamer screening. Considering the target's resemblance and co-occurrence, tryptophan was used for counter-selection after negative selection on the target-free conjugated bead matrix. Additionally, jOP-SELEX was performed to KA, QA, and Phe targets. The initial pool was attempted to be enriched for sequences that could bind to any (or all) targets by incubating the library for several rounds with an equal proportion of the three target-conjugated beads. The complete process is illustrated in Figure 4.10.

Briefly, in both SELEX approaches, a "round 0" was performed using only positive selection in order to retain every possible target-binding sequence regardless of their nonspecific interactions with the bead matrix or other targets. Negative selection was employed since round 1 to discard sequences interacting with the bead matrix. Regarding jOP-SELEX, during the first five rounds of the enrichment process, there was only negative and positive selections steps; nevertheless, once an enriched library for the three targets was obtained (R6), to further improve its specificity, it was divided into three distinct MB-SELEX, with each set designated for a specific target as a positive selection. In order to avoid any cross-reactive sequences, the remaining two targets were employed as counter-selection in equal proportions. This approach helped us to create a refined sublibrary for each target that would theoretically only contain highly specific sequences.

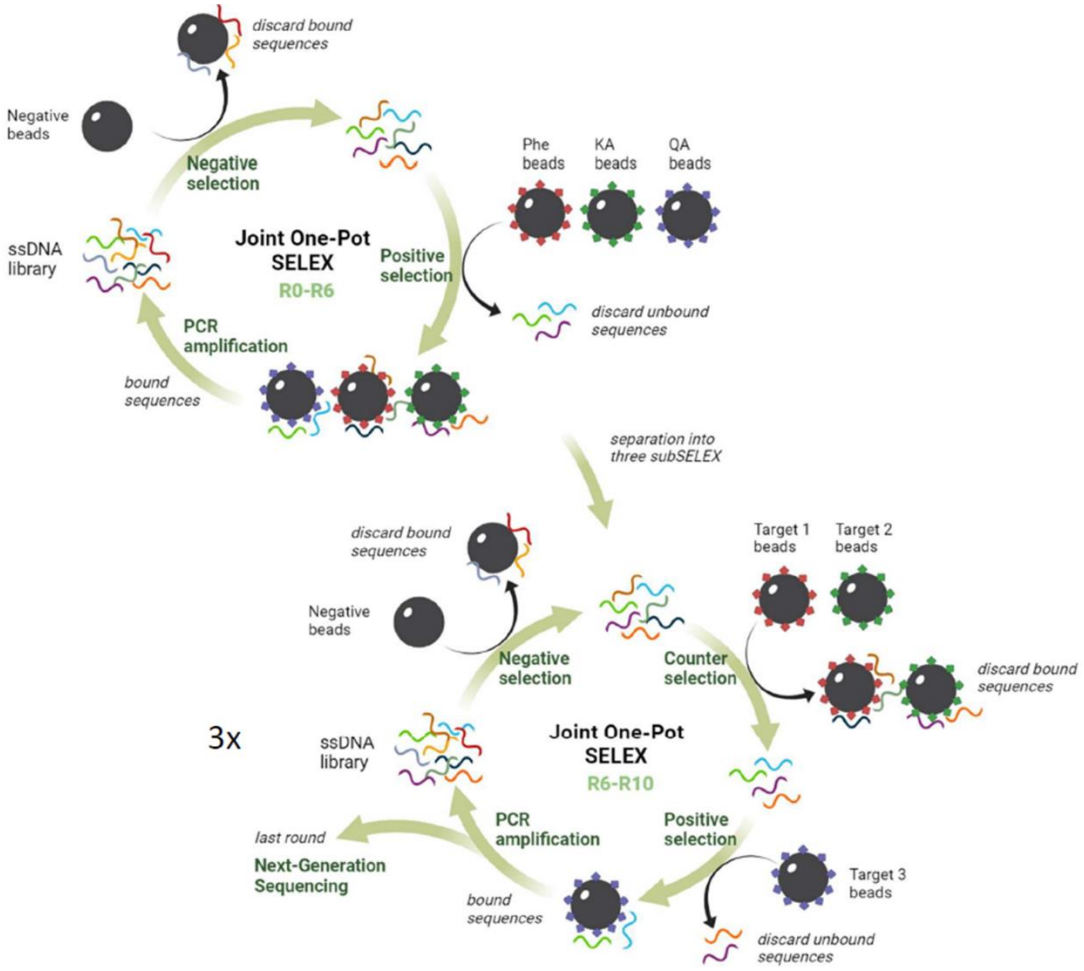


Figure 4.10. *Schematic representation of jOP-SELEX schematic workflow, from R0-R10 for 1 target as an example.*

Numerous research studies and scientific techniques have been used to optimize SELEX parameters. However, it is important to acknowledge that a significant portion of the process's success is still subject to stochasticity. As previously mentioned, several optimizations were made to experimental parameters to expedite the selection process and enhance the likelihood of identifying aptamers. Further exploration and refinement of these parameters will ultimately lead to even more favorable outcomes in this SELEX.

4.4.1.1. Magnetic bead target-conjugation and verification

By using click chemistry, which facilitates rapid and selective modular chemical reactions, target-conjugated MBs were fabricated (Figure 4.11): (i) maleimides on the MB interacted with thiol groups in the linker (AHT) and backfiller (BT) via click chemistry; [77,78](ii) the template carboxylic groups were activated using EDC/NHS, which were then bound to the amine moiety of the linker (AHT); and (iii) sulfo-NHS-acetate was used to block any unreacted primary amines. [21,79,80]

Click chemistry and EDC/NHS conjugation are well-studied coupling methods that have been established for several decades and are known for their rapid rate and efficiency.[80] Regarding Phe, potential

peptidic bonds may occur, and thus, careful pH tailoring was necessary to avoid deprotonation of the amine. To synthesize negative MBs (n-MBs) as a control, a target-free buffer incubation was employed. To ensure that the SELEX proceeded without any hindrance due to potential cross-reactivity with unblocked moieties on the MB, necessary steps were employed to irreversibly block any unreacted amine moieties by forming stable acetylates via acetylation of the surface amines with sulfo-NHS-acetate in 10 mM PBS (pH 7.5). [80–82]

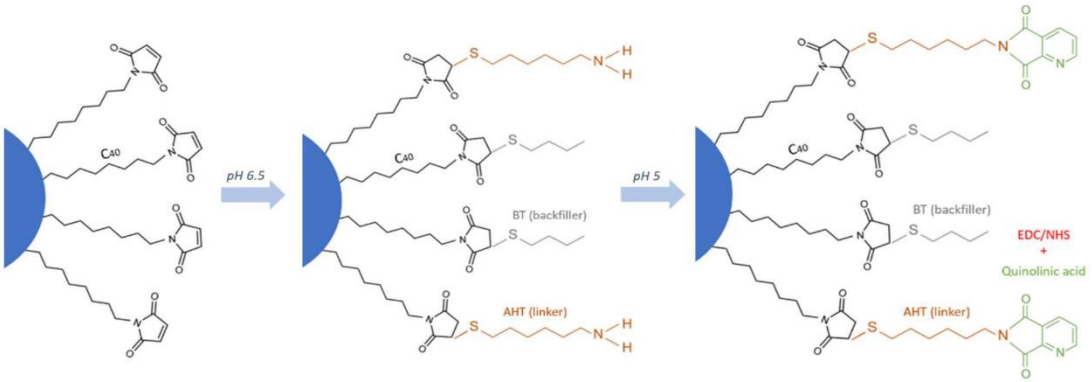


Figure 4.11. *Schematic illustration of the bead conjugation process for QA. The identical process was performed for KA, Phe, and Trp.*

As aforementioned, selecting an appropriate immobilization technique is crucial since it influences several features, such as steric hindrance, epitope availability, stability, or proper aptamer folding.

As mentioned in the "Methods" section, in order to minimize the chance of nonspecific binding to the bead matrix during the target verification, a 2% skimmed milk (w/v) solution was employed. As illustrated in Figure 4.12 (left), the n-MBs had an optical density of 0.226 ± 0.01, whereas the QA- and KA-MBs achieved higher values with an average optical density of 0.471 ± 0.0 and 0.420 ± 0.05, respectively. Unfortunately, Phe- and Trp- beads demonstrated no significant signal variation compared to the negative controls, with respective values of 0.242 ± 0.06 and 0.304 ± 0.09 (Figure 4.12, left). As a result, it was determined that only QA- and KA-MBs were successfully fabricated.

Additionally, a polymeric hydrophilic agent, PEG400, was selected as an alternative blocking agent for Phe- and Trp-beads to avoid the issues encountered. [82] After optimizing this modified protocol, considerably better results were obtained. Verified QA-beads were used as a positive control to validate the second set of target-conjugated MBs. As shown in Figure 4.12, Phe- and Trp-MBs displayed almost double the optical signal of their negative counterparts when PEG400 was used compared to their respective negative controls. Therefore, the second set of MBs was successfully validated prior to SELEX (Figure 4.12, right).

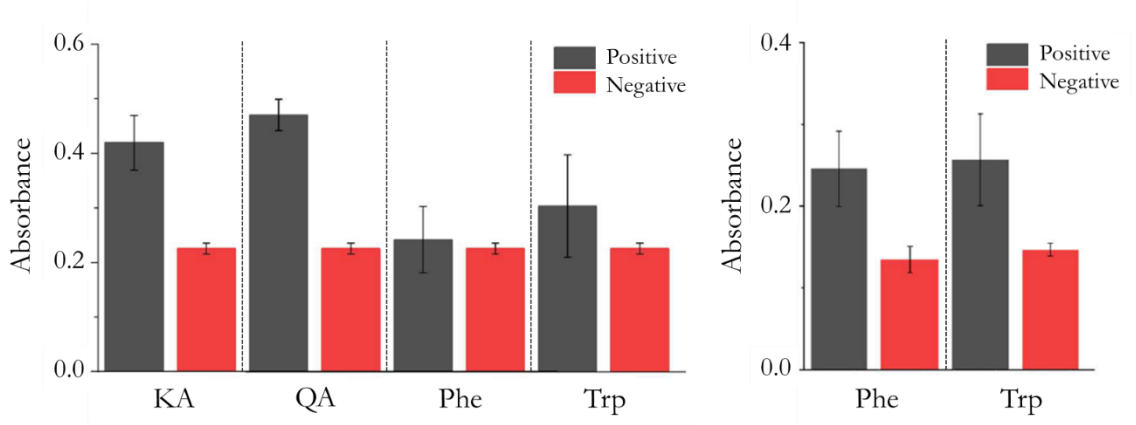


Figure 4.12. *Indirect bead-based ELISA in comparison to their negative controls using (left) skimmed milk and (right) PEG400 as a blocking agent.*

Target-conjugated MBs have been widely recognized as a flexible approach to aptamer partitioning, as they enable convenient separation of target-bound aptamers from a vast library pool under the influence of an external magnetic field. This study employed maleimide-activated MBs, just one of many commercially available beads with diverse sizes, materials, and advanced coatings for immobilization purposes. In addition, the commercial MBs employed in this study have a maleimide moiety attached to a C40 linker and an epoxy-modified MB. This unique feature allows precise control over the immobilized target's orientation and distribution. This, in turn, results in improved target density by preventing the formation of island-like agglomerates of target-AHT conjugates on the beads. It also minimizes any potential cooperativity effects or nonspecific binding with the matrix. Consequently, using AHT as the direct linker for target immobilization and BT as a backfiller (1:380 molar ratio) proved highly effective.[25,58]

4.4.2. SELEX progress

Several parameters, such as PCR conditions, agarose gels, λ digestion, and spin column purification, were optimized to evaluate the library's length, quality, and yield.[34,35,45,50] During this process, the agarose gels were examined after the pilot PCR to ensure the quality of the dsDNA generated after multiple PCR amplification cycles, as observed in Figure 4.13. This was primarily done to achieve sufficient library amplification for the target-conjugated beads without byproduct formation from overamplification in order to obtain an appropriate library for the subsequent cycles.

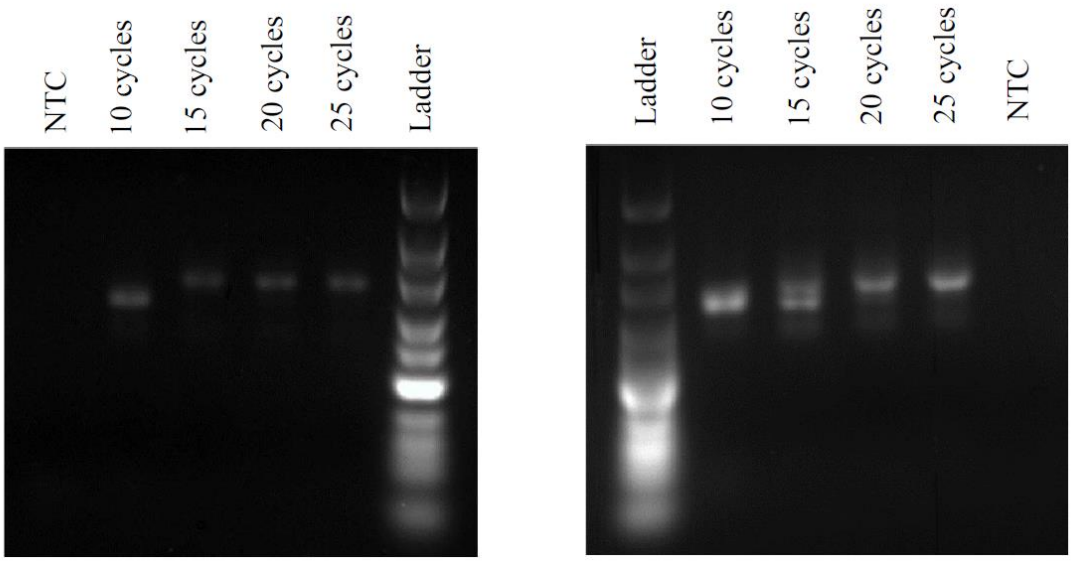


Figure 4.13. *Agarose gel electrophoresis (3% agarose, 120 V, 40 min, 1X GelGreen pre-stained) of library amplification products after 10, 15, 20, and 25 PCR cycles. On the left, using the first PCR protocol used (annealing at 59ºC for 15 s, extension at 72 ºC for 15 s). On the right, using the optimized protocol (annealing at 55ºC for 30 s, extension at 72 ºC for 30 s).*

It has been demonstrated that, during PCR amplification, an increase in the enrichment can lead to variations in the PCR cycles required to produce a visible band for positive, negative, and counter selection steps; more specifically, as SELEX rounds advance, the number of PCR cycles needed should increase for negative and counter selection steps while decreasing for positive selection.

As aforementioned, during the initial pre-enrichment round (R0), positive selection was the only incubation performed. This step can prove beneficial in capturing an initial set of target-binding sequences that may have been missed in the original library, regardless of their interaction with the bead matrix or other related targets. Amplifying these sequences can significantly improve their chances of surviving the subsequent rounds' negative selection phase.

After conducting multiple cycles of PCR, a particular byproduct emerged from the R0 pilot PCR, and after 15 PCR rounds, it exceeded the library's length (94 bp) (Figure 4.14). This trend persisted throughout both SELEX procedures. Considering this, the product of 10 cycles for both aPCR and λ digestion was selected for further rounds. To ensure that the ssDNA library was prepared for the next cycle (R1), a spin column was used to purify it. At this stage, unincorporated nucleotides, PCR primers, short byproducts, salts, enzymes, and magnetic beads were successfully removed from the samples.

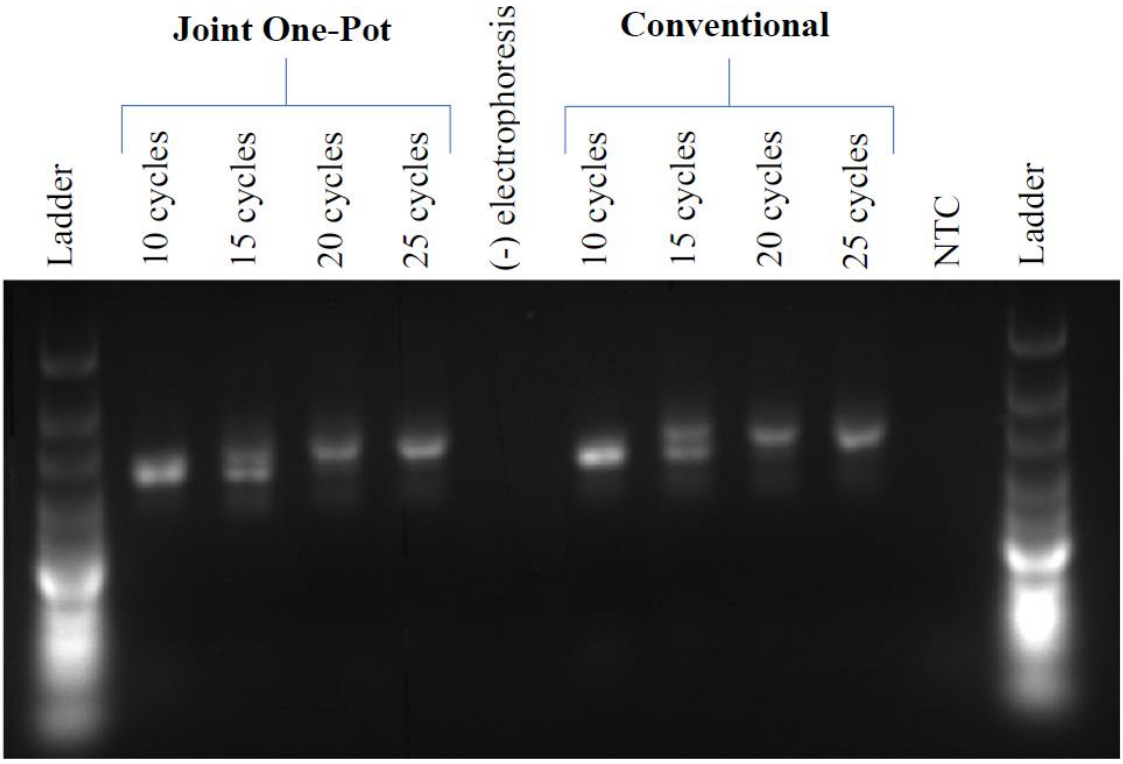


Figure 4.14. *Pilot-PCR in round 0 (R0), for both jOP- and the conventional MB-SELEX. Agarose gel electrophoresis (3% agarose, 120V, 40min, 1X GelGreen pre-stained)*

Negative selection was introduced since R1. Therefore, after conducting a pilot PCR, the optimal dsDNA yield was achieved at 20 cycles for both SELEX methods, with few byproducts identified during the pilot PCR on the positive beads (Figure 4.15, left).

Based on the results obtained, the band intensity in 5 PCR cycles of the negative selection seemed to be slightly higher compared to the positive one (Figure 4.15, right). This suggests that a comparable or larger number of sequences amplified in R0 are discarded due to the negative beads, as expected.

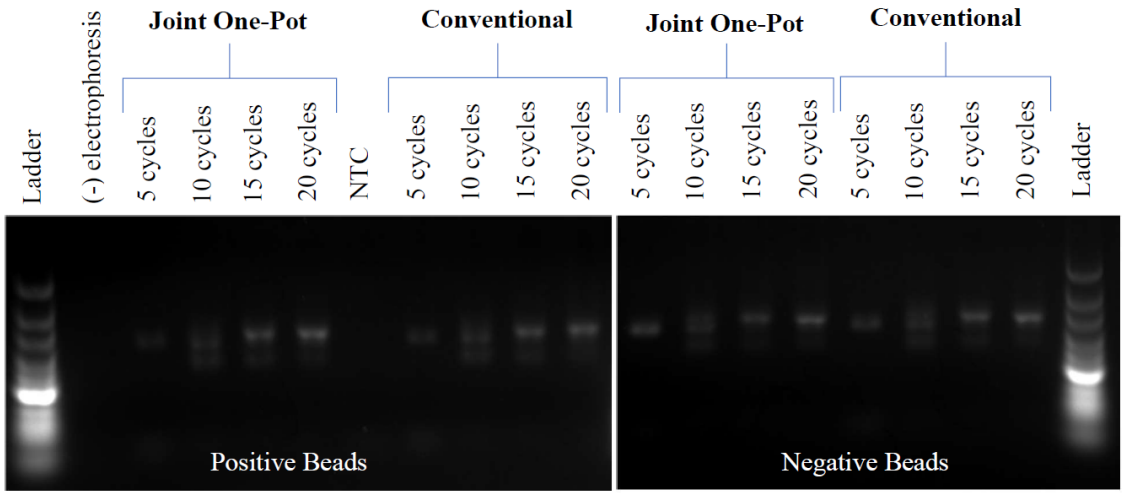


Figure 4.15. *Pilot-PCR in R1 for both SELEX. (left) positive selection. (right) negative selection. Agarose gel electrophoresis (3% agarose, 120V, 40min, 1X GelGreen pre-stained)*

In order to refine the separation of sequences with lower affinities, the next two rounds (R2 and R3) were conducted with increased stringency achieved through more rigorous washing steps following incubation with positive beads, as shown in Table 4.1 and 4.2. Interestingly, the pilot PCRs in R2 and R3 required 10 and 15 PCR cycles, respectively, indicating an increase in the library's concentration. The transition to R3 was anticipated to require additional PCR cycles due to the notably harsher washing technique. As the ladders in Figure 4.16 appeared less intense than usual, indicating less efficient DNA staining, it was unsurprising that the bands were completely invisible after only 5 PCR cycles.

Regarding the negative beads on R2, the intensities of the bands displayed a slight decrease after 10 PCR cycles compared to the positive beads. Additionally, the appearance of longer byproducts was delayed until the 20th cycle (as shown in Figure 4.16, right). This comparison helped to highlight an increase in the ratio between specific and nonspecific sequences.

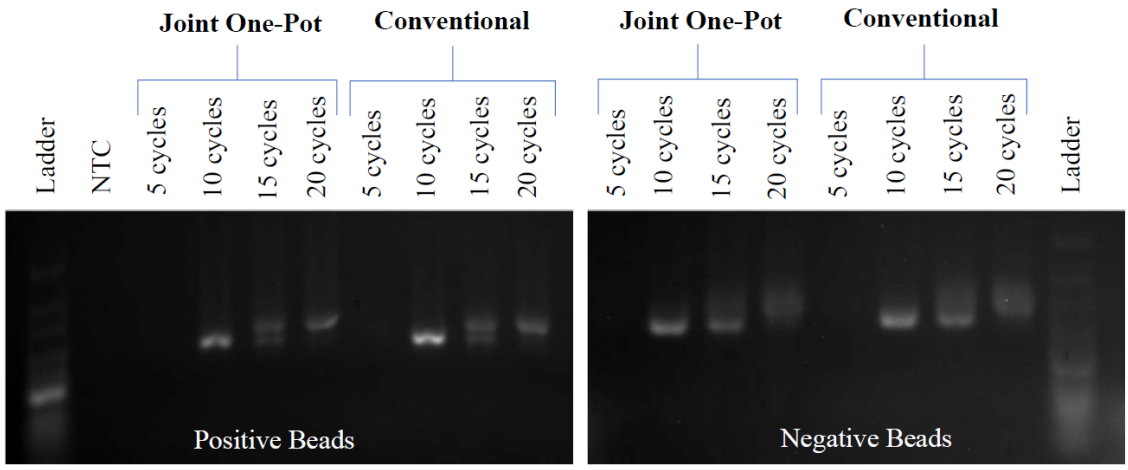


Figure 4.16. *Pilot-PCR in R2 for both SELEX. (left) positive selection (right) negative selection. Agarose gel electrophoresis (3% agarose, 120V, 40min, 1X GelGreen pre-stained)*

R4 of jOP-SELEX was performed exactly as R3, while for MB-SELEX, Trp-conjugated beads were introduced in R4 as a counter selection step. After pilot PCR, a larger byproduct (200bp) was evident after 15 cycles, which was not present in earlier gels, as indicated by red arrows in Figure 4.17. Therefore, products acquired from 10 cycles were chosen for the next round to ensure maximal amplification without producing these byproducts.

The data presented in Figure 4.17 (right) show that the pilot PCR of MB-SELEX counter selection steps shows a visible band with as few as 5 cycles. This observation implies that a large number of sequences interacted with the Trp-conjugated beads, as also evidenced in the negative selection step for both SELEX approaches (Figure 4.18).

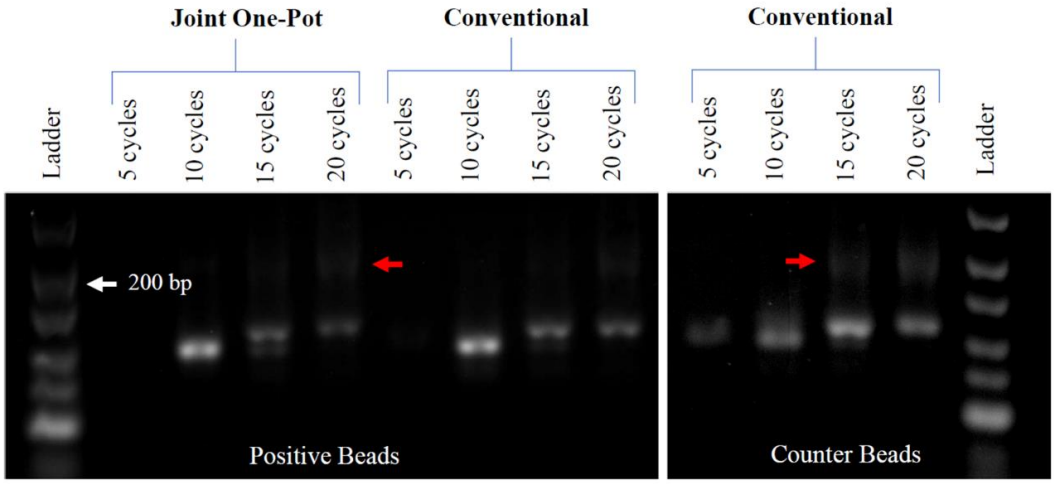


Figure 4.17. *Pilot-PCR from R4 for both SELEXs. (left) positive selection, (right) counterselection for MB-SELEX. Red arrows indicate the 200-bp estimated byproduct. Agarose gel electrophoresis (3% agarose, 120V, 40min, 1X GelGreen pre-stained)*

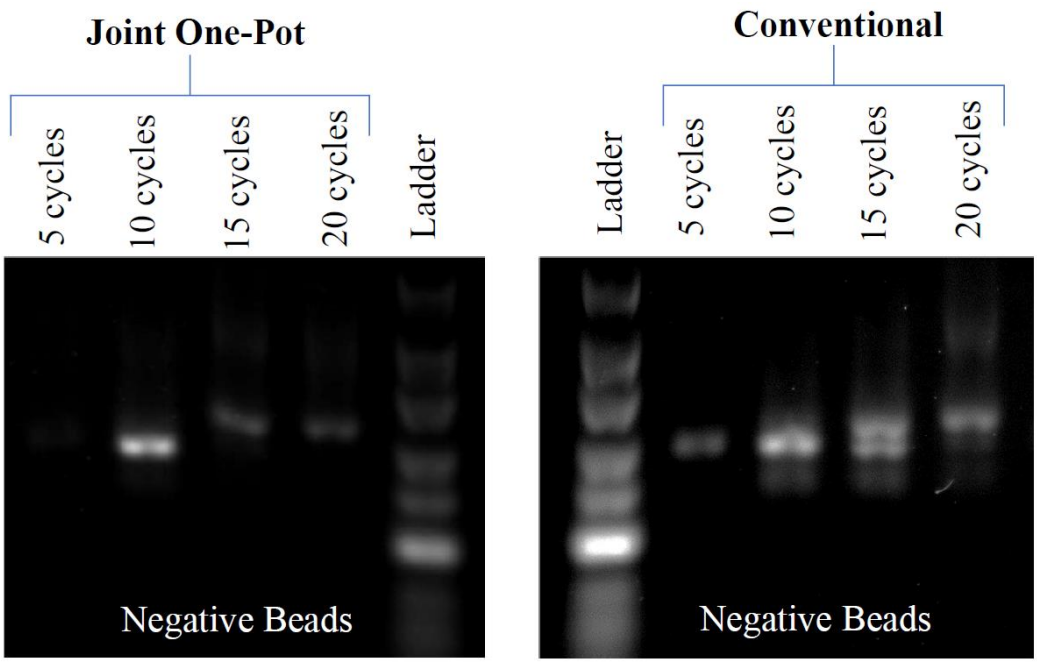


Figure 4.18. *Pilot-PCR in R4, on the negative-bound sequences for both SELEX. Agarose gel electrophoresis (3% agarose, 120V, 40min, 1X GelGreen pre-stained)*

Increasing the number of negative and counter beads from R5 onwards would be beneficial in setting harsher stringency conditions for both SELEX methods, as more nonspecific sequences would be discarded. In cases where the final application necessitates the use of target-specific aptamers rather than family-specific ones, it is recommended that additional rounds of selection be carried out. These rounds should include separated target incubation steps, where one target is used for positive selection and the remaining targets as counter-selection molecules. This approach can help prevent the occurrence of cross-reactivity and ensure the aptamer's specificity.

Regarding the jOP-SELEX, after negative selection in R7, it was divided into three independent SELEX workflows, each with its own negative and counterselection steps. As can be seen in Table 4.2, selection criteria were left unaltered from R8 to R10.

Each SELEX was analyzed in a single gel by loading samples from rounds R5 to R10 with all three selection steps: positive, negative, and counter to ensure a fair comparison of the different gels. The results depicted in Figure 4.19 suggest that the MB-SELEX exhibited a gradual increase in the intensity of positively bound sequences from R5 to R8, followed by a sharp decrease in R9 and R10 due to the harsh increase in incubation times (Table 4.1). Except for the particularly bright band observed at R8, the intensity of the counter-bound sequences was generally lower than that of the positive sequences (Figure 4.19, left). Over the course of R8 and R9, the intensity of the negative-bound sequences diminished considerably (Figure 4.19, right). Notably, the larger byproduct was much more pronounced in negative and counterselection steps, indicating that these two choices effectively removed it from the pool.

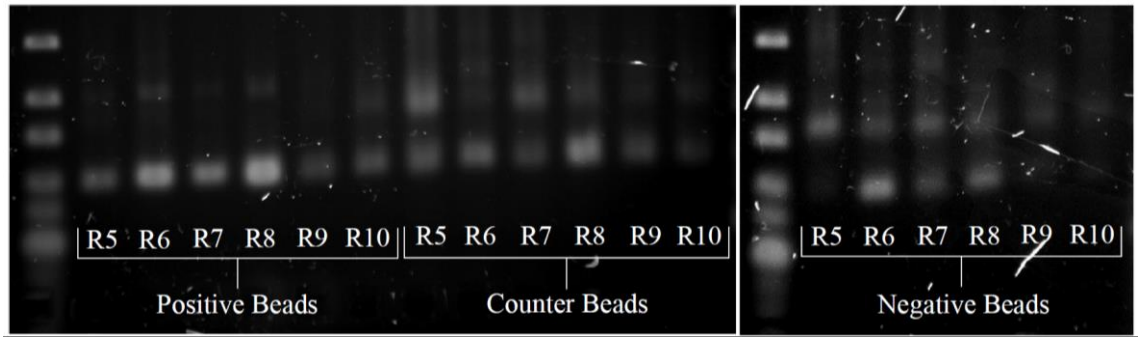


Figure 4.19. *10 PCR cycles from rounds R5 to R10 on the MB-SELEX. Agarose gel electrophoresis (3% agarose, 120V, 40min, 1X SYBRGold post-stained)*

The jOP-SELEX exhibited a remarkable increase in the ratio between the intensity of the positive- and negative-bound sequences in R6 (as depicted in Figure 4.20, left). Based on these results, the SELEX was divided into three separate SELEX workflows for each target after negative selection in R7. As illustrated in Figures 20 and 21, there was an increase in the positive selection in R8 and R10, along with a decrease in the negative selection from R8 to R10. Considering that from R8 to R10 there was a modification in the incubation periods (2h negative, 3h counter, 1h positive selection - Table 4.1 and 4.2), the counter sequences had no discernible fading as the rounds progressed mainly due to nonspecific adsorption onto the beads over the 3-hour period; nevertheless, the positive target-binding sequences still exhibited a strong signal after a 1h incubation and 5h of previously being incubated with matrix beads and structurally similar molecules (as demonstrated in Figures 4.20 and 4.21). Given more time, additional rounds would have been conducted to continue enriching target-specific sequences until the signal from the counter and negative selections almost disappeared.

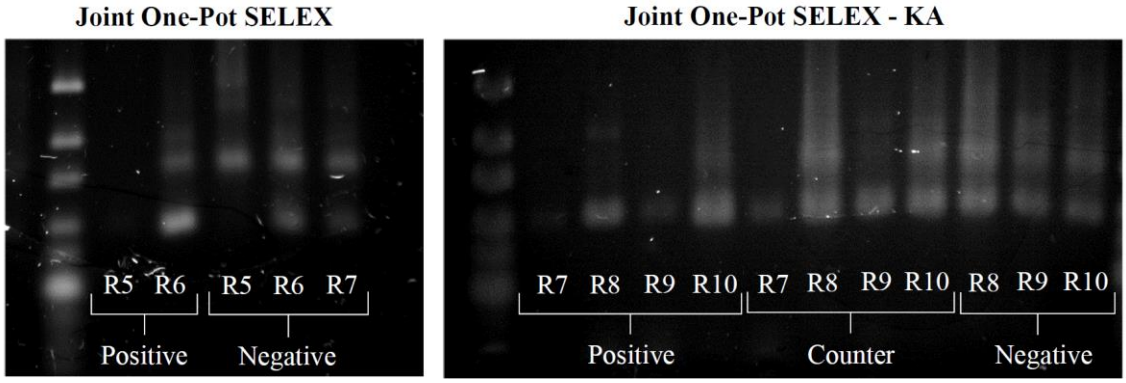


Figure 4.20. *10 PCR cycles from rounds R5 to R10 on the Joint One-Pot SELEX. (left), pre-enrichment phase, (right) jOP-SELEX division for KA-conjugated beads. Agarose gel electrophoresis (3% agarose, 120V, 40min, 1X SYBRGold post-stained)*

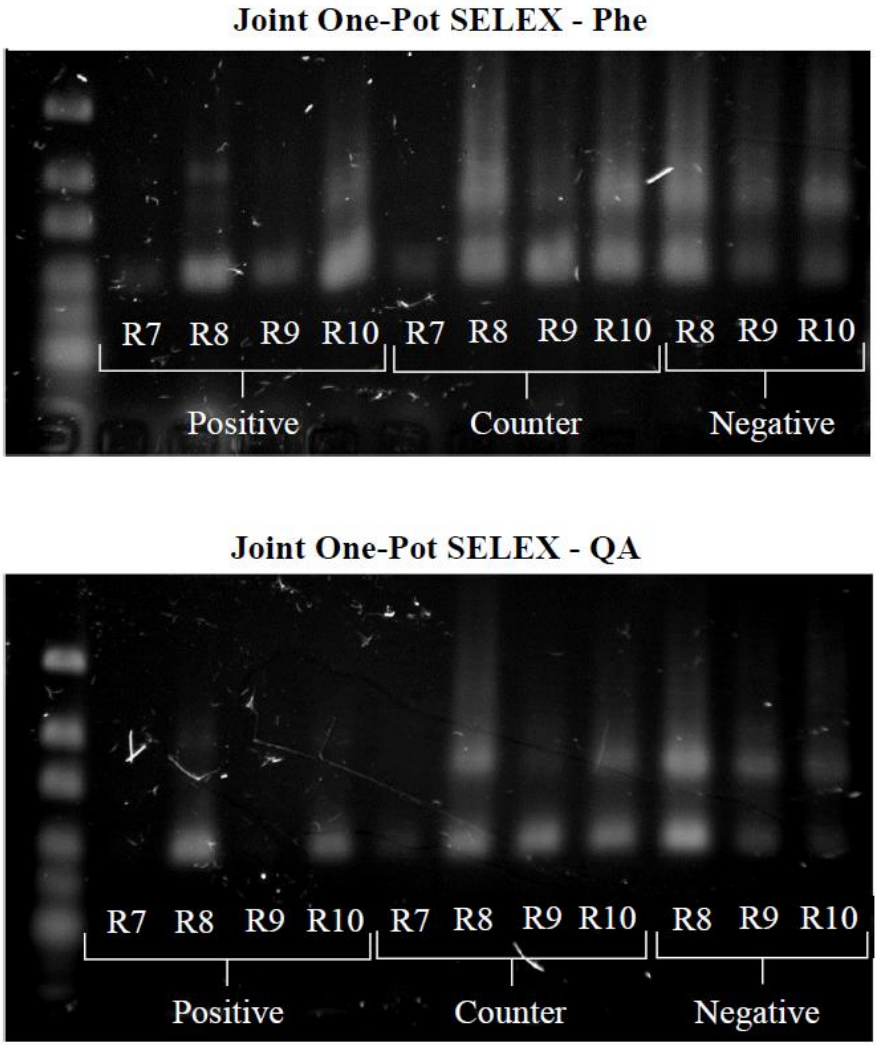


Figure 4.21. *10 PCR cycles from rounds R7 to R10 on divided jOP-SELEX. (top) Phe. (bottom) QA. Agarose gel electrophoresis (3% agarose, 120V, 40min, 1X SYBRGold post-stained)*

4.4.2.1. Enrichment monitoring during the SELEX process

To evaluate the enrichment progress in the library collections, two distinct analyses were employed: (i) monitoring the quantity of ssDNA in the libraries following the purification process using UV/Vis; and (ii) the number of PCR cycles required for the amplification step. The results of these analyses have been summarized in Table 4.3 and Figure 4.22.

Throughout the SELEX process, some fluctuations in the concentrations of DNA present in the samples were observed. A significant increase in concentration from R1 to R3 was observed despite using harsher washing procedures and performing fewer PCR cycles. However, a decline in concentration was observed during R4, coinciding with the introduction of counter-selection. Another decrease in concentration during R5 was noted, despite increasing the number of PCR cycles. The final concentrations were relatively low from R6 to R8 due to the increased stringencies for positive selection, such as harsher

washing conditions and shorter incubation periods, respectively. Reducing the number of PCR cycles required down to 10 or even 5 was also noteworthy. Although using freshly fabricated beads in R9 might have imposed a certain stringency to the process, a substantial increase in concentration was achieved with 10 cycles, and only 5 cycles in R10. By rounds 9 and 10, the negative selection had minimal occurrence and a decreasing trend in counterselection. Although it would have been preferable to submit round 10 for NGS, it was not feasible due to human errors; thus, R9 was submitted instead.

In the jOP-SELEX, the library concentration consistently increased with each round, while the number of PCR cycles required for proper amplification had a decreasing trend. However, there was an abrupt concentration reduction after the library was divided due to the dilution of the R6 library to the same volume as three separate libraries - although performing a few PCR cycles for amplicon generation could have aided. Despite only reaching 5 PCR cycles, the concentration of all three SELEX increased again, as negative and counter selection steps removed a considerable fraction of nonspecific sequences.

In summary, each SELEX approach resulted in an increase in the concentration of target-binding sequences while requiring fewer PCR cycles for amplification. These findings, along with a decrease in the fraction of negative binding sequences, indicate that the pools have been enriched. It is noteworthy that the concentrations of sequences in the initial and final rounds were comparable, despite a significant reduction in the number of PCR cycles in the final rounds compared to the initial rounds. Nevertheless, as previously noted, it is crucial to continue both SELEX approaches until there is a considerable reduction in negative and counterselection steps. Unfortunately, due to time constraints, this could not be carried out.

Table 4.3. *Rounds-wise ssDNA concentration (µM) for both SELEX. Measurements were done in triplicates.*

	Conventional SELEX	**jOP-SELEX**		
	Phe	**KA**	**QA**	**Phe**
R1	0.91 ± 0.02		0.76 ± 0.03	
R2	1.06 ± 0.04		0.91 ± 0.03	
R3	1.89 ± 0.04		1.29 ± 0.10	
R4	1.00 ± 0.05		1.31 ± 0.09	
R5	0.75 ± 0.18		1.58 ± 0.08	
R6	1.51 ± 0.25		1.35 ± 0.33	
R7	0.9 ± 0.07	0.84 ± 0.05	0.81 ± 0.12	1.12 ± 0.02
R8	0.63 ± 0.10	0.84 ± 0.17	0.89 ± 0.11	0.65 ± 0.23
R9	1.67 ± 0.10	1.52 ± 0.16	1.26 ± 0.13	1.66 ± 0.15

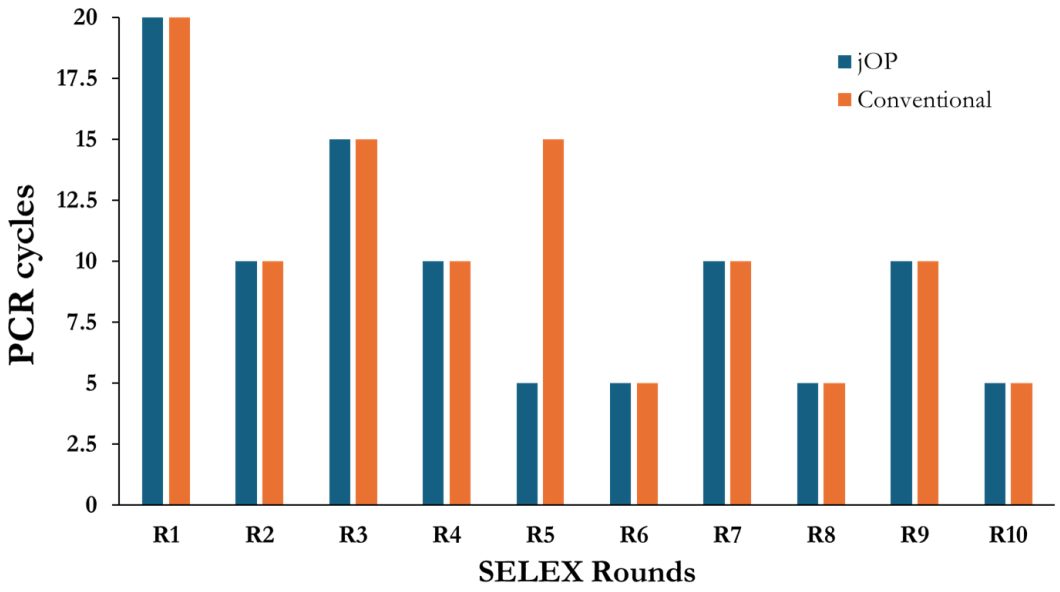
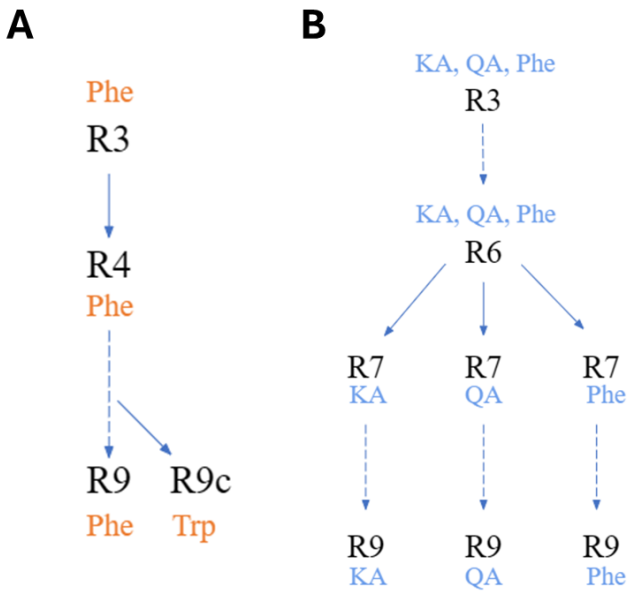


Figure 4.22. *Number of PCR cycles needed for proper library amplification round-wise. For jOP-SELEX, the PCR cycles chosen in the pilot PCR were the same for the 3 targets.*

It's worth highlighting that while the MB-SELEX exhibited a decline in negative and counterselection steps, the jOP-SELEX still showed a significant amount of nonspecific sequences in both steps. One potential explanation for this difference is that, as aforementioned, the incubation periods played an important role since the counterselection was 3x longer than the positive counterpart in the last 3 rounds (R8-R10). Additionally, the strong similarities in the targets' physicochemical properties most probably required more SELEX rounds to remove nonspecific sequences effectively. Ultimately, high-throughput sequencing of several samples throughout SELEX rounds was performed via NGS in order to determine the pools' sequence uniqueness, possibly identify patterns with overrepresentation, and design potential aptamer sequences for several purposes.

4.4.2.2. NGS Bioinformatic Analysis

The progress of the selection process was evaluated in both SELEX methods by selecting samples to be sequenced via NGS from the SELEX rounds near the introduction of negative or counterselection steps. Rounds R3 (from the MB-SELEX) and R6 (from jOP-SELEX) were chosen, as they occurred before introducing counter selection step and library division, respectively. Similarly, R4 from the MB-SELEX and the three corresponding R7 pools of jOP-SELEX were selected to evaluate any changes. The final round of each SELEX (R9) was also chosen to assess the individual enrichment of each target. Finally, the MB-SELEX R9 counter pool was selected for the same purpose. Therefore, twelve ssDNA pools were sequenced, as shown in Scheme 4.3.



Scheme 4.3. *Samples sent for NGS analysis. (A) MB-SELEX. (B) jOP-SELEX*

The quality of the obtained raw data was evaluated using the FASTQC and PEAR tools to provide general statistics. The PEAR tool was used to merge paired-end reads, filter out low-quality reads, and limit the pool size to +/-10 nt from the original library (97-nt). The pools' data format was then converted to FASTA and collapsed into unique sequences. Table 4.4 and 4.5 show the general statistics of the analysis performed using the Galaxy server and workflow, respectively.

As illustrated in the tables below, the calculated enrichment was considerably low possibly due to the low number of SELEX rounds performed. Several factors could also have contributed to this outcome, such as the colloidal stability of conjugated MBs and the limited binding sites due to target size and immobilization approach. A comprehensive bioinformatic analysis was conducted, which suggested that additional rounds of SELEX are necessary to accurately isolate aptamers towards the target molecules.

Table 4.4. *MB-SELEX*

	R3	R4	R9	R9-cT
Total Sequences	735542	283675	246225	232242
Sequence length	47-151	35-151	44-151	36-151
Sequences 87-107 pb	720974	272252	235660	224274
Unique 87-107 pb sequences	629942	235248	206753	194910
%	87.37%	86.41%	87.73%	86.91%
Top 100 (count)	354	322	454	410
%	0.0491	0.1183	0.1927	0.1828
Top 10 count	43	40	64	62
%	0.0060	0.0147	0.0272	0.0276
Round Enrichment %	0.0007	0.0015	0.0034	0.0036

***Table 4.5**. jOP-SELEX*

	R3	R6	R7-K	R7-Q	R7-P	R9-K	R9-Q	R9-P
Total Sequences	184588	245042	270049	200748	207366	265230	226987	223106
Sequence length	55-151	46-151	45-151	36-151	44-151	36-151	46-151	44-151
Sequences 87-107 pb	179285	232281	251668	188494	200287	250506	207648	217161
Unique 87-107 pb sequences	158062	206316	219989	164652	176005	217054	181239	190795
%	88.16	88.82	87.41	87.35	87.88	86.65	87.28	87.86
Top 100 (count)	308	336	380	401	400	477	428	474
%	0.1718	0.1447	0.1510	0.2127	0.1997	0.1904	0.2061	0.2183
Top 10 (count)	38	49	51	52	55	71	65	85
%	0.0212	0.0211	0.0203	0.0276	0.0275	0.0283	0.0313	0.0391
Round Enrichment %	0.0022	0.0026	0.0028	0.0037	0.0035	0.0032	0.0039	0.0055

Moreover, due to the low count in the representation of the obtained collapsed sequences, identifying and tracking them during the selection process was rendered a complex task using the traditional GALAXY workflow. Similarly, minimal overrepresentation posed a challenge in identifying shared sequence motifs using MEME (https://memesuite.org/meme/tools/meme). Due to the limitations encountered, these sequences were cross-checked and identified using Matlab code, which was written to compare selected rounds by determining the similarity percentages of complete (97-nt) and primer-trimmed sequences (53-nt) and attempting to track specific sequences throughout SELEX rounds. In the jOP-SELEX, target-binding sequences towards KA and QA were tracked with 100% similarity among sequences from R9 to R6, while Phe-specific sequences were not obtained for both SELEX approaches. However, as there is minimal sequence overrepresentation (Table 4.4 and 4.5), the obtained sequences are considered highly speculative. It is advisable not to regard them as potential candidates unless an appropriate overrepresentation is obtained. Additionally, the computational resources were inadequate for running resource-intensive software such as AptaSuite, specifically designed for comparative analysis of SELEX rounds. To address these issues, a custom-made MATLAB code was developed that allowed us to investigate parallel SELEX processes, such as jOP-SELEX after target branching, and to analyze rounds within the same SELEX experiment.

This MATLAB workflow (Scheme 4.2) proved to be effective for the requirements of the process, considering that it could identify sequences by 100% similarities in their nucleotide content in samples with almost no overrepresentation. In order words, even if overrepresentation was almost negligible, it was possible to track 3 specific sequences for some of the targets employed, as seen in Table 4.6. Therefore, this methodology may aid in aptamer identification at earlier rounds by enabling a more comprehensive analysis, even when adequate enrichment levels are not attained. Moreover, this MATLAB code could be expanded to analyze complete sequenced pools (comprising millions of sequences) if greater computational resources become available, thereby providing a versatile tool for future single- and multi-target SELEX methodologies.

Table 4.6. *Tracking of sequences using MATLAB from the Joint One-Pot SELEX in all the pools sequenced. The first number denotes the ranking, and the second one denotes the number of copies (sequence ID), as obtained in the collapsed files of unique sequences.*

	R3	R6	R7 K	R7 Q	R7 P	R9 K	R9 Q	R9 P
Seq 1.	-	1-6	3-6	7-5	-	42-4	72-4	-
Seq 2.	-	244-3	5-6	-	58-4	61-4	-	-
Seq 3	-	124-3	13-5	36-4	-	1612-3	66-4	-

4.5. CONCLUSIONS

The design and implementation of SELEX strategies in this project were critical for isolating aptamers against three ACLF-associated small-molecule targets (KA, QA, and Phe), which are structurally similar and co-occurring SMs. Based on the results obtained in agarose gels and ssDNA quantification, the MB-SELEX method exhibited promising results for screening Phe-specific aptamers, incorporating Trp as a counterselection target. The jOP-SELEX involved enriching the library for sequences capable of multi-target binding before refining the selection to target-specific aptamers. Implementing a multi-target approach, in conjunction with the use of negative and counter-selections, has demonstrated encouraging outcomes in isolating potential aptamers.

The target-conjugated MB via click chemistry and EDC/NHS methods were essential for ensuring stable and oriented target immobilization. By blocking unreacted amine moieties and using appropriate blocking agents such as milk powder and PEG400, it was possible to minimize nonspecific binding and allowed the verification of the target conjugation. As also shown in many research studies, target-conjugated MBs facilitated the successful separation of target-bound sequences from the library, highlighting the importance of proper bead conjugation techniques in the SELEX process.

Throughout the SELEX process, optimization of various parameters, including PCR conditions, lambda exonuclease digestion, agarose gels, and washing stringencies, significantly refined the selection outcomes. Based on the results obtained in the gels and quantification via UV/Vis, increasing the stringency of the procedure and adjusting PCR cycles aid in the apparent enrichment of specific aptamer sequences while reducing nonspecific sequences. The gradual increase in the intensity of positive-bound sequences and the reduction in negative-bound sequences observed in the later rounds hinted to a successful enrichment and selection of target-specific aptamers for the MB-SELEX.

As aforementioned, the ssDNA quantification indicated that the concentrations of the three targets in jOP-SELEX aligned with those of the Phe in the MB-SELEX. Enrichment monitoring through UV/Vis analysis and PCR cycle assessment provided valuable insights into the SELEX progress, as the consistent increase in library concentration and the decreasing number of PCR cycles required for amplification highlighted the efficiency of the selection process. This further suggests that the jOP-SELEX could be a viable method for isolating aptamers against multiple targets within the same timeframe typically required for a single target using conventional SELEX approaches.

Incorporating negative and counter-selections since R1 -the latter only in MB-SELEX- further aided in refining the aptamer library. Despite the challenges encountered, such as the appearance of byproducts and the need for additional SELEX rounds, the use of jOP-SELEX and MB-SELEX methods provided a robust framework for multiplexed SELEX processes, demonstrating their potential for future applications in aptamer selection.

However, as the NGS bioinformatic analysis suggested, additional selection steps were necessary to further refine the aptamer library and achieve higher specificity and enrichment levels. Unfortunately, due to an unexpected error during the purification process, the samples from Round 10 were lost, rendering it impossible for quantification, storage or sequencing. Although it wasn't feasible to repeat Round 10 due to time constraints, NGS was given priority to further analyze the progress and applicability of both SELEX approaches.

Despite the limitations encountered in computational resources and sequence overrepresentation, developing a MATLAB code for analyzing SELEX rounds aided in tracking potential target-binding sequences. If additional time and resources had been available, further rounds of SELEX would have been considered to enhance the selection and isolation of aptamers specific to the small-molecule targets KA, QA, and Phe. Subsequently, after successful optimization and validation of potential aptamer candidates through SELEX, the next step would have entailed validating the computational analysis developed for this project. This validation process would have involved comprehensive analysis of binding assays specific to small-molecule targets in order to ensure the aptamers' efficacy and reliability. This approach would have offered a promising tool for future SELEX studies, enabling comprehensive analysis of multiplexed SELEX approaches and facilitating the early identification of aptamers. Overall, the SELEX approaches described in this chapter highlight the potential of advanced multi-target SELEX strategies coupled with bioinformatic tools to simultaneously isolate highly specific aptamers for multiple targets promptly.

4.6. REFERENCES

1. Sharma S, Byrne H, O'Kennedy RJ. Antibodies and antibody-derived analytical biosensors. Essays Biochem. 2016 Jun 6;60(1):9.
2. Edelman GM. Antibody structure and molecular immunology. Science (80-). 1973;180(4088):830–40.
3. Hnasko RM. The biochemical properties of antibodies and their fragments. Methods Mol Biol. 2015;1318:1–14.
4. Mak TW, Saunders ME. The Nature of Antigen–Antibody Interaction. The Immune Response. 2006 Jan 1;121–46.
5. Conroy PJ, Hearty S, Leonard P, O'Kennedy RJ. Antibody production, design and use for biosensor-based applications. 2009 Feb 1;20(1):10–26.
6. Nimjee SM, Rusconi CP, Sullenger BA. Aptamers: An emerging class of therapeutics. Annu Rev Med. 2005;56:555–83.
7. Weigand JE, Suess B. Aptamers and riboswitches: Perspectives in biotechnology. Appl Microbiol Biotechnol. 2009 Nov;85(2):229–36.
8. Sequeira-Antunes B, Ferreira HA. Nucleic Acid Aptamer-Based Biosensors: A Review. Biomedicines. 2023 Dec 1;11(12).
9. Ellington AD, Szostak JW. In vitro selection of RNA molecules that bind specific ligands. 1990;346(6287):818–22.
10. Wilson DS, Szostak JW. In vitro selection of functional nucleic acids. Annu Rev Biochem. 1999;68(February 1999):611–47.
11. Tuerk C, Gold L. Systematic Evolution of Ligands by Exponential Enrichment: RNA Ligands to Bacteriophage T4 DNA Polymerase. Science (80-). 1990 Aug 3;249(4968):505–10.
12. McKeague M, McConnell EM, Cruz-Toledo J, Bernard ED, Pach A, Mastronardi E, et al. Analysis of In Vitro Aptamer Selection Parameters. J Mol Evol. 2015 Dec 1;81(5–6):150–61.
13. Buglak AA, Samokhvalov A V., Zherdev A V., Dzantiev BB. Methods and Applications of In Silico Aptamer Design and Modeling. Int J Mol Sci 2020, Vol 21, Page 8420. 2020 Nov 10;21(22):8420.
14. McKeague M, Derosa MC. Challenges and Opportunities for Small Molecule Aptamer Development. J Nucleic Acids. 2012 Jan 1;2012(1):748913.
15. Yu H, Alkhamis O, Canoura J, Liu Y, Xiao Y. Advances and Challenges in Small-Molecule DNA Aptamer Isolation, Characterization, and Sensor Development. Angew Chemie Int Ed. 2021 Jul 26;60(31):16800–23.
16. Hong P, Li W, Li J. Applications of aptasensors in clinical diagnostics. Sensors. 2012 Feb;12(2):1181–93.
17. Mayer G. The chemical biology of aptamers. Angew Chemie - Int Ed. 2009 Mar 30;48(15):2672–89.
18. Walter JG, Heilkenbrinker A, Austerjost J, Timur S, Stahl F, Scheper T. Aptasensors for small molecule detection. Zeitschrift fur Naturforsch - Sect B J Chem Sci. 2012;67(10):976–86.
19. Ilgu M, Nilsen-Hamilton M. Aptamers in analytics. Analyst. 2016 Mar 7;141(5):1551–8.
20. Dauphin-Ducharme P, Plaxco KW. Maximizing the signal gain of electrochemical-DNA sensors. Anal Chem. 2016;88(23):11654–62.

21. Yüce M, Kurt H. How to make nanobiosensors: Surface modification and characterisation of nanomaterials for biosensing applications. RSC Adv. 2017;7(78):49386–403.

22. Yang LF, Ling M, Kacherovsky N, Pun SH. Aptamers 101: aptamer discovery and in vitro applications in biosensors and separations. Chem Sci. 2023 May 17;14(19):4961–78.

23. Sakamoto T, Ennifar E, Nakamura Y. Thermodynamic study of aptamers binding to their target proteins. Biochimie. 2018 Feb 1;145:91–7.

24. Plach M, Schubert T. Biophysical Characterization of Aptamer-Target Interactions. Adv Biochem Eng Biotechnol. 2019;174:1–15.

25. Slavkovic S, Zhu Y, Churcher ZR, Shoara AA, Johnson AE, Johnson PE. Thermodynamic analysis of cooperative ligand binding by the ATP-binding DNA aptamer indicates a population-shift binding mechanism. Sci Reports 2020 101. 2020 Nov 3;10(1):1–10.

26. Amano R, Takada K, Tanaka Y, Nakamura Y, Kawai G, Kozu T, et al. Kinetic and Thermodynamic Analyses of Interaction between a High-Affinity RNA Aptamer and Its Target Protein. Biochemistry. 2016 Nov 15;55(45):6221–9.

27. Sakamoto T, Ennifar E, Nakamura Y. Thermodynamic study of aptamers binding to their target proteins. Biochimie. 2018 Feb 1;145:91–7.

28. Daems E, Moro G, Campos R, De Wael K. Mapping the gaps in chemical analysis for the characterisation of aptamer-target interactions. TrAC Trends Anal Chem. 2021 Sep 1;142:116311.

29. Huang M, Song J, Huang P, Chen X, Wang W, Zhu Z, et al. Molecular crowding evolution for enabling discovery of enthalpy-driven aptamers for robust biomedical applications. Anal Chem. 2019 Aug 20;91(16):10879–86.

30. Gold L, Ellington A. Introduction to SELEX. :2–47.

31. Dong Y, Wang Z, Wang S, Wu Y, Ma Y, Liu J. Introduction of SELEX and Important SELEX Variants . Aptamers Anal Appl. 2018;1–25.

32. Ruscito A, DeRosa MC. Small-molecule binding aptamers: Selection strategies, characterization, and applications. Front Chem. 2016;4(MAY):1–14.

33. Tombelli S, Mascini M. Aptamers Biosensors for Pharmaceutical Compounds. Comb Chem High Throughput Screen. 2012;13(7):641–9.

34. Kohlberger M, Gadermaier G. SELEX: Critical factors and optimization strategies for successful aptamer selection. Biotechnol Appl Biochem. 2022 Oct 1;69(5):1771–92.

35. Komarova N, Kuznetsov A. Inside the Black Box: What Makes SELEX Better? Mol 2019, Vol 24, Page 3598. 2019 Oct 7;24(19):3598.

36. Miyachi Y, Shimizu N, Ogino C, Kondo A. Selection of DNA aptamers using atomic force microscopy. Nucleic Acids Res. 2010 Mar 1;38(4):e21–e21.

37. Ruscito A, DeRosa MC. Small-molecule binding aptamers: Selection strategies, characterization, and applications. Front Chem. 2016 May 10;4(MAY):188509.

38. Pfeiffer F, Mayer G. Selection and biosensor application of aptamers for small molecules. Front Chem. 2016;4(JUN):1–21.

39. Chen L, Zhang B, Wu Z, Liu G, Li W, Tang Y. In Silico discovery of aptamers with an enhanced library design strategy. Comput Struct Biotechnol J. 2023 Jan 1;21:1005–13.

40. Tolle F, Mayer G. Preparation of SELEX samples for next-generation sequencing. Methods Mol Biol. 2016;1380:77–84.

41. Alam KK, Chang JL, Burke DH. FASTAptamer: a bioinformatic toolkit for high-throughput

sequence analysis of combinatorial selections. Mol Ther Nucleic acids. 2015 Mar 1;4(3):e230.

42. Vorobyeva MA, Davydova AS, Vorobjev PE, Pyshnyi D V., Venyaminova AG. Key Aspects of Nucleic Acid Library Design for in Vitro Selection. Int J Mol Sci 2018, Vol 19, Page 470. 2018 Feb 5;19(2):470.

43. Onaş AM, Dascălu C, Raicopol MD, Pilan L. Critical Design Factors for Electrochemical Aptasensors Based on Target-Induced Conformational Changes: The Case of Small-Molecule Targets. Biosensors. 2022;12(10).

44. Bayat P, Nosrati R, Alibolandi M, Rafatpanah H, Abnous K, Khedri M, et al. SELEX methods on the road to protein targeting with nucleic acid aptamers. Biochimie. 2018 Nov 1;154:132–55.

45. Le Dortz LL, Rouxel C, Leroy Q, Brosseau N, Boulouis HJ, Haddad N, et al. Optimized Lambda Exonuclease Digestion or Purification Using Streptavidin-Coated Beads: Which One Is Best for Successful DNA Aptamer Selection? Methods Protoc. 2022 Dec 1;5(6):89.

46. Avci-Adali M, Paul A, Wilhelm N, Ziemer G, Wendel HP. No Title. 15(1):1–11.

47. Tolle F, Wilke J, Wengel J, Mayer G. By-Product Formation in Repetitive PCR Amplification of DNA Libraries during SELEX. PLoS One. 2014 Dec 9;9(12):e114693.

48. Kago L, Hub B ilri. Introduction to PCR What is PCR ?

49. Rychlik W, Spencer WJ, Rhoads RE. Optimization of the annealing temperature for DNA amplification in vitro ; Nucleic Acids Res. 1990 Nov 21;18(21):6409–12.

50. Musheev MU, Krylov SN. Selection of aptamers by systematic evolution of ligands by exponential enrichment: Addressing the polymerase chain reaction issue. Anal Chim Acta. 2006 Mar 30;564(1):91–6.

51. Lam SY, Lau HL, Kwok CK. Capture-SELEX: Selection Strategy, Aptamer Identification, and Biosensing Application. Biosensors. 2022;12(12).

52. Spiga FM, Maietta P, Guiducci C. More DNA-aptamers for small drugs: A capture-SELEX coupled with surface plasmon resonance and high-throughput sequencing. ACS Comb Sci. 2015;17(5):326–33.

53. Yu H, Alkhamis O, Canoura J, Liu Y, Xiao Y. Advances and Challenges in Small-Molecule DNA Aptamer Isolation, Characterization, and Sensor Development. Angew Chemie - Int Ed. 2021;60(31):16800–23.

54. Yoshikawa AM, Wan L, Zheng L, Eisenstein M, Soh HT. A system for multiplexed selection of aptamers with exquisite specificity without counterselection. Proc Natl Acad Sci U S A. 2022 Mar 22;119(12):e2119945119.

55. Yue H, Chen J, Chen X, Wang X, Zhang Y, Zhou N. Systematic screening and optimization of single-stranded DNA aptamer specific for N-acetylneuraminic acid: A comparative study. Sensors Actuators B Chem. 2021 Oct 1;344:130270.

56. Huergo LF, Selim KA, Conzentino MS, Gerhardt ECM, Santos ARS, Wagner B, et al. Magnetic Bead-Based Immunoassay Allows Rapid, Inexpensive, and Quantitative Detection of Human SARS-CoV-2 Antibodies. ACS Sensors. 2021 Mar 26;6(3):703–8.

57. Tan SY, Acquah C, Sidhu A, Ongkudon CM, Yon LS, Danquah MK. SELEX Modifications and Bioanalytical Techniques for Aptamer–Target Binding Characterization. Crit Rev Anal Chem. 2016 Nov 1;46(6):521–37.

58. Ozer A, White BS, Lis JT, Shalloway D. Density-dependent cooperative non-specific binding in solid-phase SELEX affinity selection. Nucleic Acids Res. 2013 Aug 1;41(14):7167–75.

59. Komarova N, Barkova D, Kuznetsov A. Implementation of High-Throughput Sequencing (HTS)

in Aptamer Selection Technology. Int J Mol Sci. 2020 Nov 2;21(22):1–22.

60. Pantier R, Chhatbar K, Alston G, Lee HY, Bird A. High-throughput sequencing SELEX for the determination of DNA-binding protein specificities in vitro. STAR Protoc. 2022 Sep 16;3(3).

61. Thevendran R, Citartan M. Assays to Estimate the Binding Affinity of Aptamers. Talanta. 2022 Feb 1;238:122971.

62. Jing M, Bowser MT. Methods for measuring aptamer-protein equilibria: A review. Anal Chim Acta. 2011 Feb 7;686(1–2):9–18.

63. Stoltenburg R, Reinemann C, Strehlitz B. FluMag-SELEX as an advantageous method for DNA aptamer selection. Anal Bioanal Chem. 2005;383(1):83–91.

64. Jauset-Rubio M, Botero ML, Skouridou V, Aktas GB, Svobodova M, Bashammakh AS, et al. One-Pot SELEX: Identification of Specific Aptamers against Diverse Steroid Targets in One Selection. ACS Omega. 2019 Dec 3;4(23):20188–96.

65. Song Y, Zhu Z, An Y, Zhang W, Zhang H, Liu D, et al. Selection of DNA aptamers against epithelial cell adhesion molecule for cancer cell imaging and circulating tumor cell capture. Anal Chem. 2013;85(8):4141–9.

66. Marimuthu C, Tang TH, Tominaga J, Tan SC, Gopinath SCB. Single-stranded DNA (ssDNA) production in DNA aptamer generation. Analyst. 2012 Feb 20;137(6):1307–15.

67. Reinemann C, Freiin von Fritsch U, Rudolph S, Strehlitz B. Generation and characterization of quinolone-specific DNA aptamers suitable for water monitoring. Biosens Bioelectron. 2016;77:1039–47.

68. Kramat J, Suess B. Efficient Method to Identify Synthetic Riboswitches Using RNA-Based Capture-SELEX Combined with In Vivo Screening. Methods Mol Biol. 2022;2518:157–77.

69. Manea I, Casian M, Hosu-Stancioiu O, de-los-Santos-Álvarez N, Lobo-Castañón MJ, Cristea C. A review on magnetic beads-based SELEX technologies: Applications from small to large target molecules. Anal Chim Acta. 2024 Apr 8;1297:342325.

70. Nguyen VT, Kwon YS, Kim JH, Gu MB. Multiple GO-SELEX for efficient screening of flexible aptamers. Chem Commun. 2014 Aug 12;50(72):10513–6.

71. Yoshikawa AM, Wan L, Zheng L, Eisenstein M, Soh HT. A system for multiplexed selection of aptamers with exquisite specificity without counterselection. Proc Natl Acad Sci U S A. 2022;119(12):1–18.

72. Ruscito A, McConnell EM, Koudrina A, Velu R, Mattice C, Hunt V, et al. In Vitro Selection and Characterization of DNA Aptamers to a Small Molecule Target. Curr Protoc Chem Biol. 2017;9(4):233–68.

73. Fan Y, Li J, Amin K, Yu H, Yang H, Guo Z, et al. Advances in aptamers, and application of mycotoxins detection: A review. Food Res Int. 2023;170.

74. Kalra P, Dhiman A, Cho WC, Bruno JG, Sharma TK. Simple Methods and Rational Design for Enhancing Aptamer Sensitivity and Specificity. Front Mol Biosci. 2018 May 14;5(MAY):41.

75. Jiang M, Fang X, Diao H, Lv S, Zhang Z, Zhang X, et al. Semi-automated and efficient parallel SELEX of aptamers for multiple targets. Anal Methods. 2023 Apr 27;15(16):2039–43.

76. Townshend B, Xiang JS, Manzanarez G, Hayden EJ, Smolke CD. A multiplexed, automated evolution pipeline enables scalable discovery and characterization of biosensors. Nat Commun 2021 121. 2021 Mar 4;12(1):1–15.

77. Northrop BH, Frayne SH, Choudhary U. Thiol–maleimide "click" chemistry: evaluating the influence of solvent, initiator, and thiol on the reaction mechanism, kinetics, and selectivity. Polym

Chem. 2015 Apr 28;6(18):3415–30.

78. Devaraj NK, Finn MG. Introduction: Click Chemistry. Chem Rev. 2021 Jun 23;121(12):6697–8.

79. Sehgal D, Vijay IK. A Method for the High Efficiency of Water-Soluble Carbodiimide-Mediated Amidation. Anal Biochem. 1994 Apr 1;218(1):87–91.

80. Hermanson GT. Bioconjugate Techniques: Third Edition. Bioconjugate Tech Third Ed. 2013;1–1146.

81. Jiang X, Wu M, Albo J, Rao Q. Non-Specific Binding and Cross-Reaction of ELISA: A Case Study of Porcine Hemoglobin Detection. Foods 2021, Vol 10, Page 1708. 2021 Jul 23;10(8):1708.

82. Nongonierma AB, Fitzgerald RJ. Milk proteins as a source of tryptophan-containing bioactive peptides. Food Funct. 2015 Jul 8;6(7):2115–27.

GENERAL CONCLUSIONS AND FUTURE PERSPECTIVES

This section presents the key findings from a comprehensive investigation of the development of advanced (bio)sensing technologies to detect small-molecule biomarkers associated with Acute-on-Chronic Liver Failure (ACLF). The research outlines the efforts to enhance these approaches' specificity, stability, and overall efficacy, with the ultimate goal of significantly contributing to clinical diagnostics and disease prognosis. Furthermore, the research emphasizes the importance of interdisciplinary collaboration, integrating chemistry, molecular biology, and bioinformatics to address complex biosensing challenges.

In Chapter 3, the research focused on the development and application of nanoMIPs and electrochemical techniques, successfully synthesizing and characterizing electroactive nanoMIPs for kynurenic acid (KA) and N-acetylneuraminic acid (NANA). The results demonstrate the high specificity and stability of the target-specific nanoMIPs, positioning them as strong candidates for biosensing applications. Incorporating electroactive monomer significantly improved their detection capabilities, offering a reliable and highly sensitive method of biomarker analysis, even at subfemtomolar concentrations. The study also highlighted the robustness of nanoMIPs when dealing with complex samples, underscoring their potential for real-world clinical applications. Future research should prioritize the large-scale production, synthesis conditions mimicking real-world applications, and integration of nanoMIPs into portable biosensing devices, focusing on developing point-of-care diagnostic tools for ACLF and other diseases.

Chapter 4 detailed the development and optimization of aptamer selection techniques using magnetic bead (MB)- and Joint One-Pot (jOP)-SELEX approaches to isolate aptamers targeting KA, quinolinic acid (QA), and phenylalanine (Phe). Using MBs proved effective in enriching Phe-binding sequences and facilitating the simultaneous selection of multiple target-specific aptamers. Although there was minimal overrepresentation, suggested by Next-generation sequencing (NGS) and GALAXY analysis, the MATLAB analysis provided insights into sequence identification and tracking, possibly aiding in the early identification of potential aptamer candidates if proper overrepresentation would have been attained. Future work should explore and validate the broader application of this bioinformatic workflow in other SELEX processes to further optimize the selection of high-affinity aptamers for various targets.

Lastly, the findings of this thesis may pave the way for future studies and advancements. It's imperative to focus on the scalability and integration of nanoMIPs and aptamers into portable diagnostic devices and ensure a smooth transition from laboratory to real-world settings. This would create user-friendly, point-of-care tools for early diagnosis, prognosis, and monitoring of small molecules associated to ACLF and other diseases. In addition, further optimization of nanoMIPs synthesis and SELEX rounds should be considered, taking into account potential variations between production conditions and real-world usage (e.g., buffer/sample conditions, target state, intended final use, etc.). These considerations could improve biosensing parameters, expand their utility, and ensure their applicability in practical settings. It is essential

to emphasize the importance of collaborative efforts involving researchers, clinicians, and industry partners to facilitate the translation of these advancements into tangible healthcare solutions, ultimately contributing to enhanced patient care and the progression of biosensing technologies.

SUPPLEMENTARY INFORMATION

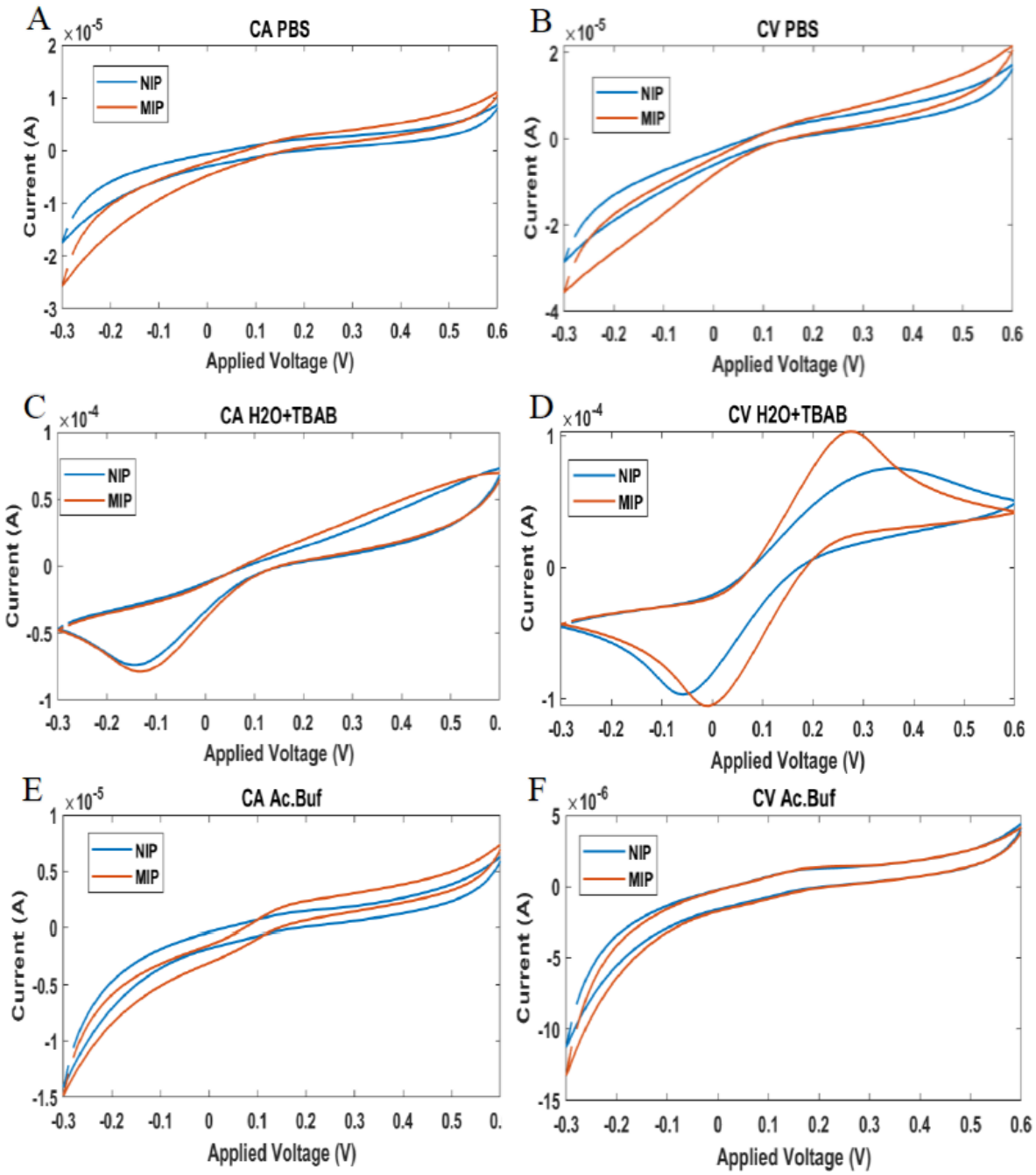


Figure S8. *CA and CV electrosynthesis using three different solvents. Solvents: 10 mM PBS, 10 mM TBAB in H_2O, and 0.5 M AcB. Blue lines correspond to NIPs, and orange ones to MIPs.*

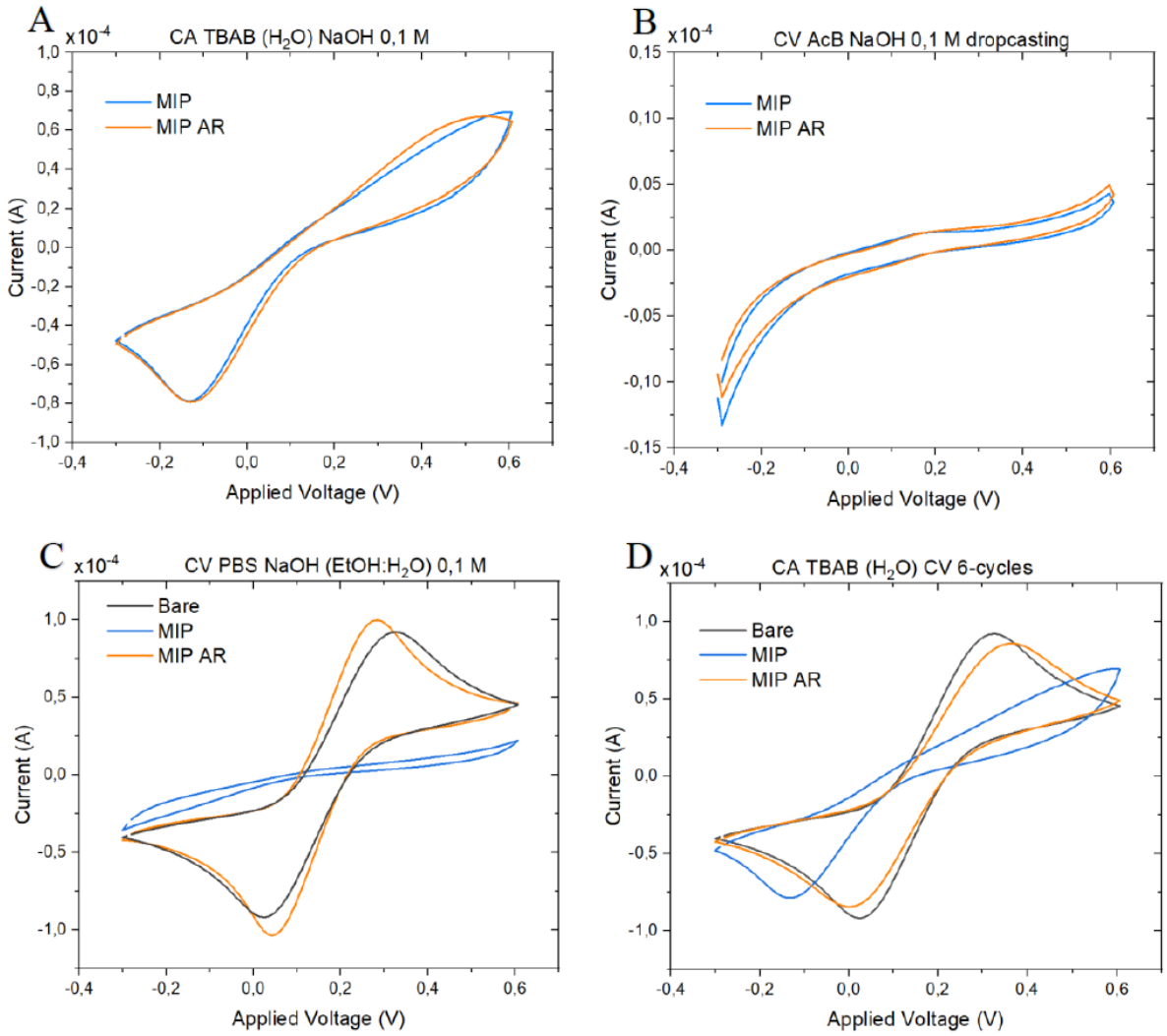


Figure 9. *Unsuccessful removal strategies. A) e-MIP with CA in TBAB and H_2O and proceeded with immersing in 0.1 M NaOH. B) e-MIP with CV in AcB and proceeded with 0.1 M NaOH drop-casting C) e-MIP with CV in PBS and proceeded with immersing in 0.1 M NaOH in EtOH:H_2O (5:1). D) e-MIP with CA in TBAB and H_2O and proceeded with 6 cycles of CV removal.*